PB2003-105809

NIST GCR 03-854

Guidelines for Evaluating Liquefaction Resistance Using Shear Wave Velocity Measurement and Simplified Procedures

National Institute of Standards and Technology
·ation, U.S. Department of Commerce

NIST GCR 03-854

Guidelines for Evaluating Liquefaction Resistance Using Shear Wave Velocity Measurement and Simplified Procedures

Prepared for
U.S. Department of Commerce
Materials and Construction Research Division
National Institute of Standards and Technology
Gaithersburg, MD 20899-8611

By
Ronald D. Andrus
Clemson University
Kenneth H. Stokoe, II
The University of Texas at Austin
Riley M. Chung
Millennium Technology Consulting International
C. Hsein Juang
Clemson University

Grant 43NANB912395

July 2003

U.S. Department of Commerce
Donald L. Evans, Secretary
Technology Administration
Phillip J. Bond, Under Secretary for Technology
National Institute of Standards and Technology
Arden L. Bement, Jr., Director

ABSTRACT

Predicting the liquefaction resistance of soil is an important step in the engineering design of new and the retrofit of existing structures in earthquake-prone regions. The procedure currently used in the U.S. and throughout much of the world to predict liquefaction resistance is termed the simplified procedure. This simplified procedure was originally developed by H. B. Seed and I. M. Idriss in the late 1960s using blow count from the Standard Penetration Test. Small-strain shear wave velocity measurements provide a promising supplement and in some cases, where only geophysical measurements are possible, may be the only alternative to the penetration-based approach. This report presents guidelines for evaluating liquefaction resistance using shear wave velocity measurements. These guidelines were written in cooperation with industry, researchers and practitioners, and evolved from workshops in 1996 and 1998 as well as review comments received on an earlier draft. The guidelines present a recommended procedure, which follows the general format of the penetration-based simplified procedure. The proposed procedure has been validated through case history data from more than 20 earthquakes and 70 measurement sites in soils ranging from clean fine sand to sandy gravel with cobbles to profiles including silty clay layers. Deterministic liquefaction resistance curves were established by applying a modified relationship between the shear wave velocity and cyclic stress ratio for the constant average cyclic shear strain suggested by R. Dobry. These curves correctly predict moderate to high liquefaction potential for over 95 % of the liquefaction case histories, and are shown to be consistent with the penetration-based curves in sandy soils. From logistic regression and Bayesian models, the recommended deterministic curve is characterized with a probability of liquefaction of about 26 %. To further validate the procedure, additional case histories are needed with all soil types that have and have not liquefied, particularly from deeper deposits (depth > 8 m) and from denser soils (shear wave velocity > 200 m/s) shaken by stronger ground motions (peak ground acceleration > 0.4 g). The guidelines serve as a resource document for practitioners and researchers involved in evaluating soil liquefaction resistance.

KEYWORDS: building technology; earthquakes; *in situ* measurements; seismic testing; shear wave velocity; soil liquefaction

ACKNOWLEDGMENTS

The NIST program to develop *Guidelines for Evaluating Liquefaction Resistance Using Shear Wave Velocity Measurements and Simplified Procedures* began in October of 1995. The initial work involved a review of proposed simplified procedures, collection of available case history data, participation in two workshops, and development of a recommended procedure. The first workshop was held on January 4-5, 1996 in Salt Lake City, Utah, and was sponsored by the National Center for Earthquake Engineering Research (NCEER). The second workshop was held on August 14-15, 1998 also in Salt Lake City, and was sponsored by the Multidisciplinary Center for Earthquake Engineering Research (MCEER, formally NCEER) and the National Science Foundation (NSF). Workshop participants included: T. Leslie Youd (Chair), Brigham Young University; Izzat M. Idriss (Co-chair), University of California at Davis; Ronald D. Andrus, formerly with National Institute of Standards and Technology; Ignacio Arango, Bechtel Corporation; John Barneich, Woodward-Clyde Consultants; Gonzalo Castro, GEI Consultants, Inc.; John T. Christian, Consulting Engineer; Ricardo Dobry, Rensselaer Polytechnic Institute; W. D. Liam Finn, University of British Columbia; Leslie F. Harder, Jr., California Department of Water Resources; Mary Ellen Hynes, U.S. Army Corps of Engineers, WES; Kenji Ishihara, Science University of Tokyo, Joseph P. Koester, U.S. Army Corps of Engineers, WES; Sam S. C. Liao, Parsons Brinckerhoff; Faiz Makdisi, Geomatrix Consultants; William F. Marcuson, III, Virginia Tech; Yoshiharu Moriwaki, Woodward-Clyde Consultants; Maurice S. Power, Geomatix Consultants; Peter K. Robertson, University of Alberta; Raymond B. Seed, University of California at Berkeley; and Kenneth H. Stokoe, II, University of Texas at Austin. The workshop participants provided expert review for the initial work.

Draft guidelines were published in a NIST technical report (*NISTIR 6277*, Andrus et al., 1999), based on the results of the initial work. Prior to publishing the draft guidelines, six technical experts were asked to review the guidelines. The six technical experts were: Ricardo Dobry; Mary Ellen Hynes; Izatt M. Idriss; Robert Pyke, Consulting Engineer; Richard D. Woods, University of Michigan; and T. Leslie Youd.

Since the publication of the draft guidelines, efforts have been made to obtain feedback on them from a broader base of practitioners and researchers. This was accomplished by distributing more than 100 copies of the draft guidelines with a request for comments. Written responses were received from the following individuals: John Barneich; Leo Brown for Robert Nigbor, GeoVision; Gonzalo Castro; A. G. Franklin, Consulting Engineer; C. Hsein Juang and Caroline J. Chen, Clemson University; Michael K. Lee and Ken Y. Lum, BC Hydro; Paul W. Mayne and James Schneider, Georgia Institute of Technology; Alan F. Rauch and James Chrisley, University of Texas at Austin; Soheil Nazarian, University of Texas at El Paso; and Zhenming Wang, Oregon Department of Geology and Mineral Industries. Comments were also received from anonymous reviewers of two journal papers summarizing this work. In addition, presentations were made at various professional meetings, including the Transportation Research Board Seventy-Eighth Annual Meeting Workshop on New Approaches to

Liquefaction Analysis. The guidelines presented herein are based on the draft guidelines, and feedback from the mail reviews, journal paper reviews, and professional meetings. The authors thank the many people who provided comments and suggestions.

The authors also thank those who provided project reports and other information presented in this report. Special thanks to Susumu Iai and Kohji Ichii of the Port and Harbour Research Institute, Osamu Matsuo of the Public Works Research Institute, Susumu Yasuda of the Tokyo Denki University, Mamoru Kanatani and Yukihisa Tanaka of the Central Research Institute for Electric Power Industry, Kohji Tokimatsu of the Tokyo Institute of Technology, Kenji Ishihara of the Science University of Tokyo, Fumio Tatsuoka of the University of Tokyo, and Takeji Kokusho of the Chuo University for the information graciously shared with the first author on Japanese liquefaction case histories and dynamic soil properties. Roman Hryciw of the University of Michigan provided information on the location of seismic cone penetration tests and liquefaction effects on Treasure Island. Ross Boulanger of the University of California at Davis provided information on liquefaction case histories at Moss Landing. Michael Bennett of the U.S. Geological Survey shared first-hand knowledge of the field performance for some of the California case histories. David Sykora of Bing Yen & Associates, Inc., graciously shared his database of shear wave velocity measurements and SPT blow counts. Tao Jiang of Clemson University assisted with the probability study described in Appendix G.

Draft copies of this report were distributed to fifteen technical experts for their final review and comment. The fifteen technical experts were: Donald G. Andersen, CH2M Hill, Gonzalo Castro, John T. Christian, Ricardo Dobry, Mary Ellen Hynes, Izzat M. Idriss, Sam S. C. Liao, James K. Mitchell, Maurice S. Power, Robert Pyke, Glenn J. Rix, Georgia Institute of Technology, Peter K. Robertson, Raymond Seed, T. Leslie Youd, and Richard D. Woods. Comments were received from several of these experts and, to the extent possible, have been incorporated into the report.

The final report was submitted to the National Institute of Standards and Technology on September 28, 2000 for review. Based on subsequent work, some minor errors are corrected in this publication.

Finally, the authors express their thanks to the staff at the National Institute of Standards and Technology. Harry Brooks, Rose Estes, Bonnie Gray and other library staff assisted with the collection of several references cited in this report. Nicholas Carino and Fahim Sadek of the Structures Division reviewed the earlier draft guidelines, and provided many helpful suggestions. William Guthrie of the Statistical Engineering Division shared insights into the logistic regression technique for determining probability. John Gross served as the Technical Information Contact for the final guidelines.

TABLE OF CONTENTS

ABSTRACT iii

ACKNOWLEDGMENTS v

TABLE OF CONTENTS vii

LIST OF TABLES xi

LIST OF FIGURES xiii

CHAPTER 1
INTRODUCTION 1
1.1 BACKGROUND 1
1.2 PURPOSE 3
1.3 REPORT OVERVIEW 4

CHAPTER 2
LIQUEFACTION EVALUATION PROCEDURE 5
2.1. CYCLIC STRESS RATIO (*CSR*) 5
2.1.1 Peak Horizontal Ground Surface Acceleration 6
2.1.2 Total and Effective Overburden Stresses 6
2.1.3 Stress Reduction Coefficient 7
2.1.3.1 Relationship by Seed and Idriss (1971) 7
2.1.3.2 Revised Relationship Proposed by Idriss (1998; 1999) 7
2.2 STRESS-CORRECTED SHEAR WAVE VELOCITY 10
2.3 CYCLIC RESISTANCE RATIO (*CRR*) 13
2.3.1 Magnitude Scaling Factor 13
2.3.1.1 Factors Recommended by 1996 NCEER Workshop 15
2.3.1.2 Revised Factors Proposed by Idriss (1999) 17
2.3.1.3 Recommended Magnitude Scaling Factors 17
2.3.2 Limiting Upper Value of V_{S1} in Sandy Soils 19
2.3.3 Limiting Upper Value of V_{S1} in Gravelly Soils 19
2.3.4 Cementation and Aging Correction Factor 20

2.4 FACTOR OF SAFETY 23
2.5 PROBABILITY-BASED EVALUATION 23
2.6 SUMMARY 24

CHAPTER 3
APPLICATION OF THE LIQUEFACTION EVALUATION PROCEDURE 29
3.1 TREASURE ISLAND FIRE STATION 29
3.2 MARINA DISTRICT WINFIELD SCOTT SCHOOL 33

CHAPTER 4
SUMMARY AND RECOMMENDATIONS 39
4.1 SUMMARY 39
4.2 FUTURE STUDIES 40

APPENDIX A
REFERENCES 43

APPENDIX B
SYMBOLS AND NOTATION 57

APPENDIX C
GLOSSARY OF TERMS 61

APPENDIX D
COMPARISON OF V_S-BASED LIQUEFACTION RESISTANCE CURVES 63
D.1 CURVE BY TOKIMATSU AND UCHIDA (1990) 63
D.2 CURVE BY ROBERTSON ET AL. (1992) 67
D.3 CURVE BY KAYEN ET AL. (1992) 69
D.4 CURVE BY LODGE (1994) 69
D.5 CURVE BY ANDRUS AND STOKOE (1997) 72
D.5.1 Cyclic Shear Strain and Cyclic Shear Stress 72
D.5.2 Dobry's Relationship Between CRR and V_{S1} 74
D.5.3 Modified CRR-V_{S1} Relationship 75
D.6 CURVE BY ANDRUS ET AL. (1999) 76
D.7 SUMMARY 76

APPENDIX E
CASE HISTORY DATA AND THEIR CHARACTERISTICS 79
E.1 SITE VARIABLES AND DATABASE CHARACTERISTICS 79
E.1.1 Earthquake Magnitude 79
E.1.2 Shear Wave Velocity Measurement 79
E.1.3 Measurement Depth 82
E.1.4 Case History 83
E.1.5 Liquefaction Occurrence 83
E.1.6 Critical Layer 84
E.1.7 Ground Water Table 87
E.1.8 Total and Effective Overburden Stresses 87
E.1.9 Average Peak Ground Acceleration 88
E.1.10 Average Cyclic Stress Ratio 88
E.1.11 Average Overburden Stress-Corrected Shear Wave Velocity 88
E.2 SAMPLE CALCULATIONS 89
E.2.1 Treasure Island Fire Station 89
E.2.2 Marina District School 91
E.3 SUMMARY 94

APPENDIX F
DEVELOPMENT OF LIQUEFACTION RESISTANCE CURVES FROM CASE HISTORY DATA 97
F.1. LIMITING UPPER V_{S1} VALUE FOR LIQUEFACTION OCCURRENCE 99
F.1.1 Sandy Soils 99
F.1.2 Gravelly Soils 109
F.2 CURVE FITTING PARAMETERS *a* AND *b* 109
F.2.1 Magnitude Scaling Factors Recommended by 1996 NCEER Workshop 109
F.2.1.1 Lower Bound of Recommended Range 109
F.2.1.2 Upper Bound of Recommended Range 110
F.2.2 Revised Magnitude Scaling Factors Proposed by Idriss (1999) 110
F.2.3 Comparison of Magnitude Scaling Factors 113
F.3 RECOMMENDED CRR-V_{S1} CURVES 113
F.4 CORRELATIONS BETWEEN V_{S1} AND PENETRATION RESISTANCE 122
F.4.1 Corrected SPT Blow Count 122
F.4.2 Normalized Cone Tip Resistance 124
F.5 SUMMARY 128

APPENDIX G
PROBABILITY-BASED LIQUEFACTION EVALUATION 129
G.1 LOGISTIC REGRESSION MODELS 130
G.1.1 Logistic Regression Model 1 130
G.1.2 Logistic Regression Model 2 132
G.2 BAYESIAN MAPPING MODEL 132
G.3 COMPARISON OF PROBABILITY MODELS 139

APPENDIX H
SUMMARY OF CASE HISTORY DATA 141

LIST OF TABLES

Table Page

2.1 Comparison of Advantages and Disadvantages of Various *In Situ* V_S Test Methods for Liquefaction Assessment 11

2.2 Magnitude Scaling Factors Obtained by Various Investigators 15

E.1 Earthquakes and Sites Used to Establish Liquefaction Resistance Curves 80

E.2 Sample Calculations for the Treasure Island Fire Station Site, Crosshole Test Array B1-B4, and the 1989 Loma Prieta Earthquake 92

E.3 Sample Calculations for the Treasure Island Fire Station Site, SASW Test Array, and the 1989 Loma Prieta Earthquake 92

E.4 Sample Calculations for the Marina District School Site and the 1989 Loma Prieta Earthquake 95

F.1 Estimates of Equivalent V_{S1} for Holocene Sands and Gravels Below the Ground Water Table with Corrected SPT **Blow Count of 30** 100

F.2 Estimates of Equivalent V_{S1} for Holocene Sands and Gravels Below the Ground Water Table with Normalized Cone Tip Resistance of 160 103

F.3 Estimates of Equivalent V_{S1} for Holocene Sands and Gravels Below the Ground Water Table with Corrected SPT **Blow Count of 21** 104

H.1 Summary Information for V_S-Based Liquefaction and Non-Liquefaction Case Histories 143

LIST OF FIGURES

Figure		Page
2.1	Relationship Between Stress Reduction Coefficient and Depth Developed by Seed and Idriss (1971) with Approximate Average Value Lines from Eq. 2.2	8
2.2	Relationship Between Average Stress Reduction Coefficient and Depth Proposed by Idriss (1998; 1999) with Average Range Determined by Seed and Idriss (1971)	9
2.3	Curves Recommended for Calculation of *CRR* from V_{S1}	14
2.4	Magnitude Scaling Factors Derived by Various Investigators with Range Recommended by the 1996 NCEER Workshop	16
2.5	Relationship Between Moment Magnitude and Various Magnitude Scales	18
2.6	Suggested Method for Determining the Correction Factor K_C from $(N_1)_{60}$, V_{S1}, and Fines Content at a Weakly Cemented Soil Site	21
2.7	Suggested Method for Determining the Correction Factor K_C from q_{c1N}, V_{S1}, and Fines Content at a Weakly Cemented Soil Site	22
2.8	Suggested Relationship for Selecting F_S Based on Probability of Liquefaction and the Recommended CRR-V_{S1} Curves	25
2.9	Curves Suggested for Probability-Based Evaluation in Clean Soils. Note that P_L = 0.26 Corresponds to the Recommended Deterministic Curve Shown in Fig. 2.3	26
3.1	Application of the Recommended Procedure to the Treasure Island Fire Station Site, Crosshole Test Array B1-B4 (Depths of 1.5 m to 14 m)	30
3.2	Application of the Recommended Procedure to the Treasure Island Fire Station Site, SASW Test Array (Depths of 2 m to 13 m)	31

Figure | Page

3.3 Liquefaction Assessment Chart for Magnitude 7 Earthquakes with Data for the 1989 Loma Prieta Earthquake and the Treasure Island Fire Station Site, Crosshole Test Array B1-B4 (Depths of 1.5 m to 14 m) 34

3.4 Liquefaction Assessment Chart for Magnitude 7 Earthquakes with Data for the 1989 Loma Prieta Earthquake and the Treasure Island Fire Station Site, SASW Test Array (Depths of 2 m to 13 m) 35

3.5 Application of the Recommended Procedure to the Marina District School Site (Depths of 3 m to 10 m) 36

3.6 Liquefaction Assessment Chart for Magnitude 7 Earthquakes with Data for the 1989 Loma Prieta Earthquake and the Marina District School Site (Depths of 3 m to 7 m) 38

D.1 Comparison of Seven Proposed CRR-V_{S1} Curves for Clean Granular Soils 64

D.2 Relationship Between Liquefaction Resistance and Normalized Shear Modulus for Various Sands with Less than 10 % Fines Determined by Cyclic Triaxial Testing 65

D.3 Liquefaction Resistance Curve for Magnitude 7.5 Earthquakes and Case History Data from Robertson et al. (1992) 68

D.4 Liquefaction Resistance Curve for Magnitude 7 Earthquake and Case History Data from Kayen et al. (1992) 70

D.5 Liquefaction Resistance Curve for Magnitude 7 Earthquakes and Case History Data from Lodge (1994) 71

D.6 Liquefaction Resistance Curve for Magnitude 7.5 Earthquakes and Uncemented Clean Soils of Holocene Age with Case History Data from Andrus and Stokoe (1997) 73

Figure Page

D.7 Revised Liquefaction Resistance Curve for Magnitude 7.5 Earthquakes and Uncemented Clean Soils of Holocene Age with Case History Data from Andrus et al. (1999) 77

E.1 Distribution of Liquefaction and Non-Liquefaction Case Histories by Earthquake Magnitude 84

E.2 Cumulative Relative Frequency of Case History Data by Critical Layer Thickness... 85

E.3 Cumulative Relative Frequency of Case History Data by Average Depth of V_S Measurements in Critical Layer 85

E.4 Distribution of Case Histories by Earthquake Magnitude, Predominate Soil Type, and Average Fines Content 86

E.5 Cumulative Relative Frequency of Case History Data by Depth to the Ground Water Table 87

E.6 Shear Wave Velocity and Soil Profiles for the Treasure Island Fire Station Site 90

E.7 Shear Wave Velocity and Soil Profiles for the Marina District School Site 93

E.8 General Configuration of the Downhole Seismic Test Using the Pseudo-Interval Method to Calculate Shear Wave Velocity 94

F.1 Curves Recommended for Calculation of *CRR* from Shear Wave Velocity Measurements Along with Case History Data Based on **Lower Bound** Values of *MSF* for the Range Recommended by the 1996 NCEER Workshop (Youd et al., 1997) and r_d Developed by Seed and Idriss (1971) 98

F.2 Variations in V_{S1} with $(N_1)_{60}$ for Uncemented, Holocene-age Sands with Less than 10 % Non-plastic Fines 101

F.3 Variations in V_{S1} with q_{c1N} for Uncemented, Holocene-age Sands with Less than 10 % Non-plastic Fines 102

Figure Page

F.4 Curve Recommended for Calculation of *CRR* from V_{S1} Measurements in Sands and Silts with $FC \geq 35$ % along with Case History Data 105

F.5 Curve Recommended for Calculation of *CRR* from V_{S1} Measurements in Sands with $FC = 20$ % along with Case History Data 106

F.6 Curve Recommended for Calculation of *CRR* from V_{S1} Measurements in Sands with $FC \leq 5$ % along with Case History Data 107

F.7 Curve Recommended for Calculation of *CRR* from V_{S1} Measurements in Gravels with $FC \leq 5$ % and $FC = 20$ % along with Case History Data 108

F.8 Curves Recommended for Calculation of *CRR* from Shear Wave Velocity Measurements Along with Case History Data Based on **Upper Bound** Values of *MSF* for the Range Recommended by the 1996 NCEER Workshop (Youd et al., 1997) and r_d Developed by Seed and Idriss (1971) 111

F.9 Curves Recommended for Calculation of *CRR* from Shear Wave Velocity Measurements Along with Case History Data Based on Revised Values of *MSF* and r_d Proposed by Idriss (1998; 1999) 112

F.10 Variation of r_d/MSF with Depth for Various Magnitudes and Proposed Relationships 114

F.11 Comparison of Liquefaction Resistance Curves and Case History Data for Procedures Recommended by the 1996 NCEER Workshop (Youd et al., 1997) and the Revised Procedures Proposed by Idriss (1998; 1999) for Clean Sands and Earthquake with Magnitude Near 5.5 115

F.12 Case History Data for Earthquakes with Magnitude Near 5.5 Based on Overburden Stress-Corrected Shear Wave Velocity and Cyclic Stress Ratio with Recommended Liquefaction Resistance Curves 116

F.13 Case History Data for Earthquakes with Magnitude Near 6 Based on Overburden Stress-Corrected Shear Wave Velocity and Cyclic Stress Ratio with Recommended Liquefaction Resistance Curves 117

Figure | Page

F.14 Case History Data for Earthquakes with Magnitude Near 6.5 Based on Overburden Stress-Corrected Shear Wave Velocity and Cyclic Stress Ratio with Recommended Liquefaction Resistance Curves ... 118

F.15 Case History Data for Earthquakes with Magnitude Near 7 Based on Overburden Stress-Corrected Shear Wave Velocity and Cyclic Stress Ratio with Recommended Liquefaction Resistance Curves ... 119

F.16 Case History Data for Earthquakes with Magnitude Near 7.5 Based on Overburden Stress-Corrected Shear Wave Velocity and Cyclic Stress Ratio with Recommended Liquefaction Resistance Curves ... 120

F.17 Case History Data for Earthquakes with Magnitude Near 8 Based on Overburden Stress-Corrected Shear Wave Velocity and Cyclic Stress Ratio with Recommended Liquefaction Resistance Curves ... 121

F.18 Relationships Between $(N_1)_{60}$ and V_{S1} for Clean Sands Implied by the Recommended CRR-V_{S1} Relationship and the 1996 NCEER Workshop Recommended CRR-$(N_1)_{60}$ Relationship (Youd et al., 1997) with Field Data for Sands with Less than 10 % Fines ... 123

F.19 Relationships Between $(N_1)_{60}$ and V_{S1} Implied by the Recommended CRR-V_{S1} Relationship and the 1996 NCEER Workshop Recommended CRR-$(N_1)_{60}$ Relationship (Youd et al., 1997) ... 125

F.20 Relationships Between q_{c1N} and V_{S1} for Clean Sands Implied by the Recommended CRR-V_{S1} Relationship and the 1996 NCEER Workshop Recommended CRR-q_{c1N} Relationship (Youd et al., 1997) with Field Data for Sands with Less than 10 % Fines ... 126

F.21 Relationships Between q_{c1N} and V_{S1} Implied by the Recommended CRR-V_{S1} Relationship and the 1996 NCEER Workshop Recommended CRR-q_{c1N} Relationship (Youd et al., 1997) ... 127

G.1 Logistic Regression Model 1 and Case History Data Adjusted for Fines Content ... 131

Figure | Page

G.2 Logistic Regression Model 2 and Case History Data Adjusted for Fines Content ... 133

G.3 Probability Density Functions and Calculated Factor of Safety for the 225 Case Histories ... 135

G.4 Calculated Values of F_S and P_L for the 225 Case Histories with the Best-Fit Relationship (Juang et al., 2002). Note that F_S is based on the Recommended Deterministic Evaluation Curves Shown in Fig. 2.3, and P_L is based on Eq. (G.6) ... 136

G.5 Relationship Between P_L and F_S for the V_S-Based Procedure (Juang et al., 2002) and the SPT-Based Procedure (Juang et al., 2000a) Determined Using Bayes' Theorem ... 137

G.6 Bayesian Mapping Model and Case History Data Adjusted for Fines Content ... 138

G.7 Comparison of the Probability-Based Logistic Regression and Bayesian Mapping Models for P_L = 26 % with the Deterministic Curve Developed by Andrus et al. (1999) for Clean Soils ... 140

CHAPTER 1

INTRODUCTION

1.1 BACKGROUND

A major cause of damage from earthquakes is liquefaction-induced ground failure. For example, direct property loss caused by liquefaction during the 1989 Loma Prieta, California earthquake (moment magnitude, M_w = 7.0) was over \$100 million (Holzer, 1998). Large indirect property loss by fire almost occurred in 1989 when liquefaction-induced ground deformation ruptured water mains that served the Marina District of San Francisco. Fortunately, the fire in the Marina District at Divisadero and Beach Streets was contained to the three-story apartment building where it ignited. It was also fortunate that the 1989 earthquake did not occur closer to the San Francisco Bay area. The cities of Kobe and Osaka, Japan were not so fortunate. The 1995 Hyogoken-Nanbu earthquake (M_w = 6.9) directly struck this metropolitan area, causing over \$100 billion in property damage (Kimura, 1996). A significant portion of the damage in Kobe can be attributed to liquefaction-induced ground deformation. These are just two of many examples of major damage caused by liquefaction-induced ground failure. Predicting soil liquefaction resistance is an important step in the engineering design of new and the retrofit of existing structures in earthquake-prone regions.

The procedure widely used in the United States and throughout much of the world for predicting the liquefaction resistance of soils is termed the *simplified procedure*. This simplified procedure was originally developed by Seed and Idriss (1971) using blow count from the Standard Penetration Test (SPT) correlated with a parameter called *cyclic stress ratio* that represents the seismic loading on the soil. Since 1971, the procedure has been revised and updated (Seed, 1979; Seed and Idriss, 1982; Seed et al., 1983; Seed et al., 1985). Correlations based on the Cone Penetration Test (CPT) and shear wave velocity measurements have also been developed by various investigators. General reviews of the simplified procedure are contained in a report by the National Research Council (1985), a workshop report edited by Youd and Idriss (1997), and a journal paper by Youd et al. (2001).

Small-strain shear wave velocity, V_S, measurements provide a promising supplement and in some cases, where only geophysical measurements are possible, may be the only alternative to the penetration-based approach. The use of V_S as an index of liquefaction resistance is soundly based because both V_S and liquefaction resistance are similarly influenced by many of the same factors (e.g., void ratio, state of stress, stress history, and geologic age).

Some advantages of using V_S are (Dobry et al., 1981; Seed et al., 1983; Stokoe et al., 1988a; Tokimatsu and Uchida, 1990): (1) Measurements are possible in soils that are hard to sample, such as gravelly soils where penetration tests may be unreliable. (2) Measurements can be performed on small laboratory specimens, allowing direct comparisons between laboratory and field behavior. (3) V_S is a basic mechanical property of soil materials, directly related to small-strain shear modulus, G_{max}, by:

$$G_{max} = \rho V_S^2 \tag{1.1}$$

where

ρ = the mass density of soil.

(4) G_{max}, or V_S, is in turn a required property in analytical procedures for estimating dynamic shearing strain in soil in earthquake site response and soil-structure interaction analyses. (5) V_S can be measured by the Spectral-Analysis-of-Surface-Waves (SASW) test method at sites where borings may not be permitted, such as capped landfills, and sites that extend for great distances where rapid evaluation is required, such as lifelines and large building complexes.

Three concerns when using V_S to evaluate liquefaction resistance are: (1) Measurements are made at small strains, whereas pore-water pressure buildup and liquefaction are medium- to high-strain phenomena (Jamiolkowski and Lo Presti, 1990; Teachavorasinskun et al., 1994; Roy et al., 1996). This concern can be significant for cemented soils, since small-strain measurements are highly sensitive to weak interparticle bonding which is eliminated at medium and high strains. It also can be significant in silty soils above the water table where negative pore water pressures can increase V_S. (2) No samples are obtained for classification of soils and identification of non-liquefiable soft clayey soils. According to the so-called Chinese criteria, non-liquefiable clayey soils have clay contents (particles smaller than 5 μm) > 15 %, liquid limits > 35 %, or moisture contents < 90 % of the liquid limit (Seed and Idriss, 1982). Andrews and Martin (2000) refined this criteria to soils with clay contents (particles smaller than 2 μm) ≥ 10 % and liquid limits ≥ 32 % (by Casagrade-type percussion apparatus) for non-liquefiable clayey soils. (3) Thin, low V_S strata may not be detected if the measurement interval is too large (USBR, 1989; Boulanger et al., 1997).

In general, borings should always be a part of the field investigation. Surface geophysical measurements and cone soundings are often conducted first to help select the best locations for borehole sampling and testing. Surface geophysical tests usually involve making measurements at several different locations, and provide general, or average, stratigraphy for sediments beneath the area tested. The ability of surface geophysical methods to resolve a layer at depth depends on the thickness, depth, and continuity of that layer, as well as the test and interpretation procedures employed. Cone soundings provide detailed stratigraphy at each test location for sediments that can be penetrated. The preferred practice when using V_S measurements to evaluate liquefaction resistance is to drill sufficient boreholes and conduct sufficient tests to detect and delineate thin liquefiable strata, to identify non-liquefiable clay-rich soils, to identify silty soils above the ground water table that might have lower values of V_S should the water table rise, and to detect liquefiable weakly cemented soils.

1.2 PURPOSE

This report presents guidelines for evaluating liquefaction resistance through shear wave velocity measurements. The guidelines are based on an earlier report entitled "Draft Guidelines for Evaluating Liquefaction Resistance Using Shear Wave Velocity Measurements and Simplified Procedures" by Andrus et al. (1999), which evolved from two workshops. The first workshop was held on January 4-5, 1996 in Salt Lake City, and was sponsored by the National Center for Earthquake Engineering Research (NCEER). The second workshop was held on August 14-15, 1998 also in Salt Lake City, and was sponsored by the Multidisciplinary Center for Earthquake Engineering Research (MCEER, formally NCEER) and the National Science Foundation (NSF). These two workshops are herein called the 1996 NCEER Workshop and 1998 MCEER Workshop. The guidelines present a recommended procedure based on the suggestions given at the workshops, as well as review comments received on the draft guidelines. The guidelines provide guidance on selecting site variables and correction factors that are consistent with the shear-wave-based procedure.

From the comments received on the earlier draft guidelines, several improvements have been made to the guidelines. The major improvements include: (1) Much of the background and development information is moved to the appendixes to provide a clearer, more practical description of the recommended procedure. (2) A table is added to compare advantages and disadvantages of the various *in situ* V_S test methods for liquefaction assessment. (3) A more comprehensive description of the database is given, particularly on the nature of the case histories of gravelly soils. (4) The results of a probability study of the V_S-based case history data are added to calibrate the recommended liquefaction resistance curve and to compare with the results of probability studies of the SPT-based case history data.

1.3 REPORT OVERVIEW

Following this introduction, Chapter 2 presents the recommended procedure for evaluating liquefaction resistance using V_S. Chapter 3 illustrates the application of the procedure using two case studies. And Chapter 4 summarizes the recommended procedure and identifies issues that remain to be resolved.

Eight appendixes are included to assist the reader, and to provide information used in the development of the guidelines. Appendix A presents a list of references cited in the guidelines. Appendix B provides a list of Symbols and Notation, and Appendix C provides a Glossary of Terms. Appendix D reviews six proposed V_S-based liquefaction resistance curves. Appendix E describes the general characteristics of case history data used to develop the recommended liquefaction resistance curves. Appendix F presents the development of the recommended curves. Appendix G considers three probability models for the case history data. Finally, Appendix H presents a summary of the case history data.

CHAPTER 2

LIQUEFACTION EVALUATION PROCEDURE

This chapter presents guidelines for using the V_S-based liquefaction evaluation procedure originally proposed by Andrus and Stokoe (1997) and subsequently updated in the report by Andrus et al. (1999) and the paper by Andrus and Stokoe (2000). The evaluation procedure follows the general format of the Seed-Idriss simplified procedure, and the general recommendations of the 1996 NCEER Workshop (Youd et al., 1997) and 1998 MCEER Workshop (Youd et al., 2001). It requires the calculation of three parameters: (1) the level of cyclic loading on the soil caused by the earthquake, expressed as a cyclic stress ratio; (2) the stiffness of the soil, expressed as an overburden stress-corrected shear wave velocity; and (3) the resistance of the soil to liquefaction, expressed as a cyclic resistance ratio. Each parameter is discussed below.

2.1 CYCLIC STRESS RATIO (*CSR*)

The cyclic stress ratio, τ_{av} / σ'_v, at a particular depth in a level soil deposit can be expressed as (Seed and Idriss, 1971):

$$CSR = \frac{\tau_{av}}{\sigma'_v} = 0.65\left(\frac{a_{\max}}{g}\right)\left(\frac{\sigma_v}{\sigma'_v}\right)r_d \qquad (2.1)$$

where

τ_{av}	=	the average equivalent uniform shear stress caused by the earthquake and is assumed to be 0.65 of the maximum induced stress,
a_{max}	=	the peak horizontal ground surface acceleration,
g	=	the acceleration of gravity,
σ_v	=	the total vertical (overburden) stress at the depth in question,
σ'_v	=	the initial effective overburden stress at the same depth, and
r_d	=	a shear stress reduction coefficient to adjust for the flexibility of the soil profile.

2.1.1 Peak Horizontal Ground Surface Acceleration

Peak horizontal ground surface acceleration is a characteristic of the ground shaking intensity, and is defined as the peak value in a horizontal ground acceleration record that would occur at the site without the influence of excess pore-water pressures or liquefaction that might develop (Youd et al., 2001).

Peak accelerations are commonly estimated using empirical attenuation relationships of a_{max} as a function of earthquake magnitude, distance from the energy source or surface project of the fault rupture, and local site conditions. Since many published attenuation relationships are based on both peak values obtained from ground motion records for the two horizontal directions (sometimes referred to as the randomly oriented horizontal component), the geometric mean (square root of the product) of the two peak values is used. According to Youd et al. (2001), use of the geometric mean is consistent with the derivation of the SPT-based procedure and is preferred for use in engineering practice. However, use of the larger of the two horizontal peak accelerations would be conservative and is allowable.

Regional or national seismic hazard maps (http://geohazards.cr.usgs.gov/eq/; Frankel et al., 2000) are also often used to estimate peak accelerations. If peak acceleration is estimated from a map, the magnitude and distance information should be obtained from the deaggregated matrices used to develop the map. The value of a_{max} selected will depend on the target level of risk and compatibility of site conditions. For site conditions not compatible with available probabilistic maps or attenuation relationships, the value of a_{max} may be corrected based on dynamic site response analyses or site class coefficients given in the latest building codes.

2.1.2 Total and Effective Overburden Stresses

Required in the calculation of σ_v and σ'_v are densities of the various soil layers, as well as characteristics of the ground water. For non-critical projects involving hard-to-sample soils below the ground water table, densities are often estimated from typical values for soils with similar grain size and penetration or velocity characteristics. Fortunately, *CSR* is not very sensitive to density, and reasonable estimates of density yield reasonable results.

The values of σ'_v and *CSR* are sensitive to the ground water table depth. Other ground water characteristics that may be significant to liquefaction evaluations include seasonal and long-term water level variations, depth of and pressure in artesian zones, and whether the water table is perched or normal.

2.1.3 Stress Reduction Coefficient

Equation 2.1 is based on Newton's second where force is equal to mass times acceleration. The coefficient r_d is added because the soil column behaves as a deformable body rather than a rigid body.

2.1.3.1 Relationship by Seed and Idriss (1971)—Values of r_d are commonly estimated from the chart by Seed and Idriss (1971) shown in Fig. 2.1. This chart was determined analytically using a variety of earthquake motions and soil conditions. Average r_d values given in the chart can be estimated using the following functions (Liao and Whitman, 1986; Robertson and Wride, 1997):

$$r_d = 1.0 - 0.00765\,z \qquad \text{for } z \leq 9.15 \text{ m} \tag{2.2a}$$

$$r_d = 1.174 - 0.0267\,z \qquad \text{for } 9.15 \text{ m} < z \leq 23 \text{ m} \tag{2.2b}$$

$$r_d = 0.744 - 0.008\,z \qquad \text{for } 23 \text{ m} < z \leq 30 \text{ m} \tag{2.2c}$$

where

z = the depth below the ground surface in meters.

Figure 2.1 shows the average r_d values approximated by Eq. (2.2). These average r_d values were suggested by the 1996 NCEER Workshop (Youd et al., 1997; 2001) for non-critical projects.

2.1.3.2 Revised Relationship Proposed by Idriss (1998; 1999)—Figure 2.2 presents revised average values of r_d proposed by Idriss (1998; 1999) for various earthquake magnitudes. The plotted curves are averages of many individual curves derived analytically by Golesorkhi (1989) under the supervision of the late Prof. H. B. Seed. They are defined by the following relationship (after Idriss, 1998; modified for depth in meters):

$$ln(r_d) = \alpha(z) + \beta(z)\,M_w \tag{2.3}$$

where

$$\alpha(z) = -1.012 - 1.126\,sin\left(\frac{z}{11.7} + 5.133\right), \text{ and} \tag{2.4}$$

$$\beta(z) = 0.106 + 0.118\,sin\left(\frac{z}{11.3} + 5.142\right). \tag{2.5}$$

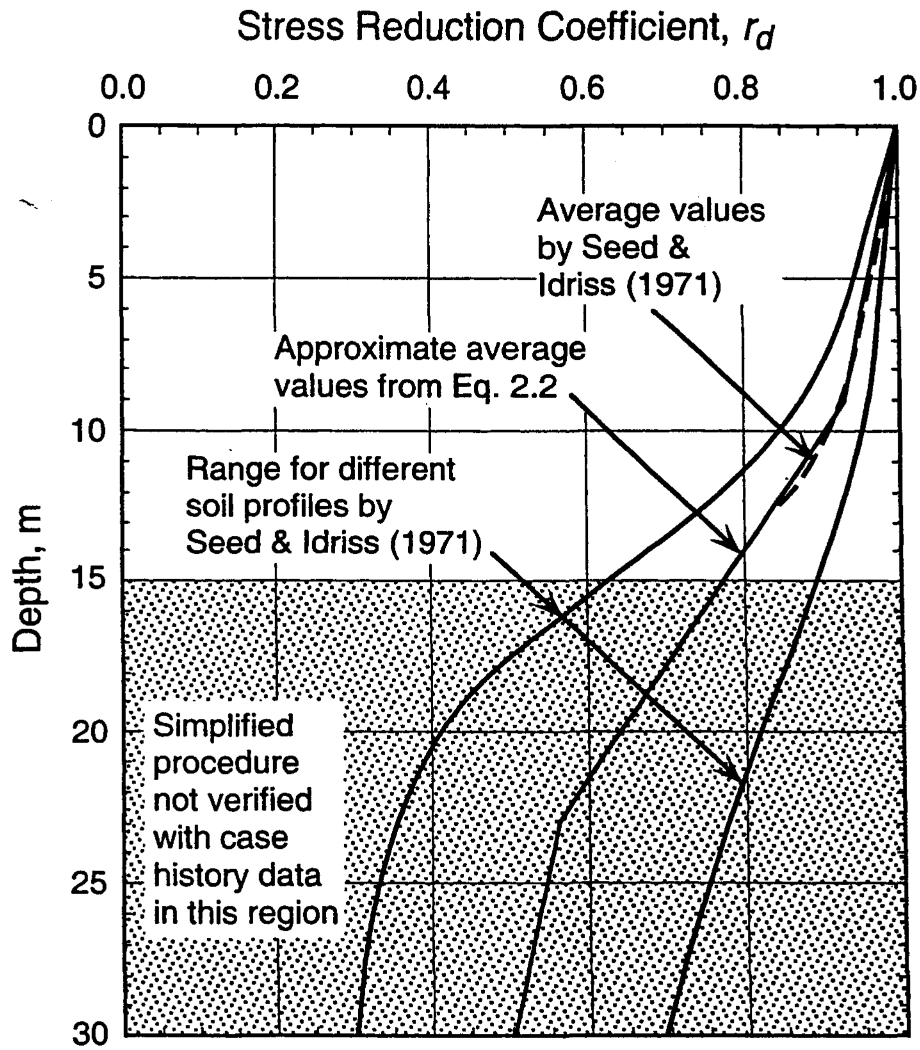

Fig. 2.1 - Relationship Between Stress Reduction Coefficient and Depth Developed by Seed and Idriss (1971) with Approximate Average Value Lines from Eq. 2.2. (after Youd et al., 1997)

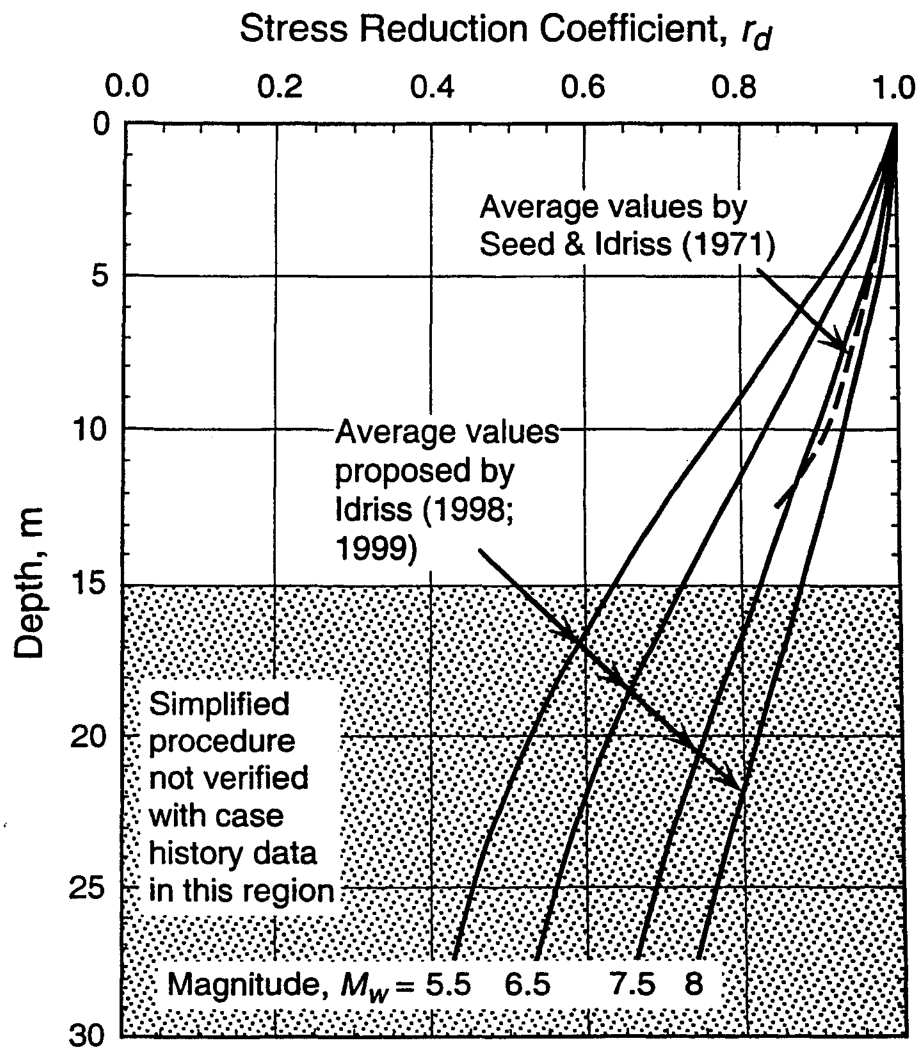

Fig. 2.2 - Relationship Between Average Stress Reduction Coefficient and Depth Proposed by Idriss (1998; 1999) with Average of Range Determined by Seed and Idriss (1971).

As shown in Fig. 2.2, the curve defined by Eq. 2.3 for M_w = 7.5 is almost identical to the average of the range published by Seed and Idriss (1971).

The scatter in the individual curves used to determine the average curves shown in Fig. 2.2, as well as Fig. 2.1, is rather large. For example, coefficients determined for a 30 m thick, loose sand deposit and magnitude 5.5 earthquakes exhibit standard deviations of about 0.1 at a depth of 5 m and 0.15 at a depth of 10 m. These standard deviation values would be larger if soil deposits of various thicknesses and stiffnesses are considered. Thus, as an alternative approach, the variation of r_d with depth may be calculated analytically using site-specific layer thicknesses and stiffnesses.

2.2 STRESS-CORRECTED SHEAR WAVE VELOCITY

The *in situ* V_S can be measured by several seismic tests including crosshole, downhole, seismic cone penetrometer (SCPT), suspension logger, and Spectral-Analysis-of-Surface-Waves (SASW). Recent reviews of these test methods are given in Woods (1994), Kramer (1996), and Ishihara (1996). ASTM D-4428M-91 provides a standard test method for crosshole seismic testing. Standard test methods do not exist for the other seismic tests. Primary advantages and disadvantages of the various *in situ* V_S test methods are presented in Table 2.1. The accuracy of each test method can be sensitive to equipment and procedural details, soil conditions, and interpretation techniques.

One important factor influencing V_S is the state of stress in soil (Hardin and Drnevich, 1972; Seed et al., 1986). Laboratory test results (Roesler, 1979; Stokoe et al., 1985; Belloti et al., 1996) show that the velocity of a propagating shear wave depends equally on principal stresses in the direction of wave propagation and the direction of particle motion. Thus, V_S measurements made with wave propagation or particle motion in the vertical direction can be related by the following empirical relationship:

$$V_S = A\ (\sigma'_v)^m\ (\sigma'_h)^m \tag{2.6}$$

where

A = a parameter that depends on the soil structure,
σ'_h = the initial effective horizontal stress at the depth in question, and
m = a stress exponent with a value of about 0.125.

Table 2.1 - Comparison of Advantages and Disadvantages of Various *In Situ* V_S Test Methods for Liquefaction Assessment.

Feature	Measurement Method				
	Crosshole	Downhole & Seismic Cone Penetrometer	Suspension Logger	Spectral-Analysis-of Surface-Waves	Surface Reflection/ Refraction
No. of boreholes (or soundings) required	2 or more	1	1	None	None
Quality control and repeatability[1]	Good	Good	Good	Good to fair; complex interpretation technique	Fair; often difficult to distinguish shear wave arrival
Resolution of soil stiffness variability[2]	Good; constant with depth	Good to fair; decreases with depth	Good at depth; poor close to the surface	Good to fair; decreases with depth; provides good global average	Fair to poor; provides coarse global average
Major component of particle motion or wave propagation in vertical direction	Yes, with vertically polarized shear waves	Yes, with test depth greater than distance between borehole and shear beam source	Yes	Yes, with vertical source	Yes, with horizontal source for reflection and vertical source for refraction
Limitations	Possible refraction problems; senses stiffer material at test depth; most expensive test method	Possible refraction problems with shallow layers; wave travel path increases with depth	Fluid-filled hole required; may not work in cased holes and soft soils; high test frequency (500 Hz-2000 Hz)	Horizontal layering assumed; poor resolution of thin layers and soft material adjacent to stiff layers; no samples recovered	In refraction test, only works for velocity increasing with depth; no samples recovered
Other	Most reliable test method	Penetration data also obtained from seismic cone; detailed layered profile with cone		Well-suited for tomo-graphic imaging large areas and testing difficult to penetrate soils	Well-suited for screening large areas

[1]Good quality depends on good equipment and procedural details, and good interpretation techniques for all methods.
[2]Resolution depends on test spacing for all methods.

Following the traditional procedures for correcting SPT blow count and CPT tip resistance, one can correct V_S to a reference overburden stress by (Sykora, 1987b; Robertson et al., 1992):

$$V_{S1} = V_S\, C_{VS} = V_S \left(\frac{P_a}{\sigma'_v} \right)^{0.25} \tag{2.7}$$

where

V_{S1} = the overburden stress-corrected shear wave velocity,
C_{VS} = a factor to correct measured shear wave velocity for overburden pressure;
P_a = a reference stress, 100 kPa or approximately atmospheric pressure, and
σ'_v = the initial effective overburden stress in kPa.

A maximum C_{VS} value of 1.4 is generally applied to V_S data at shallow depths, similar to the SPT and CPT procedures. In using Eq. (2.7), it is implicitly assumed that the initial effective horizontal stress, σ'_h, is a constant factor of the initial effective overburden stress (because both σ'_v and σ'_h affect V_S as shown in Eq. (2.6)). This factor, generally referred to as K'_o, is assumed to be approximately 0.5 at natural, level-ground sites where liquefaction has occurred or is likely to occur. Also, in applying Eq. (2.7), it is implicitly assumed that V_S is measured with both the directions of particle motion and wave propagation polarized along principal stress directions and one of those directions is vertical.

Since the direction of wave propagation and the direction of particle motion is different with respect to the stress in the soil for each *in situ* seismic test method, some variations between measured V_S is expected. These variations are minimized by performing the tests with at least a major component of wave propagation or particle motion in the vertical direction. To have a major component of wave propagation or particle motion in the vertical direction, crosshole tests are conducted with particle motion in the vertical direction, downhole and seismic cone tests are conducted at depths greater than the distance between the shear beam source and the borehole or cone sounding such that wave propagation is in the vertical direction, and SASW tests are conducted with a vertical source.

In soils above the ground water table, particularly silty soils, negative pore pressures increase the effective state of stress and, hence, the value of V_S measured in seismic tests. This effect should be considered in the estimation of σ'_v for correcting V_S to V_{S1}, and for computing *CSR* using Eq. (2.1).

2.3 CYCLIC RESISTANCE RATIO (*CRR*)

The value of *CSR* separating liquefaction and non-liquefaction occurrences for a given V_{S1}, or corrected penetration resistance, is called the cyclic resistance ratio, *CRR*. Figure 2.3 presents the *CRR*-V_{S1} curves developed by Andrus et al. (1999) for magnitude 7.5 earthquakes and uncemented, Holocene-age soils. The curves are dashed above *CRR* of about 0.35 to indicate that they are based on limited field performance data, as discussed in Appendix F. The curves do not extend much below 100 m/s, since there are no field data to support extending them to the origin. They are defined by:

$$CRR = MSF\left\{0.022\left(\frac{K_c V_{S1}}{100}\right)^2 + 2.8\left(\frac{1}{V^*_{S1} - K_c V_{S1}} - \frac{1}{V^*_{S1}}\right)\right\} \tag{2.8}$$

where

MSF = the magnitude scaling factor to account for the effect of earthquake magnitude,
V^*_{S1} = the limiting upper value of V_{S1} for cyclic liquefaction occurrence, and
K_c = a factor to correct for high V_{S1} values caused by cementation and aging.

The first (or squared) term in Eq. (2.8) is based on a relationship between *CRR* and V_{S1} for constant average cyclic strain derived by R. Dobry. The second term is a hyperbola with small value at low values of V_{S1}, and a very large value as V_{S1} approaches V^*_{S1}.

2.3.1 Magnitude Scaling Factor

The magnitude scaling factor is traditionally applied to *CRR*, rather than the cyclic loading parameter *CSR*, and equals 1 for earthquakes with a magnitude of 7.5. For magnitudes other than 7.5, Table 2.2 presents scaling factors developed by various investigators. These magnitude scaling factors were derived from laboratory test results and representative cycles of loading (Seed and Idriss, 1982; Idriss, personal communication to T. L. Youd, 1995; Idriss, 1998; Idriss, 1999), correlations of field performance data and blow count measurements (Ambrasey, 1988; Youd and Noble, 1997), estimates of seismic energy for laboratory and field data (Arango, 1996), and correlations of field performance data and *in situ* V_S measurements (Andrus and Stokoe, 1997). Figure 2.4 shows a plot of the various magnitude scaling factors along with the range recommended by the NCEER Workshop (Youd et al., 1997; 2001).

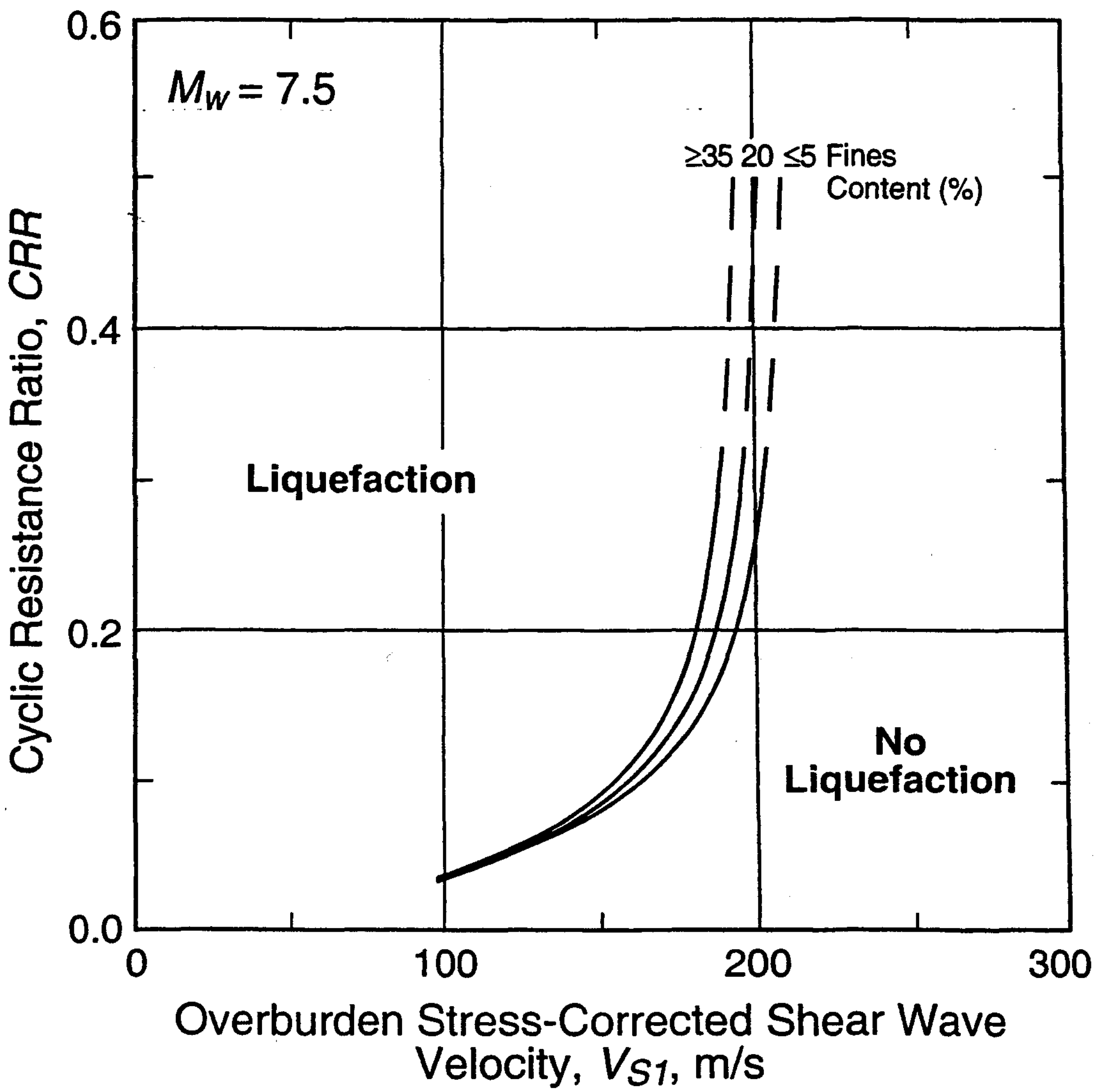

Fig. 2.3 - Curves Recommended for Calculation of *CRR* from V_{S1} (Andrus et al., 1999).

Table 2.2 - Magnitude Scaling Factors Obtained by Various Investigators. (modified from Youd and Noble, 1997)

Moment Magnitude, M_w	Magnitude Scaling Factor (MSF)										
	Seed & Idriss (1982)	Idriss (personal communication to T. L. Youd, 1995)	Idriss (1998)	Idriss (1999)	Ambraseys (1988)	Youd & Noble (1997) P_L, %			Arango (1996)**		Andrus & Stokoe (1997)
						< 20	< 30	< 50			
(1)	(2)	(3)	(4)	(5)	(6)	(7)	(8)	(9)	(10)	(11)	(12)
5.5	1.43	2.20	1.625	1.68	2.86	2.86	3.42	4.44	3.00	2.20	2.8*
6.0	1.32	1.76	1.48	1.48	2.20	1.93	2.35	2.92	2.00	1.65	2.1
6.5	1.19	1.44	1.28	1.30	1.69	1.34	1.66	1.99	1.60	1.40	1.6
7.0	1.08	1.19	1.12	1.14	1.30	1.00	1.20	1.39	1.25	1.10	1.25
7.5	**1.00**	**1.00**	**0.99**	**1.00**	**1.00**			**1.00**	**1.00**	**1.00**	**1.0**
8.0	0.94	0.84	0.88	0.87	0.67			0.73	0.75	0.85	0.8*
8.5	0.89	0.72	0.79	0.76	0.44			0.56			0.65*

*Extrapolated from scaling factors for M_w = 6, 6.5, 7, and 7.5 using $MSF = (M_w/7.5)^{-3.3}$.

**Based on equivalent uniform number of cycles and consideration of distant liquefaction sites (Column 10), and energy principles (Column 11).

Although the 1996 NCEER Workshop (Youd et al., 1997) recommended a range of magnitude scaling factors for engineering practice, a consensus has not yet been reached by the workshop participants. At the August 1998 MCEER Workshop, a revised set of magnitude scaling factors and stress reduction coefficients (see Section 2.1.3.2) were proposed by I. M. Idriss. Liao and Lum (1998) present results of a statistical analysis supporting the original Seed and Idriss (1982) factors. The magnitude scaling factors recommended by the 1996 NCEER Workshop and the revised factors proposed by Idriss (1999) are discussed below.

2.3.1.1 Factors Recommended by 1996 NCEER Workshop—The magnitude scaling factors recommended by the 1996 NCEER Workshop (Youd et al., 1997) can be represented by:

$$MSF = \left(\frac{M_w}{7.5}\right)^n \tag{2.9}$$

where

M_w = moment magnitude, and

n = an exponent.

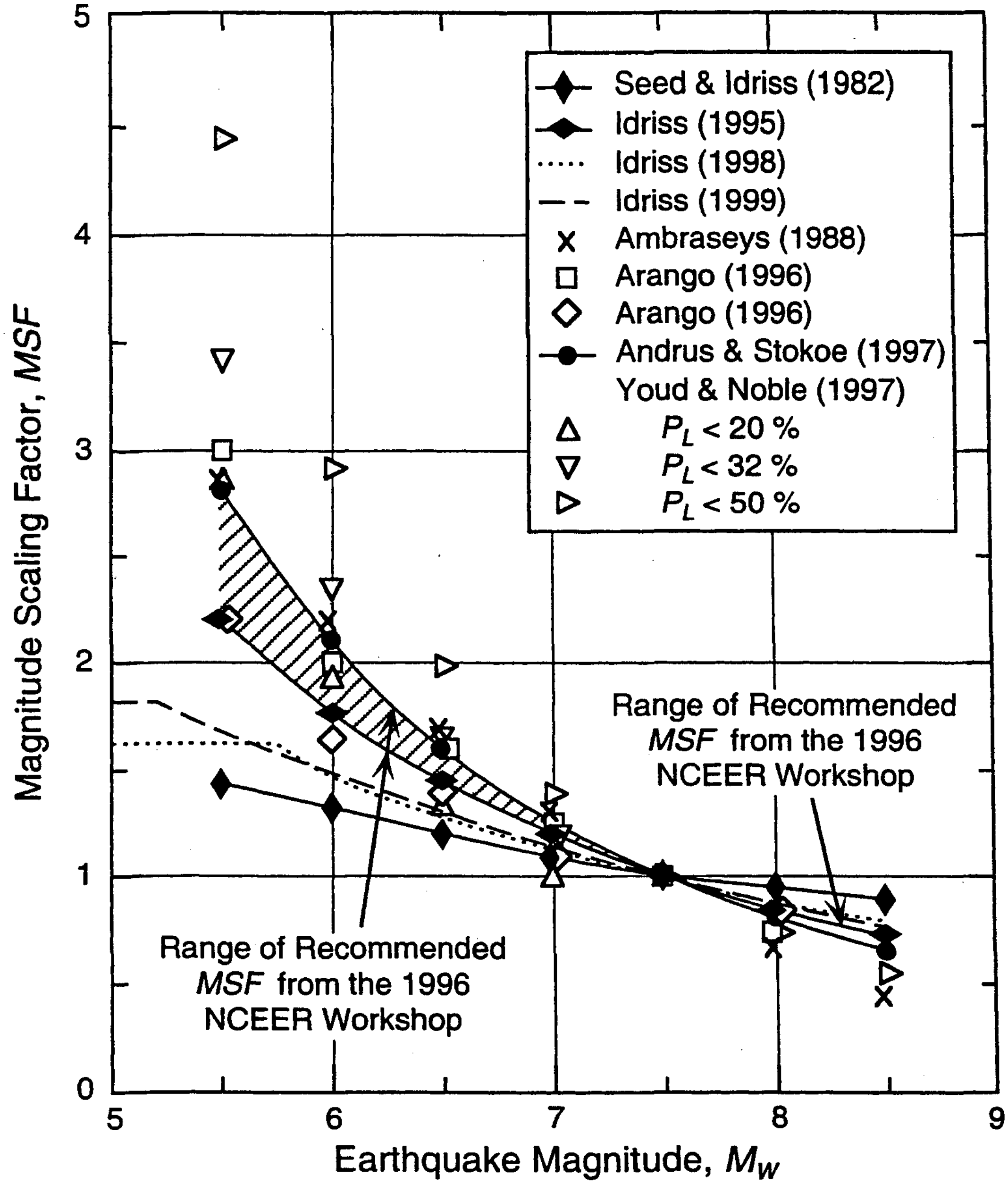

Fig. 2.4 - Magnitude Scaling Factors Derived by Various Investigators with Range Recommended by the 1996 NCEER Workshop (after Youd et al., 1997; Youd and Noble, 1997).

Moment magnitude is the scale most commonly used for engineering applications, and is preferred for liquefaction resistance calculations (Youd et al., 1997). When only other magnitude scales are available, they can be converted to M_w using the relationship of Heaton et al. (1982) shown in Fig. 2.5.

The lower bound for the range of magnitude scaling factors recommended by the 1996 NCEER Workshop is defined with n = -2.56 (Idriss, personal communication to T. L. Youd, 1995) for earthquakes with magnitudes ≤ 7.5. The upper bound of the recommended range is defined with n = -3.3 (Andrus and Stokoe, 1997) for earthquakes with magnitudes ≤ 7.5. For earthquakes with magnitudes > 7.5, the recommended factors are defined with n = -2.56. Magnitude scaling factors defined by Eq. (2.9) and average r_d values originally proposed by Seed and Idriss (1971) should be used together when applying Eqs. (2.1) and (2.8).

2.3.1.2 Revised Factors Proposed by Idriss (1999)—The magnitude scaling factors proposed by Idriss (1999) are derived using laboratory data from Yoshimi et al. (1984) and a revised relationship between representative cycles of loading and earthquake magnitude. They are defined by the following equation:

$$MSF = 6.9\exp\left(\frac{-M_w}{4}\right) - 0.06 \qquad \text{for } M_w > 5.2 \qquad (2.10a)$$

$$MSF = 1.82 \qquad \text{for } M_w \le 5.2 \qquad (2.10b)$$

where *exp* is the constant *e* raised to the power of the number given in the parentheses. Magnitude scaling factors defined by Eq. (2.10) and revised r_d proposed by Idriss (1999) should be used together when applying Eqs. (2.1) and (2.8).

2.3.1.3 Recommended Magnitude Scaling Factors—There is little difference in using magnitude scaling factors and r_d values recommended by the 1996 NCEER Workshop (Youd et al., 1997) and those proposed by Idriss (1999) for magnitudes near 7.5 and depths less than 11 m (see Appendix F, Sections F.2.2 and F.2.3). At magnitudes near 5.5, the difference is significant. The lower bound for the range of magnitude scaling factors defined by Eq. (2.9) with n = -2.56 is recommended in these guidelines because it provides more conservative assessment than with n = -3.3 for magnitudes less than 7.5. While the magnitude scaling factors defined by Eq. (2.9) with n = -2.56 are less conservative than the factors proposed by Idriss (1999) for magnitudes less than 7.5, the findings of Ambrasey (1988), I. M. Idriss (personal communication to T. L. Youd, 1995), Arango (1996), Youd and Noble (1997), and Andrus and Stokoe (1997; as indicated by the very conservative CRR-V_{S1} curves shown in Figs. F.13 and F.14) support their use.

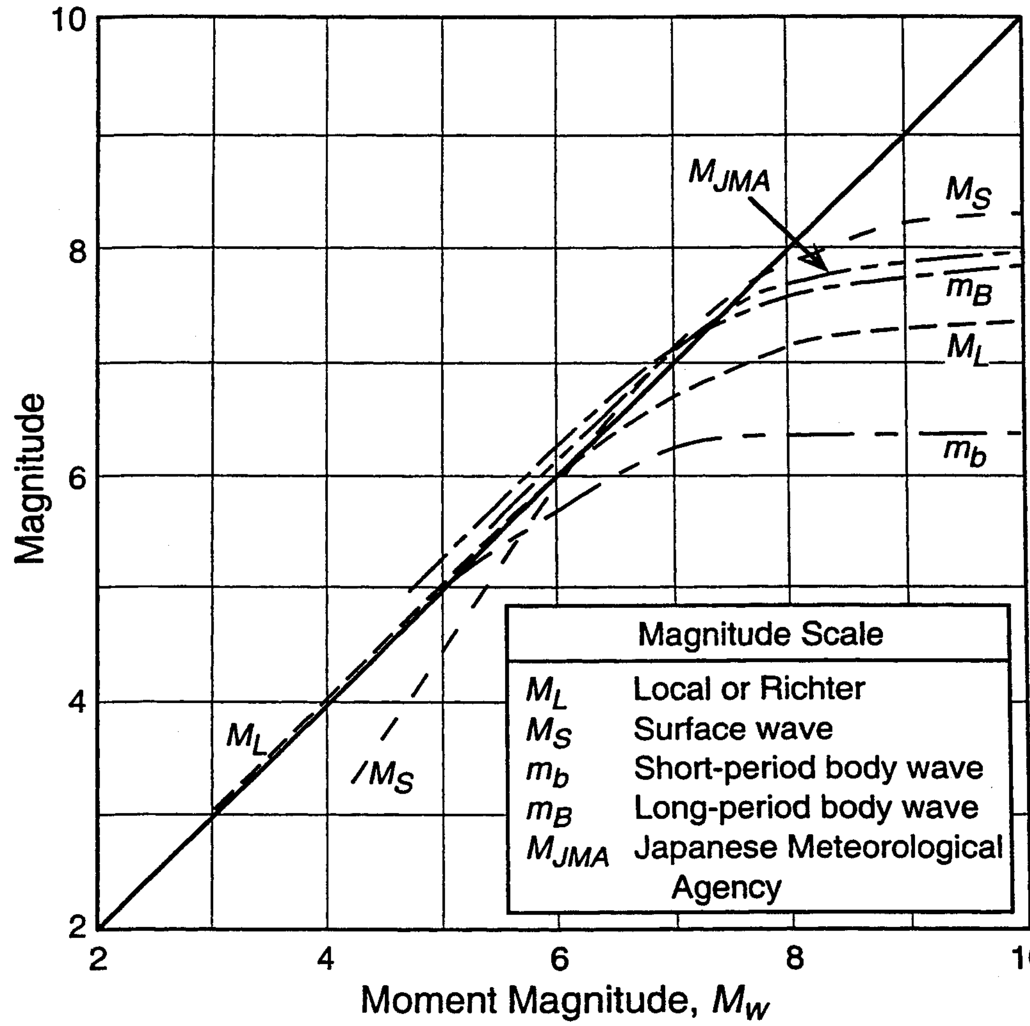

Fig. 2.5 - Relationship Between Moment Magnitude and Various Magnitude Scales (after Heaton et al., 1982).

2.3.2 Limiting Upper Value of V_{S1} in Sandy Soils

The assumption of a limiting upper value of V_{S1} is equivalent to the assumption commonly made in the SPT- and CPT-based procedures dealing with clean sands, where liquefaction is considered not possible above a corrected blow count of about 30 (Seed et al., 1985) and a corrected tip resistance of about 160 (Robertson and Wride, 1998). Upper limits for V_{S1} and penetration resistance are explained by the tendency of dense soils to exhibit dilative behavior at large strains, causing negative pore-water pressures. While it is possible in a dense soil to generate pore-water pressures close to the confining stress if large cyclic strains or many cycles are applied, the amount of water expelled during reconsolidation is dramatically less for dense soils than for loose soils. As explained by Dobry (1989), in dense soils, settlement is insignificant and no sand boils or failure take place because of the small amount of water expelled. This is important because the definition of liquefaction used to classify the field behavior here, as well as in the penetration-based procedures, is based on surface manifestations such as boils and ground cracks.

The case history data above a CSR value of about 0.35 are limited, as discussed in Appendix F. Thus, current estimates of V^*_{S1} rely, in part, on penetration-V_S correlations and, in part on the case histories. Values of V^*_{S1} can be estimated from:

$$V^*_{S1} = 215 \text{ m/s} \qquad \text{for sands with } FC \leq 5\ \% \qquad (2.11a)$$
$$V^*_{S1} = 215 - 0.5(FC-5) \text{ m/s} \qquad \text{for sands with } 5\ \% < FC < 35\ \% \qquad (2.11b)$$
$$V^*_{S1} = 200 \text{ m/s} \qquad \text{for sands and silts with } FC \geq 35\ \% \qquad (2.11c)$$

where

FC = average fines content in percent by mass.

Equations (2.8) and (2.11a) provide a CRR value of about 0.6 at $V_{S1} = 210$ m/s. A V_{S1} value of 210 m/s is considered equivalent to a corrected blow count of 30 in sands with $FC = 5$ %, based on penetration-V_S correlations.

2.3.3 Limiting Upper Value of V_{S1} in Gravelly Soils

Although the V^*_{S1} values given in Eq. (2.11) were determined for sandy soils, the case history data indicate that these limits also represent reasonable limits for gravelly soils divided into the same categories based on fines content (see Fig. F.7). This might be considered rather surprising based on the penetration-V_S correlations presented in the literature for gravelly soils. For instance, the correlation by Ohta and Goto (1978) suggested a V_{S1} value of 227 m/s for

Holocene gravels at an equivalent $(N_1)_{60}$ of 30. Similarly, the correlation by Rollins et al. (1998) provided a best-fit V_{S1} value of 232 m/s for Holocene gravels. On the other hand, all the liquefaction case history data exhibit V_{S1} values of about 200 m/s or less, suggesting that 230 m/s may be inappropriately high. To investigate further the value of V^*_{S1} in gravelly soils, laboratory studies involving V_S measurements in gravelly soils were reviewed. Kokusho et al. (1995) clearly showed that the shear wave velocity (or stiffness) of gravelly soils varies greatly and is highly dependent on the particle gradation. Weston (1996) showed similar results for coarse sands with gravels. In both cases, the results show that increasing the uniformity coefficient can significantly increase the shear wave velocity in medium dense to dense gravels. On the other hand, very loose gravelly soils, even well-graded gravels, can exhibit shear wave velocities similar to those of loose sands (Kokusho et al., 1995). The case history data presented in Fig. F.7 support the premise that gravelly soils that are loose enough to exhibit significant liquefaction effects (boils, ground cracks, etc.) have shear wave velocities similar to loose sands. Hence, the boundaries developed for sandy soils are recommended as preliminary boundaries for gravelly soils. However, additional work is clearly needed to understand the relationship between V_{S1} and liquefaction resistance of gravels.

2.3.4 Cementation and Aging Correction Factor

The recommended CRR-V_{S1} curves shown in Fig. 2.3 are limited to the characteristics of the database used to develop them. The database consists of relatively level ground sites with the following general characteristics: (1) uncemented soils of Holocene age; (2) average depths less than about 10 m; (3) ground water table depths between 0.5 m and 6 m, and (4) all V_S measurements are from below the water table. Correction factors may be used to extend the curves to site conditions different from the database.

The correction factor K_c is 1 for areas of uncemented, Holocene-age soils. For Pleistocene-age soils (>10 000 years), average estimates of K_c range from 0.6 to 0.8 based on the penetration-V_{S1} correlations by Rollins et al. (1998a) and Ohta and Goto (1978), respectively. Figures 2.6 and 2.7 illustrate two methods for estimating the value of K_c using SPT and CPT test results, respectively. Shown in the figures are correlations for clean sands and silty soils implied by the CRR-V_{S1} relationship defined by Eq. (2.8) and 1996 NCEER Workshop recommended CRR-penetration relationships (Youd et al., 1997). In the example, the measured values of V_{S1}, $(N_1)_{60}$, q_{c1N}, and fines content are 220 m/s, 8, 55, and 10 %, respectively. The V_{S1}-penetration correlations in Figs. 2.6 and 2.7 suggest a K_c value between 0.71 and 0.75, respectively, for these conditions. The K_c value is assumed to be the ratio of the predicted value of V_{S1}, based on the corrected penetration resistance and fines content, to the measured value of V_{S1}.

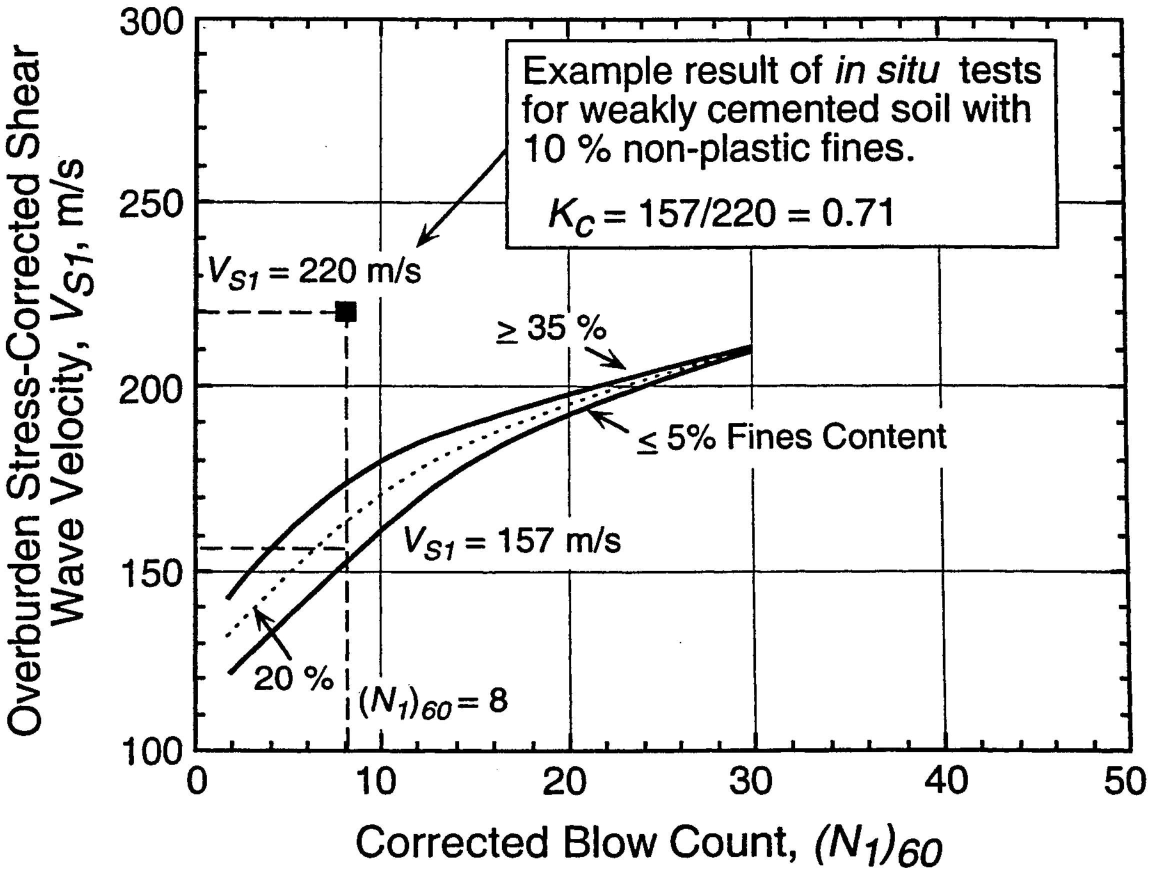

Fig. 2.6 - Suggested Method for Determining the Correction Factor K_C from $(N_1)_{60}$, V_{S1}, and Fines Content at a Weakly Cemented Soil Site.

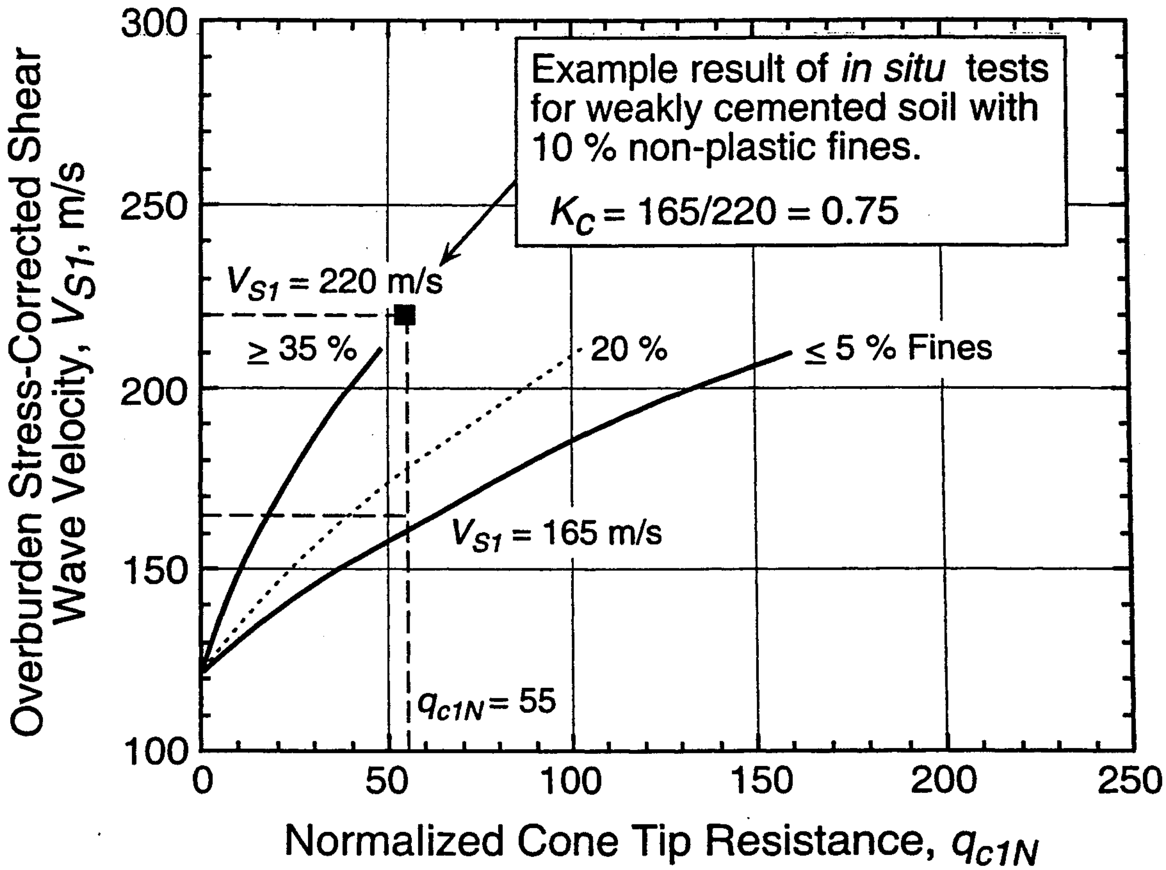

Fig. 2.7 - Suggested Method for Determining the Correction Factor K_c from q_{c1N}, V_{S1}, and Fines Content at a Weakly Cemented Soil Site.

The method for estimating K_c described above assumes that the strain level induced during penetration testing is the same strain level causing liquefaction, which may not be true because pore-water pressure buildup to liquefaction can occur at medium strains in several loading cycles (Dobry et al., 1982; Seed et al., 1983). The method also assumes that liquefaction potential, blow count, and cone penetration resistance are <u>not</u> affected by cementation, which may not be a reasonable assumption. Hence, this suggested method should be used cautiously and with engineering judgment.

2.4 FACTOR OF SAFETY

A common way to quantify the potential for liquefaction is in terms of a factor of safety. The factor of safety, F_S, against liquefaction can be defined by:

$$F_S = \frac{CRR}{CSR} \tag{2.12}$$

By convention, liquefaction is predicted to occur when $F_S \leq 1$. When $F_S > 1$, liquefaction is predicted not to occur.

As is the case with the SPT- and CPT-based charts, it is possible that liquefaction could occur outside the region of predicted liquefaction shown in Fig. 2.3. Consequently, the Building Seismic Safety Council (1997, page 158) suggests a factor of safety of 1.2 to 1.5 is appropriate when applying the Seed-Idriss simplified procedure in engineering design. The acceptable value of F_S for a particular site will depend on several factors, including the type and importance of structure and the potential for ground deformation. Based on V_S-SPT blow count correlations (see Section F.4) and probability studies (see Section G.2), the recommended V_S-based procedure is as conservative as the SPT-based procedure outlined by Seed et al. (1985) and updated by the NCEER Workshop (Youd et al., 2001). Thus, the same range of factor of safety is recommended for the V_S-based method.

2.5 PROBABILITY-BASED EVALUATION

Probability of liquefaction, P_L, is required information for making risk-based design decisions. As discussed in Appendix G, the relationship between P_L and F_S for the deterministic procedure described above can be expressed as (Juang et al., 2002; modified from Juang et al., 2001a):

$$P_L = \frac{1}{1+\left(\frac{F_S}{0.73}\right)^{3.4}} \tag{2.13}$$

In Eq. (2.13), a F_S value of 1 corresponds to points on the deterministic curves shown in Fig. 2.3. Thus, on average, the deterministic curves are characterized by a P_L value of 26 %. This average P_L value is similar to probability estimates determined for the SPT-based curves (Liao et al., 1988; Youd and Noble, 1997; Juang et al., 2000a). The relationship defined by Eq. (2.13) is plotted in Fig. 2.8, and provides the link between the probabilistic and deterministic methods. By combining Eqs. (2.8), (2.12) and (2.13), one can obtain a family of P_L curves for risk-based design. The family of P_L curves for magnitude 7.5 earthquakes and soils with $FC \leq 5$ % is presented in Fig. 2.9.

It is important to note that Figs. 2.8 and 2.9 are developed assuming F_S to be a fixed variable, and possible variations in *CRR* and *CSR* are not considered directly. Previous studies by Juang et al. (2000b) and Chen and Juang (2000) concluded that practically the same P_L-F_S relationship would be obtained even if the uncertainties in *CSR* and *CRR* were incorporated in the formulation for P_L. Thus, in general, if the variations of *CRR* and *CSR* are not too great, the figures can be used directly without considering the variations (Juang et al., 2001b).

2.6 SUMMARY

In this chapter, guidelines are presented for evaluating liquefaction resistance through V_S measurements using the procedure outlined in Andrus and Stokoe (2000). The procedure can be summarized in the following ten steps:

1. From available subsurface data, develop detailed profiles of V_S, soil type, fines content and, if possible, soil density and penetration resistance. Identify the depth of the ground water table, noting any seasonal fluctuations and artesian pressures.

2. Calculate the values of σ_v and σ'_v for each measurement depth at which seismic testing has been performed.

3. Correct the V_S measurements to the reference overburden stress of 100 kPa using Eq. (2.7). The correction factor C_{VS} is limited to a maximum value of 1.4 at shallow depths.

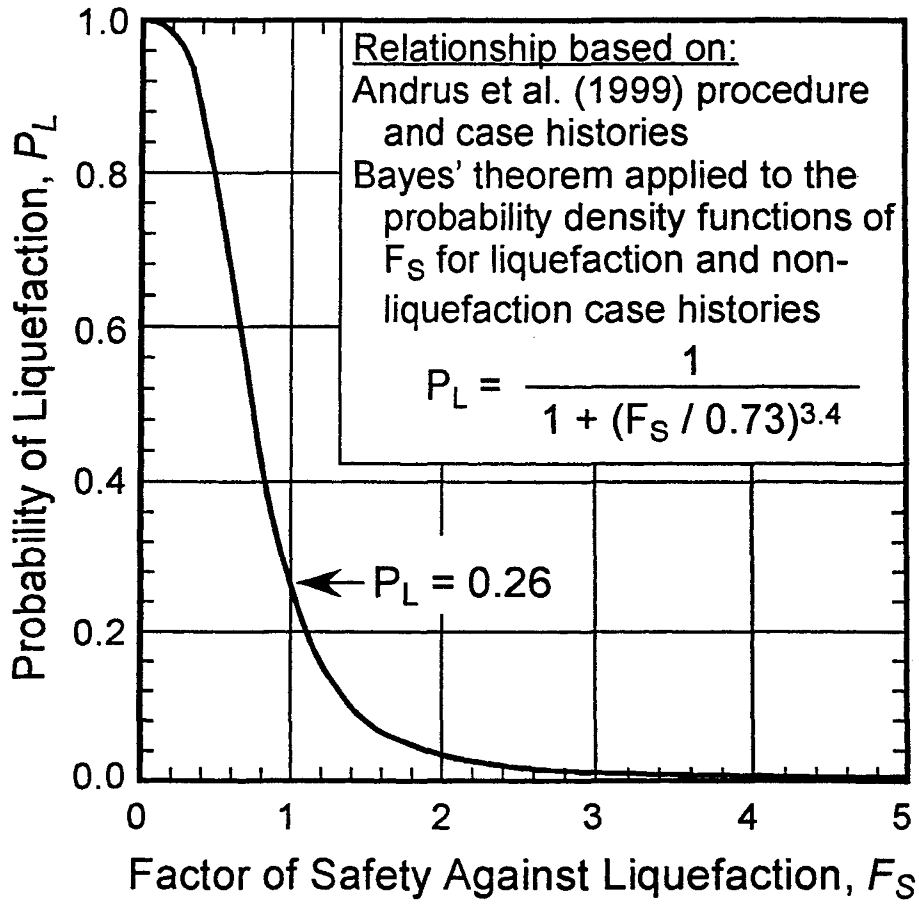

Fig. 2.8 - Suggested Relationship for Selecting F_S Based on Probability of Liquefaction and the Recommended CRR-V_{S1} Curves. (Juang et al., 2002)

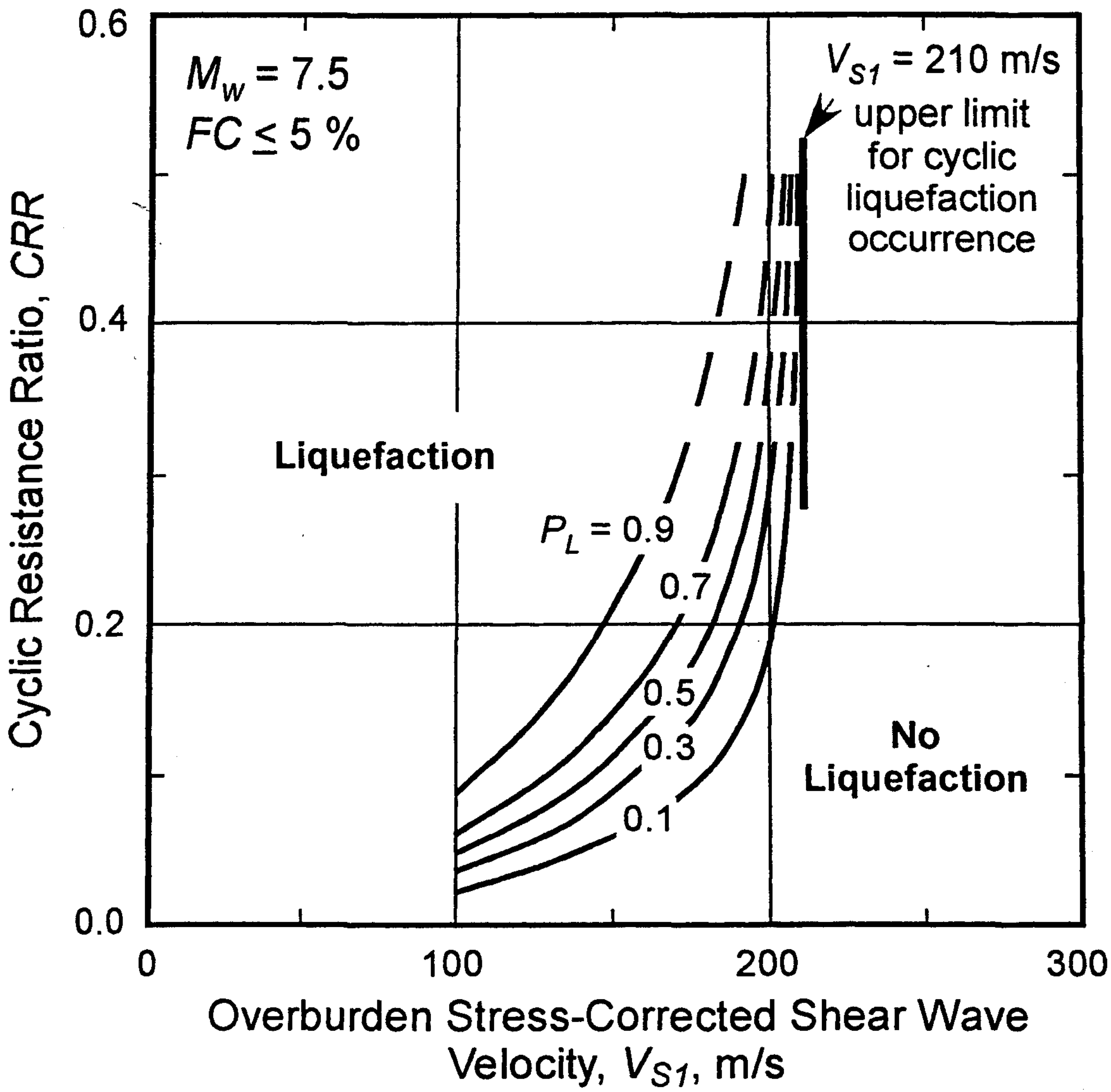

Fig. 2.9 - Curves Suggested for Probability-Based Evaluation in Clean Soils. Note that P_L = 0.26 Corresponds to the Recommended Deterministic Curve Shown in Fig. 2.3. (Juang et al., 2002)

4. Determine the value of V_{S1}^* for each measurement depth using Eq. (2.11) which is recommended for sandy as well as gravelly soils. If the fines content is unknown, assume 215 m/s for V_{S1}^*.

5. Determine the value of K_c. K_c can be assumed equal to 1, if the soil to be evaluated is uncemented and less than 10 000 years old. If the soil conditions are unknown and penetration data are not available, assume 0.6 for K_c.

6. Determine the design earthquake magnitude and expected value of a_{max}.

7. Calculate *CSR* for each measurement depth below the water table using Eq. (2.1). The value of r_d can be estimated from the average curve originally proposed by Seed and Idriss (1971).

8. Calculate *CRR* for each value of V_{S1} using Eqs. (2.8) and (2.9) with $n = -2.56$. It is important to note that Eq. (2.8) is for extreme behavior where boils and ground cracks occur.

9. Calculate the value of F_S for each value of V_{S1} using Eq. (2.12). By convention, liquefaction is predicted to occur when $F_S \leq 1$, and not to occur when $F_S > 1$.

10. Plot the values of V_{S1}, *CSR*, *CRR* and F_S to visually note how they vary with depth, and how many points fall in the regions of liquefaction and no liquefaction.

The deterministic V_S-based procedure outlined above is characterized with an average probability of liquefaction of 26 %. In other words, a soil with a calculated $F_S = 1$ has a 26 % chance of liquefaction occurrence based on the case histories analyzed in this study. As mentioned previously, the V_S-based procedure is as conservative as the SPT-based procedure by Seed et al. (1985). A factor of safety of 1.2 to 1.5, as suggested by the Building Seismic Safety Council (1997, page 158), is considered appropriate for design of typical buildings using the SPT- and V_S-based procedures. This range of factor of safety corresponds to a probability of liquefaction of about 8 % (for $F_S = 1.5$) to 16 % (for $F_S = 1.2$). The acceptable value of F_S for a particular site will depend on several factors, including the type and importance of structure and the potential for ground deformation. For critical structures, a smaller probability of liquefaction might be required. Equation (2.13) provides an important link between F_S and P_L, and is suggested for probability liquefaction evaluations.

CHAPTER 3

APPLICATION OF THE LIQUEFACTION EVALUATION PROCEDURE

To illustrate the application of the liquefaction evaluation procedure described in Chapter 2, two sites shaken by the 1989 Loma Prieta, California, earthquake ($M_w = 7$) are considered below. The two sites are Treasure Island Fire Station and Marina District Winfield Scott School.

3.1 TREASURE ISLAND FIRE STATION

Treasure Island is a man-made island located in the San Francisco Bay along the Bay Bridge between the cities of San Francisco and Oakland. It was constructed in 1936-37 by hydraulic filling behind a perimeter rock dike. The perimeter dike served to contain the hydraulic fill and was raised in sections over the previously placed fill. In 1991, Treasure Island was selected as a national geotechnical experimentation site. Much of the work to date at the Treasure Island national geotechnical experimentation site centers arounds a ground response experiment (de Alba and Faris, 1996) with six accelerometers and eight piezometers operating at various elevations near the fire station.

Extensive field tests have been conducted near the Treasure Island fire station to characterize ground conditions. Figures 3.1 and 3.2 present V_S and general soil profiles for the site. The V_S profile shown in Fig. 3.1(a) is from Fuhriman (1993), and was determined by crosshole testing. The V_S profile shown in Fig. 3.2(a) is based on unpublished SASW test results by The University of Texas at Austin in 1992. From the description by de Alba et al. (1994), the upper 4.5 m of soil consists of silty sand fill, possibly formed by dumping. Between depths of 4.5 m and 12.2 m, the soil consists of silty sand to clayey sand, formed by hydraulic filling. Beneath the hydraulic fill are natural clayey soils. The ground water table lies near the ground surface at a depth of 1.4 m.

During the 1989 Loma Prieta earthquake, a seismograph station at the fire station recorded ground surface accelerations. Unlike recordings at other seismograph stations located on soft-soils in the Bay area, there is a sudden drop in the recorded acceleration at about 15 seconds and small motion afterward (Idriss, 1990). De Alba et al. (1994) attribute this behavior to liquefaction of an underlying sand layer, although no sand boils or ground cracks occurred at the site. The nearest liquefaction effect observed is a sand boil located 100 m from the site (Geometric Consultants, 1990; Bennett, 1994; Power et al., 1998).

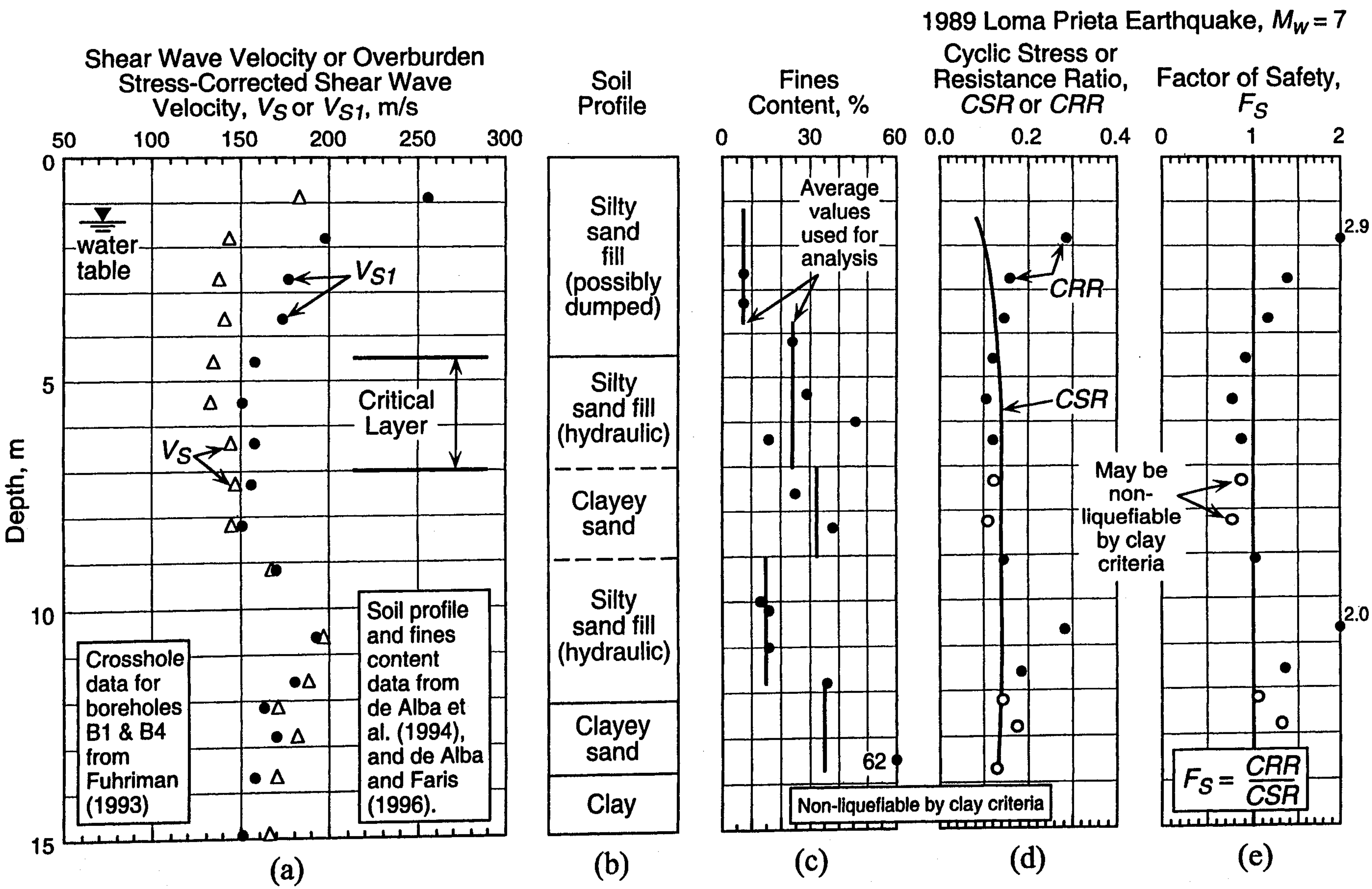

Fig. 3.1 - Application of the Recommended Procedure to the Treasure Island Fire Sation Site, Crosshole Test Array B1-B4 (Depth of 1.5 m to 14 m).

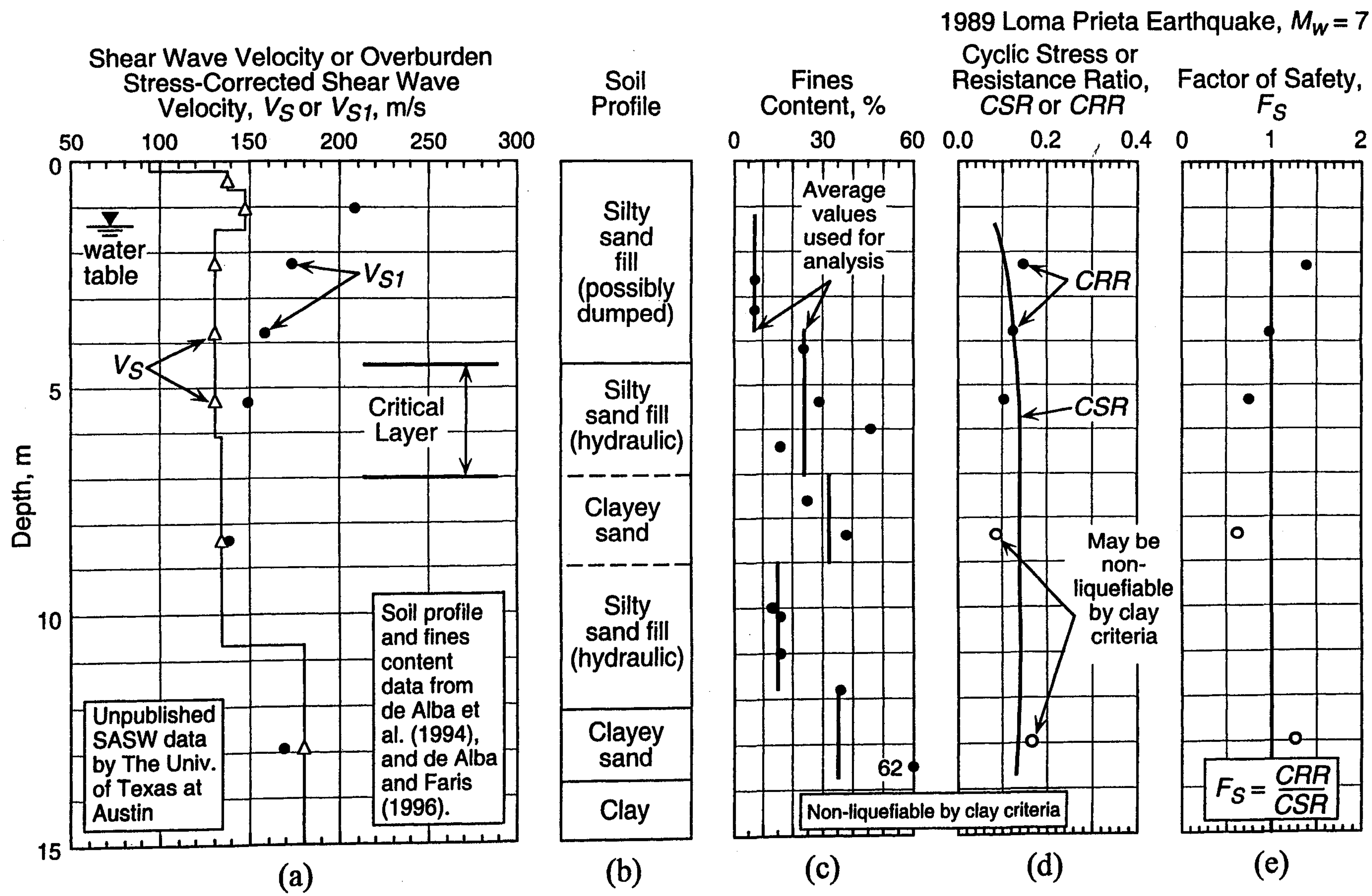

Fig. 3.2 - Application of the Recommended Procedure to the Treasure Island Fire Sation Site, SASW Test Array (Depths of 2 m to 13 m).

Figure 3.1 presents the liquefaction evaluation for the crosshole test array B1-B4 and the 1989 Loma Prieta earthquake. Values of V_{S1} and CSR shown in Figs. 3.1(a) and 3.1(d), respectively, are calculated assuming densities of 1.76 Mg/m^3 above the water table and 1.92 Mg/m^3 below the water table. Based on peak values of 0.16 g and 0.11 g recorded in two horizontal directions at the fire station during the 1989 earthquake (Brady and Shakal, 1994), a geometric mean value of 0.13 g is used to calculate CSR. Stress reduction coefficients are estimated using the average curve by Seed and Idriss (1971) shown in Fig. 2.1.

For the crosshole measurement at a depth of 4.6 m, values of CSR and V_{S1} are calculated as follows:

$$CSR \quad = 0.65\left(\frac{a_{max}}{g}\right)\left(\frac{\sigma_v}{\sigma'_v}\right)r_d = 0.65\left(\frac{0.13g}{g}\right)\left(\frac{84.0}{52.7}\right)0.97 = 0.131 \tag{3.1}$$

and

$$V_{S1} \quad = V_S\left(\frac{P_a}{\sigma'_v}\right)^{0.25} = 134\left(\frac{100}{52.7}\right)^{0.25} = 158 \text{ m/s} \tag{3.2}$$

Assuming an average fines content of 24 %, from Fig. 3.1(c), and a K_c value of 1, the values of V^*_{S1}, CRR, and F_S are calculated by:

$$V^*_{S1} \quad = 215 - 0.5(FC\text{-}5) = 215 - 0.5(24\text{-}5) = 206 \text{ m/s} \tag{3.3}$$

and

$$\begin{aligned} CRR \quad &= \left\{a\left(\frac{K_c V_{S1}}{100}\right)^2 + b\left(\frac{1}{V^*_{S1} - K_c V_{S1}} - \frac{1}{V^*_{S1}}\right)\right\} MSF \\ &= \left\{0.022\left(\frac{158}{100}\right)^2 + 2.8\left(\frac{1}{206-158} - \frac{1}{206}\right)\right\}\left(\frac{7}{7.5}\right)^{-2.56} \\ &= 0.119 \end{aligned} \tag{3.4}$$

and

$$F_S \quad = \frac{CRR}{CSR} = \frac{0.119}{0.131} = 0.91 \tag{3.5}$$

Since the value of F_S is less than 1, liquefaction is predicted at this depth.

Values of F_S shown in Fig. 3.1(e) are less than 1 for the depths of 4 m to about 9 m. Between the depths of 4 m and 7 m, the sand contains non-plastic fines and is considered liquefiable. Between the depths of 7 m and 9 m, the soil exhibits plastic characteristics and may be non-liquefiable by the simple clay criteria (see Section 1.1). Thus, the layer most likely to liquefy, or the critical layer, lies between the depths of 4 m and 7 m.

Figure 3.2 presents the liquefaction evaluation for the SASW test array. Locations of V_S measurements for the SASW test array are assumed at the center of the layer used in forward modeling of surface wave measurements. Values of F_S shown in Fig. 3.2(e) are less than 1 between the depths of about 3.5 m and 11 m. The lowest values of F_S in the non-plastic soil is 0.75 at a depth of 5.3 m. This F_S value is similar to the lowest F_S value of 0.77 determined from crosshole measurements in the critical layer.

Figures 3.3 and 3.4 present the liquefaction evaluations directly on the recommended liquefaction assessment chart for the crosshole test array and SASW test array, respectively. Plots of this type are particularly useful in comparing the range and distribution of V_{S1} and CSR values with the case histories used to develop the assessment chart. Based on Fig. F.15, the assessment chart is well supported within the range of the Treasure Island Fire Station data.

Although no sand boils or ground cracks occurred at the fire station during the 1989 earthquake, the prediction of liquefaction agrees with the conclusion stated above that liquefaction of an underlying sand cause the sudden drop in the acceleration time histories recorded at this site (de Alba et al., 1994). A similar sudden drop in the strong ground motion recordings occurred at the Port Island Downhole Array site in Kobe, Japan, during the 1995 Hyogo-ken Nanbu earthquake (Aguirre and Irikura, 1997), where liquefaction and sand boils did occur. It is possible that the 4 m thick layer capping the site, predicted not to liquefy, as shown in Figs. 3.1(e) and 3.2(e), prevented the formation of sand boils at the ground surface (Ishihara, 1985).

3.2 MARINA DISTRICT WINFIELD SCOTT SCHOOL

Kayen et al. (1990) conducted downhole seismic tests at the Winfield Scott School in the Marina District of San Francisco. Figures 3.5(a) and 3.5(b) present the V_S and soil profiles for the site. The V_S profile was originally determined based on best-fit line segments through travel time measurements plotted versus depth. However, the layering assumed in the best-fit segment method did not seem appropriate for the fill. Figures 3.5(a) presents the V_S profile for the site determined using the pseudo-interval method (see Appendix E). Figure 3.5(c) presents a profile of fines content that are based on information provided by Kayen et al. (1990). The upper 7.6 m of soil at the site consists of sand with 1 % to 8 % fines. The ground water table lies at a depth of 2.7 m.

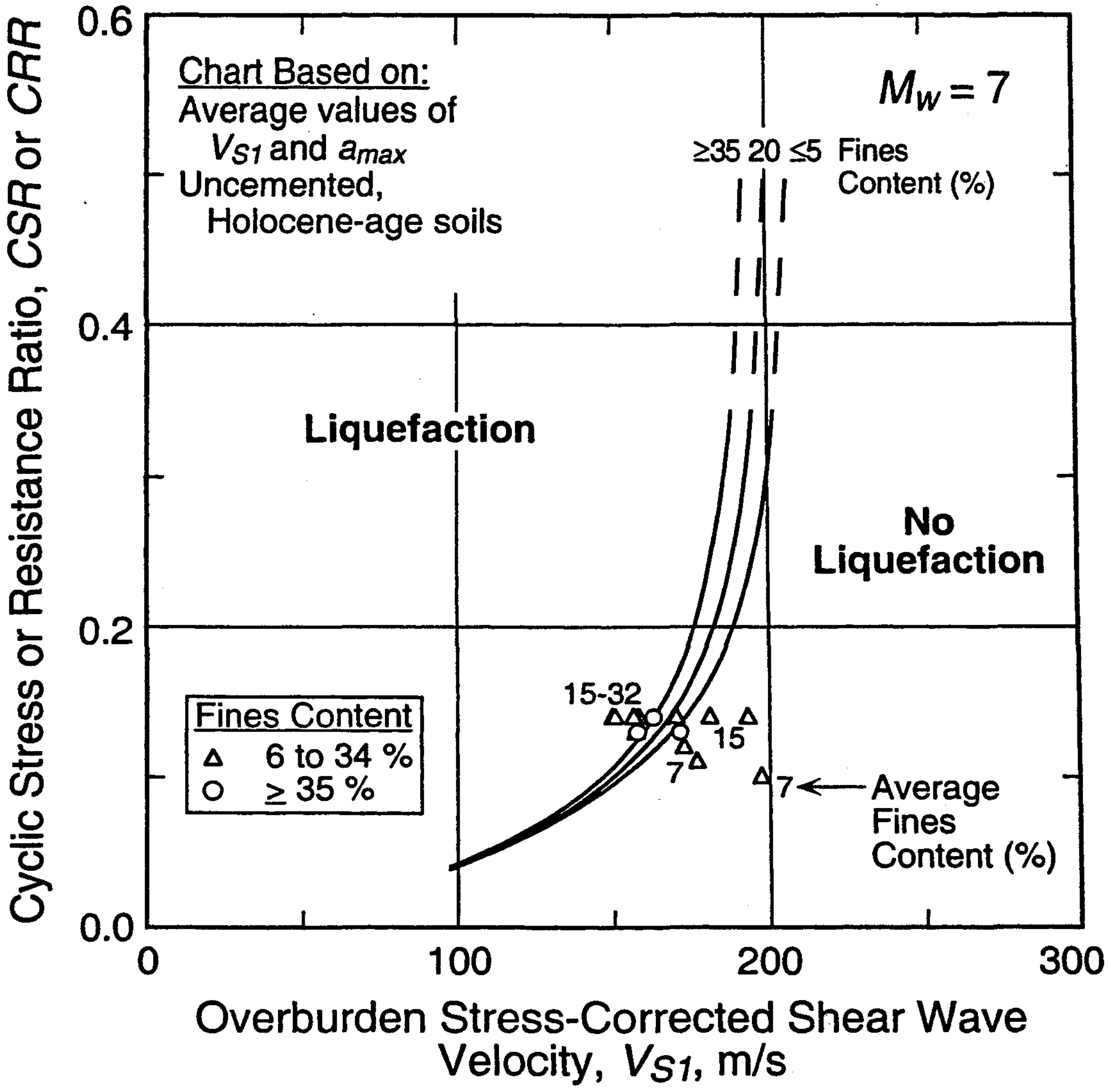

Fig. 3.3 - Liquefaction Assessment Chart for Magnitude 7 Earthquakes with Data for the 1989 Loma Prieta Earthquake and the Treasure Island Fire Station Site, Crosshole Test Array B1-B4 (Depths of 1.5 m to 14 m).

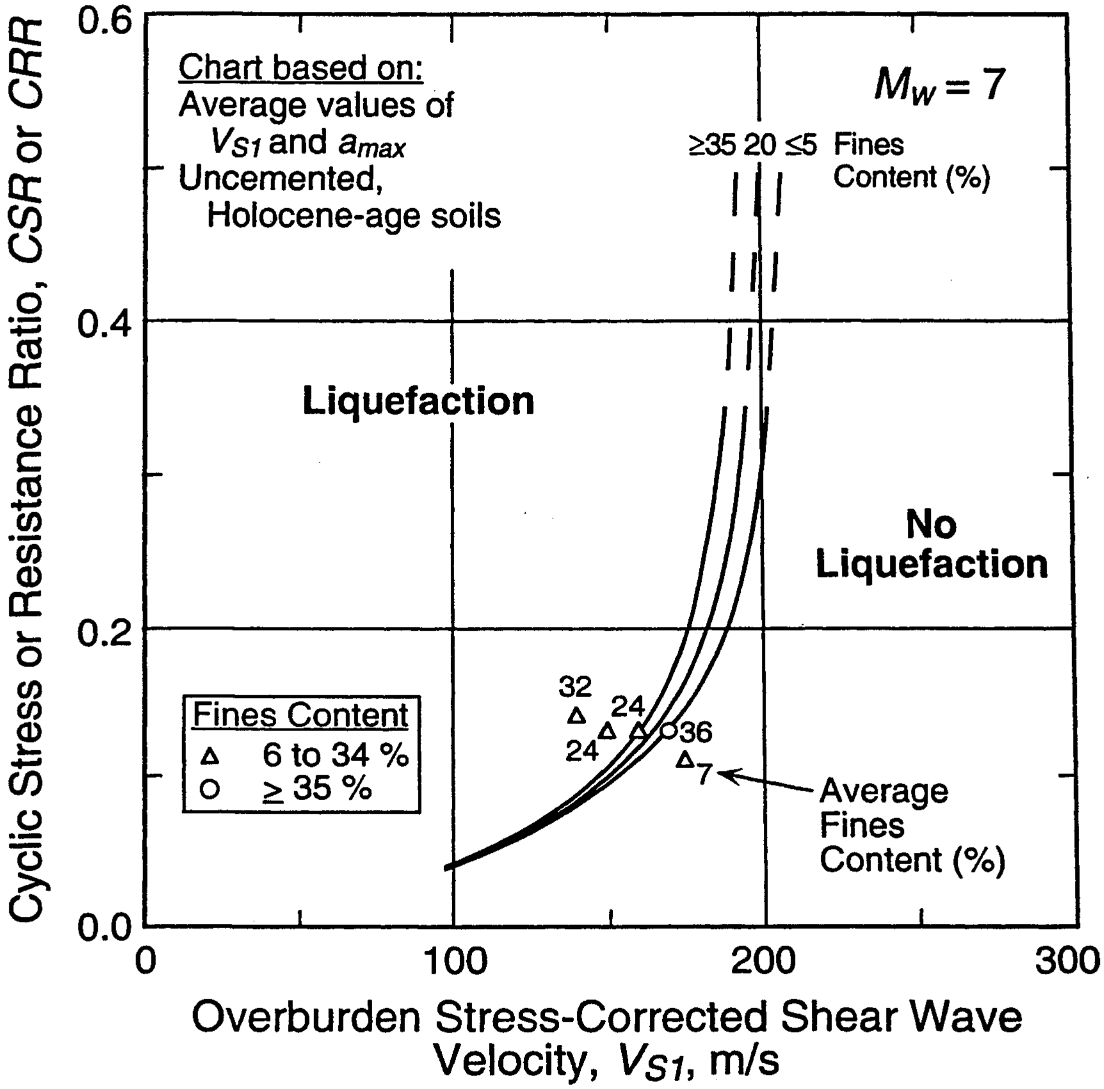

Fig. 3.4 - Liquefaction Assessment Chart for Magnitude 7 Earthquakes with Data for the 1989 Loma Prieta Earthquake and the Treasure Island Fire Station Site, SASW Test Array (Depths of 2 m to 13 m).

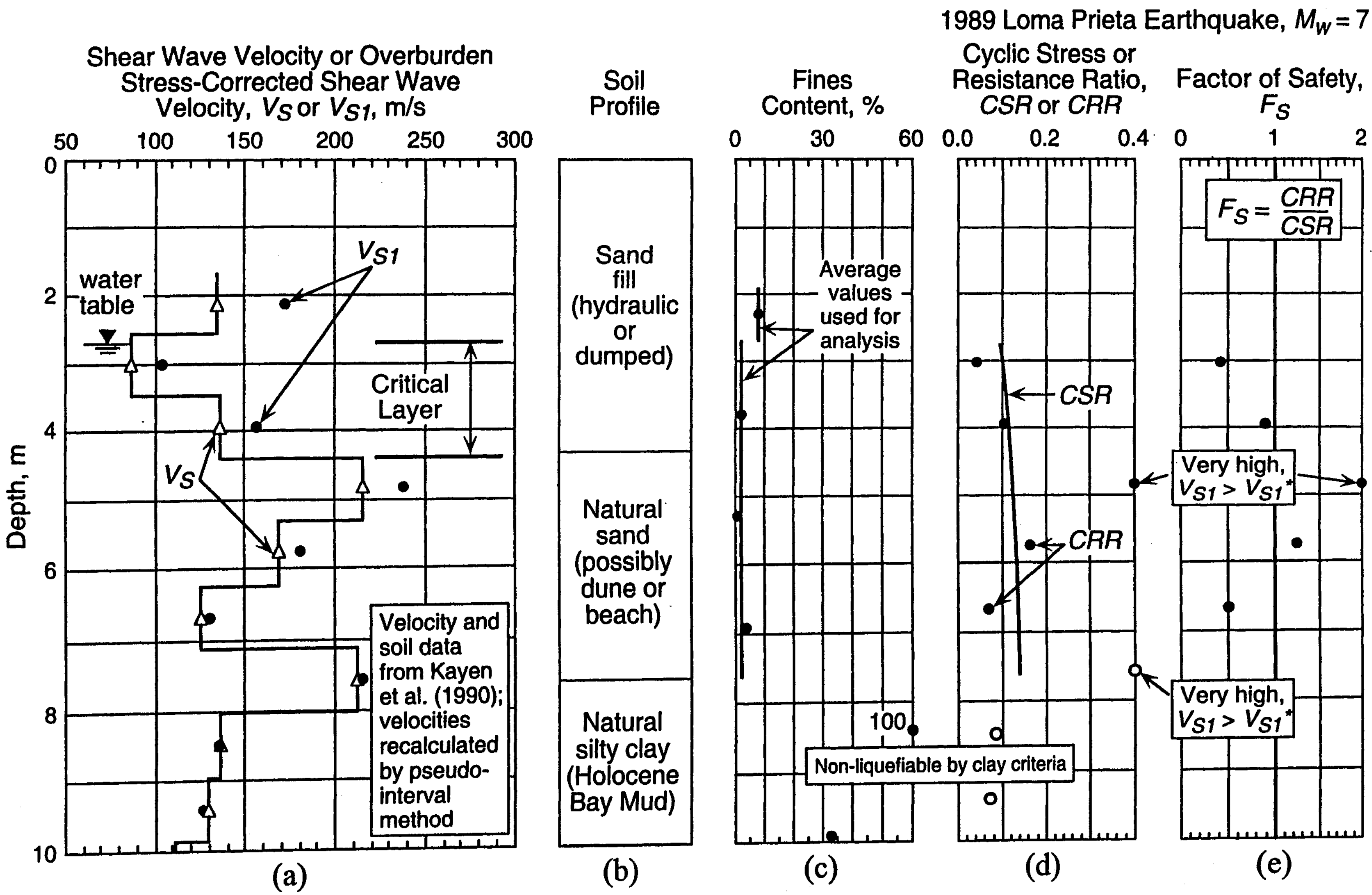

Fig. 3.5 - Application of the Recommended Procedure to the Marina District School Site (Depths of 3 m to 10 m).

Many structures, pavements, and public works near the school sustained heavy damage during the 1989 Loma Prieta earthquake (Kayen et al., 1990). This damage was due to liquefaction of the sand fill. From maps prepared by Pease and O'Rourke (1995), the site lies on the margin of the 1906 water front and artificial fill where about 40 mm of settlement occurred. Mapped sand boils and ground cracks lie just east of the site. Based on these observations, this site is classified as a liquefaction site during this earthquake.

The Marina District and Treasure Island are located about 82 km from the 1989 surface fault rupture. Assuming a distance of 82 km from the fault rupture, the attenuation relationship by Idriss (1991) for 1989 strong ground motion records from soft-soil sites provides a median value of 0.16 g. This value is slightly higher than the geometric mean value of 0.13 g for the two peak horizontal accelerations recorded at Treasure Island fire station. Thus, a peak horizontal ground surface acceleration of 0.15 g, the average of these two estimates, is assumed in the analysis.

Figure 3.5 presents the liquefaction evaluation for the Marina District School site and the 1989 Loma Prieta earthquake. Values of V_{S1} and CSR are calculated assuming densities of 1.76 Mg/m^3 above the water table and 1.92 Mg/m^3 below the water table. They are plotted in Fig. 3.5(a) and 3.5(d) at the depths midway between receiver locations. Since the sand is uncemented and less than 10 000 years old, the value of K_c is 1. Calculated values of F_S are 0.42, 0.90, and 0.51 at the depths of 3 m, 4 m, and 6.7 m within the sand fill. The silty clay layer beneath the sand fill is non-liquefiable by the simple clay criteria (see Section 1.1). Thus, having the lowest average value of F_S, the sand fill just below the water table between the depths of 2.7 m and 4.4 m is identified as the critical layer that liquefied. A prediction of liquefaction agrees with the observed field behavior.

Figure 3.6 present the liquefaction evaluation directly on the recommended liquefaction assessment chart for the Marina District. Based on Fig. F.15, the assessment chart is well supported within the range of the Marina District data.

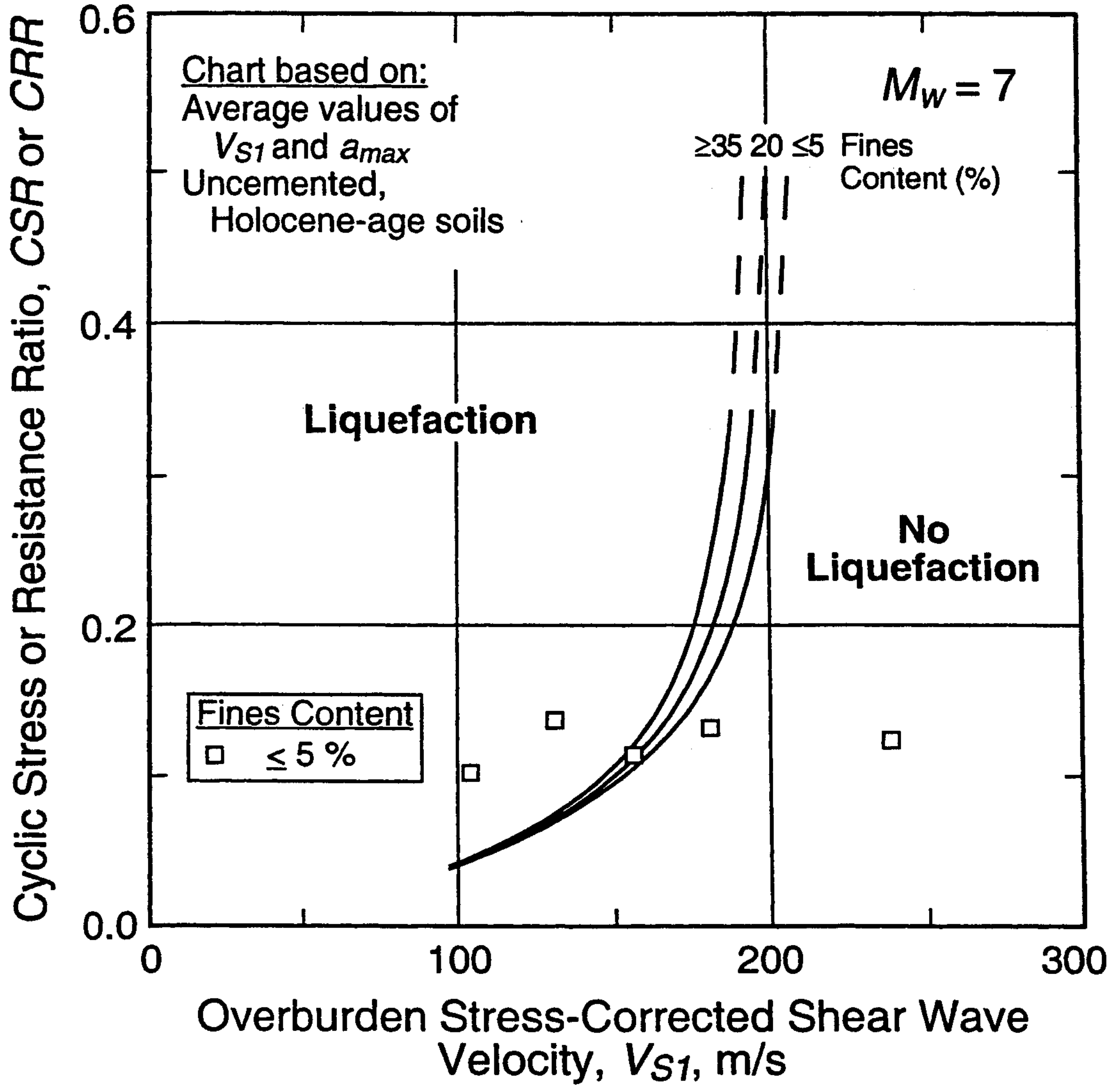

Fig. 3.6 - Liquefaction Assessment Chart for Magnitude 7 Earthquakes with Data for the 1989 Loma Prieta Earthquake and the Marina District School Site (Depths of 3 m to 7 m).

CHAPTER 4

SUMMARY AND RECOMMENDATIONS

4.1 SUMMARY

Presented in this report are guidelines for evaluating the liquefaction resistance of soils through shear wave velocity, V_S, measurements. The guidelines are based on an earlier report entitled "Draft Guidelines for Evaluating Liquefaction Resistance Using Shear Wave Velocity Measurements and Simplified Procedures." From comments received on the earlier report, the draft guidelines are updated in this report. The guidelines present a recommended procedure for evaluating soil liquefaction resistance and guidance for its use.

The recommended procedure follows the general format of the simplified penetration-based procedure originally proposed by Seed and Idriss (1971). Cyclic stress ratios, *CSR*, are calculated using Eq. (2.1), with the average stress reduction coefficient estimated from Fig. 2.1. Shear wave velocity measurements are corrected for overburden stress using Eq. (2.7). Figure 2.3 presents the recommended evaluation curves for uncemented, Holocene-age soils and magnitude 7.5 earthquakes. These curves are defined by Eq. (2.8) with $MSF = 1$, $V^*_{S1} = 200$ m/s to 215 m/s (depending on fines content), and $K_c = 1$. Equation (2.8) can be adjusted for other magnitude earthquakes using *MSF* values defined by Eq. (2.9) with $n = -2.56$. Corrections for cemented and aged soils are suggested in Section 2.3.4. A ten-step summary of the procedure is given in Section 2.6.

The recommended liquefaction evaluation curves, defined by Eq. (2.8), are based on a modified relationship between overburden stress-corrected shear wave velocity, V_{S1}, and *CSR* for constant average cyclic shear strain suggested by R. Dobry. As discussed in Section 2.3 and Appendix F, the quadratic relationship proposed by Dobry is modified so that it is asymptotic to some limiting upper value of V_{S1}. This limit is related to the tendency of dense granular soils to exhibit dilative behavior at large strains, as well as the fact that dense soils expel dramatically less water during reconsolidation than loose soils. Liquefaction and non-liquefaction case histories from 26 earthquakes and more than 70 measurement sites in soils ranging from clean fine sand to sandy gravel with cobbles to profiles including silty clay layers are analyzed to determine the parameters of Eq. (2.8). Penetration-V_S correlations are also considered. The evaluation curves correctly bound over 95 % of the case histories where liquefaction occurred.

By constructing relationships between V_{S1} and penetration resistance from the recommended evaluation curves and plotting available *in situ* test data, it is shown that the V_{S1}-based evaluation curves are generally more conservative than the penetration-based evaluation curves. From logistic regression and Bayesian interpretation techniques (see Appendix G), the recommended curve for clean soils is characterized with an average probability of 26 %.

Caution should be exercised when applying the procedure to sites where conditions are different from the case history data. The case history data used to develop the procedure are limited to relatively level ground sites with the following general characteristics: (1) uncemented soils of Holocene age; (2) average depths less than about 10 m; and (3) ground water table depths between 0.5 m and 6 m. All V_S measurements are from below the water table. About three-quarters of the case history data are for soils with fines content greater than 5 %. Almost half of the case histories are for earthquakes with magnitudes near 7.

Three concerns when using shear wave velocity as an indicator of liquefaction resistance are (1) its higher sensitivity (when compared with the penetration-based methods) to weak interparticle bonding, (2) the lack of a physical sample for identifying non-liquefiable clayey soils, and (3) not detecting thin liquefiable strata because the test interval is too large. The preferred practice is to drill sufficient boreholes and conduct sufficient other *in situ* tests to detect thin liquefiable strata, identify non-liquefiable clay-rich soils, identify silty soils above the ground water table that might have lower values of V_S should the water table rise, and detect liquefiable weakly cemented soils.

4.2 FUTURE STUDIES

The following future studies are recommended:

1. Additional well-documented case histories with all types of soil that have and have not liquefied during earthquakes should be compiled, particularly from deeper deposits (depth > 8 m) and from denser soils ($V_S > 200$ m/s) shaken by stronger ground motions ($a_{max} > 0.4$ g), to further validate the recommended curves. Also, case histories from lower magnitude earthquakes ($M_w < 7$) may improve estimates of the magnitude scaling factor.

2. Laboratory and field studies should be conducted to further refine estimates of V^*_{S1}, the limiting value of V_{S1} for cyclic liquefaction occurrence. For example, careful laboratory studies may identify more clearly the influence of fines content, gravel content, and particle gradation on V^*_{S1}. Additional careful penetration-V_S correlation studies may also help refine the V^*_{S1} estimates.

3. Laboratory studies should also be conducted to evaluate the implied assumption observed in Fig. 2.3 that at low values of V_{S1} (say 100 m/s) liquefaction resistance is independent of fines content.

4. Additional work is needed to evaluate the significance of ignoring soil type and horizontal stress in the overburden correction.

5. Standard test procedures exist only for the crosshole test. Standard test methods should be developed for the other *in situ* seismic tests.

APPENDIX A

REFERENCES

Abdel-Haq, A., and Hryciw, R. D. (1998). "Ground Settlement in Simi Valley Following the Northridge Earthquake," *Journal of Geotechnical and Geoenvironmental Engineering*, ASCE, Vol. 124, No. 1, pp. 80-89.

Aguirre, J., and Irikura, K. (1997). "Nonlinearity, Liquefaction, and Velocity Variation of Soft Soil Layers in Port Island, Kobe, During the Hyogo-ken Nanbu Earthquake," *Bulletin of the Seismological Society of America*, Vol. 85, No. 5, pp. 1244-1258.

Ambraseys, N. N. (1988). "Engineering Seismology," *Earthquake Engineering and Structural Dynamics*, Vol. 17, p. 1-105.

American Society of Testing and Materials, ASTM, D-4428M-91. "Standard Test Methods for Crosshole Seismic Testing," *Annual Book of ASTM Standards*, Vol. 4.08.

Andrews, D. C. A., and Martin, G. R. (2000). "Criteria for Liquefaction of Silty Soils," Proceedings, Twelfth World Conference on Earthquake Engineering, held January 29-February 5, Auckland, New Zealand.

Andrus, R. D. (1994). "In Situ Characterization of Gravelly Soils That Liquefied in the 1983 Borah Peak Earthquake," *Ph.D. Dissertation*, The University of Texas at Austin, 533 p.

Andrus, R. D., and Stokoe, K. H., II (1997). "Liquefaction Resistance Based on Shear Wave Velocity," *NCEER Workshop on Evaluation of Liquefaction Resistance of Soils*, Technical Report NCEER-97-0022, T. L. Youd and I. M. Idriss, Eds., held 4-5 January 1996, Salt Lake City, UT, National Center for Earthquake Engineering Research, Buffalo, NY, pp. 89-128.

Andrus, R. D., and Stokoe, K. H., II (2000). "Liquefaction Resistance of Soils from Shear Wave Velocity," *Journal of Geotechnical and Geoenvironmental Engineering*, ASCE, Vol. 126, No. 11, pp. 1015-1025.

Andrus, R. D., Stokoe, K. H., II, Bay, J. A., and Chung, R. M. (1998a). "Delineation of Densified Sand at Treasure Island by SASW Testing," *Geotechnical Site Characterization*, P. K. Robertson and P. W. Mayne, Eds., A. A. Balkema, Rotterdam, Netherlands, pp. 459-464.

Andrus, R. D., Stokoe, K. H., II, Chung, R. M., and Bay, J. A. (1998b). "Liquefaction Evaluation of Densified Sand at Approach to Pier 1 on Treasure Island, California, Using SASW Method," *NISTIR 6230*, Nat. Institute of Standards and Technology, Gaithersburg, MD, 75 p.

Andrus, R. D., Stokoe, K. H., II, Bay, J. A., and Youd, T. L. (1992). "In Situ V_S of Gravelly Soils Which Liquefied," *Proceedings, Tenth World Conference on Earthquake Engineering*, held 19-24 July 1992, Mardrid, Spain, A. A. Balkema, Rotterdam, Netherlands, pp. 1447-1452.

Andrus, R. D., Stokoe, K. H., II, and Chung, R. M. (1999). "Draft Guidelines for Evaluating Liquefaction Resistance Using Shear Wave Velocity Measurements and Simplified Procedures," *NISTIR 6277*, Nat. Institute of Standards and Technology, Gaithersburg, MD, 121 p.

Andrus, R. D., and Youd, T. L. (1987). "Subsurface Investigation of a Liquefaction-Induced Lateral Spread, Thousand Springs Valley, Idaho," *Geotechnical Laboratory Miscellaneous Paper GL-87-8*, U.S. Army Engineer Waterways Experiment Station, Vicksburg, MS, 131 p.

Arango, I. (1996). "Magnitude Scaling Factors for Soil Liquefaction Evaluations," *Journal of Geotechnical Engineering*, ASCE, Vol. 122, No. 11, pp. 929-936.

Arulanandan, K., Yogachandran, C., Meegoda, N. J., Ying, L., and Zhauji, S. (1986). "Comparison of the SPT, CPT, SV and Electrical Methods of Evaluating Earthquake Induced Liquefaction Susceptibility in Ying Kou City During the Haicheng Earthquake," *Use of In Situ Tests in Geotechnical Engineering*, Geotechnical Special Publication No. 6, S. P. Clemence, Ed., ASCE, pp. 389-415.

Barrow, B. L. (1983). "Field Investigation of Liquefaction Sites in Northern California," *Geotechnical Engineering Thesis GT83-1*, The University of Texas at Austin, 213 p.

Bennett, M. J., Youd, T. L., Harp, E. L., and Wieczorek, G. F. (1981). "Subsurface Investigation of Liquefaction, Imperial Valley Earthquake, California, October 15, 1979," *Open-File Report 81-502*, U.S. Geological Survey, Menlo Park, CA, 83 p.

Bennett, M. J., McLaughlin, P. V., Sarmiento, J. S., and Youd, T. L. (1984). "Geotechnical Investigation of Liquefaction Sites, Imperial Valley, California," *Open-File Report 84-252*, U.S. Geological Survey, Menlo Park, CA, 103 p.

Bennett, M. J., and Tinsley, J. C. (1995). "Geotechnical Data from Surface and Subsurface Samples Outside of and within Liquefaction-Related Ground Failures Caused by the October 17, 1989, Loma Prieta Earthquake, Santa Cruz and Monterey Counties, California," *Open-File Report 95-663*, U.S. Geological Survey, Menlo Park, CA.

Bierschwale, J. G., and Stokoe, K. H., II (1984). "Analytical Evaluation of Liquefaction Potential of Sands Subjected to the 1981 Westmorland Earthquake," *Geotechnical Engineering Report GR-84-15*, The University of Texas at Austin, 231 p.

Boulanger, R. W., Idriss, I. M., and Mejia, L. H. (1995). "Investigation and Evaluation of Liquefaction Related Ground Displacements at Moss Landing During the 1989 Loma Prieta Earthquake," *Report No. UCD/CGM-95/02*, University of California at Davis.

Boulanger, R. W., Mejia, L. H., and Idriss, I. M. (1997). "Liquefaction at Moss Landing During Loma Prieta Earthquake," *Journal of Geotechnical and Geoenviromental Engineering*, ASCE, Vol. 123, No. 5, pp. 453-467.

Brady, A. G., and Shakal, A. F. (1994). "Strong-Motion Recordings," *The Loma Prieta, California, Earthquake of October 17, 1989--Strong Ground Motion*, U.S. Geological Survey Professional Paper 1551-A, R. D. Borcherdt, Ed., U.S. Gov. Printing Office, Washington, D.C., pp. A9-A38.

Building Seismic Safety Council (1997). "NEHRP Recommended Provisions for Seismic Regulations for New Buildings and Other Structures, Part 2: Commentary," *FEMA 303*, Federal Emergency Management Agency, Washington, D.C.

Chen, C. J., and Juang, C. H. (2000). "Calibration of SPT- and CPT-based Liquefaction Evaluation Methods," *Innovations and Applications in Geotechnical Site Characterization*, Geotechnical Special Publication, No. 97, P. Mayne and R. Hryciw, eds., ASCE, pp. 49-64.

de Alba, P., Baldwin, K., Janoo, V., Roe, G., and Celikkol, B. (1984). "Elastic-Wave Velocities and Liquefaction Potential," *Geotechnical Testing Journal*, ASTM, Vol. 7, No. 2, pp. 77-87.

de Alba, P., Benoît, J., Pass, D. G., Carter, J. J., Youd, T. L., and Shakal, A. F. (1994). "Deep Instrumentation Array at the Treasure Island Naval Station," *The Loma Prieta, California, Earthquake of October 17, 1989--Strong Ground Motion*, U.S. Geological Survey Professional Paper 1551-A, R. D. Borcherdt, Ed., U.S. Gov. Printing Office, Washington, D.C., pp. A155-A168.

de Alba, P., and Faris, J. R. (1996). "Workshop on Future Research Deep Instrumentation Array, Treasure Island NGES, July 27, 1996: Report to the Workshop Current State of Site Characterization and Instrumentation," University of New Hampshire at Durham, 45 p.

Dobry, R. (1989). "Some Basic Aspects of Soil Liquefaction during Earthquakes," *Earthquake Hazards and the Design of Constructed Facilities in the Eastern United States*, K. H. Jacob and C. J. Turkstra, Eds., New York Academy of Sciences, Vol. 558, pp. 172-182.

Dobry, R., and Ladd, R. S. (1980). Discussion to "Soil Liquefaction and Cyclic Mobility Evaluation for Level Ground During Earthquakes," by. H. B. Seed and "Liquefaction Potential: Science versus Practice," by R. B. Peck, *Journal of the Geotechnical Engineering Division*, ASCE, Vol. 106, GT. 6, pp. 720-724.

Dobry, R., Ladd, R. S., Yokel, F. Y., Chung, R. M., Powell, D. (1982). "Prediction of Pore Water Pressure Buildup and Liquefaction of Sands During Earthquakes by the Cyclic Strain Method," *NBS Building Science Series 138*, National Bureau of Standards, Gaithersburg, MD, 152 p.

Dobry, R., Stokoe, K. H., II, Ladd, R. S., and Youd, T. L. (1981). "Liquefaction Susceptibility from S-Wave Velocity," *Proceedings, In Situ Tests to Evaluate Liquefaction Susceptibility*, ASCE National Convention, held 27 October 1981, St. Louis, MO.

Dobry, R., Baziar, M. H., O'Rourke, T. D., Roth, B. L., and Youd, T. L. (1992). "Liquefaction and Ground Failure in the Imperial Valley, Southern California During the 1979, 1981 and 1987 Earthquakes," *Case Studies of Liquefaction and Lifeline Performance During Past Earthquakes*, Technical Report NCEER-92-0002, T. O'Rourke and M. Hamada, Eds., National Center for Earthquake Engineering Research, Buffalo, NY, Vol. 2.

Drnevich, V. P., and Richart, F. E., Jr. (1970). "Dynamic Prestraining of Dry Sand," *Journal of the Soil Mechanics and Foundations Division*, ASCE, Vol. 96, No. SM2, pp. 453-469.

EPRI (1992). *Lotung Large-Scale Seismic Test Strong Motion Records*, EPRI NP-7496L, Electric Power Research Institute, Palo Alto, CA, Vols. 1-7.

Finn, W. D. L., and Bhatia, S. K. (1981). "Prediction of Seismic Pore-water Pressures," *Proceedings, Tenth International Conference on Soil Mechanics and Foundation Engineering*, Vol. 3, A. A. Balkema Publishers, Rotterdam, Netherlands, pp. 201-206.

Frankel, A. D., Mueller, C. S., Barnhard, T. P., Leyendecker, E. V., Wesson, R. L., Harmsen, S. C., Klein, F. W., Perkins, D. M., and Dickman, N. (2000). "USGS National Seismic Hazard Maps," *Earthquake Spectra*, EERI, Vol. 16, No. 1, pp. 1-19.

Fuhriman, M. D. (1993). "Crosshole Seismic Tests at Two Northern California Sites Affected by the 1989 Loma Prieta Earthquake," *M.S. Thesis*, The University of Texas at Austin, 516 p.

Geomatrix Consultants (1990). "Results of Field Exploration and Laboratory Testing Program for Perimeter Dike Stability Evaluation Naval Station Treasure Island San Francisco, California," Project No. 1539.05, report prepared for U.S. Navy, Naval Facilities Engineering Command, Western Division, San Bruno, CA, Vol. 2.

Gibbs, J. F., Fumal, T. E., Boore, D. M., and Joyner, W. B. (1992). "Seismic Velocities and Geologic Logs from Borehole Measurements at Seven Strong-Motion Stations that Recorded the Loma Prieta Earthquake," *Open-File Report 92-287*, U.S. Geological Survey, Menlo Park, CA, 139 p.

Golesorkhi, R. (1989). "Factors Influencing the Computational Determination of Earthquake-Induced Shear Stresses in Sandy Soils," *Ph.D. Dissertation*, University of California at Berkeley, 369 p.

Hanshin Expressway Public Corporation (1998). "The Hanshin Expressway Geological Database, Volume for Seismic Damage Reconstruction of Route No. 3, the Kobe Line, and Route No. 5, the Harbor Line," 224 p. (in Japanese).

Hamada, M., Isoyama, R., and Wakamatsu, K. (1995). *The 1995 Hyogoken-Nanbu (Kobe) Earthquake: Liquefaction, Ground Displacement and Soil Condition in Hanshin Area*, Waseda University, Tokyo, Japan, 194 p.

Harder, L. F., Jr., and Boulanger, R. (1997). "Application of $K_?$ and $K_?$ Correction Factors," *NCEER Workshop on Evaluation of Liquefaction Resistance of Soils*, Technical Report NCEER-97-0022, T. L. Youd and I. M. Idriss, Eds., held 4-5 January 1996, Salt Lake City, UT, National Center for Earthquake Engineering Research, Buffalo, NY, pp. 167-190.

Hardin, B. O., and Drnevich, V. P. (1972). "Shear Modulus and Damping in Soils: Design Equations and Curves," *Journal of the Soil Mechanics and Foundations Division*, ASCE, Vol. 98, SM7, pp. 667-692.

Heaton, T. H., Tajima, F., and Mori, A. W. (1982). "Estimating Ground Motions Using Recorded Accelerograms," Report by Dames and Moore to Exxon Production Res. Co., Houston Texas.

Holzer, T. L., Ed. (1998). "Map Showing Locations of Ground-Failures and Damage to Facilities on Treasure Island Attributed to the 1989 Loma Prieta Earthquake," *The Loma Prieta, California Earthquake of October 17, 1989--Liquefaction*, U.S. Geological Survey Professional Paper 1551-B, U.S. Gov. Printing Office, Washington, D.C., B1-B8.

Hryciw, R. D. (1991). "Post Loma Prieta Earthquake CPT, DMT and Shear Wave Velocity Investigations of Liquefaction Sites in Santa Cruz and on Treasure Island," Final Report to the U.S. Geological Survey, Award No. 14-08-0001-G1865, University of Michigan at Ann Arbor, 68 p.

Hryciw, R. D., Rollins, K. M., Homolka, M., Shewbridge, S. E., and McHood, M. (1991). "Soil Amplification at Treasure Island During the Loma Prieta Earthquake," *Proceedings, Second International Conference on Recent Advances in Geotechnical Earthquake Engineering and Soil Dynamics*, S. Prakash, Ed., held 11-15 March 1991, St. Louis, MO, University of Missouri at Rolla, Vol. II, pp. 1679-1685.

Hryciw, R. D., Shewbridge, S. E., Kropp, A., and Homolka, M. (1998). "Postearthquake Investigation at Liquefaction Sites in Santa Cruz and on Treasure Island," *The Loma Prieta, California Earthquake of October 17, 1989--Liquefaction*, U.S. Geological Survey Professional Paper 1551-B, T. L. Holzer, Ed., U.S. Gov. Printing Office, Washington, D.C., pp. B165-B180.

Hynes, M. E. (1988). "Pore Pressure Generation Characteristics of Gravel Under Undrainded Cyclic Loading," *Ph.D. Dissertation*, University of California, Berkeley.

Hynes, M. E., and Olsen, R. S. (1998). "Influence of Confining Stress on Liquefaction Resistance," *Proceedings, International Workshop on the Physics and Mechanics of Soil Liquefaction*, held 10-11 September 1998, Baltimore, MD, A. A. Balkema, Rotterdam, Netherlands.

Iai, S., Morita, T., Kameoka, T., Matsunaga, Y., and Abiko, K. (1995). "Response of a Dense Sand Deposit During 1993 Kushiro-Oki Earthquake," *Soils and Foundations*, Japanese Society of Soil Mechanics and Foundation Engineering, Vol. 35, No. 1, pp. 115-131.

Idriss, I. M. (1990). "Response of Soft Soil Sites During Earthquakes," *H. Bolton Seed Memorial Symposium*, BiTech Publishers, Vancouver, B.C., Vol. 2, pp. 273-289.

Idriss, I. M. (1991). "Earthquake Ground Motions at Soft Soil Sites," *Proceedings, Second International Conference on Recent Advances in Geotechnical Earthquake Engineering and Soil Dynamics*, S. Prakash, Ed., held 11-15 March 1991, St. Louis, MO, University of Missouri at Rolla, Vol. III, pp. 2265-2272.

Idriss, I. M. (1998). "Evaluation of Liquefaction Potential, Consequences and Mitigation--An Update," Presentation notes for Geotechnical Society Meeting, held 17 February 1998, Vancouver, Canada.

Idriss, I. M. (1999). "An Update of the Seed-Idriss Simplified Procedure for Evaluating Liquefaction Potential," Presentation notes for Transportation Research Board Workshop on New Approaches to Liquefaction Analysis, held 10 January 1999, Washington, D.C.

Inatomi, T., Zen, K., Toyama, S., Uwabe, T., Iai, S. Sugano, T., Terauchi, K., Yokota, H., Fujimoto, K., Tanaka, S., Yamazaki, H., Koizumi, T., Nagao, T., Nozu, A., Miyata, M., Ichii, K., Morita, T., Minami, K., Oikawa, K., Matsunaga, Y., Ishii, M., Sugiyama, M., Takasaki, N., Kobayashi, N., and Okashita, K. (1997). "Damage to Port and Port-related Facilities by the 1995 Hyogoken-Nanbu Earthquake," *Technical Note No. 857*, Port and Harbour Research Institute, Yokosuka, Japan, 1762 p.

Ishihara, K. (1985). "Stability of Natural Deposits During Earthquakes," *Proceedings, Eleventh International Conference on Soil Mechanics and Foundation Engineering*, A. A. Balkema Publishers, Rotterdam, Netherlands, pp. 321-376.

Ishihara, K., Shimizu, K., and Yamada, Y. (1981). "Pore Water Pressures Measured in Sand Deposits During an Earthquake," *Soils and Foundations*, Japanese Society of Soil Mechanics and Foundation Engineering, Vol. 21, No. 4, pp. 85-100.

Ishihara, K., Anazawa, Y., and Kuwano, J. (1987). "Pore Water Pressures and Ground Motions Monitored During the 1985 Chiba-Ibaragi Earthquake," *Soils and Foundations*, Japanese Society of Soil Mechanics and Foundation Engineering, Vol. 27, No. 3, pp. 13-30.

Ishihara, K., Muroi, T., and Towhata, I. (1989). "In-situ Pore Water Pressures and Ground Motions During the 1987 Chiba-Toho-Oki Earthquake," *Soils and Foundations*, Japanese Society of Soil Mechanics and Foundation Engineering, Vol. 29, No. 4, pp. 75-90.

Ishihara, K., Karube, T., and Goto, Y. (1997). "Summary of the Degree of Movement of Improved Masado Reclaimed Land," *Proceedings, 24th JSCE Earthquake Engineering Symposium*, Japan Society of Civil Engineering, held 24-26 July 1997, Kobe, Japan, Vol. 1, pp. 461-464 (in Japanese).

Ishihara, K., Kokusho, T., Yasuda, S., Goto, Y., Yoshida, N., Hatanaka, M., and Ito, K. (1998). "Dynamic Properties of Masado Fill in Kobe Port Island Improved through Soil Compaction Method," Summary of Final Report by Geotechnical Research Collaboration Committee on the Hanshin-Awaji Earthquake, Obayashi Corporation, Tokyo, Japan.

Jamiolkowski, M., and Lo Presti, D. C. F. (1990). "Correlation Between Liquefaction Resistance and Shear Wave Velocity," *Soils and Foundations*, Japanese Society of Soil Mechanics and Foundation Engineering, Vol. 32, No. 2, pp. 145-148.

Juang, C. H., and Chen, C. J. (2000). "A Rational Method for Development of Limit State for Liquefaction Evaluation Based on Shear Wave Velocity," *International Journal of Numerical and Analytical Methods in Geomechanics*, Vol. 24, pp. 1-27.

Juang, C. H., and Jiang, T. (2000). "Assessing Probability Methods for Liquefaction Potential Evaluation," *Soil Dynamics and Liquefaction, Geotechnical Special Publication*, ASCE, GeoDenver 2000 Conference, pp. 148-162.

Juang, C. H., Rosowsky, D. V., and Tang, W. H. (1999). "A Reliability-Based Method for Assessing Liquefaction Potential of Sandy Soils," *Journal of Geotechnical and Geoenvironmental Engineering*, ASCE, Vol. 125, No. 8, pp. 684-689.

Juang, C. H., Chen, C. J., Jiang, T., and Andrus, R. D. (2000a). "Risk-Based Liquefaction Potential Evaluation Using SPT," *Canadian Geotechnical Journal*, Vol. 37, No. 6, pp. 1195-1208.

Juang, C. H., Chen, C. J., Rosowsky, D. V., and Tang, W. H. (2000b). "CPT-based Liquefaction Analysis, Part II: Reliability for Design," *Géotechnique*, The Institution of Civil Engineers, Vol. 50, No. 5, pp. 593-599.

Juang, C. H., Andrus, R. D., Jiang, T., and Chen, C. J. (2001a). "Probability-Based Liquefaction Evaluation Using Shear Wave Velocity Measurements," *Proceedings, Fourth International Conference on Recent Advances in Geotechnical Earthquake Engineering and Soil Dynamics*, S. Prakash, Ed., held 26-31 March 2001, San Diego, Calif., University of Missouri at Rolla, Paper 4.25.

Juang, C. H., Jiang, T., Andrus, R. D. and Lee, D.-H. (2001b). "Assessing Probabilistic Methods for Liquefaction Potential Evaluation—An Update," *Proceedings, Fourth International Conference on Recent Advances in Geotechnical Earthquake Engineering and Soil Dynamics*, S. Prakash, Ed., held 26-31 March 2001, San Diego, Calif., University of Missouri at Rolla, Paper 4.23.

Juang, C. H., Jiang, T., and Andrus, R. D. (2002). "Assessing Probability-based Methods for Liquefaction Potential Evaluations," *Journal of Geotechnical and Geoenvironmental Engineering*, ASCE. (accepted for publication)

Kayabali, K. (1996). "Soil Liquefaction Evaluation Using Shear Wave Velocity," *Engineering Geology*, Elsevier Publisher, New York, NY, Vol. 44, No. 4, pp. 121-127.

Kayen, R. E., Liu, H. -P., Fumal, T. E., Westerland, R. E., Warrick, R. E., Gibbs, J. F., and Lee, H. J. (1990). "Engineering and Seismic Properties of the Soil Column at Winfield Scott School, San Francisco," *Effects of the Loma Prieta Earthquake on the Marina District San Francisco, California*, Open-file Report 90-253, U.S. Geological Survey, Menlo Park, CA, pp. 112-129.

Kayen, R. E., Mitchell, J. K., Seed, R. B., Lodge, A., Nishio, S., and Coutinho, R. (1992). "Evaluation of SPT-, CPT-, and Shear Wave-Based Methods for Liquefaction Potential Assessment Using Loma Prieta Data," *Proceedings, Fourth Japan-U.S. Workshop on Earthquake Resistant Design of Lifeline Facilities and Countermeasures for Soil Liquefaction*, Technical Report NCEER-92-0019, M. Hamada and T. D. O'Rourke, Eds., held 27-29 May 1992, Honolulu, Hawaii, National Center for Earthquake Engineering Research, Buffalo, NY, Vol. 1, pp. 177-204.

Kimura, M. (1996). "Damage Statistics," *Soils and Foundations, Special Issue on Geotechnical Aspects of the January 17, 1995 Hyogoken-Nambu Earthquake*, Japanese Geotechnical Society, pp. 1-5.

Kokusho, T., Tanaka, Y., Kudo, K., and Kawai, T. (1995a). "Liquefaction Case Study of Volcanic Gravel Layer during 1993 Hokkaido-Nansei-Oki Earthquake," *Third International Conference on Recent Advances in Geotechnical Earthquake Engineering and Soil Dynamics*, S. Prakash, Ed., held 2-7 March 1995, St. Louis, MO, University of Missouri at Rolla, Vol. I, pp. 235-242.

Kokusho, T., Yoshida, Y., and Tanaka, Y. (1995b). "Shear Wave Velocity in Gravelly Soils with Different Particle Gradings," *Static and Dynamic Properties of Gravelly Soils*, Geotechnical Special Publication No. 56, M. D. Evans and R. J. Fragaszy, Eds., ASCE, pp. 92-106.

Kokusho, T., Tanaka, Y., Kawai, T., Kudo, K., Suzuki, K., Tohda, S., and Abe, S. (1995c). "Case Study of Rock Debris Avalanche Gravel Liquefied During 1993 Hokkaido-Nansei-Oki Earthquake," *Soils and Foundations*, Japanese Geotechnical, Vol. 35, No. 3, pp. 83-95.

Lee, N. J. (1993). "Experimental Study of Body Wave Velocities in Sand Under Anisotripic Conditions," *Ph.D. Dissertation*, The University of Texas at Austin, 503 p.

Lee, S. H. (1986). "Investigation of Low-Amplitude Shear Wave Velocity in Anisotripic Material," *Ph.D. Dissertation*, The University of Texas at Austin, 395 p.

Liao, S. S. C., and Lum, K. Y. (1998). "Statisitical Analysis and Application of the Magnitude Scaling Factor in Liquefaction Analysis," *Geotechnical Earthquake Engineering and Soil Dynamics III*, Geotechnical Special Publication No. 75, P. Dakoulas, M. Yegian, and R. D. Holtz, eds., ASCE, Vol. 1, pp. 410-421.

Liao, S. S. C., and Whitman, R. V. (1986). "Overburden Correction Factors for SPT in Sands," *Journal of Geotechnical Engineering*, ASCE, Vol. 112, No. 3, pp. 373-377.

Liao, S. S., C., Veneziano, D., and Whitman, R. V. (1988). "Regression Models for Evaluating Liquefaction Probability," *Journal of Geotechnical Engineering*, ASCE, Vol. 114, No. 4, pp. 389-411.

Lodge, A. L. (1994). "Shear Wave Velocity Measurements for Subsurface Characterization," *Ph.D. Dissertation*, University of California at Berkeley.

Marcuson, W. F., III, and Bieganousky, W. A. (1977). "SPT and Relative Density in Coarse Sands," *Journal of Geotechnical Engineering Division*, ASCE, Vol. 103, No. 11, pp. 1295-1309.

Martin, G. R., Finn, W. D. L., and Seed, H. B. (1975). "Fundamentals of Liquefaction Under Cyclic Loading," *Journal of the Geotechnical Engineering Division*, ASCE, Vol. 101, No. GT5, pp. 423-483.

Mitchell, J. K., Lodge, A. L., Coutinho, R. Q., Kayen, R. E., Seed, R. B., Nishio, S., and Stokoe, K. H., II (1994). "Insitu Test Results from Four Loma Prieta Earthquake Liquefaction Sites: SPT, CPT, DMT, and Shear Wave Velocity," *Report No. UCB/EERC-94/04*, Earthquake Engineering Research Center, University of California at Berkeley, 171 p.

National Research Council (1985). *Liquefaction of Soils During Earthquakes*, National Academy Press, Washington, D. C., 240 p.

Ohta, Y., and Goto, N. (1978). "Physical Background of the Statistically Obtained S-Wave Velocity Equation in Terms of Soil Indexes," *Butsuri-Tanko (Geophysical Exploration)*, Vol. 31, No. 1, pp. 8-17 (in Japanese; translated by Y. Yamamoto).

Olsen, R. S. (1997). "Cyclic Liquefaction Based on the Cone Penetrometer Test," *NCEER Workshop on Evaluation of Liquefaction Resistance of Soils*, Technical Report NCEER-97-0022, T. L. Youd and I. M. Idriss, Eds., held 4-5 January 1996, Salt Lake City, UT, National Center for Earthquake Engineering Research, Buffalo, NY, pp. 225-276.

Park, T., and Silver, M. L. (1975). "Dynamic Soil Properties Required to Predict the Dynamic Behavior of Elevated Transportation Structures," *Report DOT-TST-75-44*, U.S. Department of Transportation, Washington, D.C.

Pease, J. W., and O'Rourke, T. D. (1995). "Liquefaction Hazards in the San Francisco Bay Region: Site Investigation, Modeling, and Hazard Assessment at Areas Most Seriously Affected by the 1989 Loma Prieta Earthquake," Report to the U.S. Geological Survey, Cornell University, Ithaca, NY, 176 p.

Pillai, V. S., and Byrne, P. M. (1994). "Effect of Overburden Pressure on Liquefaction Resistance of Sand," *Canadian Geotechnical Journal*, Vol. 31, pp. 53-60.

Power, M. S., Egan, J. A., Shewbridge, S. E., deBecker, J., and Faris, J. R. (1998). "Analysis of Liquefaction-Induced Damage on Treasure Island," *The Loma Prieta, California Earthquake of*

October 17, 1989--Liquefaction, U.S. Geological Survey Professional Paper 1551-B, T. L. Holzer, Ed., U.S. Gov. Printing Office, Washington, D.C., pp. B87-B119.

Poulos, S. J., Castro, G., and France, J. W. (1985). "Liquefaction Evaluation Procedure," *Journal of Geotechnical Engineering*, ASCE, Vol. 111, No. 6, pp. 772-792.

Pyke, R. M., Seed, H. B., and Chan, C. K. (1975). "Settlement of Sands Under Multi-Directional Shaking," *Journal of the Geotechnical Engineering Division*, ASCE, Vol. 101, No. GT4, pp. 379-398.

Rauch, A. F., Duffy, M., and Stokoe, K. H., II (2000). "Laboratory Correlation of Liquefaction Resistance with Shear Wave Velocity," *Soil Dynamics and Liquefaction, Geotechnical Special Publication*, ASCE, GeoDenver 2000 Conference.

Rashidian, M. (1995). "Undrained Shearing Behavior of Gravelly Sands and Its Relation with Shear Wave Velocity," *Thesis*, Geotechnical Engineering Laboratory, Department of Civil Engineering, University of Tokyo, Japan, 343 p.

Redpath, B. B. (1991). "Seismic Velocity Logging in the San Francisco Bay Area," Report to the Electric Power Research Institute, Palo Alto, CA, 34 p.

Robertson, P. K., Woeller, D. J., and Finn, W. D. L. (1992). "Seismic Cone Penetration Test for Evaluating Liquefaction Potential Under Cyclic Loading," *Canadian Geotechnical Journal*, Vol. 29, pp. 686-695.

Robertson, P. K., and Wride, C. E. (1997). "Cyclic Liquefaction and its Evaluation Based on the SPT and CPT," *NCEER Workshop on Evaluation of Liquefaction Resistance of Soils*, Technical Report NCEER-97-0022, T. L. Youd and I. M. Idriss, Eds., held 4-5 January 1996, Salt Lake City, UT, Nat. Center for Earthquake Engineering Research, Buffalo, NY, pp. 41-87.

Robertson, P. K., and Wride, C. E. (1998). "Evaluating Cyclic Liquefaction Potential Using the Cone Penetration Test," *Canadian Geotechnical Journal*, Vol. 35, No. 3, pp. 442-459.

Roesler, S. K. (1979). "Anisotropic Shear Modulus Due to Stress Anisotropy," *Journal of the Geotechnical Engineering Division*, ASCE, Vol. 105, No. GT7, pp. 871-880.

Rollins, K. M., Evans, M. D., Diehl, N. B., and Daily, W. D., III (1998a). "Shear Modulus and Damping Relationships for Gravels," *Journal of Geotechnical and Geoenvironmental Engineering*, ASCE, Vol. 124, No. 5, pp. 396-405.

Rollins, K. M., Diehl, N. B., and Weaver, T. J. (1998b). "Implications of V_S-BPT $(N_1)_{60}$ Correlations for Liquefaction Assessment in Gravels," *Geotechnical Earthquake Engineering and Soil Dynamics III*, Geotechnical Special Publication No. 75, P. Dakoulas, M. Yegian, and B. Holtz, Eds., ASCE, Vol. I, pp. 506-517.

Roy, D., Campanella, R. G., Byrne, P. M., and Hughes, J. M. O. (1996). "Strain Level and Uncertainty of Liquefaction Related Index Tests," *Uncertainty in the Geologic Environment: From Theory to Practice*, Geotechnical Special Publication No. 58, C. D. Shackelford, P. P. Nelson, and M. J. S. Roth, Eds., ASCE, Vol. 2, pp. 1149-1162.

Sato, K., Kokusho, T., Matsumoto, M., and Yamada, E. (1996). "Nonlinear Seismic Response and Soil Property During Strong Motion," *Soils and Foundations, Special Issue on Geotechnical Aspects of the January 17, 1995 Hyogoken-Nambu Earthquake*, Japanese Geotechnical Society, pp. 41-52.

Seed, H. B. (1979). "Soil Liquefaction and Cyclic Mobility Evaluation for Level Ground during Earthquakes," *Journal of the Geotechnical Engineering Division*, ASCE, Vol. 105, GT2, pp. 201-255.

Seed, H. B. (1983). "Earthquake-Resistant Design of Earth Dams," *Proceedings, Symposium on Seismic Design of Embankments and Caverns*, held 6-10 May 1983, Philadelphia, PA, ASCE, pp. 41-64.

Seed, H. B., and Idriss, I. M. (1971). "Simplified Procedure for Evaluating Soil Liquefaction Potential," *Journal of the Soil Mechanics and Foundations Division*, ASCE, Vol. 97, SM9, pp. 1249-1273.

Seed, H. B., and Idriss, I. M. (1982). *Ground Motions and Soil Liquefaction During Earthquakes*, Earthquake Engineering Research Institute, Berkeley, CA, 134 p.

Seed, H. B., Idriss, I. M., and Arango, I. (1983). "Evaluation of Liquefaction Potential Using Field Performance Data," *Journal of Geotechnical Engineering*, ASCE, Vol. 109, No. 3, pp. 458-482.

Seed, H. B., Tokimatsu, K., Harder, L. F., and Chung, R. M. (1985). "Influence of SPT Procedures in Soil Liquefaction Resistance Evaluations," *Journal of Geotechnical Engineering*, ASCE, Vol. 111, No. 12, pp. 1425-1445.

Seed, H. B., Wong, R. T., Idriss, I. M., and Tokimatsu, K. (1986). "Moduli and Damping Factors for Dynamic Analysis of Cohesionless Soils," *Journal of Geotechnical Engineering*, ASCE, Vol. 112, No. 11, pp. 1016-1032.

Seed, R. B., and Harder, L. F., Jr. (1990). "SPT-Based Analysis of Cyclic Pore Pressure Generation and Undrained Residual Strength," *Proceedings, H. Bolton Seed Memorial Symposium*, J. M Duncan, Ed., BiTech Publishers, Vancouver, B.C., Vol. 2, pp. 351-376.

Shen, C. K., Li, X. S., and Wang, Z. (1991). "Pore Pressure Response During 1986 Lotung Earthquakes," *Proceedings, Second International Conference on Recent Advances in Geotechnical Earthquake Engineering and Soil Dynamics*, S. Prakash, Ed., held 11-15 March 1991, St. Louis, MO, University of Missouri at Rolla, Vol. I, pp. 557-563.

Shibata, T., Oka, F., and Ozawa, Y. (1996). "Characteristics of Ground Deformation Due to Liquefaction," *Soils and Foundations, Special Issue on Geotechnical Aspects of the January 17, 1995 Hyogoken-Nambu Earthquake*, Japanese Geotechnical Society, pp. 65-79.

Silver, M. L., and Seed, H. B. (1971). "Volume Changes in Sands During Cyclic Loading," *Journal of the Soil Mechanics and Foundations Division*, ASCE, Vol. 97, No. SM9, pp. 1171-1182.

Stokoe, K. H., II, and Nazarian, S. (1985). "Use of Rayleigh Waves in Liquefaction Studies," *Measurement and Use of Shear Wave Velocity for Evaluating Dynamic Soil Properties*, R. D. Woods, Ed., ASCE, pp. 1-17.

Stokoe, K. H., II, Andrus, R. D., Bay, J. A., Fuhriman, M. D., Lee, N. J., and Yang, Y. (1992). "SASW and Crosshole Seismic Test Results from Sites that Did and Did not Liquefy During the 1989 Loma Prieta, California Earthquake," Geotechnical Engineering Center, Department of Civil Engineering, The University of Texas at Austin.

Stokoe, K. H., II, Lee, S. H. H., and Knox, D. P. (1985). "Shear Moduli Measurements Under True Triaxial Stresses," *Proceedings, Advances in the Art of Testing Soil Under Cyclic Conditions*, ASCE, pp. 166-185.

Stokoe, K. H., II, Nazarian, S., Rix, G. J., Sanchez-Salinero, I., Sheu, J.-C., and Mok, Y. J. (1988a). "In Situ Seismic Testing of Hard-to-Sample Soils by Surface Wave Method," *Earthquake Engineering and Soil Dynamics II--Recent Advances in Ground-Motion Evaluation*, Geotechnical Special Publication No. 20, J. L. Von Thun, Ed., ASCE, pp. 264-289.

Stokoe, K. H., II, Andrus, R. D., Rix, G. J., Sanchez-Salinero, I., Sheu, J. C., and Mok, Y. J. (1988b). "Field Investigation of Gravelly Soils Which Did and Did Not Liquefy During the 1983 Borah Peak, Idaho, Earthquake," *Geotechnical Engineering Report GR 87-1*, The University of Texas at Austin, 206 p.

Stokoe, K. H., II, Roesset, J. M., Bierschwale, J. G., and Aouad, M. (1988c). "Liquefaction Potential of Sands from Shear Wave Velocity," *Proceedings, Ninth World Conference on Earthquake Engineering*, Tokyo, Japan, Vol. III, pp. 213-218.

Sykora, D. W. (1987a). "Examination of Existing Shear Wave Velocity and Shear Modulus Correlations in Soils," *Geotechnical Laboratory Miscellaneous Paper GL-87-22*, U.S. Army Engineer Waterways Experiment Station, Vicksburg, MS.

Sykora, D. W. (1987b). "Creation of a Data Base of Seismic Shear Wave Velocities for Correlation Analysis," *Geotechnical Laboratory Miscellaneous Paper GL-87-26*, U.S. Army Engineer Waterways Experiment Station, Vicksburg, MS.

Sykora, D. W., and Stokoe, K. H., II (1982), "Seismic Investigation of Three Heber Road Sites After October 15, 1979 Imperial Valley Earthquake," *Geotechnical Engineering Report GR82-24*, The University of Texas at Austin, 76 p.

Teachavorasinskun, S., Tatsuoka, F., and Lo Presti, D. C. F. (1994). "Effects of the Cyclic Prestaining on Dilatancy Characteristics and Liquefaction Strength of Sand," *Pre-failure Deformation of Geomaterials*, S. Shibuya, T. Mitachi, and S. Miura, Eds., A. A. Balkema, Rotterdam, Netherlands, pp. 75-80.

Tokimatsu, K., Kuwayama, S., and Tamura, S. (1991a). "Liquefaction Potential Evaluation Based on Rayleigh Wave Investigation and Its Comparison with Field Behavior," *Proceedings, Second International Conference on Recent Advances in Geotechnical Earthquake Engineering and Soil Dynamics*, S. Prakash, Ed., held 11-15 March 1991, St. Louis, MO, University of Missouri at Rolla, Vol. I, pp. 357-364.

Tokimatsu, K., Kuwayma, S., Abe, A., Nomura, S., and Tamura, S. (1991b). "Considerations to Damage Patterns in the Marina District During the Loma Prieta Earthquake Based on Rayleigh Wave Investigation," *Proceedings, Second International Conference on Recent Advances in Geotechnical Earthquake Engineering and Soil Dynamics*, S. Prakash, Ed., held 11-15 March 1991, St. Louis, MO, University of Missouri at Rolla, Vol. II, pp. 1649-1654.

Tokimatsu, K., and Uchida, A. (1990). "Correlation Between Liquefaction Resistance and Shear Wave Velocity," *Soils and Foundations*, Japanese Society of Soil Mechanics and Foundation Engineering, Vol. 30, No. 2, pp. 33-42.

United States Bureau of Reclamation, USBR (1989). "Seismic Design and Analysis," *Design Standards No. 13 - Embankment Dams*, USBR, Denver, CO, Chapter 13.

Vaid, Y. P., Chern, J. C., and Tumi, H. (1985). "Confining Pressure, Grain Angularity, and Liquefaction," *Journal of Geotechnical Engineering*, ASCE, Vol. 111, No. 10, pp. 1229-1235.

Vaid, Y. P., and Thomas, J. (1994). "Liquefaction and Postliquefaction Behavior of Sand," *Journal of Geotechnical Engineering*, ASCE, Vol. 121, No. 2, pp. 163-173.

Weston, T. R. (1996). "Effects of grain size and particle distribution on the stiffness and damping of granular soils at small strains," *MS Thesis*, The University of Texas at Austin.

Woods, R. D., Ed. (1994). *Geophysical Characterization of Sites*, A. A. Balkema, Rotterdam, Netherlands.

Yoshimi, Y., Tokimatsu, K., Kaneko, O., and Makihara, Y. (1984). "Undrained Cyclic Shear Strength of Dense Niigata Sand," *Soils and Foundations*, Japanese Society of Soil Mechanics and Foundation Engineering, Vol. 24, No. 4, pp. 131-145.

Yoshimi, Y., Tokimatsu, K., and Hosaka, Y. (1989). "Evaluation of Liquefaction Resistance of Clean Sands Based on High-Quality Undisturbed Samples," *Soils and Foundations*, Japanese Society of Soil Mechanics and Foundation Engineering, Vol. 29, No. 1, pp. 93-104.

Youd, T. L. (1972). "Compaction of Sands by Repeated Shear Straining," *Journal of the Soil Mechanics and Foundations Division*, ASCE, Vol. 98, No. SM7, pp. 709-725.

Youd, T. L., and Noble, S. K. (1997). "Liquefaction Criteria Based on Statistical and Probabilistic Analyses," *NCEER Workshop on Evaluation of Liquefaction Resistance of Soils*, Technical Report NCEER-97-0022, T. L. Youd and I. M. Idriss, Eds., held 4-5 January 1996, Salt Lake City, UT, National Center for Earthquake Engineering Research, Buffalo, NY, pp. 201-215.

Youd, T. L., and Bennett, M. J. (1983). "Liquefaction Sites, Imperial Valley, California," *Journal of Geotechnical Engineering*, ASCE, Vol. 109, No. 3, pp. 440-457.

Youd, T. L., Harp, E. L., Keefer, D. K., and Wilson, R. C. (1985). "The Borah Peak, Idaho Earthquake of October 28, 1983 - Liquefaction," *Earthquake Spectra*, Earthquake Engineering Research Institute, El Cerrito, CA, Vol. 2, No. 1, pp. 71-89.

Youd, T. L., and Holzer, T. L. (1994). "Piezometer Performance at Wildlife Liquefaction Site, California," *Journal of Geotechnical Engineering*, ASCE, Vol. 120, No. 6, pp. 975-995.

Youd, T. L., and Hoose, S. N. (1978). "Historic Ground Failures in Northern California Triggered by Earthquakes," *U.S. Geological Survey Professional Paper 993*, U.S. Government Printing Office, Washington, D.C., 177 p.

Youd, T. L., and Idriss, I. M., eds. (1997). *NCEER Workshop on Evaluation of Liquefaction Resistance of Soils*, Technical Report NCEER-97-0022, held 4-5 January 1996, Salt Lake City, UT, National Center for Earthquake Engineering Research, Buffalo, NY, 276 p.

Youd, T. L., Idriss, I. M., Andrus, R. D., Arango, I., Castro, G., Christian, J. T., Dobry, R., Finn, W. D. L., Harder, L. F., Jr., Hynes, M. E., Ishihara, K., Koester, J. P., Liao, S. S. C., Marcuson, W. F., III, Martin, G. R., Mitchell, J. K., Moriwaki, Y., Power, M. S., Robertson, P. K., Seed, R. B., and Stokoe, K. H., II (1997). "Summary Report," *NCEER Workshop on Evaluation of Liquefaction Resistance of Soils*, Technical Report NCEER-97-0022, T. L. Youd and I. M. Idriss, Eds., held 4-5 January 1996, Salt Lake City, UT, National Center for Earthquake Engineering Research, Buffalo, NY, pp. 1-40.

Youd, T. L., Idriss, I. M., Andrus, R. D., Arango, I., Castro, G., Christian, J. T., Dobry, R., Finn, W. D. L., Harder, L. F., Jr., Hynes, M. E., Ishihara, K., Koester, J. P., Liao, S. S. C., Marcuson, W. F., III, Martin, G. R., Mitchell, J. K., Moriwaki, Y., Power, M. S., Robertson, P. K., Seed, R. B., and Stokoe, K. H., II (2001). "Liquefaction Resistance of Soils: Summary Report from the 1996 NCEER and 1998 NCEER/NSF Workshops on Evaluation of Liquefaction Resistance of Soils," *Journal of Geotechnical and Geoenvironmental Engineering*, ASCE, Vol. 127, No. 10, pp. 817-833.

Yu, P., and Richart, F. E., Jr. (1984). "Stress Ratio Effects on Shear Modulus of Dry Sands," *Journal of Geotechnical Engineering*, ASCE, Vol. 110, No. 3, pp. 331-345.

APPENDIX B

SYMBOLS AND NOTATION

The following symbols and notation are used in this report:

A	=	parameter that depends on soil structure;
a	=	parameter related to slope of CRR-V_{S1} curve;
a_1, a_2, a_3	=	regression coefficients;
a_{max}	=	peak horizontal ground surface acceleration;
B_1, B_2	=	parameters relating V_{S1} and penetration resistance;
b	=	parameter related to slope of CRR-V_{S1} curve;
b_1, b_2, b_3, b_4	=	regression coefficients;
CRR	=	average cyclic resistance ratio;
CRR_{tx}	=	CRR for cyclic triaxial tests;
CRR_1	=	CRR corrected for high overburden stress;
$CRR_{7.5}$	=	CRR for magnitude 7.5 earthquakes;
CSR	=	cyclic stress ratio;
C_{VS}	=	factor to correct V_S for overburden pressure;
D_{50}	=	median grain size by mass;
DA	=	double-amplitude axial strain;
D_r	=	relative density;
exp	=	the constant e raised to the power of a given number;
F_1, F_2	=	age and soil type factors for correlating V_S and N_j;
FC	=	fines content (particles smaller than 75 μm);
F_S	=	factor of safety;
f	=	high overburden stress exponent;
$f(e_{min})$	=	function of minimum void ratio;
$f(V_{S1})$	=	function of V_{S1};
$f(x)$	=	function of x (= F_S);
$f(\gamma_{av})$	=	function of average peak cyclic shear strain;
$f_L(F_S)$	=	probability density function of calculated F_S for liquefaction case histories;
$f_{NL}(F_S)$	=	probability density function of calculated F_S for non-liquefaction case histories;

G	=	shear modulus;
G_{max}	=	small-strain shear modulus;
G_N	=	G_{max} corrected for confining stress and void ratio;
$(G)_{\gamma_{av}}$	=	secant shear modulus at γ_{av};
g	=	acceleration of gravity;
K_c	=	cementation and aging correction factor;
K_{fc}	=	fines content correction factor;
K'_o	=	coefficient of effective lateral earth pressure at rest;
K_σ	=	high overburden stress correction factor;
ln	=	natural logarithm function;
MSF	=	magnitude scaling factor;
M_w	=	earthquake moment magnitude;
m	=	stress exponent;
N_j	=	SPT blow count in Japanese practice;
N_{60}	=	SPT energy-corrected blow count;
$(N_1)_{60}$	=	SPT energy- and overburden stress-corrected blow count;
n	=	magnitude scaling factor exponent;
P_a	=	reference overburden stress (= 100 kPa);
P_L	=	probability of liquefaction occurrence
r_c	=	factor to account for effects of multidirectional shaking;
r_d	=	shear stress reduction coefficient;
sin	=	sine function;
S_{res}	=	residual standard deviation;
V_S	=	small-strain shear wave velocity;
V_{S1}	=	overburden stress-corrected V_S;
$V_{S1,CS}$	=	equivalent clean soil value of V_{S1};
V^*_{S1}	=	limiting upper value of V_{S1} for liquefaction occurrence;
V_{S1m}	=	mean stress-corrected V_S;
z	=	depth;
$\alpha(z)$	=	function of depth;
$\beta(z)$	=	function of depth;
γ_{av}	=	average peak cyclic shear strain;
μ	=	mean;
ρ	=	mass density of soil;
σ	=	standard deviation;
σ_d	=	cyclic deviator stress in cyclic triaxial tests;
σ'_h	=	initial effective horizontal confining stress;
σ'_m	=	mean effective confining stress;
σ'_o	=	initial effective confining stress in cyclic triaxial tests;

σ_v	=	total vertical (or overburden) stress;
σ'_v	=	initial effective vertical (or overburden) stress;
τ_{av}	=	average cyclic equivalent uniform shear stress generated by earthquake; and
τ_{max}	=	maximum cyclic shear stress generated by earthquake.

APPENDIX C

GLOSSARY OF TERMS

The following definitions apply to this report:

Case History	An earthquake and a test array.
Critical Layer	The layer of non-plastic soil below the ground water table where corrected values of shear wave velocity and penetration are the least, and where cyclic stress ratios are the greatest.
Liquefaction Occurrence	Surface manifestations of excess pore-water pressure at depth, such as sand boils, ground cracks and fissures, and ground settlement.
Moment Magnitude	An earthquake magnitude scale defined in terms of energy.
Overburden Stress-Corrected Shear Wave Velocity	Shear wave velocity measurement corrected to a reference vertical (or overburden) stress of 100 kPa.
Peak Horizontal Ground Surface Acceleration	The peak value in a horizontal ground surface acceleration record that would occur at the site in the absence of liquefaction or excess pore-water pressures.
Shear Wave Velocity	The velocity of a propagating shear wave within a material with either the direction of wave propagation or the direction of particle motion in the vertical direction.
Shear Wave	A body wave with the direction of particle motion transverse to the direction of wave propagation.

Test Array	The two boreholes used for crosshole measurements, the borehole and source used for downhole measurements, the cone sounding and source used for seismic cone measurements, the borehole used for suspension logging measurements, or the line of receivers used for Spectral-Analysis-of-Surface-Waves (SASW) measurements.

APPENDIX D

COMPARISON OF V_S-BASED LIQUEFACTION RESISTANCE CURVES

During the past two decades, several studies have been conducted to investigate the relationship between V_S and liquefaction resistance. These studies involved laboratory tests (Dobry et al., 1981; Dobry et al., 1982; de Alba et al., 1984; Hynes, 1988; Tokimatsu and Uchida, 1990; Tokimatsu et al., 1991a; Rashidian, 1995; Rauch et al., 2000), analytical investigations (Bierschwale and Stokoe, 1984; Stokoe et al., 1988c; Andrus, 1994), penetration-V_S correlations (Seed et al., 1983; Lodge, 1994; Kayabali, 1996; Rollins et al., 1998b; Andrus et al., 1999), or field performance observations (Stokoe and Nazarian, 1985; Robertson et al., 1992; Kayen et al., 1992; Andrus and Stokoe, 1997; Andrus et al., 1999; Juang and Chen, 2000; Andrus and Stokoe, 2000; Juang et al., 2001a). Many of the liquefaction evaluation procedures developed from these studies follow the general format of the Seed-Idriss simplified procedure, where V_S is corrected to a reference overburden stress and correlated with the cyclic stress, or resistance, ratio.

This appendix reviews seven proposed liquefaction evaluation curves based on *CRR* and V_{S1}. The seven *CRR*-V_{S1} curves are shown in Fig. D.1. Each of the curves is briefly discussed below.

D.1 CURVE BY TOKIMATSU AND UCHIDA (1990)

The best-fit curve by Tokimatsu and Uchida (1990) shown in Fig. D.1 was determined from laboratory cyclic triaxial test results for various sands with less than 10 % fines (silt and clay) and 15 cycles of loading. Figure D.2 presents the cyclic triaxial test results. The solid symbols in Fig. D.2 correspond to specimens obtained by the *in situ* freezing technique. The open symbols correspond to specimens reconstituted in the laboratory. Tokimatsu and Uchida defined the cyclic resistance ratio for cyclic triaxial tests, CRR_{tx}, as the ratio of cyclic deviator stress to initial effective confining stress, $\sigma_d/2\sigma'_o$ when the double-amplitude (or peak-to-peak)

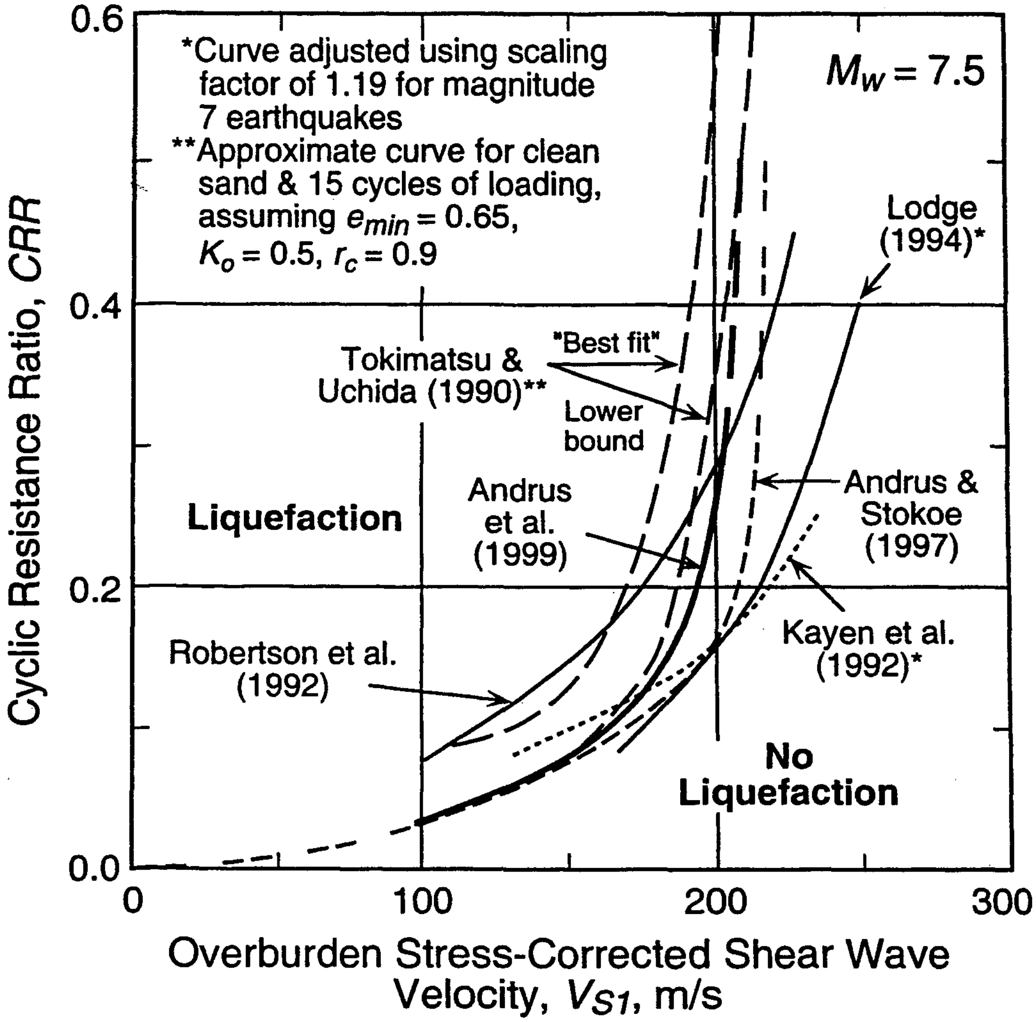

Fig. D.1 - Comparison of Seven Proposed CRR-V_{S1} Curves for Clean Granular Soils.

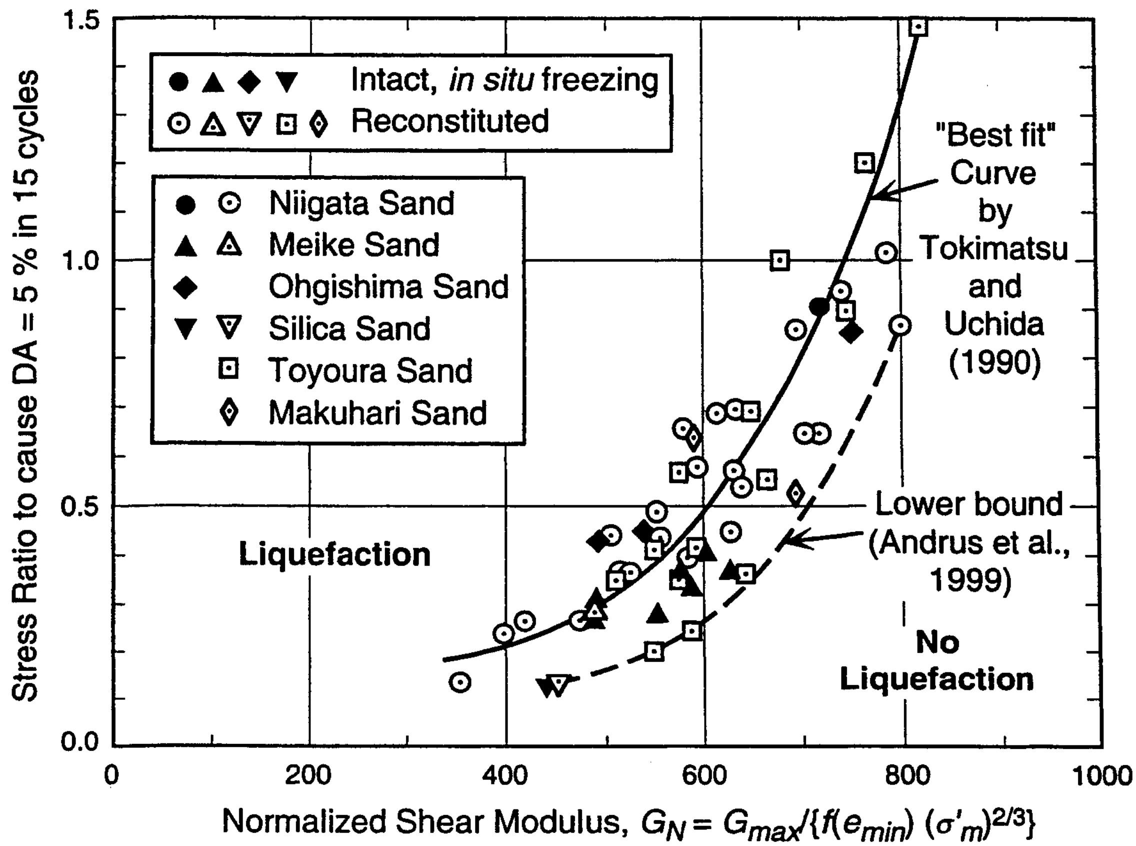

Fig. D.2 - Relationship Between Liquefaction Resistance and Normalized Shear Modulus for Various Sands with Less than 10 % Fines Determined by Cyclic Triaxial Testing. (modified from Tokimatsu and Uchida, 1990) axial strain, DA, reaches 5 %. They measured the elastic shear modulus of the specimen at a shear strain of 10^{-3} % just prior to the liquefaction test. This small-strain shear modulus was normalized to correct for the influence of confining pressure and void ratio by:

$$G_N = \frac{G_{\max}}{f(e_{\min})(\sigma'_m)^{2/3}} \tag{D.1}$$

and

$$f(e_{min}) = \frac{(2.17-e_{\min})^2}{1+e_{\min}} \tag{D.2}$$

where

G_N	=	the normalized shear modulus,
e_{min}	=	the minimum void ratio determined by standard test method, and
σ'_m	=	the mean effective confining stress.

Tokimatsu and Uchida selected an exponent of 2/3 rather than 1/2, as determined by Hardin and Drnevich (1972), because it seemed that a slightly better correlation could be obtained. Values of e_{min} ranged from 0.61 to 0.91 for the sands tested. The actual values of void ratio in each test were greater than e_{min}, with values ranging from about 0.65 to about 1.4.

By combining Eqs. (1.1) and (D.1), one obtains the following relationship for converting G_N to mean stress-corrected V_S:

$$V_{S1m} = V_S\left(\frac{1}{\sigma'_m}\right)^{0.33} = \left(\frac{G_N f(e_{\min})}{\rho}\right)^{0.5} \tag{D.3}$$

where

V_{S1m}	=	mean stress-corrected V_S, and
σ'_m	=	the mean effective confining stress in kgf/cm^2 (1 kgf/cm^2 = 98 kPa).

Tokimatsu and Uchida (1990) suggested using 0.65 as an average value of e_{min} for clean sands.

The overburden stress-corrected V_S and V_{S1m} can be related by:

$$V_{S1m} = V_S \left(\frac{1}{\sigma'_v}\right)^{0.33} \left(\frac{3}{1+2K'_o}\right)^{0.33} \approx V_{S1} \left(\frac{1}{\sigma'_v}\right)^{0.08} \left(\frac{3}{1+2K'_o}\right)^{0.33} \tag{D.4}$$

where

K'_o = the coefficient of lateral earth pressure at rest ($= \sigma'_h / \sigma'_v$).

Values of V_{S1} for the best fit curve by Tokimatsu and Uchida (1990) shown in Fig. D.1 are determined (Andrus et al., 1999; after Tokimatsu et al., 1991a) from Fig. D.2 using Eqs. (D.3) and (D.4), and assuming $K'_o = 0.5$, $e_{min} = 0.65$, $\sigma'_m = 100$ kPa, and soil density of 1.9 Mg/m^3.

For converting CRR_{tx} to an equivalent field CRR, Tokimatsu and Uchida (1990) suggested the following expression originally proposed by Seed (1979):

$$CRR = \frac{(1+2K'_o)}{3} \, r_c \, (CRR_{tx}) \tag{D.5}$$

where

r_c = a constant to account for the effects of multi-directional shaking with a value between 0.9 and 1.0.

Values of CRR for the best fit curve by Tokimatsu and Uchida shown in Fig. D.1 are determined from Fig. D.2 using Eq. (D.5) and assuming $K'_o = 0.5$ and $r_c = 0.9$.

Because the other liquefaction resistance curves shown in Fig. D.1 were drawn to bound liquefaction case histories, the more conservative lower bound curve for the laboratory test results by Tokimatsu and Uchida (1990) also is shown. This curve was drawn (Andrus et al., 1999) from Fig. D.2 following the procedure outlined above.

D.2 CURVE BY ROBERTSON ET AL. (1992)

The bounding curve by Robertson et al. (1992) was developed using field performance data from primarily sites in Imperial Valley, California, along with data from four other sites, as shown in Fig. D.3. The soil at these sites contained as much as 35 % fines. Robertson et al. corrected V_S using Eq. (2.7). The shape of their curve was based on the analytical results of

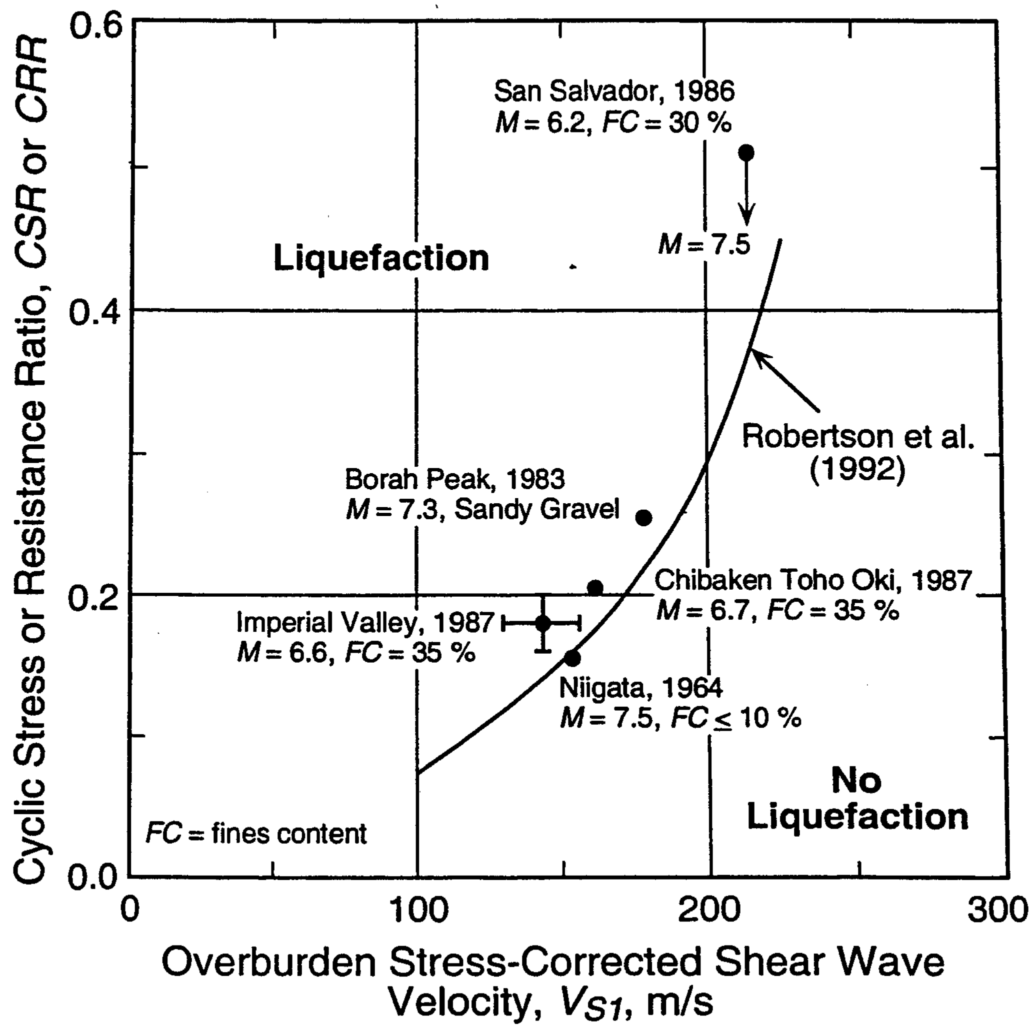

Fig. D.3 - Liquefaction Resistance Curve for Magnitude 7.5 Earthquakes and Case History Data from Robertson et al. (1992).

Bierschwale and Stokoe (1984). They reasoned that the curve should pass close to the Imperial Valley (Wildlife site) data point, since liquefaction did and did not occur at this site during the 1987 Superstition Hills (M_w = 6.5) and Elmore Ranch (M_w = 6.2) earthquakes, respectively. Robertson et al. used magnitude scaling factors similar to those suggested by Seed and Idriss (1982), Column 2 of Table 2.2, to position their curve for magnitude 7.5 earthquakes.

D.3 CURVE BY KAYEN ET AL. (1992)

Kayen et al. (1992) studied four sites that did and did not liquefy during the 1989 Loma Prieta, California, earthquake (M_w = 7.0). The four sites are: Port of Richmond, Bay Bridge Toll Plaza, Port of Oakland, and Alameda Bay Farm Island South Loop Road. The fines content for soils at these sites ranged from less than 5 % to as much as 57 %. Values of V_S were measured by the SCPT method and corrected for overburden stress using Eq. (2.7). Figure D.4 presents their data and bounding curve. The curve by Kayen et al. shown in Fig. D.1 was adjusted for magnitude 7.5 earthquakes by assuming a *MSF* of 1.19 (see Column 3 of Table 2.2).

D.4 CURVE BY LODGE (1994)

Lodge (1994) considered the same sites that Kayen et al. (1992) studied, as well as other sites shaken by the 1989 Loma Prieta earthquake. The curve by Lodge was developed as follows. First, cyclic stress ratios for the entire soil profile at each site were calculated. Second, available SPT blow counts were corrected for overburden pressure and energy. Soil layers with high and low liquefaction potential were identified with the procedure of Seed et al. (1985). Soil layers with corrected blow count within 3 of the SPT-based curve were eliminated due to uncertainties in the correlation. Third, V_S measurements from SCPT and crosshole tests were corrected for overburden stress using Eq. (2.7). Fourth, on a "meter by meter" basis, values of V_{S1} and cyclic stress ratio were plotted for both layer types, those which were predicted liquefiable and those which were predicted non-liquefiable. Fifth, published data for sites shaken by the 1983 Borah Peak, Idaho, and 1964 Niigata, Japan, earthquakes were added to the plot. Finally, a curve was drawn to include all liquefiable layers, as shown in Fig. D.5. The curve by Lodge shown in Fig. D.1 was adjusted for magnitude 7.5 earthquakes by assuming a *MSF* of 1.19 (see Column 3 of Table 2.2).

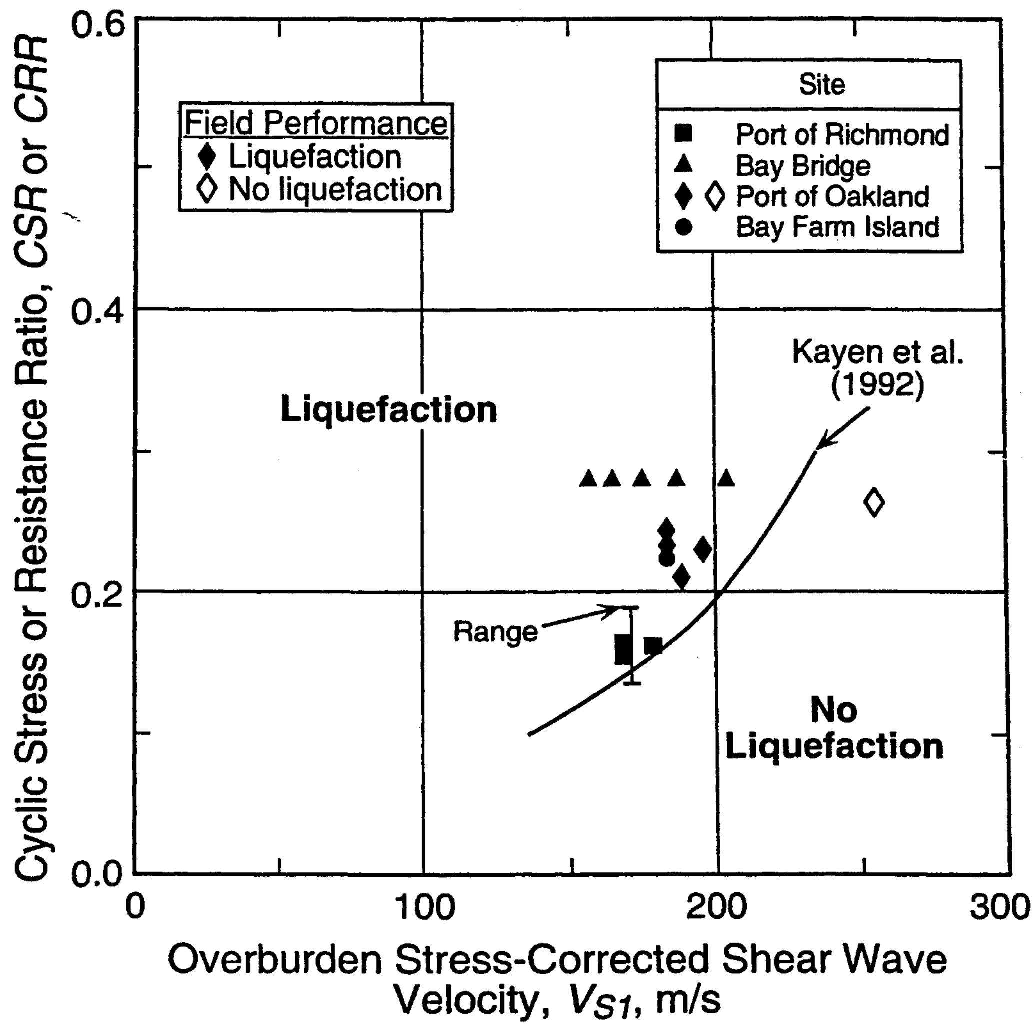

Fig. D.4 - Liquefaction Resistance Curve for Magnitude 7 Earthquake and Case History Data from Kayen et al. (1992).

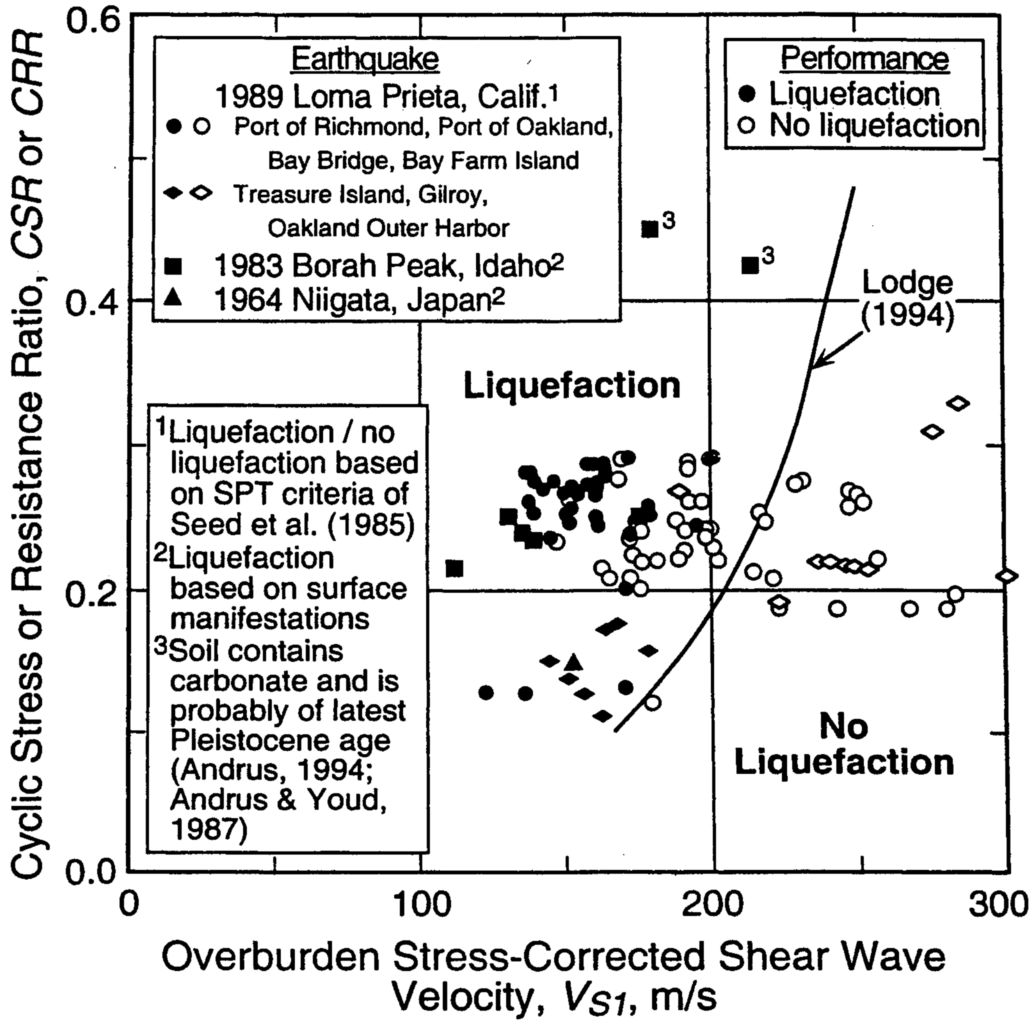

Fig. D.5 - Liquefaction Resistance Curve for Magnitude 7 Earthquakes and Case History Data from Lodge (1994).

D.5 CURVE BY ANDRUS AND STOKOE (1997)

The curve by Andrus and Stokoe (1997) shown in Fig. D.1 was developed for the proceedings of the 1996 NCEER Workshop (Youd and Idriss, eds., 1997). Several suggestions were offered at, and after, the workshop concerning how site variables should be define, as well as the shape of the boundary curve separating liquefaction and no liquefaction. Following the suggestions and using field performance data from 20 earthquakes and *in situ* V_S measurements from over 50 sites in soils ranging from clean fine sand to sandy gravel with cobbles to profiles including silty clay layers, Andrus and Stokoe constructed curves for uncemented, Holocene-age soils with various fines content. The values of V_S were corrected using Eq. (2.7). The curve by Andrus and Stokoe (1997) for fines content ≤ 5 % along with the case history data are presented in Fig. D.6. The shape of the curve by Andrus and Stokoe (1997) was based on a modified relationship between V_{S1} and CSR for constant average cyclic shear strain suggested by R. Dobry.

D.5.1 Cyclic Shear Strain and Cyclic Shear Stress

Liquefaction results from the rearranging of soil particles and the tendency for decrease in volume. Experimental and theoretical studies show that decrease in volume is more closely related to cyclic strain than cyclic stress (Silver and Seed, 1971); a threshold cyclic strain exists below which neither rearrangement of soil particles nor decrease in volume take place (Drnevich and Richart, 1970; Youd, 1972; Pyke et al., 1975), and no pore water pressure buildup occurs (Dobry et al., 1981; Seed et al., 1983); and that there is a predictable correlation between cyclic shear strain and pore pressure buildup of saturated soils (Martin et al., 1975; Park and Silver, 1975; Finn and Bhatia, 1981; Dobry et al., 1982; Hynes, 1988). The threshold cyclic strain is limited to a narrow range of variation, ranging from about 0.005 % for gravels to 0.01 % for normally consolidated clean sands and silty sands to 0.03 % for overconsolidated clean sands. In addition, cyclic strain-controlled test results are less affected than stress-controlled tests by factors such as density, confining stress, anisotropic confining stress, fabric and prestaining (Martin et al., 1975; Dobry and Ladd, 1980; Dobry et al., 1982; Hynes, 1988). It should also be noted that the steady state approach to liquefaction evaluation by Poulos et al. (1985) is based on a triggering strain level. These findings confirm the fact that cyclic strain is more fundamentally related to pore pressure buildup than cyclic stress, and are strong arguments in favor of a cyclic strain approach to liquefaction evaluation.

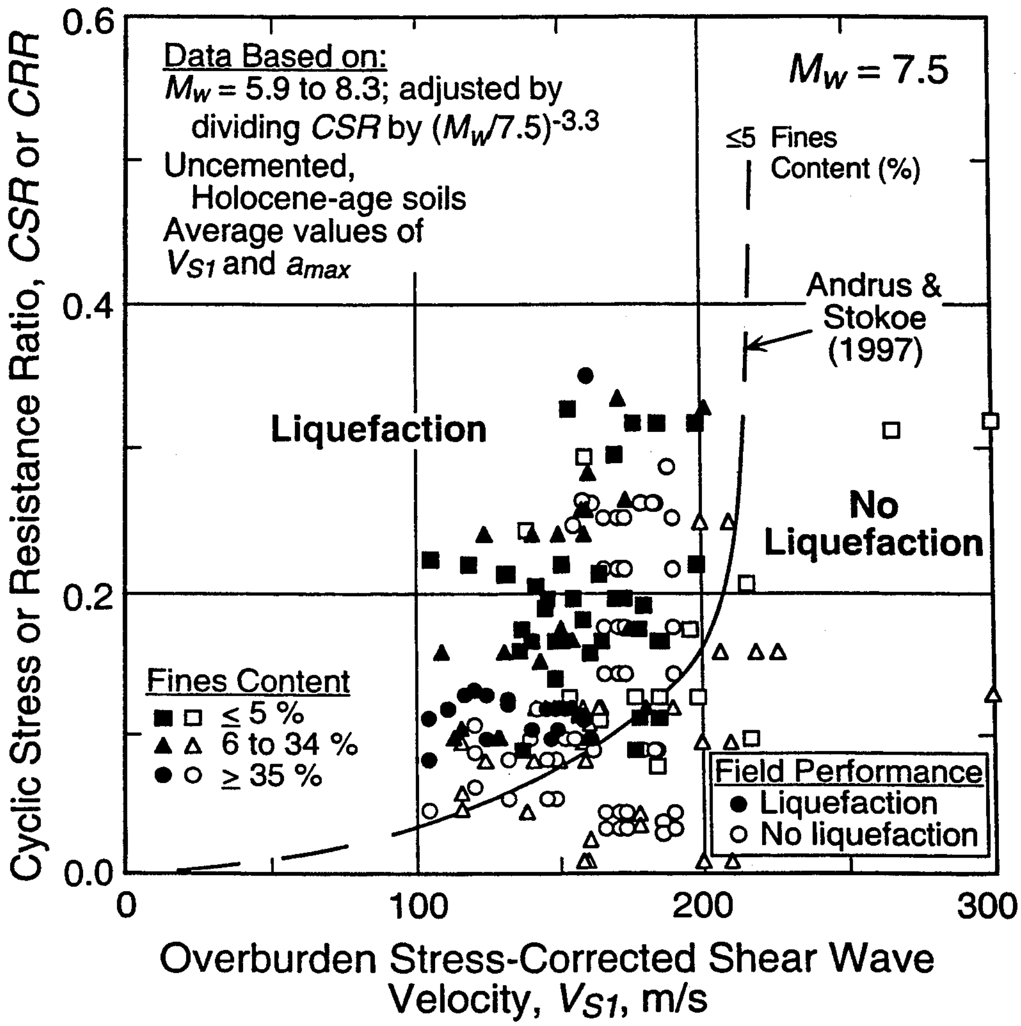

Fig. D.6 - Liquefaction Resistance Curve for Magnitude 7.5 Earthquakes and Uncemented Clean Soils of Holocene Age with Case History Data from Andrus and Stokoe (1997).

Cyclic shear strain and cyclic shear stress can be related by the following equation:

$$\gamma_{av} = \frac{\tau_{av}}{(G)_{\gamma_{av}}} \tag{D.6}$$

where

γ_{av} = the average peak cyclic shear strain during a cyclic stress-controlled test of uniform cyclic shear stress τ_{av}, and

$(G)_{\gamma_{av}}$ = the secant shear modulus at γ_{av} during the same cyclic test.

In the cyclic strain approach proposed by Dobry et al. (1982), the average cyclic shear strain caused by an earthquake is estimated from:

$$\gamma_{av} = 0.65\,\frac{a_{\max}}{g}\,\frac{\sigma_v r_d G_{\max}}{\rho V_S^2 (G)_{\gamma_{av}}} \tag{D.7}$$

Equation (D.7) is obtained by combining Eqs. (1.1), (2.1) and (D.6). The variation of shear modulus with strain is commonly expressed in terms of $(G)_{\gamma_{av}}/G_{max}$, called the *modulus reduction factor*. The modulus reduction factor can be estimated from an experimentally determined correlation. Neither pore pressure buildup nor liquefaction will occur when γ_{av} is less than the threshold strain. When γ_{av} is greater than the threshold strain, then pore pressure buildup can occur. The amount of pore pressure buildup can also be estimated from an experimentally determined correlation.

D.5.2 Dobry's Relationship Between *CRR* and V_{S1}

R. Dobry (personal communication to R. D. Andrus, 1996) derived a relationship between V_{S1} and *CSR* for constant average cyclic shear strain using Eqs. (1.1) and (D.6). Combining Eqs. (1.1) and (D.6), and dividing both sides by σ'_v leads to:

$$\frac{\tau_{av}}{\sigma'_v} = \gamma_{av}\left(\frac{\rho}{\sigma'_v}\right)\frac{(G)_{\gamma_{av}}}{G_{\max}}V_S^2 \tag{D.8}$$

For an overburden stress of 100 kPa, $V_S = V_{S1}$ and curves of constant average cyclic strain can be expressed by:

$$CSR = \frac{\tau_{av}}{\sigma'_v} = f(\gamma_{av})\ (V_{S1})^2 \tag{D.9}$$

where

$$f(\gamma_{av}) = \gamma_{av}\left(\frac{\rho}{P_a}\right)\frac{(G)_{\gamma_{av}}}{G_{\max}} \tag{D.10}$$

Since CSR equals CRR at the point separating liquefaction from no liquefaction, Eq. (D.9) provides an analytical basis for establishing the CRR-V_{S1} curve at low values of V_{S1} (say $V_{S1} \leq$ 125 m/s) and extending them to zero at $V_{S1} = 0$.

D.5.3 Modified *CRR*-V_{S1} Relationship

Andrus and Stokoe (1997) reasoned that the curve separating liquefiable and non-liquefiable soils would become asymptotic to some limiting upper value of V_{S1}. They modified Eq. (D.9) to:

$$CRR = \left\{a\left(\frac{V_{S1}}{100}\right)^2 + b\left(\frac{1}{V^*_{S1} - V_{S1}} - \frac{1}{V^*_{S1}}\right)\right\} MSF \tag{D.11}$$

where

V^*_{S1} = the limiting upper value of V_{S1} for liquefaction occurrence, and
a, b = curve fitting parameters.

The first term in Eq. (D.11) is a form of Eq. (D.9), assuming $f(\gamma_{av})$ is independent of initial effective confining pressure and of pore water pressure buildup. The second term is a hyperbola with a small value at low values of V_{S1}, and a very large value as V_{S1} approaches V^*_{S1}.

The curve by Andrus and Stokoe (1997) shown in Figs. D.1 and D.6 is defined by Eqs. (D.11) and (2.9) with $a = 0.03$, $b = 0.9$, $n = -3.3$, and $V^*_{S1} = 220$ m/s.

D.6 CURVE BY ANDRUS ET AL. (1999)

Since the publication of the 1996 NCEER Workshop proceedings (Youd and Idriss, eds., 1997), the case history data compiled by Andrus and Stokoe (1997) have been revised based on new information, and expanded to include field performance data from 26 earthquakes and more than 70 measurements sites. Also, the 1998 MCEER Workshop was held to discuss developments since the 1996 workshop. From the suggestions given at the second workshop and using the expanded database, the curve proposed by Andrus and Stokoe (1997) was revised in the report by Andrus et al. (1999) and paper by Andrus and Stokoe (2000). The revised curve for uncemented soils with fines content ≤ 5 % along with the case history data are shown in Fig. D.7. The development of the revised curve is discussed in Appendix F.

D.7 SUMMARY

Seven proposed curves relating *CRR* and V_{S1} were discussed in this Appendix. Many of the differences among the seven curves (see Fig. D.1) can be explained by the following four factors: (1) The best-fit curve by Tokimatsu and Uchida (1990) is more of a median curve, while the other curves bound the liquefaction case history data. (2) Portions of the proposed curves are based on limited data, and the investigator(s) have assumed different levels of conservatism. In particular, the curves by Robertson et al. (1992), Kayen et al. (1992), and Lodge (1994) were based on little or no data above V_{S1} of 200 m/s, and were conservatively drawn in this region. (3) Methods for selecting some site variables and correction factors are different among investigator(s). (4) Some errors exist in the database by Andrus and Stokoe (1997), and lead to more conservative curve than the updated curve by Andrus et al. (1999) above a V_{S1} value of 150 m/s. Thus, the *CRR*-V_{S1} curve proposed by Andrus et al. (1999) for clean soils is recommended because it was based on the largest, most correct case history data set and procedures recommended by the 1996 NCEER Workshop (Youd et al., 1997).

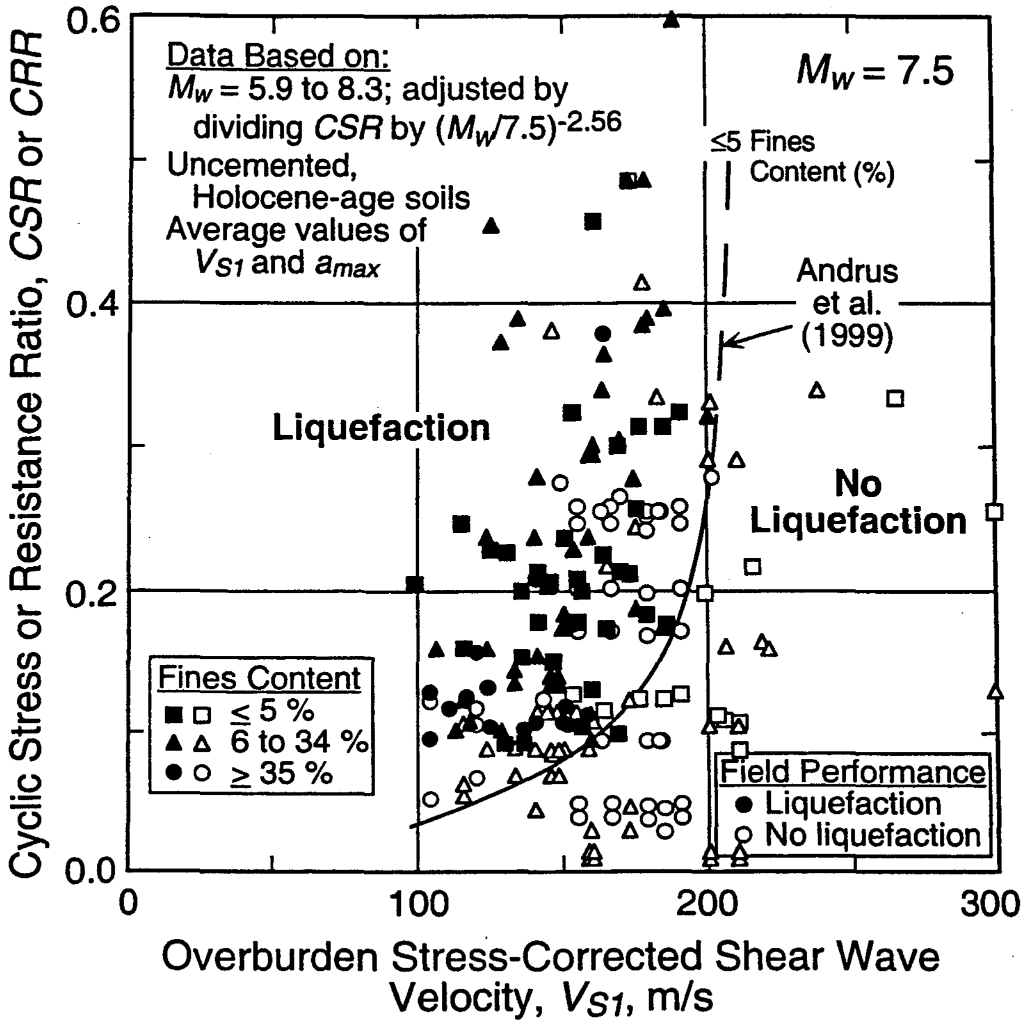

Fig. D.7 - Revised Liquefaction Resistance Curve for Magnitude 7.5 Earthquakes and Uncemented Clean Soils of Holocene Age with Case History Data from Andrus et al. (1999).

APPENDIX E

CASE HISTORY DATA AND THEIR CHARACTERISTICS

Shear wave velocity measurements have been made for field liquefaction studies at many sites during the past twenty years. Table E.1 presents a list of over 70 sites and 26 earthquakes that have been investigated. Of the 26 earthquakes listed, 9 occurred in the United States; and the other 15 in Japan, Taiwan, and China. The field performance information for these earthquakes along with the V_S measurements provides an important opportunity to determine the relationship between liquefaction resistance and V_S directly from case histories. A detailed summary of available case history data is presented in Appendix H. This appendix describes the site variables and characteristics of the database.

E.1 SITE VARIABLES AND DATABASE CHARACTERISTICS

E.1.1 Earthquake Magnitude

Earthquake magnitudes for the 26 earthquakes listed in Table E.1 range from 5.3 to 8.3, based on the moment magnitude scale. Moment magnitude is the scale most commonly used for engineering applications, and is the preferred scale for liquefaction resistance calculations (Youd et al., 1997). When other magnitude scales are reported by the investigator(s), they are converted to M_w using the relationship of Heaton et al. (1982) shown in Fig. 2.5.

E.1.2 Shear Wave Velocity Measurement

At the more than 70 investigation sites listed in Table E.1, shear wave velocity measurements were made with 139 test arrays. A test array is defined in this report as the two boreholes used for crosshole measurements, the borehole and source used for downhole measurements, the cone sounding and source used for seismic cone measurements, the borehole used for suspension logging measurements, or the line of receivers used for Spectral-Analysis-of-Surface-Waves (SASW) measurements. Of the 139 test arrays, 39 are crosshole, 21 downhole, 27 seismic cone, 15 suspension logger, 36 SASW, and one is unknown.

Table E.1 - Earthquakes and Sites Used to Establish Liquefaction Resistance Curves

Earthquake (1)	Moment Magnitude (2)	Site (3)	Reference (4)
1906 San Francisco, California	7.7	Coyote Creek; Salinas River (North, South)	Youd & Hoose (1978); Barrow (1983); Bennett & Tinsley (1995)
1957 Daly City, California	5.3	Marina District (2, 3, 4, 5, School)	Kayen et al. (1990); Tokimatsu et al. (1991b); T. L. Youd (personal communication to R. D. Andrus, 1999)
1964 Niigata, Japan	7.5	Niigata City (A1, C1, C2, Railway Station)	Yoshimi et al. (1984; 1989); Tokimatsu et al. (1991a)
1975 Haicheng, China	7.3	Chemical Fiber; Construction Building; Fishery & Shipbuilding; Glass Fiber; Middle School; Paper Mill	Arulanandan et al. (1986)
1979 Imperial Valley, California 1981 Westmorland, California 1987 Elmore Ranch, California 1987 Superstition Hills, California	6.5 5.9 5.9 6.5	Heber Road (Channel fill, Point bar); Kornbloom; McKim; Radio Tower; Vail Canal; Wildlife	Bennett et al. (1981; 1984); Sykora & Stokoe (1982); Youd & Bennett (1983); Bierschwale & Stokoe (1984); Stokoe & Nazarian (1984); Dobry et al. (1992); Youd & Holzer (1994)
1980 Mid-Chiba, Japan 1985 Chiba-Ibaragi-Kenkyo, Japan	5.9 6.0	Owi Island No. 1	Ishihara et al. (1981; 1987)
1983 Borah Peak, Idaho	6.9	Andersen Bar; Goddard Ranch; Mackay Dam Downstream Toe; North Gravel Bar; Pence Ranch	Youd et al. (1985); Stokoe et al. (1988a); Andrus et al. (1992); Andrus (1994)
1986 Event LSST2, Taiwan Event LSST3, Taiwan Event LSST4, Taiwan Event LSST6, Taiwan Event LSST7, Taiwan Event LSST8, Taiwan Event LSST12, Taiwan Event LSST13, Taiwan Event LSST16, Taiwan	5.3 5.5 6.6 5.4 6.6 6.2 6.2 6.2 7.6	Lotung LSST Facility	Shen et al. (1991); EPRI (1992)
1987 Chiba-Toho-Oki, Japan	6.5	Sunamachi	Ishihara et al. (1989)

Table E.1 (cont.) - Earthquakes and Sites Used to Establish Liquefaction Resistance Curves.

Earthquake (1)	Moment Magnitude (2)	Site (3)	Reference (4)
1989 Loma Prieta, California	7.0	Bay Bridge Toll Plaza, Bay Farm Island (Dike, South Loop Road); Port of Oakland; Port of Richmond	Stokoe et al. (1992); Mitchell et al. (1994)
		Coyote Creek; Salinas River (North, South);	Barrow (1983); M. J. Bennett (personal communication to R. D. Andrus, 1995); Bennett and Tinsley (1995)
		Marina District (2, 3, 4, 5, school)	Kayen et al. (1990); Tokimatsu et al. (1991b)
		Moss Landing (Harbor Office, Sandholdt Road, State Beach)	Boulanger et al. (1995); Boulanger et al. (1997)
		Santa Cruz (SC02, SC03, SC04, SC05, SC13, SC14)	Hryciw (1991); Hryciw et al. (1998)
		Treasure Island Fire Station	Hryciw et al. (1991); Redpath (1991); Gibbs et al. (1992); Furhriman (1993); Andrus (1994); de Alba et al. (1994)
		Treasure Island Perimeter (Approach to Pier, UM03, UM05, UM06, UM09)	Geomatrix Consultants (1990); Hryciw (1991); R. D. Hryciw (personal communication to R. D. Andrus, 1998); Hryciw et al. (1998); Andrus et al. (1998a, 1998b)
1993 Kushiro-Oki, Japan	8.3	Kushiro Port (2, D)	Iai et al. (1995); S. Iai (personal communication to R. D. Andrus, 1997)
1993 Hokkaido-Nansei-Oki, Japan	8.3	Pension House	Kokusho et al. (1995a, 1995b, 1995c)
		Hakodate Port	S. Iai (personal communication to R. D. Andrus, 1997)
1994 Northridge, California	6.7	Rory Lane	Abdel-Haq & Hryciw (1998)

Table E.1 (cont.) - Earthquakes and Sites Used to Establish Liquefaction Resistance Curves.

Earthquake (1)	Moment Magnitude (2)	Site (3)	Reference (4)
1995 Hyogo-Ken Nanbu, Japan	6.9	Hanshin Expressway 5 (3, 10, 14, 25, 29); Kobe-Nishinomiya Expressway (3, 17, 23, 28)	Hamada et al. (1995); Hanshin Expressway Public Corporation (1998)
		KNK; Port Island (Downhole Array); SGK	Sato et al. (1996); Shibata et al. (1996)
		Port Island (Common Factory)	Ishihara et al. (1997); Ishihara et al. (1998)
		Kobe Port (7C); Port Island (1C, 2C)	Inatomi et al. (1997); Hamada et al. (1995)
		Kobe Port (LPG Tank Yard)	S. Yasuda (personal communication to R. D. Andrus, 1997)

Values of V_S reported by the investigator(s) are used directly. The one exception is for the downhole array located at the Marina District School site in San Francisco, California. A reevaluation of the field data indicates that V_S values reported for the critical layer at this site are too high. They are recalculated using the pseudo-interval method, as discussed in Section E.2.2. Only the crosshole measurements made with shear waves having particle motion in the vertical direction are used. Crosshole measurements near the critical layer boundary that seem high, and could represent refracted waves, are not included in the average. Some V_S values are from measurements made before the earthquake, others followed the earthquake. No adjustments are made to compensate for changes in soil density and V_S due to ground shaking.

E.1.3 Measurement Depth

In situ V_S measurements may be reported at discrete depths or for continuous intervals, depending on the test method. When velocities are reported for continuous intervals, as is typically the case for downhole, seismic cone, suspension logger and SASW measurements, the depth to the center of each interval is assumed. Thus, if the reported V_S profile has ten velocity layers, it is assumed that the profile consists of ten "measurements" with depths at the center of each layer.

E.1.4 Case History

In this report, a case history is defined as a seismic event and a test array. For example, at the Treasure Island Fire Station site, crosshole measurements were made between five different pairs of boreholes, downhole measurements were made by two different investigators, seismic cone measurements were made at one location, and SASW measurements were made along one alignment. Thus, a total of nine case histories are identified for the Fire Station site and the 1989 Loma Prieta, California earthquake. At the Marina District School site, downhole measurements were made at one location. Estimates of ground surface acceleration at this site are available for the 1957 Daly City and 1989 Loma Prieta earthquakes. Thus, two case histories are identified for the Marina District School site. Combining the 26 seismic events and 139 test arrays, a total of 225 case histories are obtained with 149 from the United States, 36 from Taiwan, 34 from Japan, and 6 from China.

The two exceptions to this definition are the Owi Island No. 1 site and the Moss Landing Sandholdt Road UC-4 site where additional subsurface information is available. At Owi Island, pore pressure transducers recorded pore-water pressure buildup for two separate layers. At Moss Landing, inclinometer measurements indicated lateral movement in an upper loose layer and no lateral movement in a lower dense layer. Thus, two case histories are identified for each of these two test arrays.

E.1.5 Liquefaction Occurrence

It is important to realize that the occurrence of liquefaction, in this evaluation, is based on the appearance of surface evidence, such as sand boils, ground cracks and fissures, and ground settlement. Case histories are classified as non-liquefaction when no liquefaction effects were observed. At the Owi Island No. 1, Lotung LSST Facility, Sunamachi, Wildlife (1987 earthquakes), and Port Island sites, the assessment of liquefaction or non-liquefaction occurrence is supported by pore-water pressure measurements. In addition, liquefaction occurrence is assigned (in This Report) to the Treasure Island, California, Fire Station case histories where the strong ground motion records from the 1989 Loma Prieta earthquake exhibit a sudden drop at about 15 seconds and small motion afterward (Idriss, 1990), indicating liquefaction (de Alba et al., 1994). Of the 225 case histories, 99 are liquefaction case histories and 126 are non-liquefaction case histories. Figure E.1 shows the distribution of case histories with earthquake magnitude.

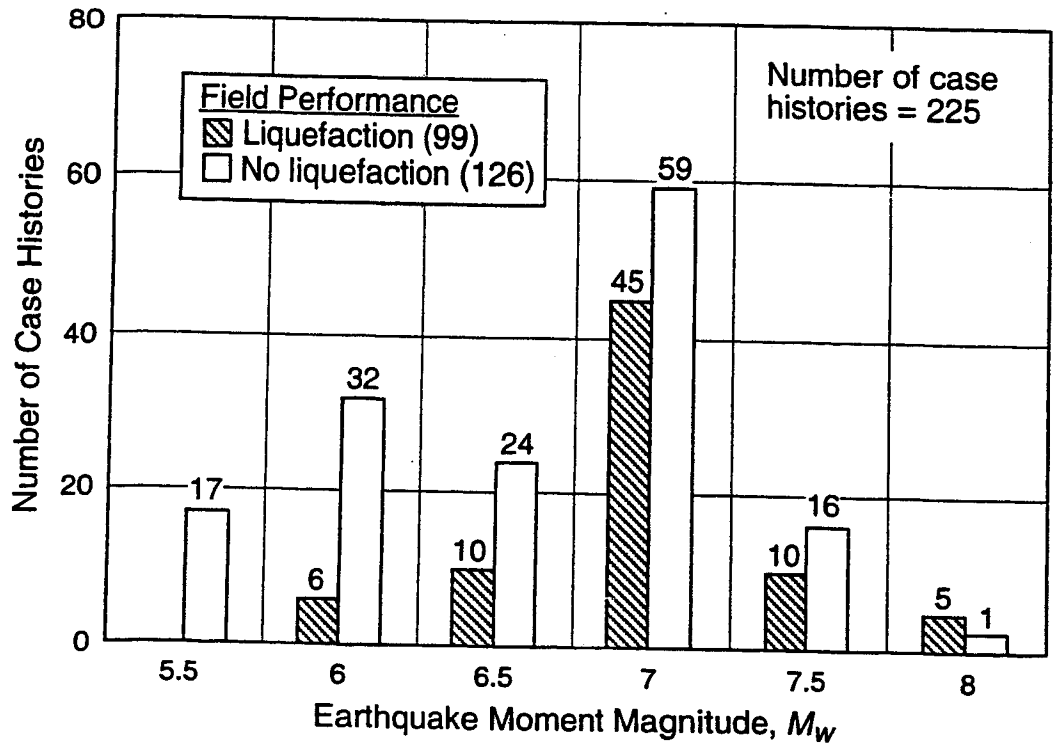

Fig. E.1 - Distribution of Liquefaction and Non-Liquefaction Case Histories by Earthquake Magnitude.

E.1.6 Critical Layer

The layer of soil most likely to liquefy at a site, or the critical layer, is the layer of non-plastic soil below the ground water table where values of V_{S1}, as defined in Chapter 2, and penetration resistance are generally the least and cyclic stress ratio relative to V_{S1} is the greatest. Figure E.2 presents the cumulative relative frequency distributions for the case histories by critical layer thickness and predominate soil type (gravel, or sand and silt). Critical layer thicknesses range from 1 m to as much as 15 m. About 50 % of the case histories have a critical layer thickness less than 3.5 m; 90 % of the case histories have a critical layer thickness less than 7 m. Overall, the layer thicknesses for the gravel cases are less than the layer thicknesses for the sand and silt cases

Figure E.3 presents the cumulative relative frequency distributions for the case histories by average V_S measurement depth in the critical layer and predominate soil type. The average measurement depths are between 2 m and 11 m for nearly all case histories. Over 50 % of the case histories have average measurement depths less than 5.5 m. About 90 % of the case histories have average measurement depths less than 8 m. Overall, the measurement depths for the gravel cases are less than the measurement depths for the sand and silt cases.

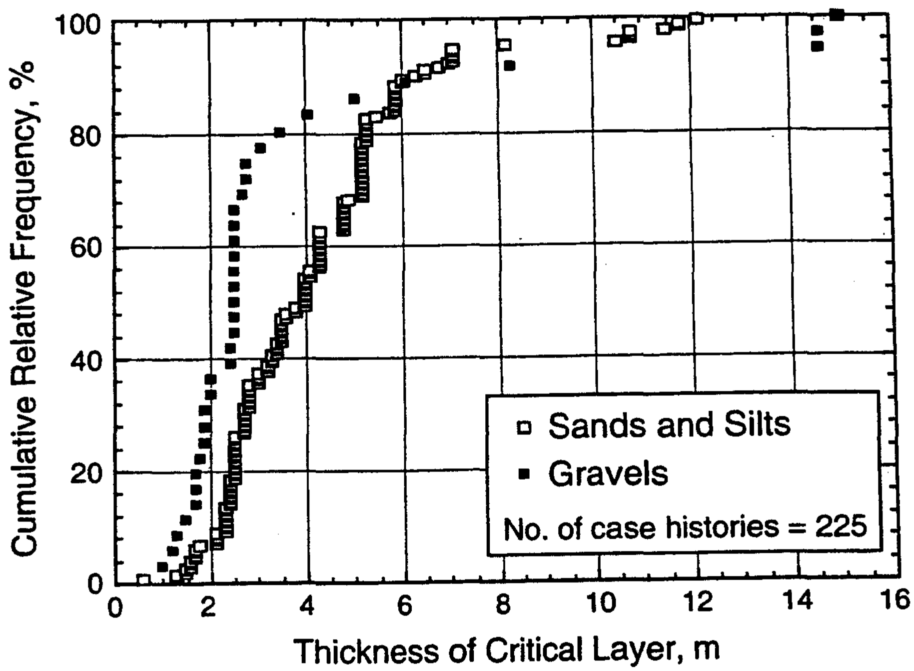

Fig. E.2 - Cumulative Relative Frequency of Case History Data by Critical Layer Thickness.

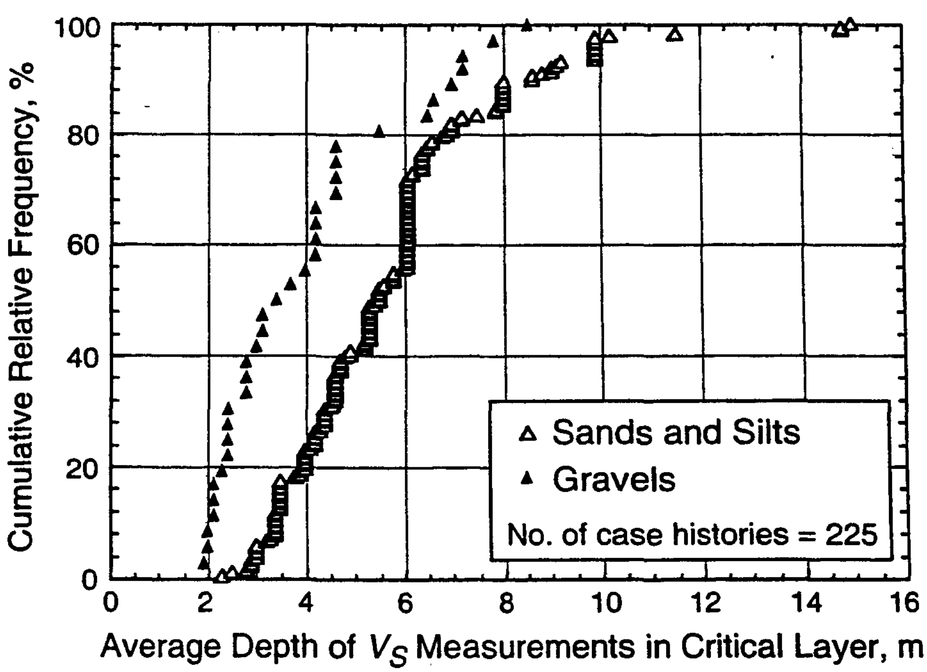

Fig. E.3 - Cumulative Relative Frequency of Case History Data by Average Depth of V_S Measurements in Critical Layer.

Materials comprising the critical layers range from clean fine sand to sandy gravel with cobbles to profiles including silty clay layers. In Fig. E.4, the distribution of case histories with earthquake magnitude, predominate soil type (gravel, or sand and silt) and average fines content (silt and clay) is presented. Of the 225 case histories, 28 were for sands with fines content *(FC)* ≤ 5 %, 90 for sands with *FC* = 6 % to 34 %, 71 for sands and silts with *FC* ≥ 35 %, 26 for gravels with FC ≤ 5 %, and 10 for gravels with *FC* = 6 % to 34 %.

About 70 % of the case histories are for natural soils deposits, with many formed by alluvial processes. The other 30 % are for hydraulic or dumped fills. Eight of the fills have been densified by soil improvement techniques.

At least 85 % of the case histories are of Holocene age (< 10 000 years). Although the age of the other 15 % is unknown, they are believed to be also of Holocene age.

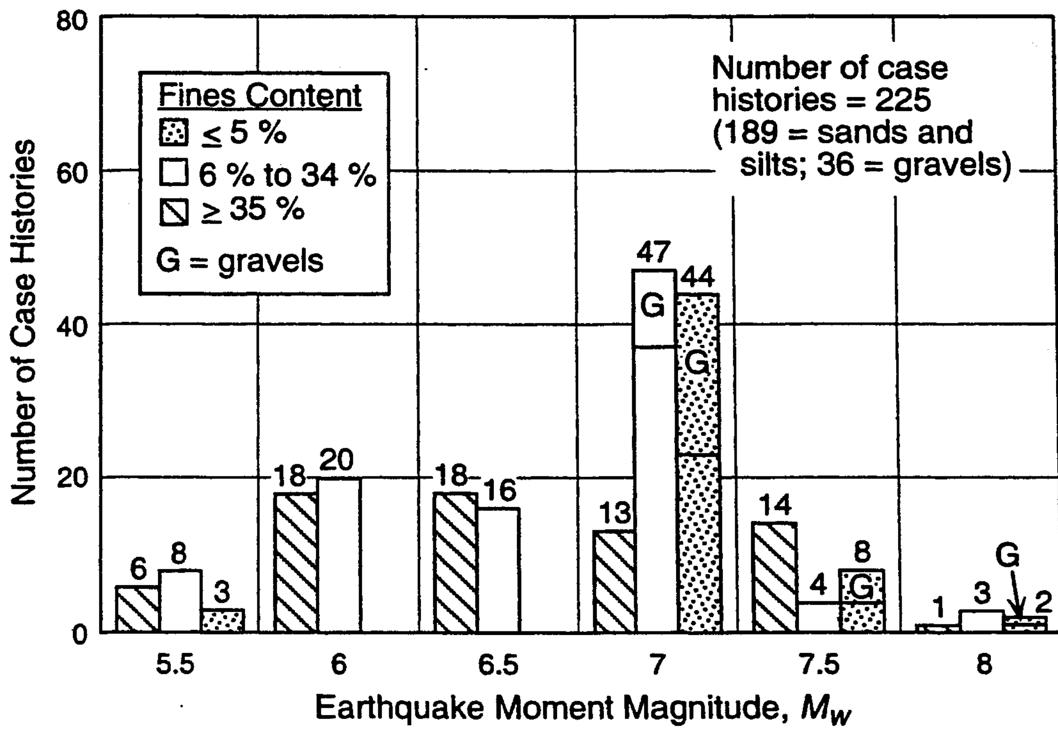

Fig. E.4 - Distribution of Case Histories by Earthquake Magnitude, Predominate Soil Type, and Average Fines Content.

E.1.7 Ground Water Table

Figure E.5 presents the cumulative relative frequency distributions for the case histories by depth to the ground water table and predominate soil type. The ground water table for nearly all case histories lies between depths of 0.5 m and 6 m. Nearly 60 % of the case histories have water table depths less than 2 m. About 90 % of the case histories have water table depths less than 4.5 m.

Artesian pressures are reported for the Lotung Large-Scale Seismic Test (LSST) Facility site in Taiwan. At this site, the pore-water pressure distribution is assumed to vary linearly from a pressure head of 8.1 m at a depth of 7 m to a pressure head of 1.9 m at a depth of 2 m.

E.1.8 Total and Effective Overburden Stresses

Values of total and effective overburden stresses are estimated using densities reported by the investigator(s). When no densities are reported, typical values for soils with similar grain size, penetration and velocity characteristics are assumed. In most instances, the assumed densities are 1.76 Mg/m^3 for soils above the water table and 1.92 Mg/m^3 for soils below the water table.

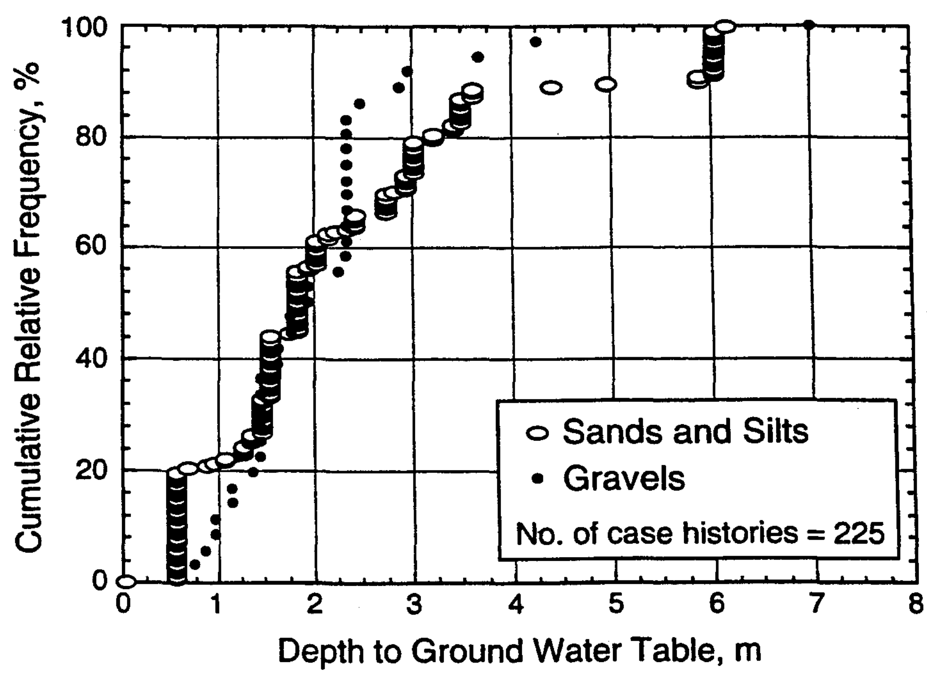

Fig. E.5 - Cumulative Relative Frequency of Case History Data by Depth to the Ground Water Table.

E.1.9 Average Peak Ground Acceleration

Average values of peak horizontal ground surface acceleration, a_{max}, are determined by averaging estimates reported by the investigator(s) and estimates made as part of this study using attenuation relationships developed from published ground surface acceleration data. Because many published attenuation relationships are based on both peak values obtained from ground motion records for the two horizontal directions (sometimes referred to as the randomly oriented horizontal component), the geometric mean (square root of the product) of the two peak values is used. Use of the geometric mean is consistent with the development of the SPT-based procedure (Youd et al., 1997; 2001). For the cases in this study, the difference between the geometric mean and arithmetic mean values is generally small, within about 5 %.

E.1.10 Average Cyclic Stress Ratio

Cyclic stress ratios, *CSR*, are first calculated for each "measurement" depth within the critical layer using Eq. 2.1 and then averaged. Values of r_d are estimated using the average relationship developed by Seed and Idriss (1971) shown in Fig. 2.1. These r_d values are used to follow the traditional format of the SPT- and CPT-based procedures where the magnitude scaling factor is used to account for all effects of earthquake magnitude.

E.1.11 Average Overburden Stress-Corrected Shear Wave Velocity

Values of V_S within the critical layer are first corrected for overburden stress using Eq. 2.7 and then averaged. The number of values included in the average range from 1 to 22 (see Appendix H). Values of C_{VS} used to correct measured shear wave velocities range from 1.4 to 0.9 for most of the data. About 80 % of the case histories have two to seven values in the average. No adjustments are made for possible variations between seismic test methods due to different source-receiver orientations with respect to the stress state in the soil. In the calculations, each site is assumed to be level ground.

E.2 SAMPLE CALCULATIONS

Calculations for two sites shaken by the 1989 Loma Prieta, California earthquake (M_w = 7.0) are presented below to illustrate how values of *CSR* and overburden stress-corrected shear wave velocity, V_{S1}, are determined. The two sites are Treasure Island Fire Station and Marina District School.

E.2.1 Treasure Island Fire Station

Treasure Island is a man-made island located in the San Francisco Bay along the Bay Bridge between the cities of San Francisco and Oakland. It was constructed in 1936-37 by hydraulic filling behind a perimeter rock dike.

Extensive field tests have been conducted at the fire station on Treasure Island. Figure E.6 presents two V_S profiles for the site. The V_S profile determined by crosshole testing is from Fuhriman (1993). The other V_S profile is based on unpublished SASW test results by The University of Texas at Austin in 1992. Also presented in Fig. E.6 is the soil profile for the site. From the description by de Alba et al. (1994), the upper 4.5 m of soil consists of silty sand fill, possibly formed by dumping. Between depths of 4.5 m and 12.2 m, the soil consists of silty sand to clayey sand, formed by hydraulic filling. Beneath the hydraulic fill are natural clayey soils. The ground water table lies near the ground surface at a depth of 1.4 m. The critical layer is determined to be between depths of 4.5 m and 7 m, where the soil is non-plastic, lies below the water table, and exhibits the lowest values of V_{S1} relative to the highest values of *CSR* in the layer (see Fig. 3.1).

During the 1989 Loma Prieta earthquake, a seismograph station at the fire station recorded ground surface accelerations. The peak values in the two horizontal accelerometer records are 0.16 g and 0.11 g (Brady and Shakal, 1994).

Sample calculations for the crosshole and SASW test arrays are summarized in Tables E.2 and E.3, respectively. The data points used in the calculations are shown by the open symbols in Fig. E.6. Total and effective overburden stresses are calculated assuming densities of 1.76 Mg/m^3 above the water table and 1.92 Mg/m^3 below the water table. Stress reduction coefficients are estimated using the average curve by Seed and Idriss (1971) shown in Fig. 2.1. The geometric mean of the two peak values observed in the horizontal ground surface acceleration records is 0.13 g. Using these parameters, values of *CSR* and V_{S1} are calculated for the crosshole measurement at depth of 4.6 m as follows:

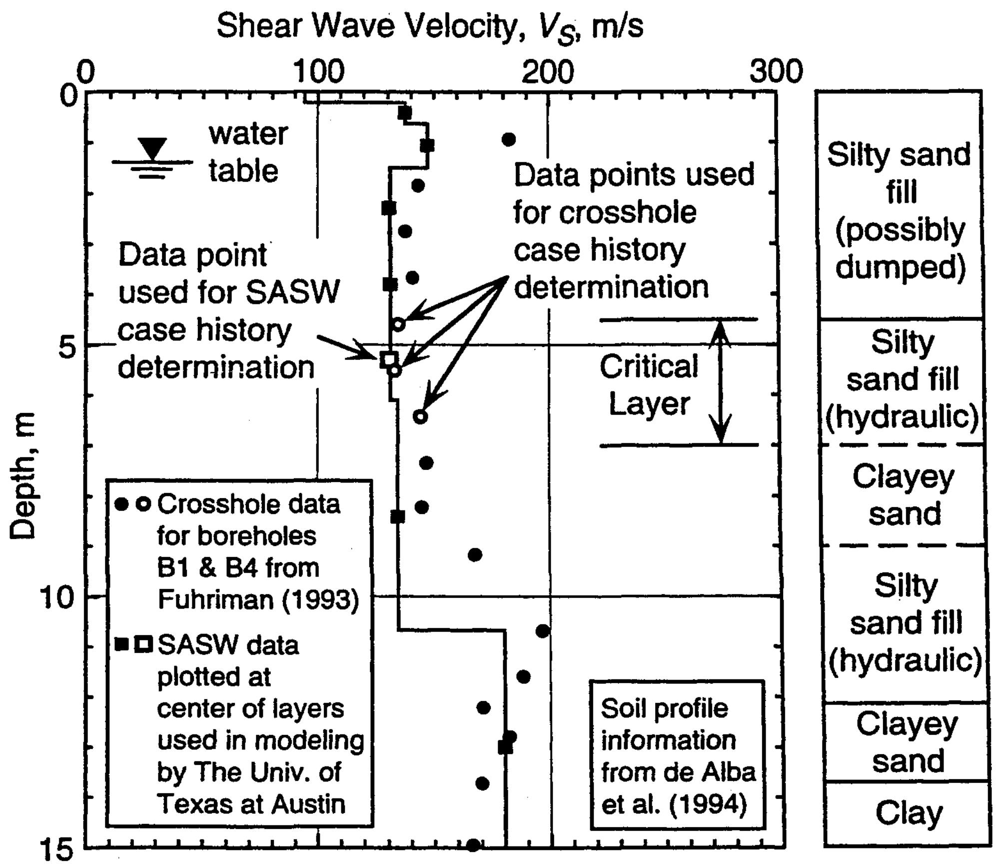

Fig. E.6 - Shear Wave Velocity and Soil Profiles for the Treasure Island Fire Station Site.

$$CSR = 0.65\left(\frac{a_{\max}}{g}\right)\left(\frac{\sigma_v}{\sigma'_v}\right)r_d = 0.65\left(\frac{0.13g}{g}\right)\left(\frac{84.0}{52.7}\right)0.97 = 0.131 \qquad \text{(E.1)}$$

and

$$V_{S1} = V_S\left(\frac{P_a}{\sigma'_v}\right)^{0.25} = 134\left(\frac{100}{52.7}\right)^{0.25} = 158 \text{ m/s} \qquad \text{(E.2)}$$

Representative values of CSR and V_{S1} used to defined the two case histories are determined by averaging values for each "measurement" depth within the critical layer, as shown in Tables E.2 and E.3.

E.2.2 Marina District School

Kayen et al. (1990) conducted downhole seismic tests at the Winfield Scott School in the Marina District of San Francisco. Figure E.7 presents soil and velocity profiles for the site. The critical layer lies between depths of 2.7 m, the ground water table depth, and 4.3 m, the base of sand fill. The average V_S profile shown in Fig. E.7 was determined by Kayen et al., and was based on best-fit line segments through travel time measurements plotted versus depth. The second V_S profile is determined using the pseudo-interval method (This Report), as illustrated in Fig. E.8. Both methods should provide similar average values over the same depth interval. However, the layering assumed for the best-fit line segment method does not seem appropriate for the fill. For this reason, values of V_S based on the pseudo-interval method are used in this analysis.

As discussed in Section 3.2, the Marina District of San Francisco experienced a peak horizontal ground surface acceleration of about 0.15 g during the 1989 Loma Prieta earthquake.

Sample calculations for the Marina District School site are summarized in Table E.4. The locations of V_S measurements are assumed midway between receiver positions, as shown in Fig. E.7. Total and effective overburden stresses are estimated assuming densities of 1.76 Mg/m^3 above the water table and 1.92 Mg/m^3 below the water table. The ground water table is at a depth of about 2.7 m. Average values of CSR and V_{S1} defining the case history are determined by averaging values for the two "measurement" depths, as shown in Table E.4

Table E.2 - Sample Calculations for the Treasure Island Fire Station Site, Crosshole Test Array B1- B4, and the 1989 Loma Prieta Earthquake.

Measurement Number (1)	Average Depth, m (2)	Measured Shear Wave Velocity, V_S, m/s (3)	Total Overburden Stress[1], kPa (4)	Effective Overburden Stress[1], kPa (5)	Stress Reduction Coefficient[2], r_d (6)	Cyclic Stress Ratio[3], CSR (7)	Overburden Stress-Corrected Shear Wave Velocity, V_{S1}, m/s (8)
1	4.57	134	84.0	52.7	0.97	0.13	158
2	5.49	133	111.3	60.9	0.96	0.14	150
3	6.40	144	118.5	69.2	0.95	0.14	158
	====	====	===	====	====	====	====
Average	5.5	137	101.3	60.9	0.96	0.14	155

[1]Assuming water table at 1.4 m; and material densities are 1.76 Mg/m^3 above the water table and 1.92 Mg/m^3 below the water table.
[2]Based on average values determined by Seed and Idriss (1971).
[3]Assuming peak horizontal ground surface acceleration is 0.13 g.

Table E.3 - Sample Calculations for the Treasure Island Fire Station Site, SASW Test Array, and the 1989 Loma Prieta Earthquake.

Measurement Number (1)	Average Depth, m (2)	Measured Shear Wave Velocity, V_S, m/s (3)	Total Overburden Stress[1], kPa (4)	Effective Overburden Stress[1], kPa (5)	Stress Reduction Coefficient[2], r_d (6)	Cyclic Stress Ratio[3], CSR (7)	Overburden Stress-Corrected Shear Wave Velocity, V_{S1}, m/s (8)
1	5.34	131	98.4	59.6	0.96	0.14	149
	====	====	===	====	====	====	====
Average	5.3	131	98.4	59.6	0.96	0.14	149

[1]Assuming water table at 1.4 m; and material densities are 1.76 Mg/m^3 above the water table and 1.92 Mg/m^3 below the water table.
[2]Based on average values determined by Seed and Idriss (1971).
[3]Assuming peak horizontal ground surface acceleration is 0.13 g.

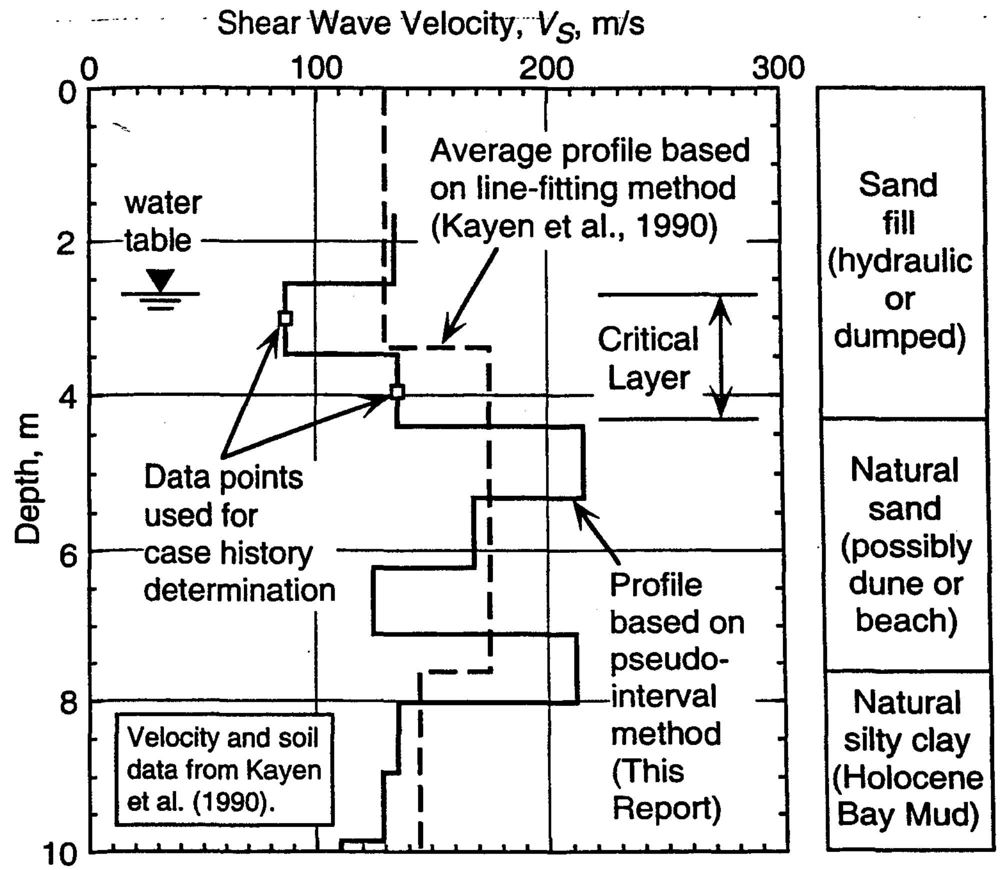

Fig. E.7 - Shear Wave Velocity and Soil Profiles for the Marina District School Site (Kayen et al., 1990).

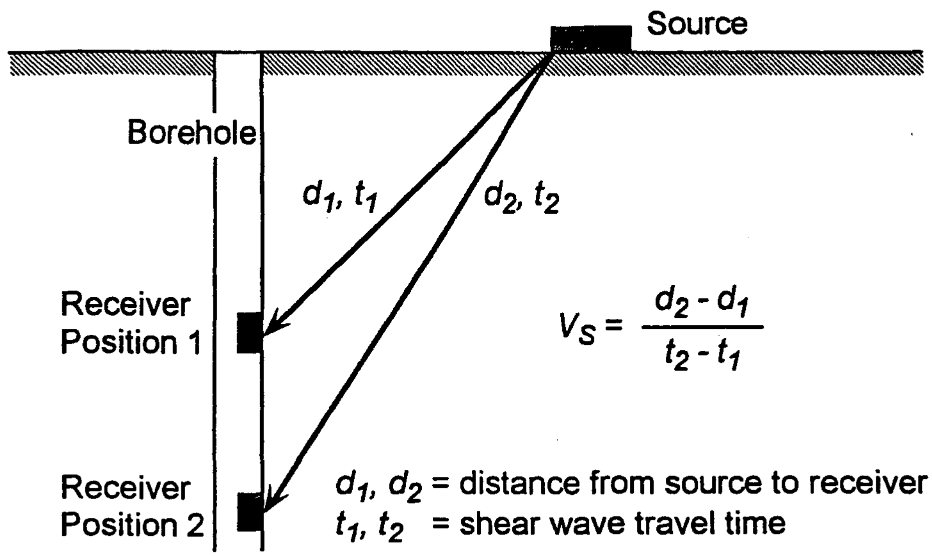

Fig. E.8 - General Configuration of the Downhole Seismic Test Using the Pseudo-Interval Method to Calculate Shear Wave Velocity.

E.3 SUMMARY

The case history data described in this chapter are limited to level and gently sloping sites with the following characteristics:

(1) average critical layer depths less than 10 m;
(2) uncemented soils of Holocene age;
(3) ground water table depths between 0.5 m and 6 m; and
(4) all V_S measurements from below the water table.

Of the 225 case histories, 57 are for soils with FC $\leq$ 5 %, 98 for soils with FC = 6 % to 34 %, and 70 with FC $\geq$ 35 %. About 20 % of the case histories are for soils containing more than 10 % gravel. Nearly 50 % of the case histories are for earthquake magnitudes near 7.

Table E.4 - Sample Calculations for the Marina District School Site and the 1989 Loma Prieta Earthquake.

Measurement Number (1)	Average Depth, m (2)	Measured Shear Wave Velocity[1], V_S, m/s (3)	Total Overburden Stress[2], kPa (4)	Effective Overburden Stress[2], kPa (5)	Stress Reduction Coefficient[3], r_d (6)	Cyclic Stress Ratio[4], *CSR* (7)	Overburden Stress-Corrected Shear Wave Velocity, V_{S1}, m/s (8)
1	3.02	87	52.6	49.9	0.98	0.10	104
2	3.94	136	70.0	58.2	0.97	0.11	156
	====	====	===	====	====	====	====
Average	3.5	112	61.3	54.1	0.98	0.11	130

[1]Based on pseudo-interval method.

[2]Assuming water table at 2.7 m; and material densities are 1.76 Mg/m^3 above the water table and 1.92 Mg/m^3 below the water table.

[3]Based on average values determined by Seed and Idriss (1971).

[4]Assuming peak horizontal ground surface acceleration is 0.15 g.

APPENDIX F

DEVELOPMENT OF LIQUEFACTION RESISTANCE CURVES FROM CASE HISTORY DATA

In the process of developing the liquefaction evaluation chart shown in Fig. 2.3 all case histories were initially plotted on the same chart. This aggregation was accomplished through an adjustment procedure; that is, the *CSR* values in each case history were adjusted to an earthquake with M_w = 7.5 by dividing by Eq. (2.9) with n = -2.56. As done in penetration evaluation procedures, the sandy soil case histories were separated into three categories: (1) sands with average $FC \leq 5$ %; (2) sands with average FC = 6 % to 34 %; and (3) sands and silts with average $FC \geq 35$ %. For consistency, the gravelly soil case histories also were divided into the same three categories based on fines content. However, no case histories exist in the database with gravel having FC $\geq$ 35 %. All data are plotted in Fig. F.1 along with the recommended CRR-V_{S1} curves. Development of these curves is discussed in this appendix.

The shape of the CRR-V_{S1} curves shown in Fig. F.1 is based on a modified relationship between shear wave velocity and cyclic stress ratio for constant average cyclic shear strain suggested by R. Dobry. The modified relationship is expressed as (Andrus and Stokoe, 1997):

$$CRR_{7.5} = \left\{ a\left(\frac{V_{S1}}{100}\right)^2 + b\left(\frac{1}{V_{S1}^* - V_{S1}} - \frac{1}{V_{S1}^*}\right)\right\} \qquad \text{(F.1)}$$

where

$CRR_{7.5}$ = CRR for magnitude 7.5 earthquakes,
V_{S1}^* = the limiting upper value of V_{S1} for liquefaction occurrence, and
a, b = curve fitting parameters.

As discussed in Section D.5, the first (quadratic) term of Eq. (F.1) is a form of Dobry's relationship given by Eq. (D.9). The second term is a hyperbola with a small value at low values of V_{S1}, and a very large value as V_{S1} approaches V_{S1}^*.

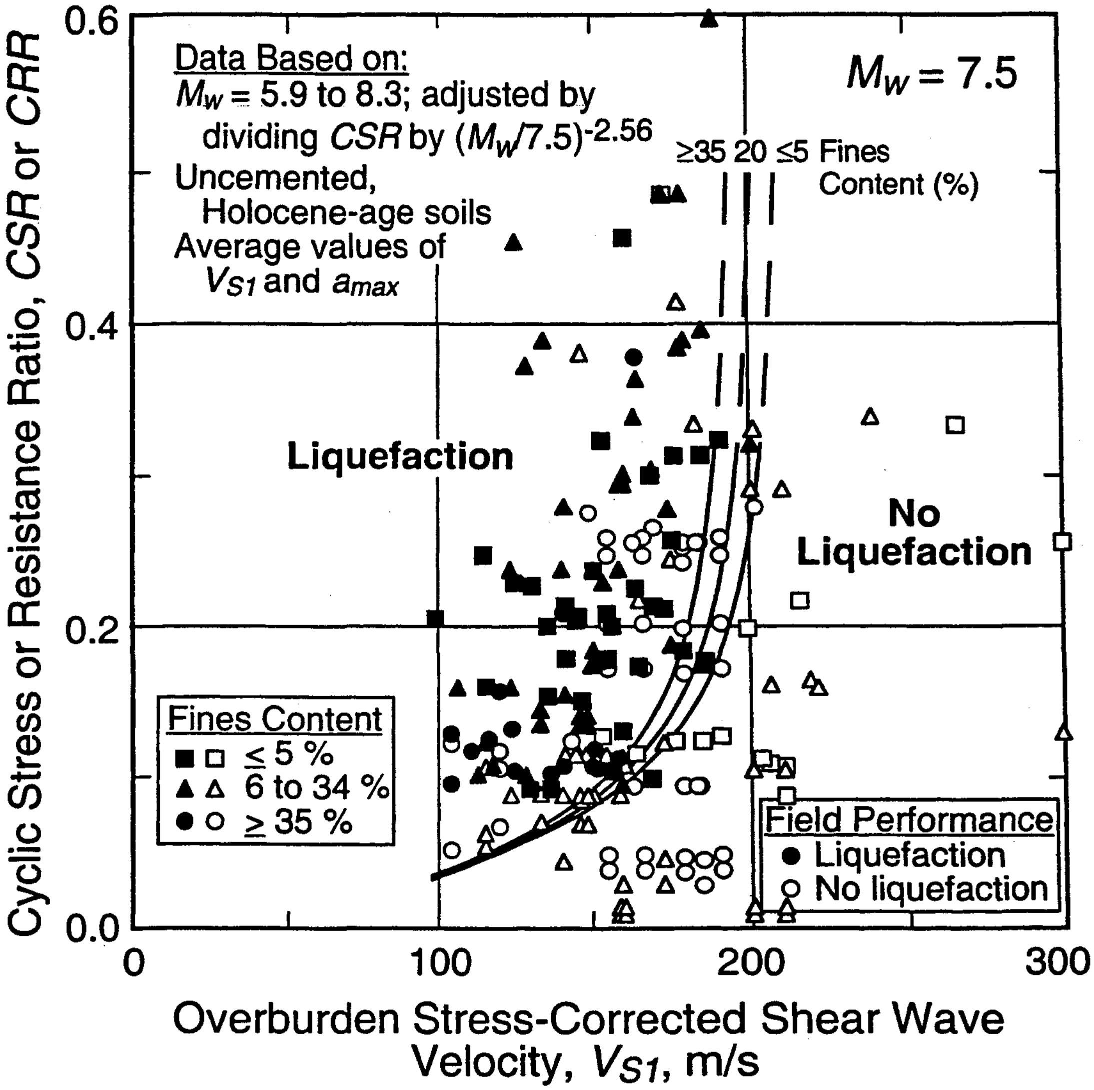

Fig. F.1 - Curves Recommended for Calculation of *CRR* from Shear Wave Velocity Measurements Along with Case History Data Based on **Lower Bound** Values of *MSF* for the Range Recommended by the 1996 NCEER Workshop (Youd et al., 1997) and r_d Developed by Seed and Idriss (1971).

F.1 LIMITING UPPER V_{S1} VALUE FOR LIQUEFACTION OCCURRENCE

As shown in Fig. F.1, *CSR*-values above about 0.35 are limited in the case history data. Thus, current estimates of V^*_{S1} rely, in part, on penetration-shear wave velocity correlations and, in part, on the data trend in Fig. F.1.

F.1.1 Sandy Soils

In the SPT-based procedure, a corrected blow count, $(N_1)_{60}$, of 30 is assumed as the limiting upper value for liquefaction occurrence in sands with ≤ 5 % silt and clay (Seed et al., 1985; Youd et al., 1997). Table F.1 presents estimates of equivalent V_{S1} for corrected blow count of 30. The correlation by Ohta and Goto (1978) modified to a blow count with a theoretical free-fall energy of 60 % (Seed et al., 1985) suggested equivalent V_{S1} values of 207 m/s for Holocene sands, assuming that a depth of 10 m is equivalent to an effective overburden stress of 100 kPa. The stress-corrected crosshole measurements compiled by Sykora (1987b) for Holocene sands and non-plastic silty sands below the ground water table, with $(N_1)_{60}$ between 25 and 35, exhibited an average V_{S1} value of 206 m/s and standard deviation of 41 m/s. Finally, the case history data in this study were used to investigate the V_{S1} and $(N_1)_{60}$ relationship for well-documented sand layers with less than 10 % fines. These data are presented in Fig. F.2 along with the best-fit relationship that can be expressed as:

$$V_{S1} = B_1\left[(N_1)_{60}\right]^{B_2} \tag{F.2}$$

where $B_1 = 93.2 \pm 6.5$ and $B_2 = 0.231 \pm 0.022$ for soils with fines content < 10 %, and with V_{S1} in m/s and $(N_1)_{60}$ in blows/0.3 m. The plotted data exhibit a mean V_{S1} value of 204 m/s at a $(N_1)_{60}$ value of 30 and residual standard deviation, S_{res}, of 12 m/s.

In the CPT-based procedure, a normalized cone tip resistance, q_{c1N}, of 160 is assumed as the limiting upper value for liquefaction occurrence in sands with ≤ 5 % silt and clay (Youd et al., 1997; Robertson and Wride, 1998). Figure F.3 presents average values of V_{S1} and q_{c1N} for soil layers with less than 10 % fines at several sites listed in Table E.1. Also shown in Fig. F.3 is the best-fit relationship for the plotted data, which can be expressed as:

$$V_{S1} = B_1\left[q_{c1N}\right]^{B_2} \tag{F.3}$$

where $B_1 = 88.2 \pm 15.5$ and $B_2 = 0.154 \pm 0.037$ for soils with fines content < 10 %, and with V_{S1} in m/s and q_{c1N} is normalized tip resistance based on procedures by Robertson and Wride (1998). As noted in Table F.2, the plotted data exhibit a mean V_{S1} value of 193 m/s at a q_{c1N} value of 160 and residual standard deviation of 19 m/s.

Table F.1 - Estimates of Equivalent V_{S1} for Holocene Sands and Gravels Below the Ground Water Table with Corrected SPT **Blow Count of 30**.

Reference (1)	Relationship (2)	Equivalent V_{S1} Estimate (m/s) (3)	Assumptions (4)
Ohta & Goto (1978); also given in report by Sykora (1987a, page 29)	$V_S = 69\ (N_j)^{0.173}\ z^{0.195}\ F_1 F_2$ N_j = SPT blow count measured in Japanese practice z = depth, m F_1 = 1.00 for Holocene-age soils F_2 = 1.085 for sands; 1.189 for gravel ...best-fit relationship for 289 sets of SPT and V_S measurements from Japan	207 ...for Holocene sands 227 ...for Holocene gravels	1. $N_j = 60/67\ N_{60}$ 2. $N_{60} = 30$ 3. z = 10 m is equivalent to an overburden stress of 100 kPa 4. All measurements are from below the ground water table
Sykora (1987b, page 90); This Report	Correlation between $(N_1)_{60}$ and crosshole V_S, normalized to effective overburden stress, measurements for Holocene sands and non-plastic silty sands below the ground water table at sites in U.S.A.; 16 sets of measurements (with known SPT equipment)	206 ...for Holocene sands and non-plastic silty sands below the water table ...standard deviation is 41 m/s	1. Average for V_{S1} values with $(N_1)_{60}$ between 25 and 35 2. σ'_v = 100 kPa
Rollins et al. (1998a)	$V_S = 53\ (N_{60})^{0.19}\ (\sigma'_v)^{018}$ ...best-fit relationship using equivalent N_{60}-values from Becker Penetration Tests and V_S measurements; 186 points from 7 Holocene gravel sites	232 ...for Holocene gravels ...most of data lie within ±25 % of relationship	1. $N_{60} = 30$ 2. σ'_v = 100 kPa 3. All measurements are from below the ground water table
This Report (see Fig. F.2)	$V_{S1} = B_1\ [(N_1)_{60}]^{B2}$ B_1 = 93.2 ± 6.5 B_2 = 0.231 ± 0.022 ...best-fit relationship for uncemented, Holocene-age sands with less than 10 % non-plastic fines; 25 sets of average SPT and V_S measurements all from below the water table	204 ...for Holocene clean sands below the water table ...residual standard deviation is 12 m/s	1. Average for V_{S1} with $(N_1)_{60} = 30$ 2. σ'_v = 100 kPa 3. Corrected blow count based on procedures given in Seed et al. (1985) and Robertson and Wride (1997; 1998)

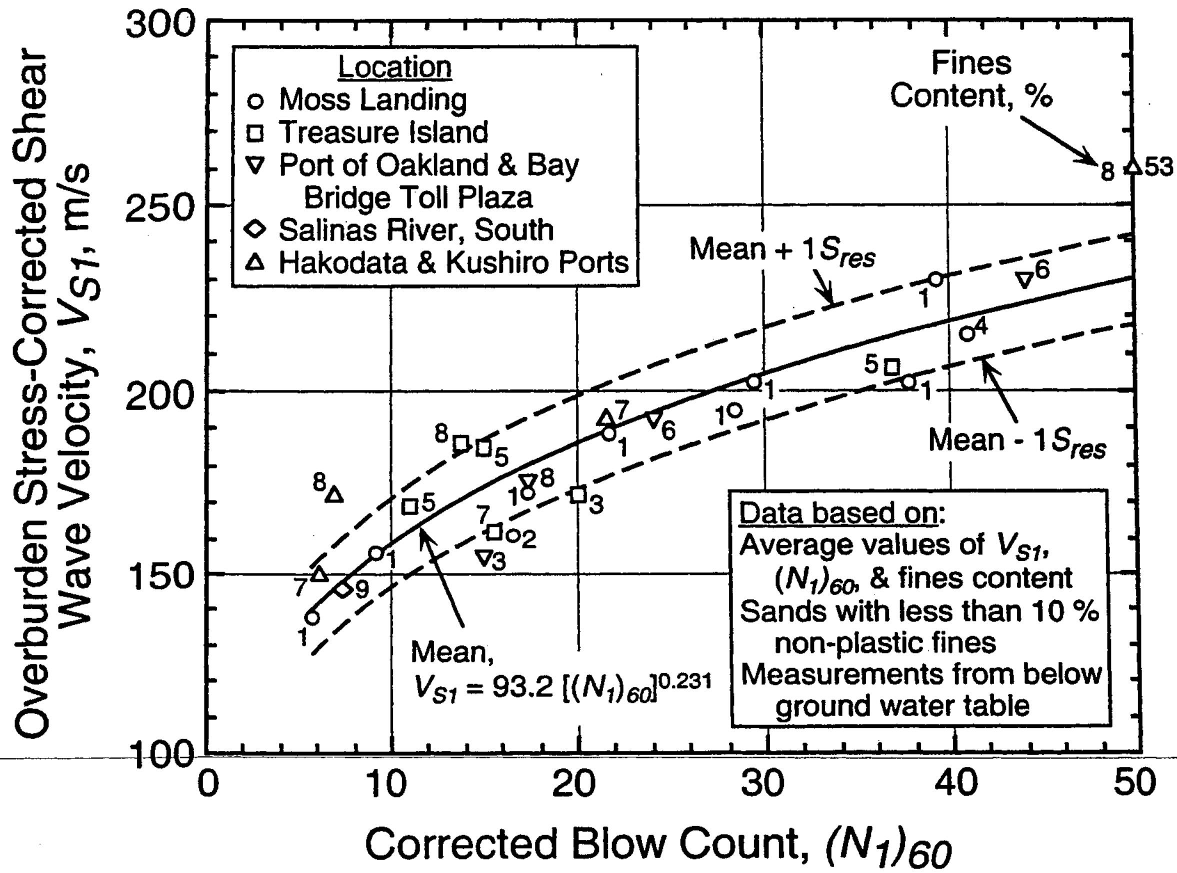

Fig. F.2 - Variations in V_{S1} with $(N_1)_{60}$ for Uncemented, Holocene-age Sands with Less than 10 % Non-Plastic Fines.

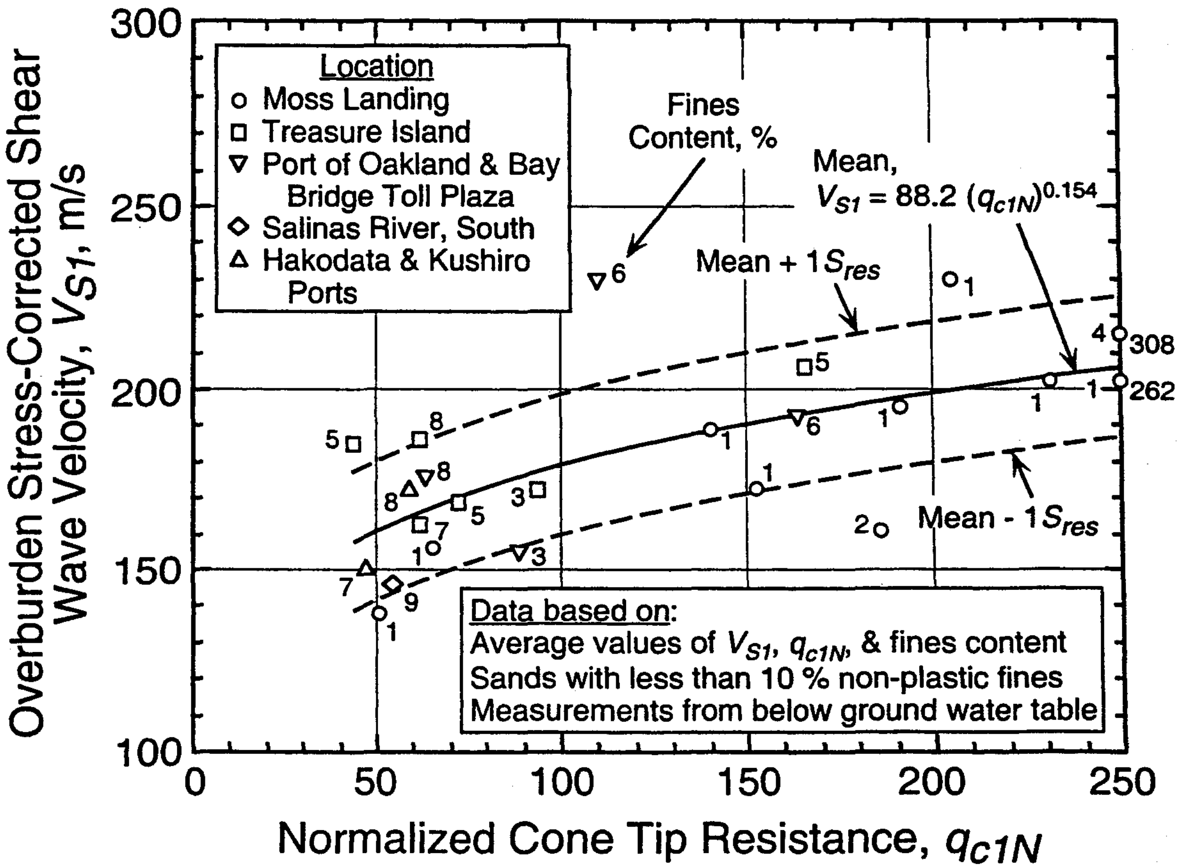

Fig. F.3 - Variations in V_{S1} with q_{c1N} for Uncemented, Holocene-age Sands with Less than 10 % Non-Plastic Fines.

Table F.2 - Estimates of Equivalent V_{S1} for Holocene Sands Below the Ground Water Table with Normalized Cone Tip Resistance of 160.

Reference (1)	Relationship (2)	Equivalent V_{S1} Estimate (m/s) (3)	Assumptions (4)
This Report (see Fig. F.3)	$V_{S1} = B_1 \, (q_{c1N})^{B2}$ $B_1 = 88.2 \pm 15.5$ $B_2 = 0.154 \pm 0.037$ ...best-fit relationship for uncemented, Holocene-age sands with less than 10 % non-plastic fines; 23 sets of average SPT and V_S measurements all from below the water table	193 ...for Holocene clean sands below the water table ...residual standard deviation is 19 m/s	1. Average for V_{S1} with $q_{c1N} = 160$ 2. $\sigma'_v = 100$ kPa 3. Normalized tip resistance based on procedures given in Robertson and Wride (1997; 1998)

From these estimates, a V_{S1} value of 210 m/s is assumed equivalent to an $(N_1)_{60}$ value of 30 in clean sands ($\leq$ 5 % fines). A limiting upper V_{S1} value of 210 m/s for cyclic liquefaction occurrence at CSR = 0.6 is less than the general consensus value of 230 m/s suggested at the 1998 MCEER Workshop. As a result, Figs. F.2 and F.3 were added specifically to provide additional evidence to support the use of 210 m/s in clean sands.

For sandy and silty soils with FC $\geq$ 35 %, the SPT-based chart by Seed et al. (1985) indicates a limiting upper $(N_1)_{60}$ value of about 21 for cyclic liquefaction occurrence. Table F.3 presents estimates of equivalent V_{S1} for blow count of 21. The correlation by Ohta and Goto (1978) suggested equivalent V_{S1} values of 195 m/s for Holocene sands. The stress-corrected crosshole compiled by Sykora (1987b) for Holocene sands and non-plastic silty sands below the ground water table, with $(N_1)_{60}$ between 16 and 26, exhibited an average value of 199 m/s and standard deviation of 36 m/s. From these estimates, a V_{S1} value of 195 m/s is assumed equivalent to an $(N_1)_{60}$ value of 21 in non-plastic soils with FC $\geq$ 35 %.

To permit the CRR-V_{S1} curves for magnitude 7.5 earthquakes shown in Fig. F.1 to have V_{S1} values between 195 m/s and 210 m/s at CRR near 0.6, values of V^*_{S1} are assumed to range linearly from 200 m/s to 215 m/s, respectively. The relationship between V^*_{S1} and fines content, FC, can be expressed by:

$V^*_{S1} = 215$ m/s	for sands with $FC \leq 5$ %	(F.4a)
$V^*_{S1} = 215 - 0.5(FC-5)$ m/s	for sands with 5 % $< FC <$ 35 %	(F.4b)
$V^*_{S1} = 200$ m/s	for sands and silts with $FC \geq 35$ %	(F.4c)

To illustrate how well the recommended CRR-V_{S1} curves defined by Eqs. (F.1) and (F.4) fit the case history data, the data separated by soil type, are presented in Figs. F.4 through F.7. The recommended curves provide reasonable bounds for all the case history data above a CSR value of 0.35, supporting the use of the suggested V^*_{S1} values for sands and silts, as well as gravels. The use of these V^*_{S1} values for gravels is discussed below.

Table F.3 - Estimates of Equivalent V_{S1} for Holocene Sands and Gravels Below the Ground Water Table with Corrected SPT **Blow Count of 21**.

Reference (1)	Relationship (2)	Equivalent V_{S1} Estimate (m/s) (3)	Assumptions (4)
Ohta & Goto (1978); also given in report by Sykora (1987a, page 29)	$V_S = 69\ (N_j)^{0.173}\ z^{0.195}\ F_1F_2$ N_j = SPT blow count measured in Japanese practice z = depth, m F_1 = 1.00 for Holocene-age soils F_2 = 1.085 for sands; 1.189 for gravel ...best-fit relationship for 289 sets of SPT and V_S measurements from Japan	195 ...for Holocene sands 214 ...for Holocene gravels	1. $N_j = 60/67\ N_{60}$ 2. $N_{60} = 21$ 3. z = 10 m is equivalent to an overburden stress of 100 kPa 4. All measurements are from below the ground water table
Sykora (1987b, page 90); This Report	Correlation between $(N_1)_{60}$ and crosshole V_S, normalized to effective overburden stress, measurements for Holocene sands and non-plastic silty sands below the water table at sites in U.S.A.; 31 sets of measurements (with known SPT equipment)	199 ...for Holocene sands and non-plastic silty sands below the water table ...standard deviation is 36 m/s	1. Average for V_{S1} values with $(N_1)_{60}$ between 16 and 26 2. σ'_v = 100 kPa
Rollins et al. (1998a)	$V_S = 53\ (N_{60})^{0.19}\ (\sigma'_v)^{018}$ ...best-fit relationship using equivalent N_{60}-values from Becker Penetration Tests and V_S measurements; 186 points from 7 Holocene gravel sites	217 ...for Holocene gravels ...most of data lie within ±25 % of relationship	1. $N_{60} = 21$ 2. σ'_v = 100 kPa 3. All measurements are from below the ground water table

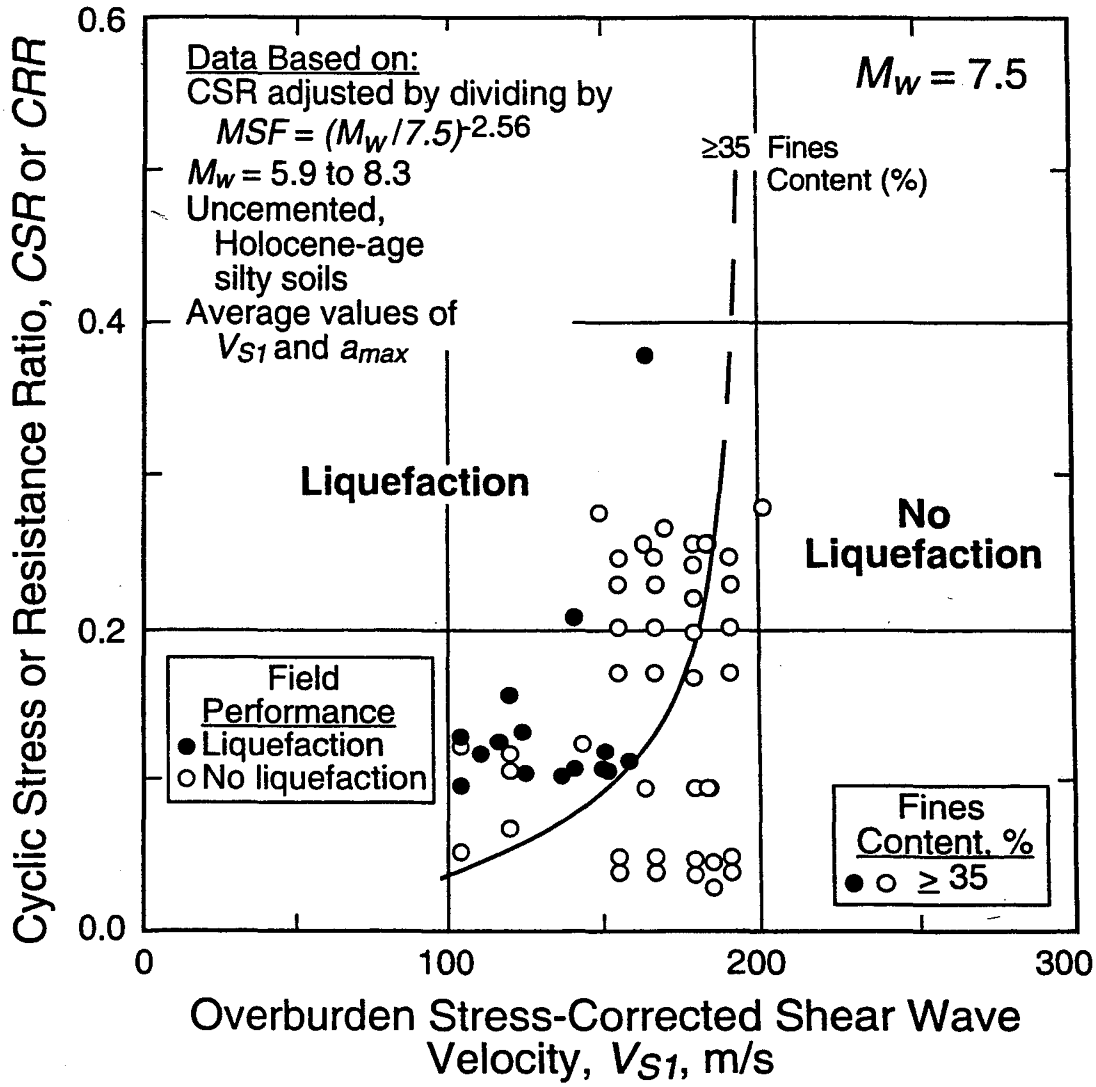

Fig. F.4 - Curve Recommended for Calculation of *CRR* from V_{S1} Measurements in Sands and Silts with $FC \geq 35$ % along with Case History Data.

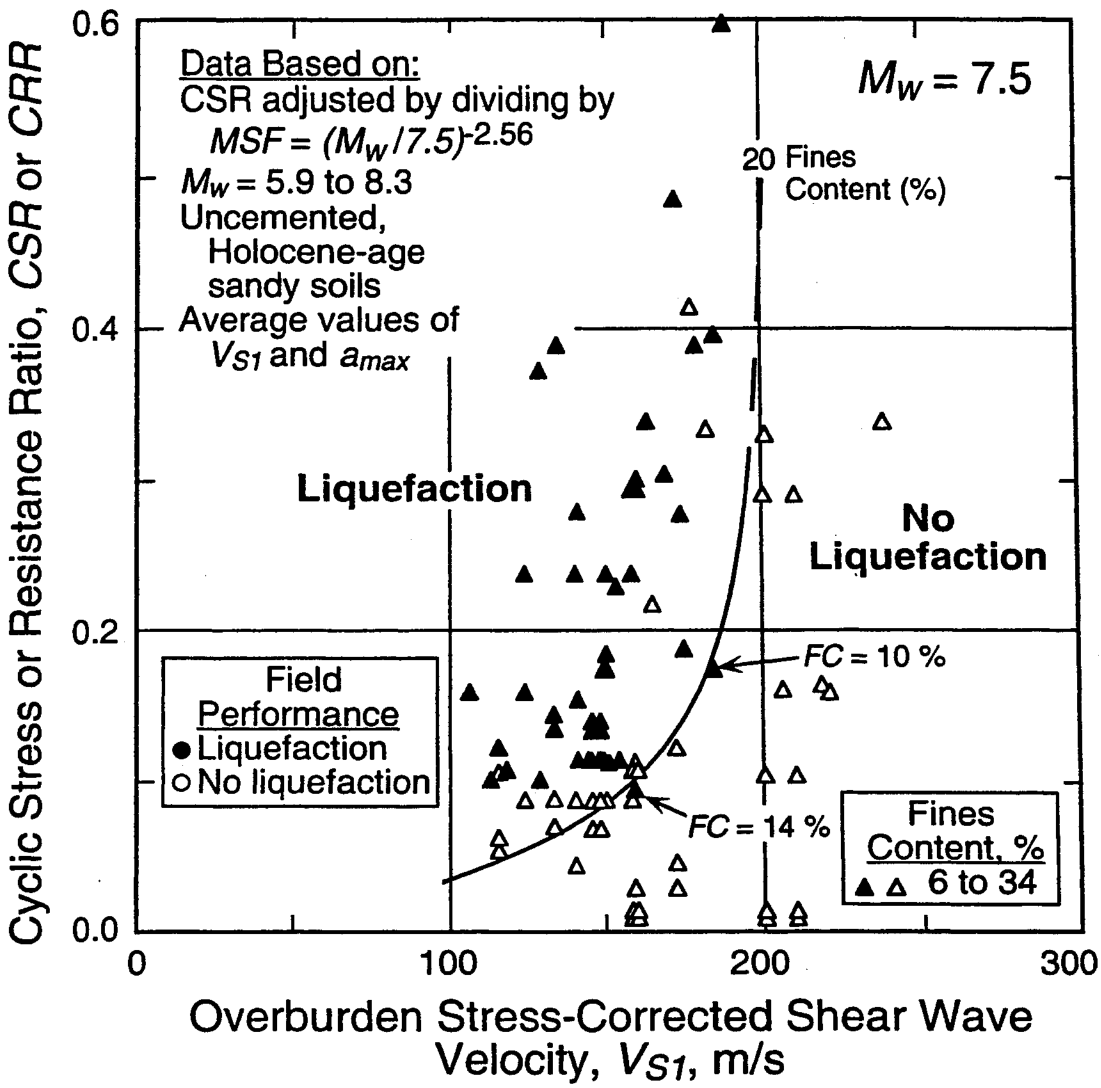

Fig. F.5 - Curve Recommended for Calculation of *CRR* from V_{S1} Measurements in Sands with *FC* = 20 % along with Case History Data.

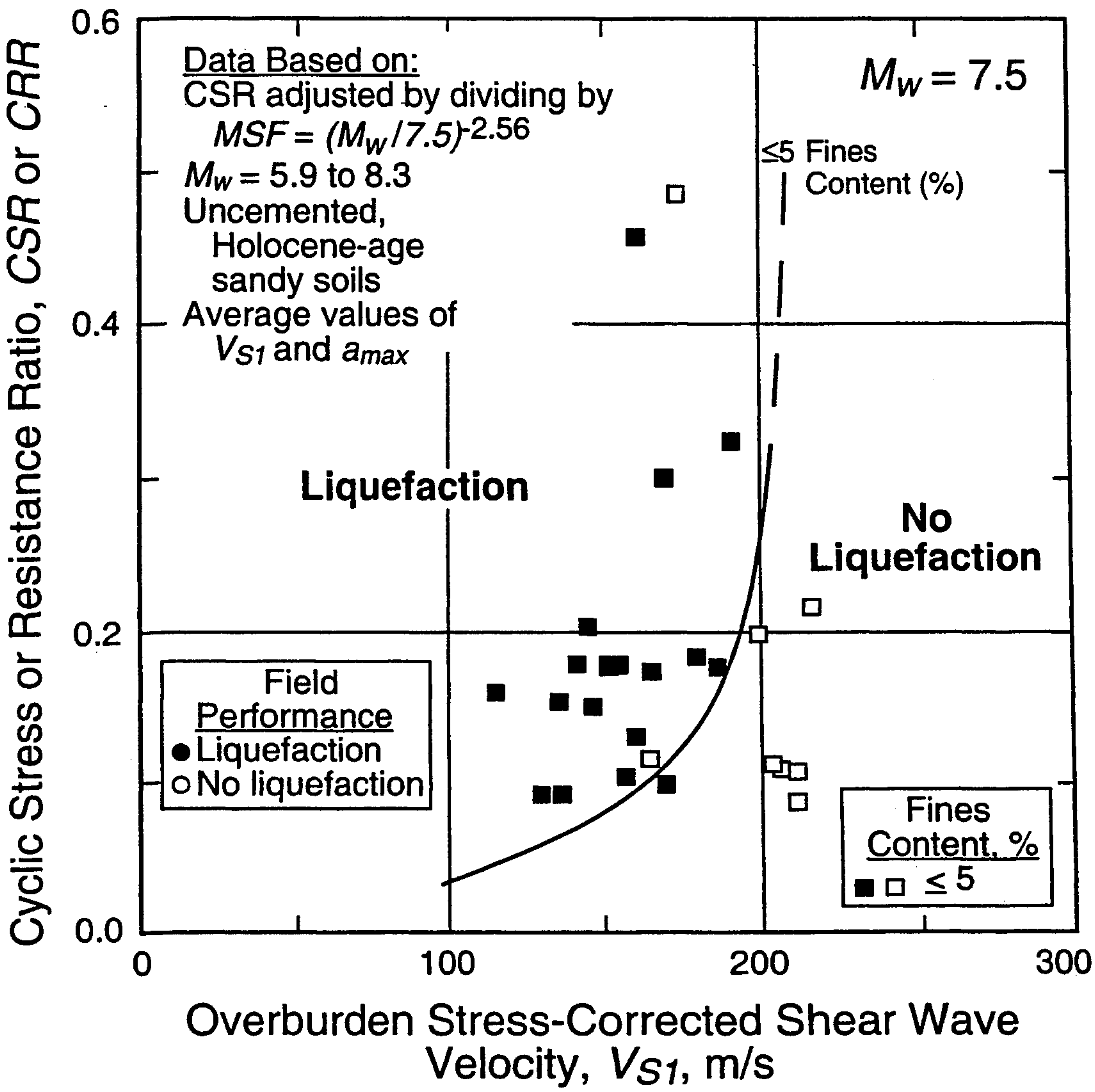

Fig. F.6 - Curve Recommended for Calculation of *CRR* from V_{S1} Measurements in Sands with $FC \leq 5$ % along with Case History Data.

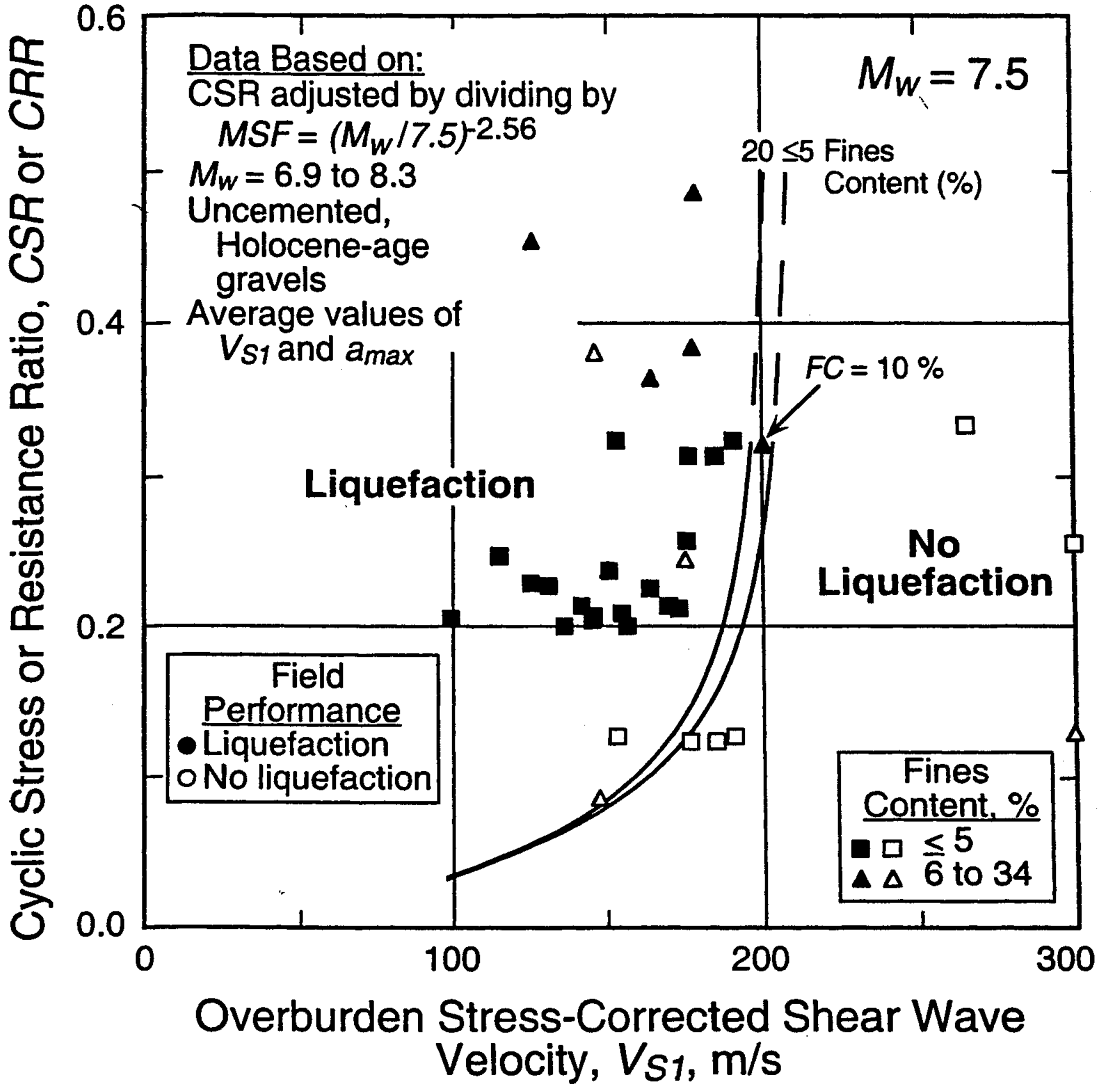

Fig. F.7 - Curves Recommended for Calculation of *CRR* from V_{S1} Measurements in Gravels with $FC \leq 5$ % and $FC = 20$ % along with Case History Data.

F.1.2 Gravelly Soils

Although the V^*_{S1} values given in Eq. (F.4) were determined for sandy soils, the results presented in Fig. F.7 indicate that these limits also represent reasonable limits for gravelly soils divided into the same categories based on fines content. This might be considered rather surprising, based on the penetration-V_S correlations presented in the literature for gravelly soils. For instance, as noted in Table F.1, the correlation by Ohta and Goto (1978) suggested a V_{S1} value of 227 m/s for Holocene gravels at an equivalent $(N_1)_{60}$ of 30. Similarly, the correlation by Rollins et al. (1998a) provided a best-fit value of 232 m/s for Holocene gravels. On the other hand, all the liquefaction case history data shown in Figs. F.4 through F.7 exhibit V_{S1} values of about 200 m/s or less, suggesting that 230 m/s may be inappropriately high.

To investigate further the value of V^*_{S1} in gravelly soils, laboratory studies involving V_S measurements in gravelly soils were reviewed. Kokusho et al. (1995b) clearly showed that the shear wave velocity of gravelly soils varies greatly and is highly dependent on the particle gradation. Weston (1996) showed similar results for coarse sands with gravels. In both cases, the results show that increasing the uniformity coefficient can significantly increase the shear wave velocity in medium dense to dense gravels. On the other hand, very loose gravelly soils, even well-graded gravels, can exhibit shear wave velocities similar to those of loose sands (Kokusho et al., 1995b). The case history data presented in Fig. F.7 supports the premise that gravelly soils that are loose enough to exhibit significant liquefaction effects (boils, ground cracks, etc.) have shear wave velocities similar to loose sands. Hence, the authors recommend the boundaries developed for sandy soils as preliminary boundaries for gravelly soils. However, additional work is clearly needed to understand the relationship between V_{S1} and liquefaction resistance of gravels.

F.2 CURVE FITTING PARAMETERS *a* AND *b*

The curve fitting parameters a and b in Eq. (F.1) can be approximated from the case history data assuming the values of V^*_{S1} given in Eq. (F.4) and a *MSF* relationship. Three *MSF* relationships representing the range of proposed magnitude scaling factors (see Section 2.3.1) are considered below to establish the values of a and b in Eq. (F.1).

F.2.1 Magnitude Scaling Factors Recommended by 1996 NCEER Workshop

F.2.1.1 Lower Bound of Recommended Range—Figure F.1 presents the case history data for magnitude 5.9 to 8.3 earthquakes adjusted using the lower bound for the range of magnitude scaling factors recommended by the 1996 NCEER workshop (Youd et al., 1997). The lower bound is defined by Eq. (2.9) with n = -2.56, as discussed in Section 2.3.1. Also shown in Fig. F.1 are three recommended *CRR*-V_{S1} curves for earthquakes with magnitude near 7.5 and various fines content. The three curves were determined through an iterative process of varying the values of *a* and *b* until nearly all the liquefaction case histories were bound by the curves with the least amount of non-liquefaction case histories in the liquefaction region. The final values of *a* and *b* used to draw the curves were 0.022 and 2.8, respectively.

Of the 99 liquefaction case histories, only two liquefaction case histories incorrectly lie in the no liquefaction region. The two liquefaction case histories shown in Fig. F.1 that incorrectly lie in the no liquefaction region are two sites at Treasure Island (UM05 and UM09) where liquefaction was marginal during the 1989 Loma Prieta earthquake (M_w = 7). The sites are located along the perimeter of Treasure Island. Mapped liquefaction effects generated by the 1989 earthquake near the UM05 site are ground cracks with 50 to 90 mm of horizontal displacement (R. D. Hryciw, personal communication to R. D. Andrus, 1998; Power et al., 1998). The nearest mapped sand boil is located 60 m away from the site. At the UM09 site, as much as 90 mm of vertical displacement was observed adjacent to a building located 60 m inland from the site. These displacements are small compared to the meters of displacement that are expected to occur during larger ground shaking. Thus, liquefaction was marginal at the UM05 and UM09 sites, and sloping ground may have been a factor. It is interesting to note that similar incorrect evaluations also are obtained when one uses the SPT and CPT data for these two sites. The SPT- and CPT-based evaluations for the UM05 site are discussed in Section F.3.1.

F.2.1.2 Upper Bound of Recommended Range—Figure F.8 presents the case history data for magnitude 5.9 to 8.3 earthquakes adjusted using the upper bound for the range of magnitude scaling factors recommended by the 1996 NCEER Workshop (Youd et al., 1997). The upper bound is defined by Eq. (2.9) with n = -3.3, as discussed in Section 2.3.1. Also shown in Fig. F.8 are the three *CRR*-V_{S1} curves from Fig. F.1. Many case histories plot lower in Fig. F.8 than in Fig. F.1, because the M_w is less than 7.5 for most of the data. The downward shift in the liquefaction data points near the curves at *CRR* of about 0.08 is less than 0.01. This difference is not significant, and is within the accuracy of the plotted case history data.

F.2.2 Revised Magnitude Scaling Factors Proposed by Idriss (1999)

Figure F.9 presents the case history data for magnitude 5.9 to 8.3 earthquakes adjusted using the revised magnitude scaling factors and stress reduction coefficients proposed by Idriss (1999, as discussed in Section 2.3.1. Also shown in Fig. F.9 are the three *CRR*-V_{S1} curves from Fig. F.1. Many of the case history data shown in Fig. F.9 plot higher than case history data in Fig. F.1, because the M_w is less than 7.5 for most of the data. The upward shift in the liquefaction data points near the curves at *CRR* of about 0.08 is less than 0.01. Again, this difference is not significant, and is within the accuracy of the plotted case history data.

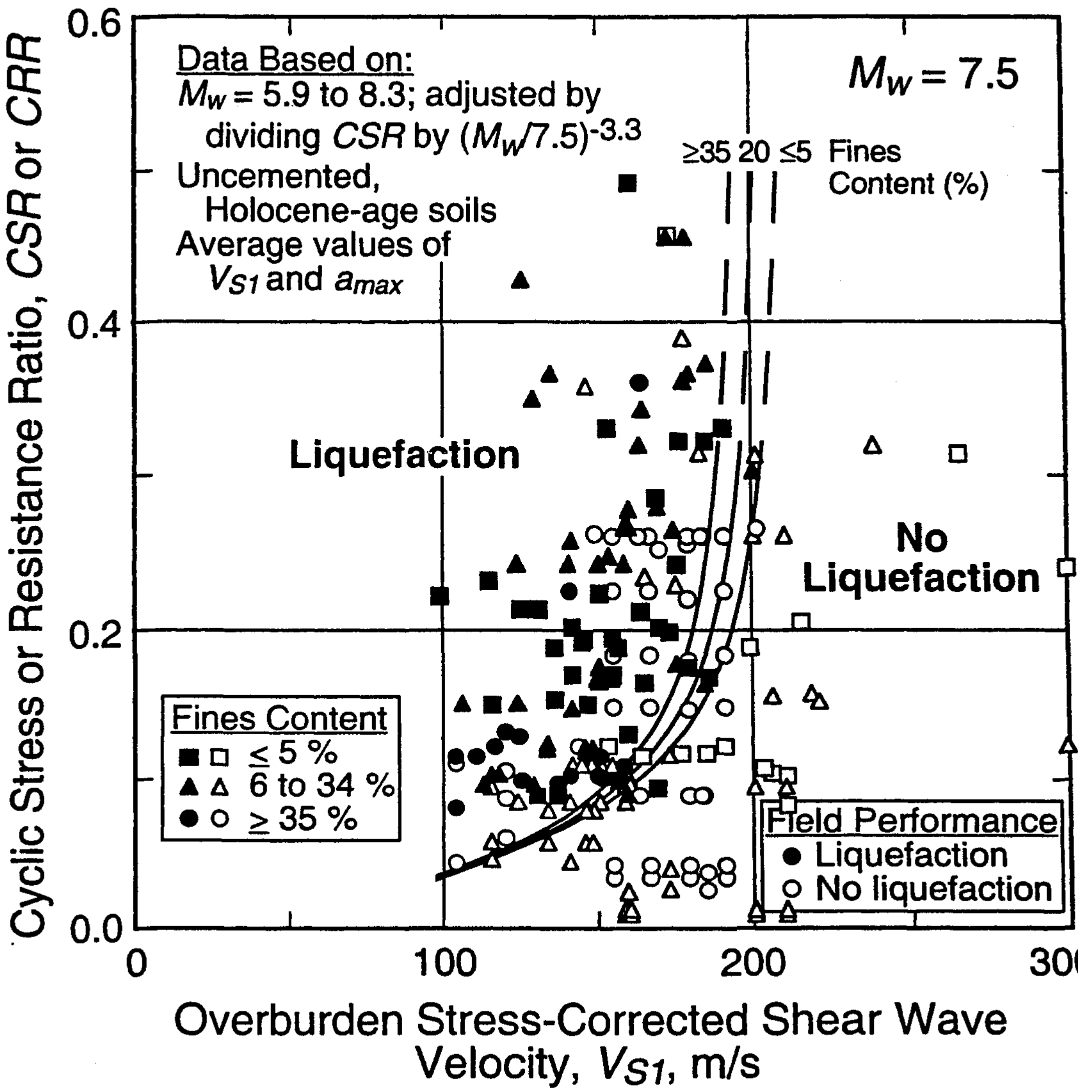

Fig. F.8 - Curves Recommended for Calculation of *CRR* from Shear Wave Velocity Measurements Along with Case History Data Based on **Upper Bound** Values of *MSF* for the Range Recommended by the 1996 NCEER Workshop (Youd et al., 1997) and r_d Developed by Seed and Idriss (1971).

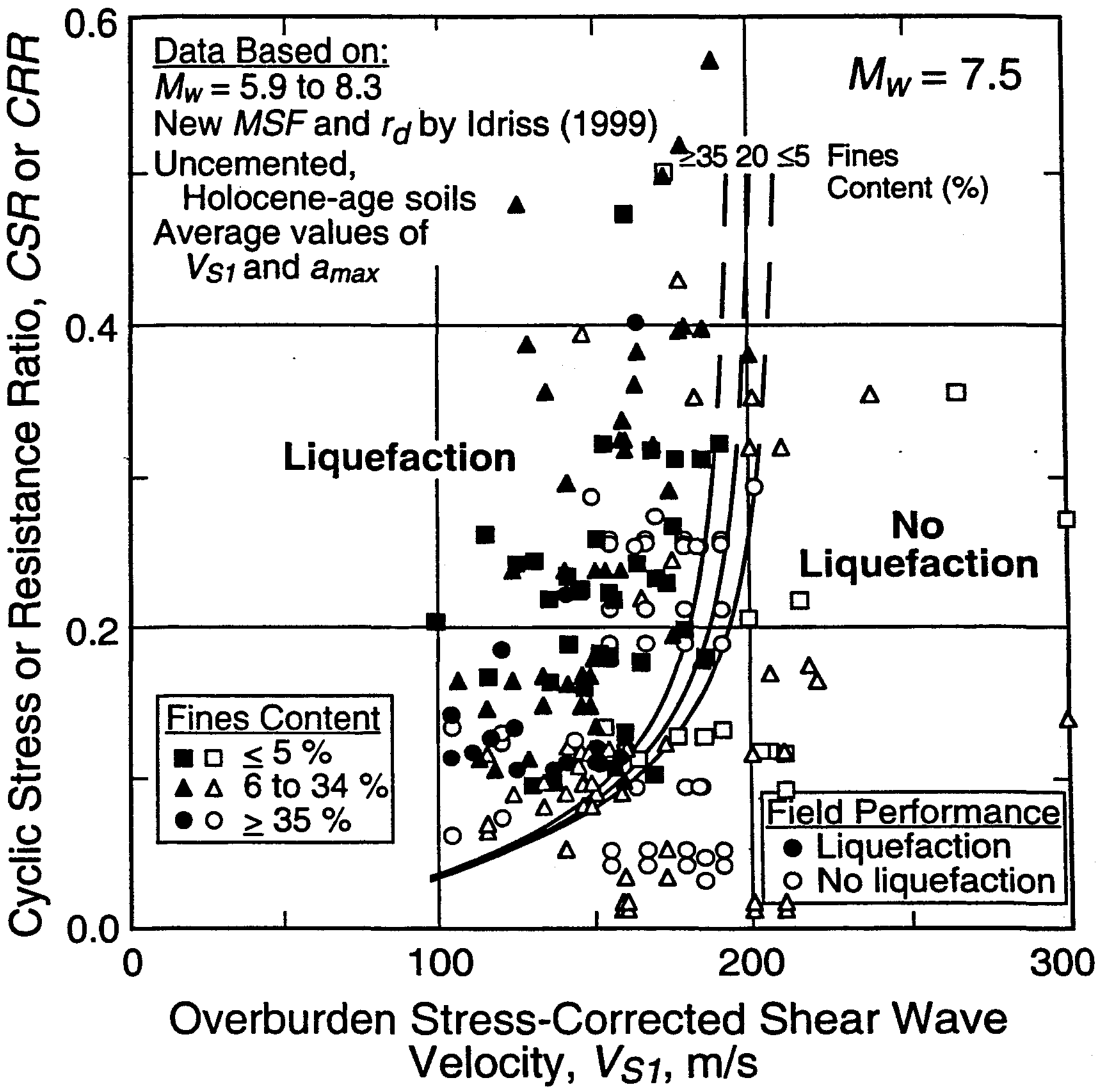

Fig. F.9 - Curves Recommended for Calculation of *CRR* from Shear Wave Velocity Measurements Along with Case History Data Based on Revised Values of *MSF* and r_d Proposed by Idriss (1999).

F.2.3 Comparison of Magnitude Scaling Factors

The proposed relationships for *MSF* can be compared directly by combining them with the appropriate stress reduction coefficient into one factor. This factor is the product of r_d and the reciprocal of *MSF*. Figure F.10 presents values of r_d/MSF for the range recommended by the 1996 NCEER Workshop (Youd et al., 1997) and those proposed by Idriss (1999). As shown in the figure, there is not much difference between the two sets of r_d/MSF values for magnitude of 7.5 and depth less than 11 m. At magnitudes near 5.5 and shallow depths, the difference between r_d/MSF values proposed by Idriss (1999) and values recommended by the 1996 NCEER Workshop is as much as 50 %. Thus, at magnitudes less than about 7, the difference in using values of *MSF* and r_d proposed by Idriss (1999) and those adopted by the NCEER Workshop (Youd et al., 1997) is significant in the calculation of *CSR*.

For example, Fig. F.11 presents two liquefaction resistance curves for earthquakes with magnitude near 5.5 and clean soils ($FC \leq 5$ %). The upper curve was obtained by multiplying values of *CRR* defining the curve for $FC \leq 5\%$ in Fig. F.1 by 2.2, the lower *MSF* recommended by the 1996 NCEER Workshop for magnitude 5.5 earthquakes (see Eq. (2.9) with n = -2.56). The lower curve was obtained by multiplying values of *CRR* defining the curve for $FC \leq 5$ % in Fig. F.1 by 1.68, the *MSF* proposed by Idriss (1999) for magnitude 5.5 earthquakes (see Eq. (2.10)). Also shown in Fig. F.11 are the available case history data for clean sands determined using average stress reduction coefficients proposed by Seed and Idriss (1971) and Idriss (1998). The two curves in Fig. F.11 exhibit differences in *CRR* of about 0.02 at $V_{S1} = 100$ m/s and 0.1 at $V_{S1} = 200$ m/s.

F.3 RECOMMENDED *CRR*-V_{S1} CURVES

From the discussion presented above, the recommended *CRR*-V_{S1} curves are defined by Eqs. (F.1), (2.9) and (F.4) with $a = 0.022$, $b = 2.8$, and $n = -2.56$. The recommended curves for moment magnitudes ranging from 5.5 though 8 are presented in Figs. F.12 through F.17, respectively, along with the case history data. The value of -2.56 for n is recommended for determining magnitude scaling factors because it provides more conservative *CRR*-V_{S1} curves than -3.3, which is the n value defining the upper bound of the range of *MSFs* suggested by the 1996 NCEER Workshop (Youd et al., 1997) for magnitudes less than 7.5. Although the magnitude scaling factors defined by Eq. (2.9) with $n = -2.56$ provide less conservative *CRR*-V_{S1} curves than the factors proposed by Idriss (1999) for magnitudes less than 7.5, the factors determined of Ambraseys (1988), I. M. Idriss (personal communication to T. L. Youd, 1995), Arango (1996), Youd and Noble (1997), and Andrus and Stokoe (1997; as indicated by the very conservative *CRR*-V_{S1} curves shown in Figs. F.13 and F.14) supported their use.

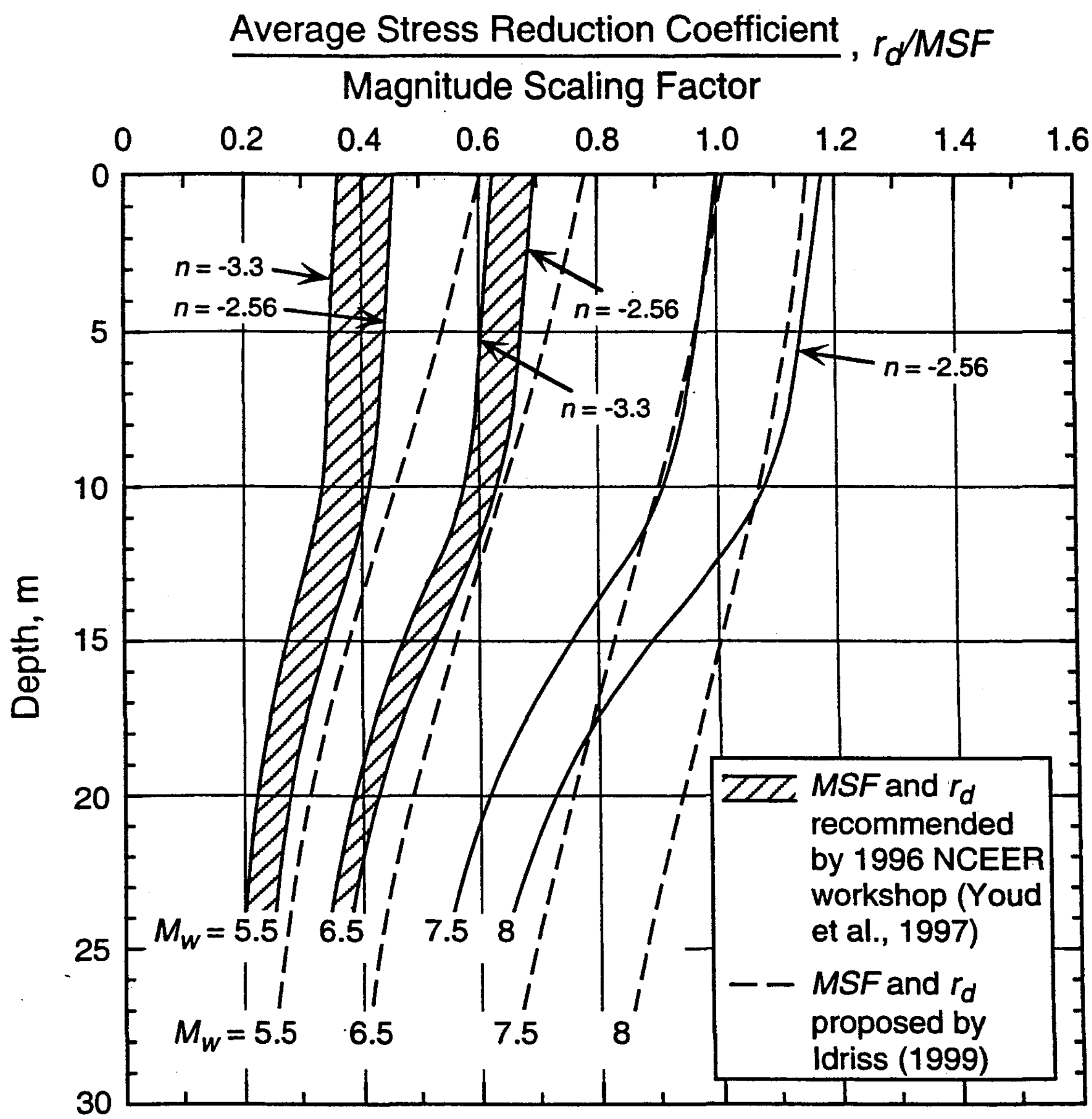

Fig. F.10 - Variation of r_d/MSF with Depth for Various Magnitudes and Proposed Relationships.

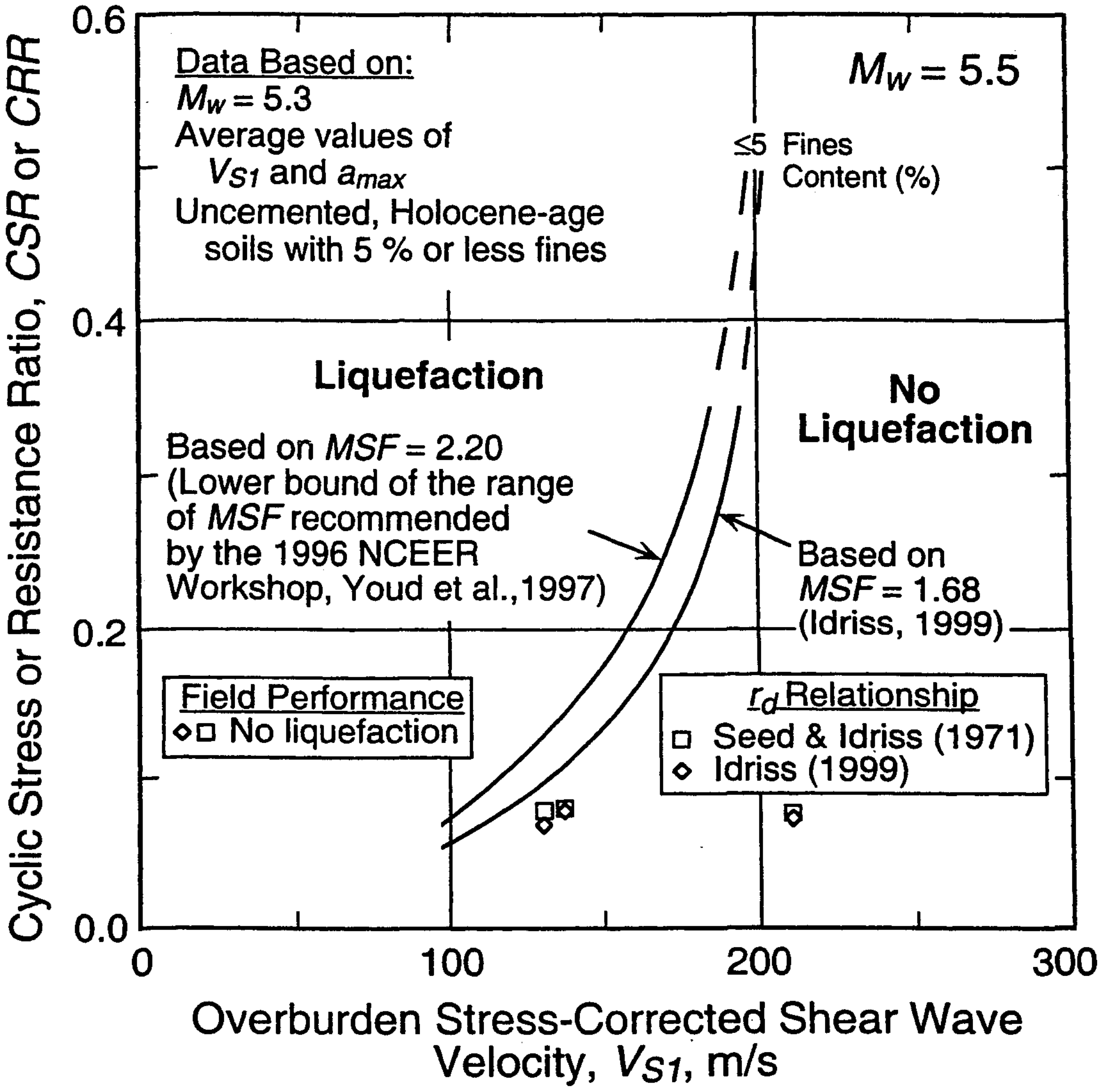

Fig. F.11 - Comparison of Liquefaction Resistance Curves and Case History Data for Procedures Recommended by the 1996 NCEER Workshop (Youd et al., 1997) and the Revised Procedures Proposed by Idriss (1999) for Clean Sands and Earthquakes with Magnitude Near 5.5.

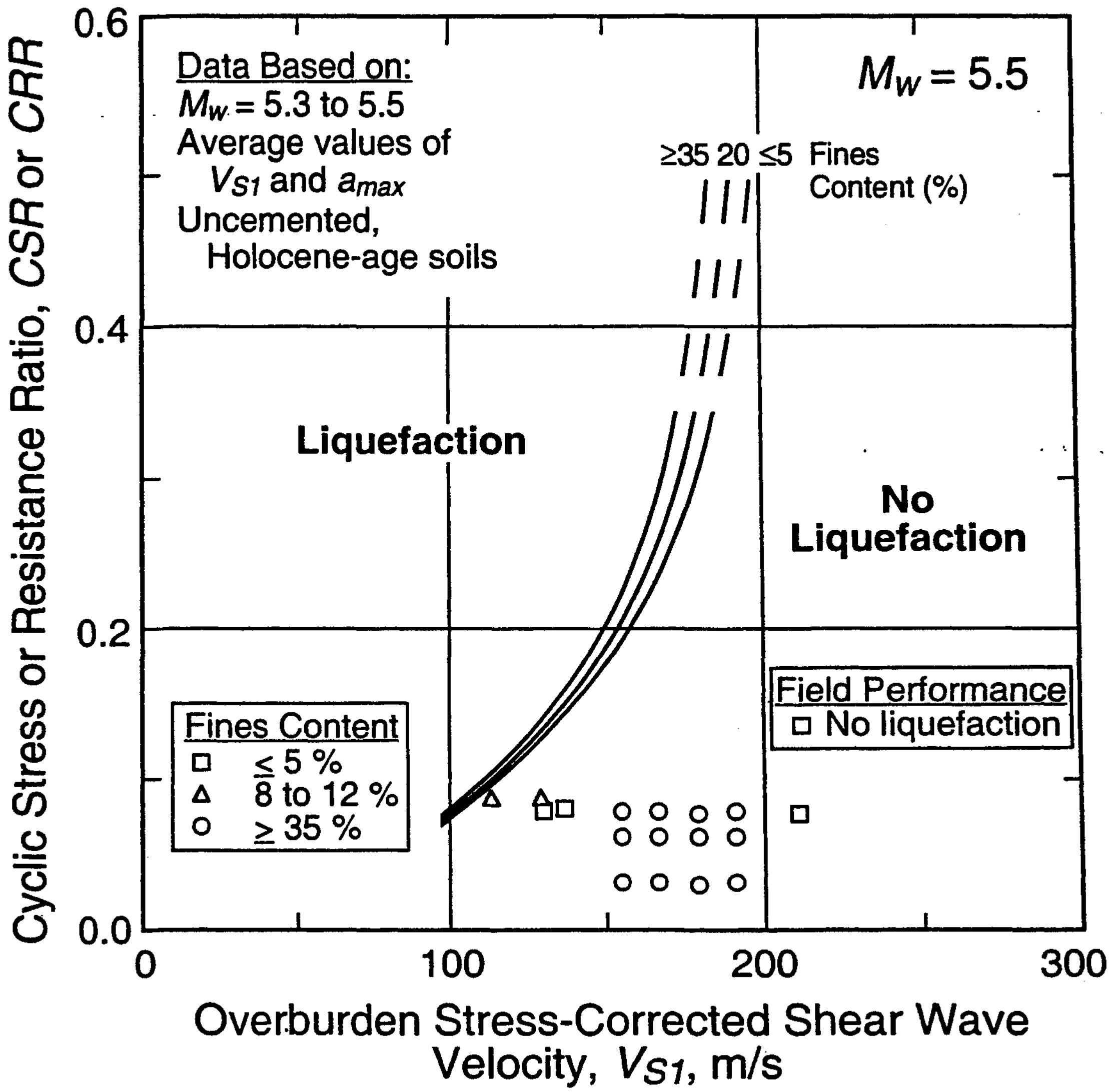

Fig. F.12 - Case History Data for Earthquakes with Magnitude Near 5.5 Based on Overburden Stress-Corrected Shear Wave Velocity and Cyclic Stress Ratio with Recommended Liquefaction Resistance Curves.

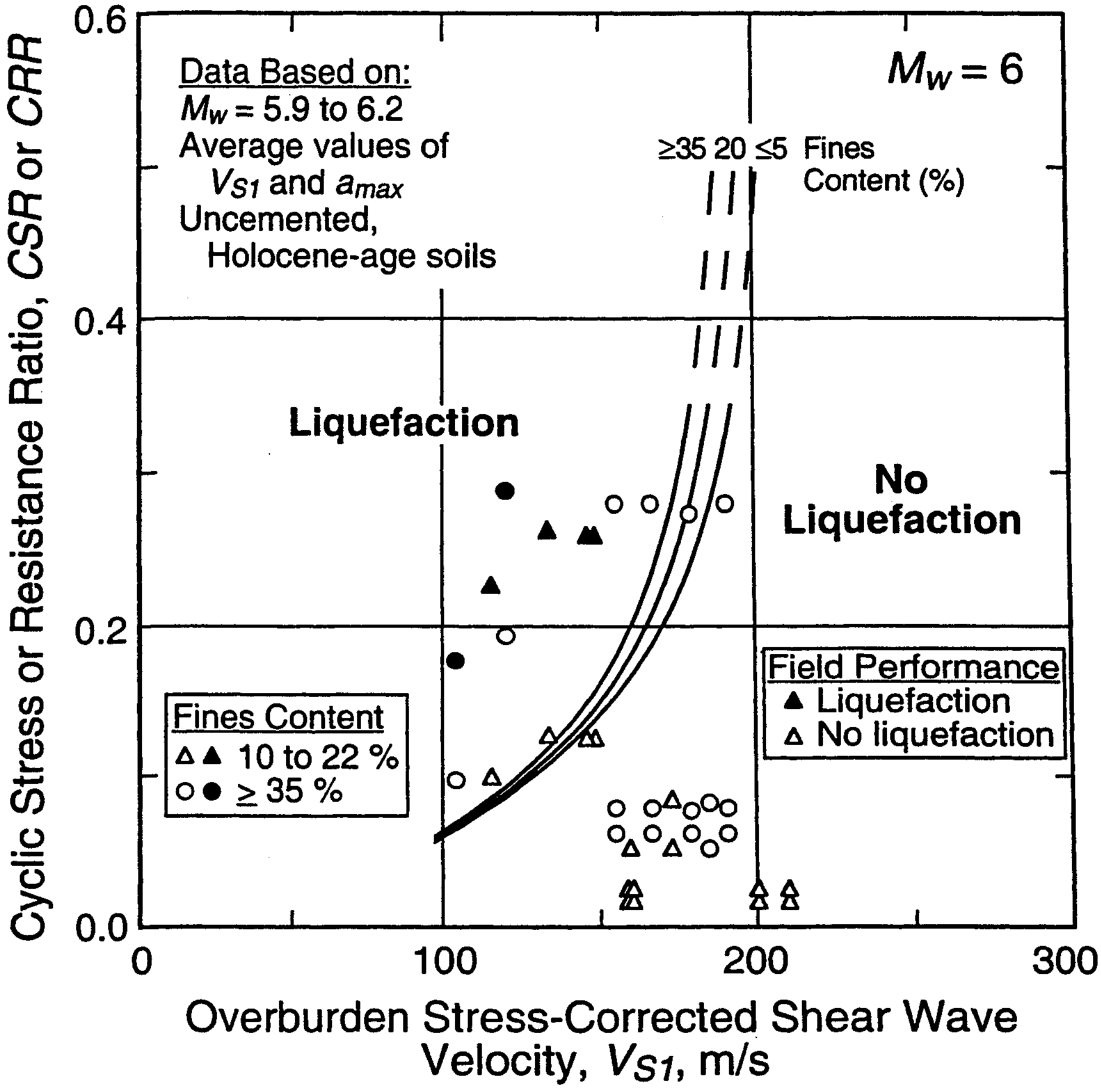

Fig. F.13 - Case History Data for Earthquakes with Magnitude Near 6 Based on Overburden Stress-Corrected Shear Wave Velocity and Cyclic Stress Ratio with Recommended Liquefaction Resistance Curves.

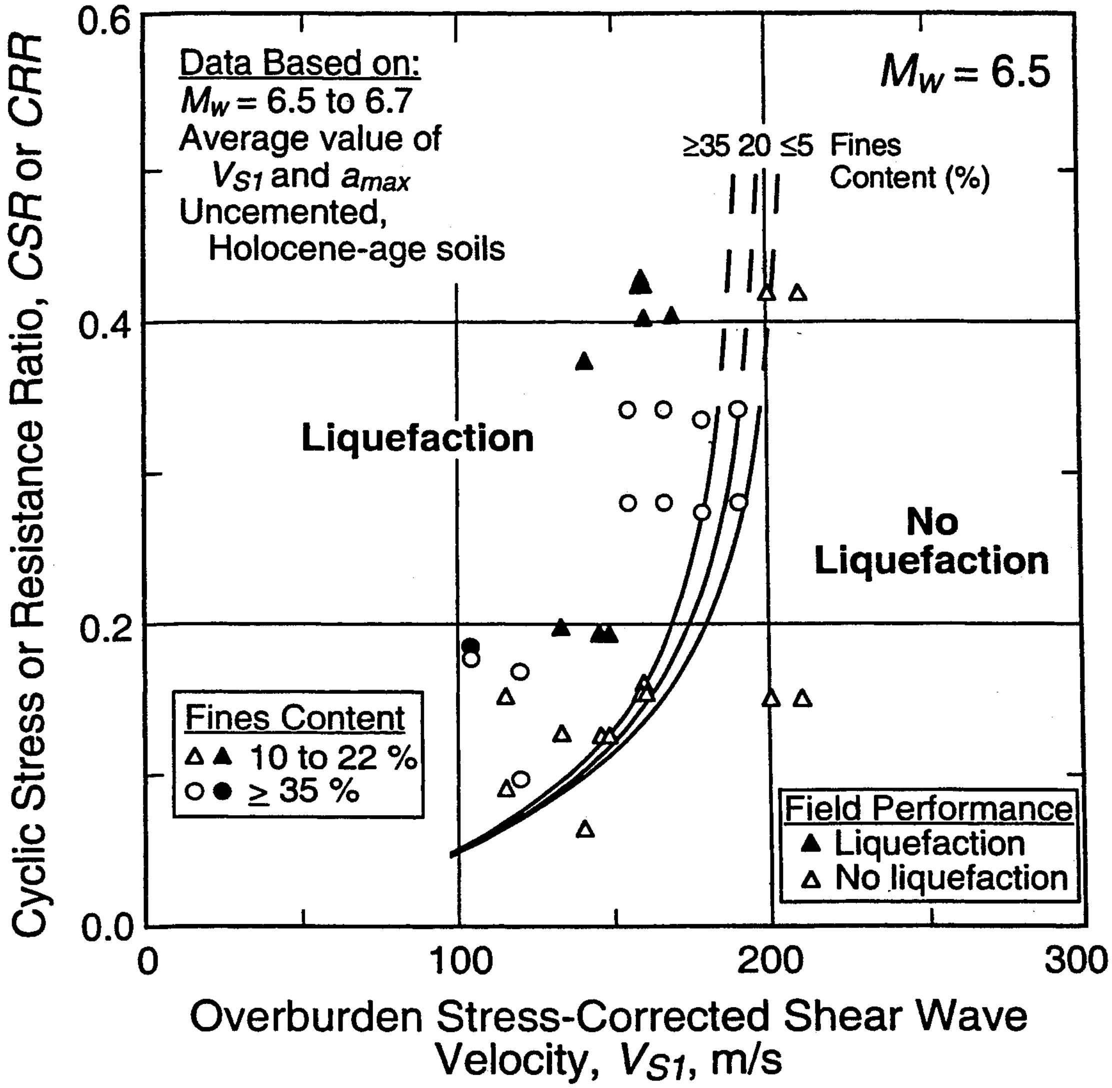

Fig. F.14 - Case History Data for Earthquakes with Magnitude Near 6.5 Based on Overburden Stress-Corrected Shear Wave Velocity and Cyclic Stress Ratio with Recommended Liquefaction Resistance Curves.

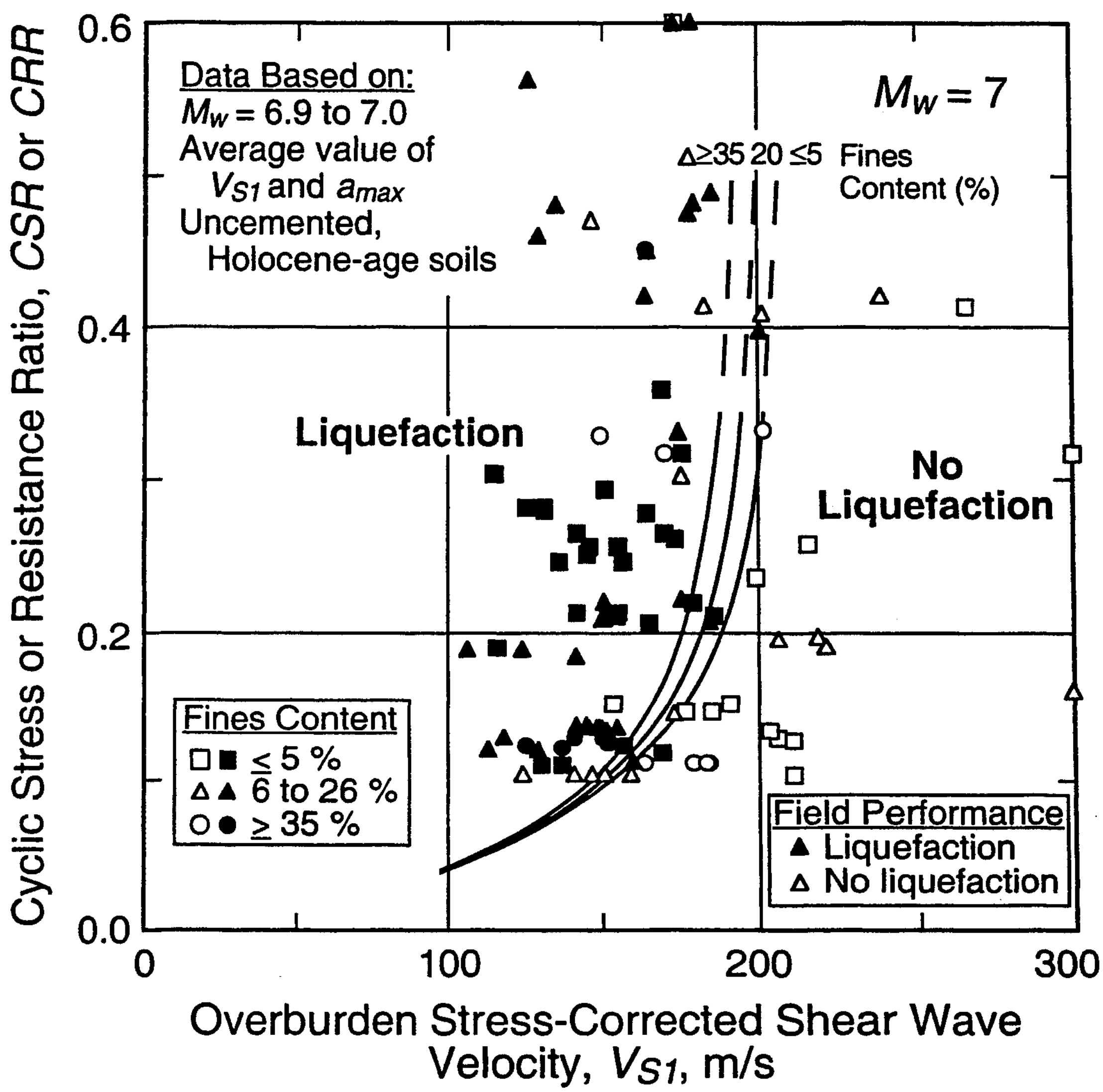

Fig. F.15 - Case History Data For Earthquakes with Magnitude Near 7 Based on Overburden Stress-Corrected Shear Wave Velocity and Cyclic Stress Ratio with Recommended Liquefaction Resistance Curves.

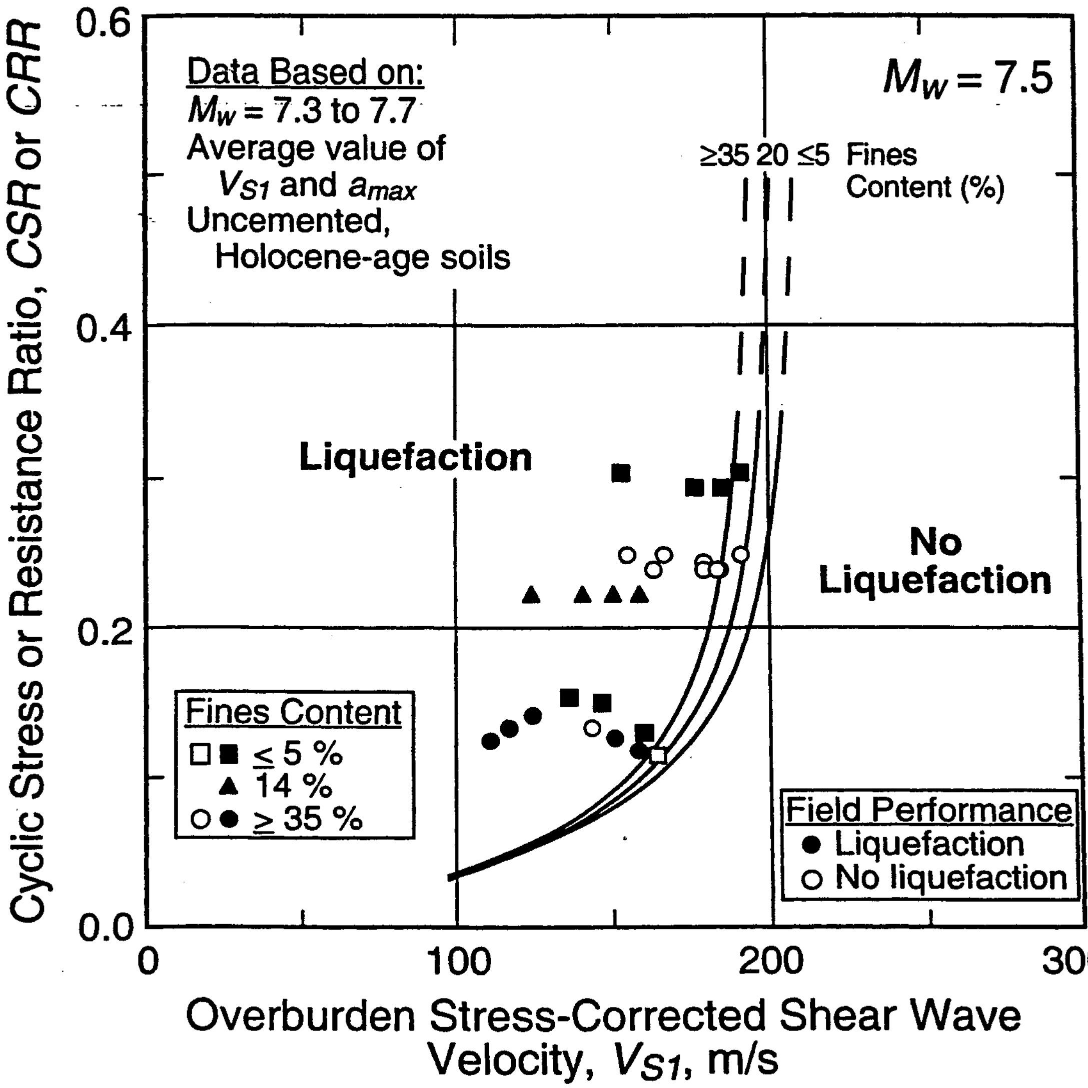

Fig. F.16 - Case History Data for Earthquakes with Magnitude Near 7.5 Based on Overburden Stress-Corrected Shear Wave Velocity and Cyclic Stress Ratio with Recommended Liquefaction Resistance Curves.

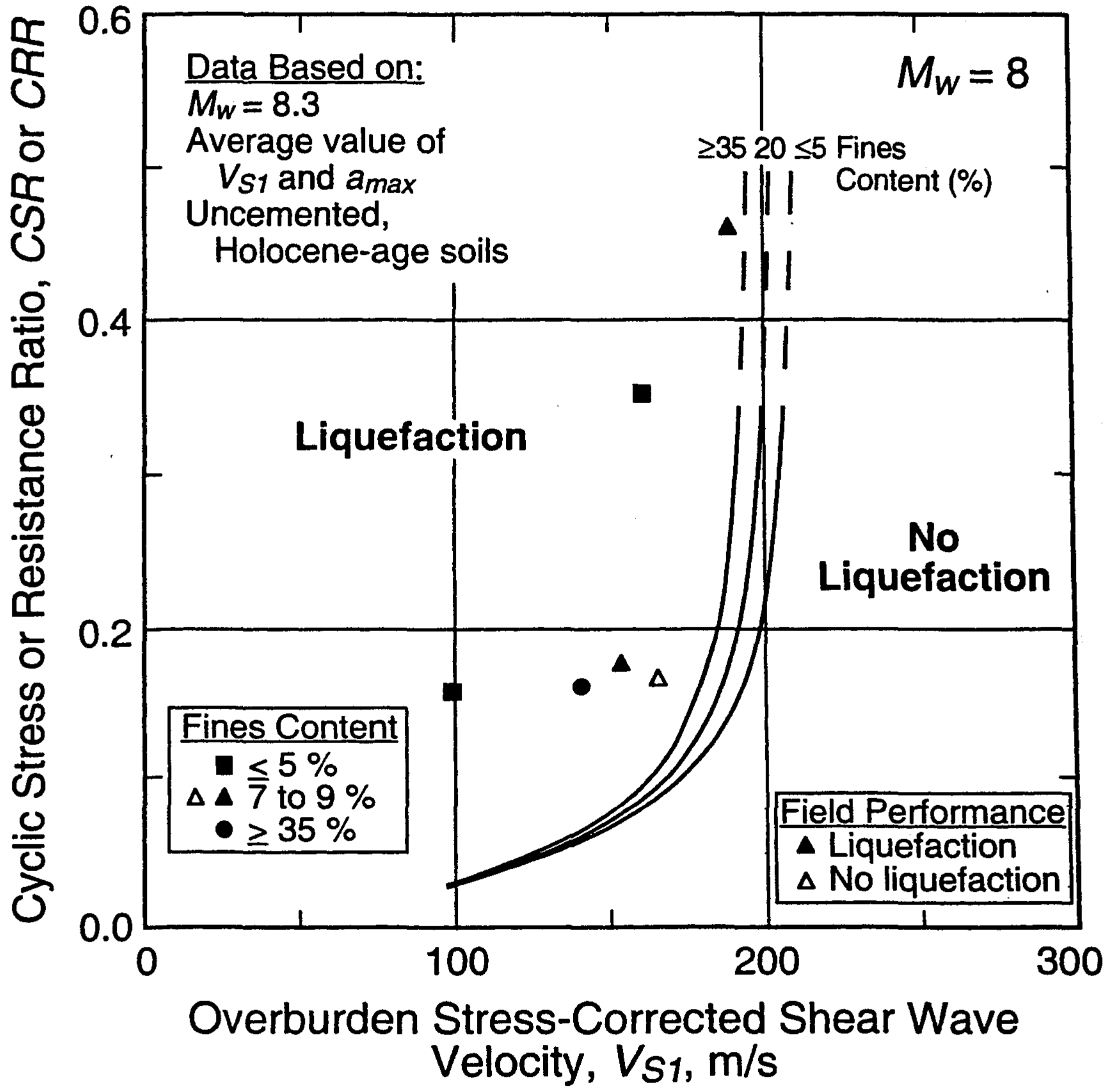

Fig. F.17 - Case History Data for Earthquakes with Magnitude Near 8 Based on Overburden Stress-Corrected Shear Wave Velocity and Cyclic Stress Ratio with Recommended Liquefaction Resistance Curves.

The recommended CRR-V_{S1} curves shown in Figs. F.12 through F.17 are dashed above CRR of about 0.35 to indicate that they are based on limited field performance data. The curves do not extend much below 100 m/s, because there are no field data to support extending them to the origin. It is important to note that these boundary curves are for extreme behavior, where boils and ground cracks occur.

F.4 CORRELATIONS BETWEEN V_{S1} AND PENETRATION RESISTANCE

One can obtain correlations between V_{S1} and corrected penetration resistance from the recommended CRR-V_{S1} relationships given in Fig. F.1 and 1996 NCEER Workshop (Youd et al., 1997) recommended SPT- and CPT-based relationships for magnitude 7.5 earthquakes by plotting values with equal CRR.

F.4.1 Corrected SPT Blow Count

Figure F.18 presents the correlation of V_{S1} with $(N_1)_{60}$ for clean soils ($\leq$ 5 % fines), based on the recommended CRR-V_{S1} and CRR-$(N_1)_{60}$ relationships. Also shown are the field data and mean curve for sands with less than 10 % non-plastic fines from Fig. F.2. The correlation derived from the CRR relationships lies between the mean and the mean $+1S_{res}$ curves. The flatter slope below $(N_1)_{60}$ of 6 exhibited by the CRR-based correlation can be explained by different assumed minimal values of CRR. The CRR-V_{S1} relationship for magnitude 7.5 earthquakes and $FC \leq 5$ % shown in Fig. F.1 provides a CRR of 0.033 for V_{S1} = 100 m/s, the lowest V_{S1} value shown in the figure. The 1996 NCEER Workshop recommended a CRR value of 0.05 for $(N_1)_{60} = 0$. The difference between minimal values of CRR is small, and is near the accuracy of both procedures.

The CRR-based correlation shown in Fig. F.18, along with the plotted field data, provide a simple method of comparing the V_{S1}- and $(N_1)_{60}$-based liquefaction evaluation procedures. Both procedures provide similar predictions of liquefaction potential, when the data point lies on the CRR-based curve. When the data point plots below the CRR-based curve, the V_{S1}-based liquefaction evaluation procedure provides the more conservative prediction. When the data point plots above the CRR-based curve, the SPT-based liquefaction evaluation procedure provides the more conservative prediction. Because most of the data points shown in Fig. F.18 plot below the CRR-based curve, the V_{S1}-based procedure provides an overall more conservative prediction of liquefaction resistance than does the SPT-based procedure for these sites.

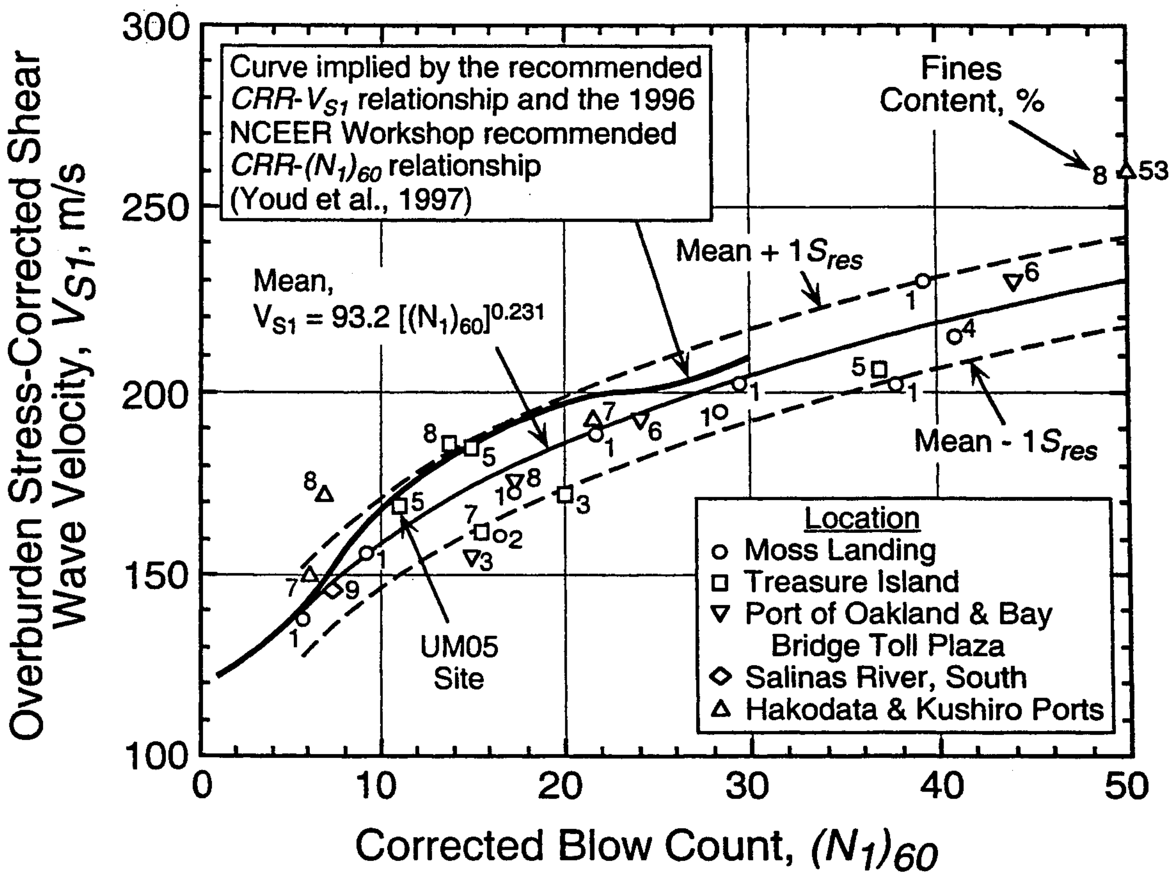

Fig. F.18 - Relationships Between $(N_1)_{60}$ and V_{S1} for Clean Sands Implied by the Recommended CRR-V_{S1} Relationship and the 1996 NCEER Workshop Recommended CRR-$(N_1)_{60}$ Relationship (Youd et al., 1997) with Field Data for Sands with Less than 10 % Fines.

The data point for the Treasure Island UM05 site, which incorrectly lies in the region of no liquefaction shown in Fig. F.1, plots just below the *CRR*-based curve, as shown in Fig. F.18. Thus, this case history also incorrectly plots in the region of no liquefaction on the SPT-based liquefaction evaluation chart. Furthermore, the SPT-based procedure provides a slightly less conservative prediction of liquefaction resistance than the shear-wave-based procedure for this case history.

Although the *CRR*-based curve shown in Fig. F.18 generally trends parallel to the mean curve, there is a small hump between corrected blow counts of 8 and 26. This hump suggests that either the *CRR*-V_{S1} relationship is more conservative or the *CRR*-$(N_1)_{60}$ relationship is less conservative in this range.

Similarly, as shown in Fig. F.19, a correlation between V_{S1} with $(N_1)_{60}$ for soils with $\geq$ 35 % fines can be derived from the recommended *CRR*-V_{S1} and *CRR*-$(N_1)_{60}$ relationships. Figure F.19 provides the basis for the method of estimating the cementation and aging correction factor, K_c, suggested in Section 2.3.4 (see Fig. 2.6).

F.4.2 Normalized Cone Tip Resistance

Figure F.20 presents the correlation of V_{S1} with q_{c1N} for clean sands with median grain size, D_{50}, between 0.25 mm and 2.0 mm, based on the recommended *CRR*-V_{S1} and *CRR*-q_{c1N} relationships. Also shown are the field data and mean curve for clean sands with less than 10 % non-plastic fines from Fig. F.3. The correlation derived from the *CRR* relationships lies between the mean and the mean $+1S_{res}$ curves for V_{S1} = 170 m/s, indicating that the V_{S1}-based procedure provides an overall more conservative prediction of liquefaction resistance than does the CPT-based procedure for these sites. For V_{S1} < 170, the *CRR*-based correlation lies close to the mean curve, indicating that both procedure provide an overall similar prediction. The slope of the *CRR*-based correlation below q_{c1N} of 20 may be explained by the different assumed minimal values of *CRR*, as discussed in Section F.4.1.

The data point for the Treasure Island UM05 site, which incorrectly lies in the region of no liquefaction shown in Fig. F.1, plots on the *CRR*-based curve, as shown in Fig. F.20. Thus, the CPT-based procedure provides a similar incorrect prediction of no liquefaction for this site.

Similarly, as shown in Fig. F.21, a correlation between V_{S1} with q_{c1N} for soils with $\geq$ 35 % fines can be derived from the recommended *CRR*-V_{S1} and *CRR*-$(N_1)_{60}$ relationships. Figure F.21 provides the basis for the method of estimating the cementation and aging correction factor, K_c, suggested in Section 2.3.4 (see Fig. 2.7).

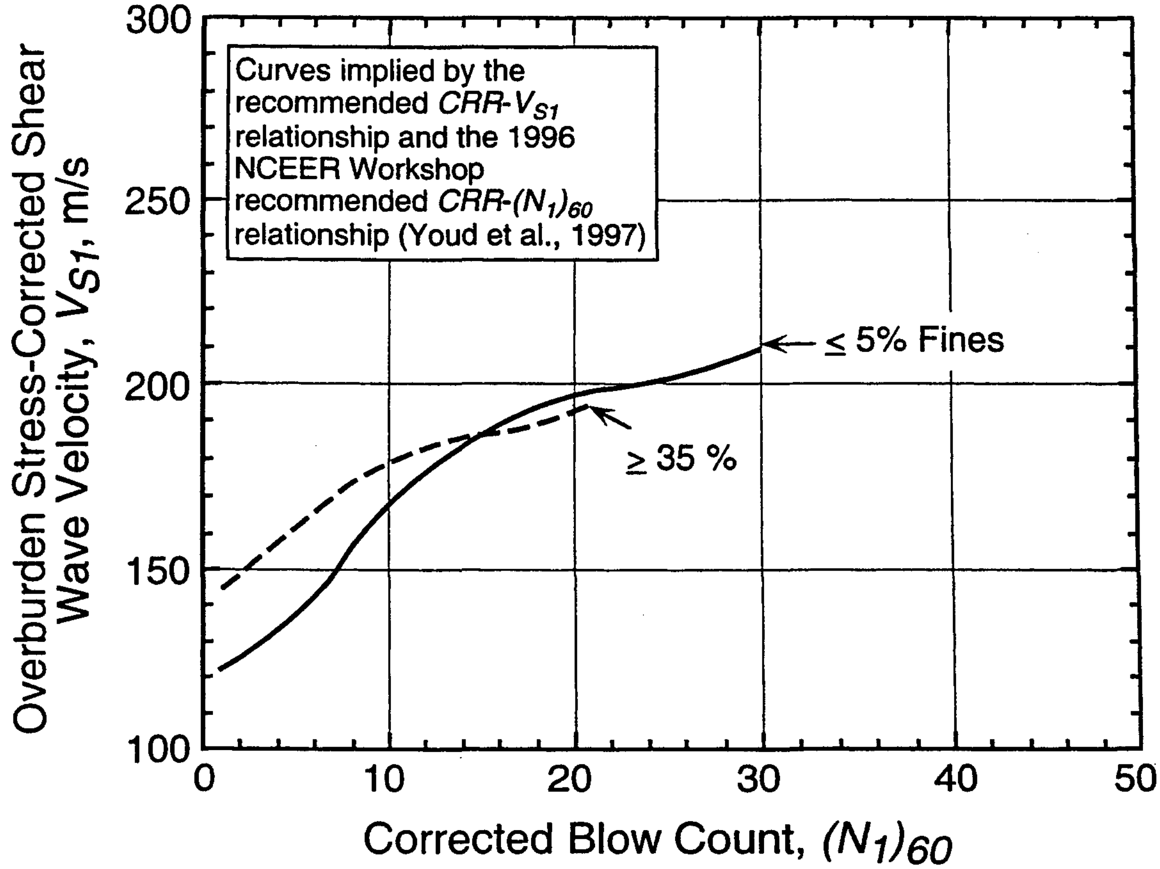

Fig. F.19 - Relationships Between $(N_1)_{60}$ and V_{S1} Implied by the Recommended CRR-V_{S1} Relationship and the 1996 NCEER Workshop Recommended CRR-$(N_1)_{60}$ Relationship (Youd et al., 1997).

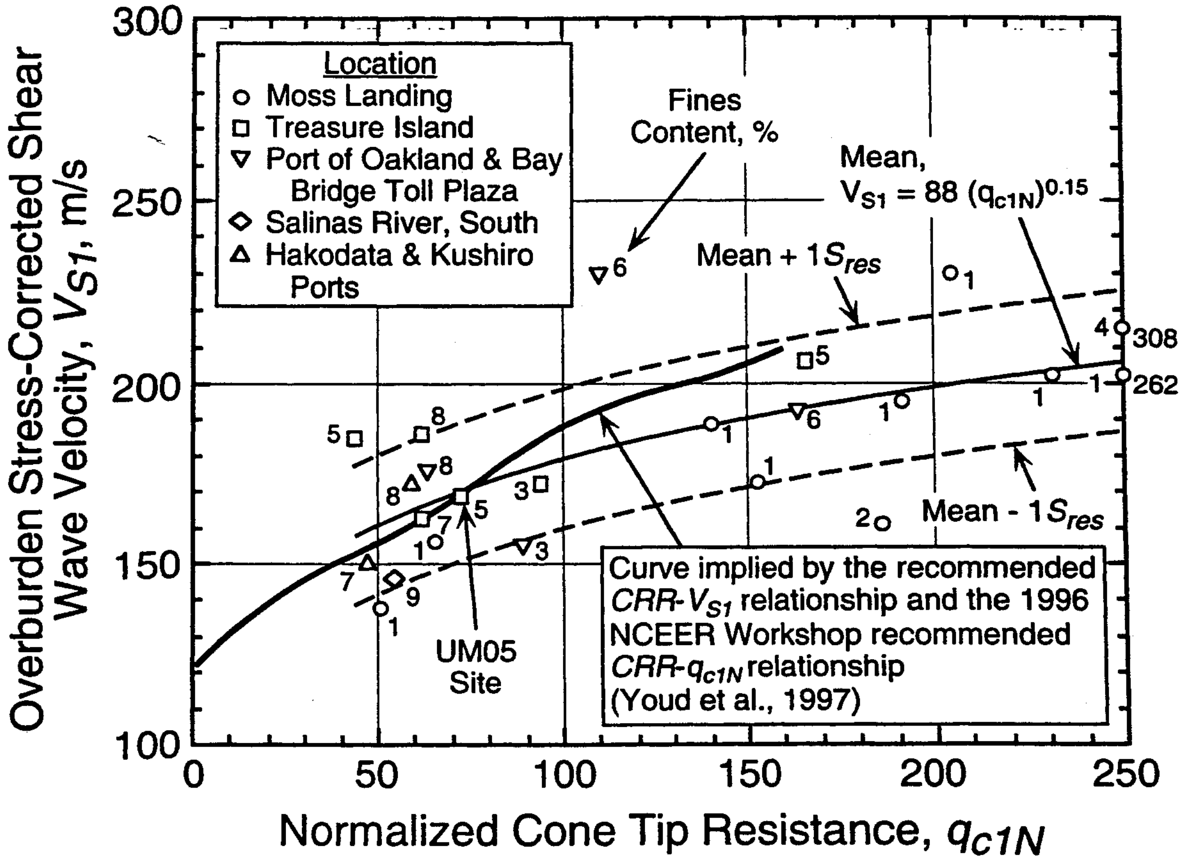

Fig. F.20 - Relationships Between q_{c1N} and V_{S1} for Clean Sands Implied by the Recommended CRR-V_{S1} Relationship and the 1996 NCEER Workshop Recommended CRR-q_{c1N} Relationship (Youd et al., 1997) with Field Data for Sands with Less than 10 % Fines.

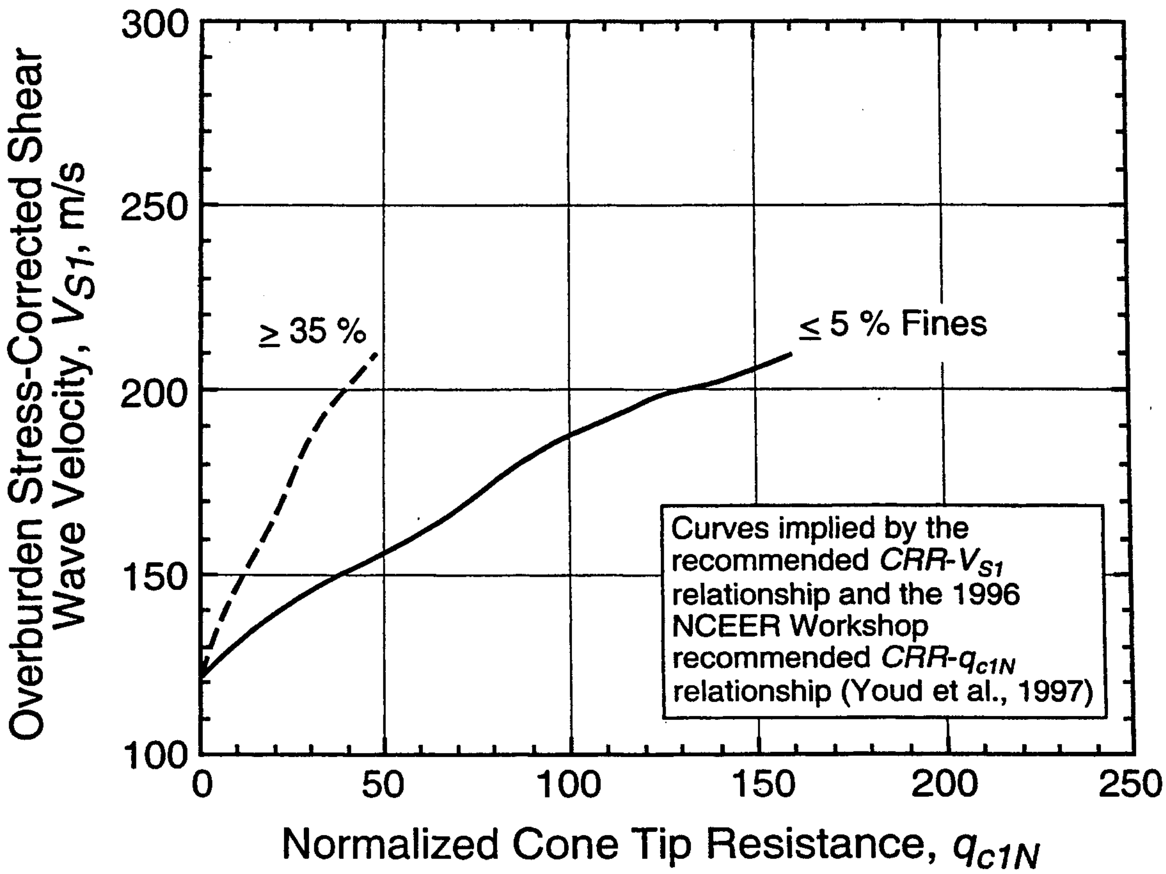

Fig. F.21 - Relationships Between q_{c1N} and V_{S1} Implied by the Recommended CRR-V_S Relationship and the 1996 NCEER Workshop Recommended CRR-q_{c1N} Relationship (Youd et al., 1997).

F.5 SUMMARY

The development of the recommended CRR-V_{S1} curves was outlined in this appendix. The recommended curves are based on a modified relationship between shear wave velocity and cyclic stress ratio for constant average cyclic shear strain suggested by R. Dobry. They are defined by Eqs. (F.1), (F.4) and (2.9) with $a = 0.022$, $b = 2.8$, and $n = -2.56$. The curve fitting parameters a and b are determined through an iterative process that involved varying their values until nearly all the liquefaction case histories were bound by the curves with the least amount of non-liquefaction case histories in the liquefaction region. Three *MSF* relationships are considered in determining the values of a and b. Equation (F.4), which provides a relationship between the limiting upper V_{S1} value and fines content, is based, in part, on the case history data and, in part, on penetration shear wave velocity correlations. From penetration-V_S correlations, the recommended CRR-V_{S1} curves appear to be somewhat more conservative than the penetration-based curves recommended by the 1996 NCEER Workshop (Youd et al., 1997).

APPENDIX G

PROBABILITY-BASED LIQUEFACTION EVALUATION

This appendix presents three probability models for the case history data listed in Appendix H. The probability models are based on the work of Juang et al. (2001a; 2002), and are derived using logistic regression and Bayesian interpretation techniques. They are compared with the deterministic evaluation curve by Andrus et al. (1999) for clean soils ($FC \leq 5$ %) shown in Fig. 2.3. The probability models provide a means of objectively calibrating the deterministic liquefaction evaluation curve.

To develop the probability models, values of V_{S1} are adjusted to a clean soil equivalent. The procedure for adjusting V_{S1} values involves two steps. First, a CRR value is determined using Eq. (2.8) for each case history. Second, for each value of CRR, a clean soil equivalent V_{S1} value is determined using Eq. (2.8) with V^*_{S1} = 215 m/s. Thus, this adjustment procedure, maintains the ratio of CRR to CSR (or factor of safety). The adjustment procedure can be expressed by:

$$V_{S1,CS} = K_{fc} V_{S1} \quad \text{(G.1)}$$

where

$V_{S1,CS}$ = the equivalent clean soil value of V_{S1}, and
K_{fc} = a fines content correction to adjust V_{S1} values to a clean soil equivalent.

Values of K_{fc} can be approximated using the following equation (Juang et al., 2001a; 2002):

$$K_{fc} = 1, \quad \text{for } FC \leq 5\ \% \quad \text{(G.2a)}$$
$$K_{fc} = 1 + (FC - 5) f(V_{S1}), \quad \text{for } FC = 6\ \% \text{ to } 34\ \% \quad \text{(G.2b)}$$
$$K_{fc} = 1 + 30 f(V_{S1}), \quad \text{for } FC \geq 35\ \% \quad \text{(G.2c)}$$

where

$$f(V_{S1}) = 0.009 - 0.0109\left(\frac{V_{S1}}{100}\right) + 0.0038\left(\frac{V_{S1}}{100}\right)^2 \qquad \text{(G.3)}$$

Equations (G.1) through (G.3) provide an approximate mathematical description of the adjustment procedure. The adjusted case history data are plotted in Figs. G.1 and G.2 along with two probability models determined using logistic regression. The logistic regression-based probability models, as well as a Bayesian-based probability model, are discussed below.

G.1 LOGISTIC REGRESSION MODELS

G.1.1 Logistic Regression Model 1

The first logistic regression-based probability model, called Model 1, is similar in form to the model used by Liao et al. (1988) for analyzing SPT-based case histories. The probability equation for Model 1 is given by (Juang et al., 2001a; 2002):

$$\ln\left[\frac{P_L}{1-P_L}\right] = a_1 + a_2\, V_{S1,CS} + a_3 \ln(CSR_{7.5}) \qquad \text{(G.4)}$$

where

P_L = the probability that liquefaction will occur,
a_1, a_2, a_3 = regression coefficients, and
$CSR_{7.5}$ = CSR adjusted to $M_w = 7.5$.

The mean values of a_1, a_2, and a_3 are 14.8967, -0.0611, and 2.6418, respectively. The standard deviations associated with the coefficients are 2.1637, 0.0098, and 0.4268, respectively. The Nagelkerke coefficient (equivalent to R^2) of this regression is 0.58. Probability curves for Model 1 are presented in Fig. G.1. From the figure, Model 1 appears to provide reasonable P_L curves within the limits of most of the data. However, the Model 1 curves may be inappropriately too conservative at high values of $V_{S1,CS}$ (say > 200 m/s), since a corrected velocity of 210 m/s is considered equivalent to a corrected blow count of 30 in clean sands and liquefaction is generally assumed not possible above this value.

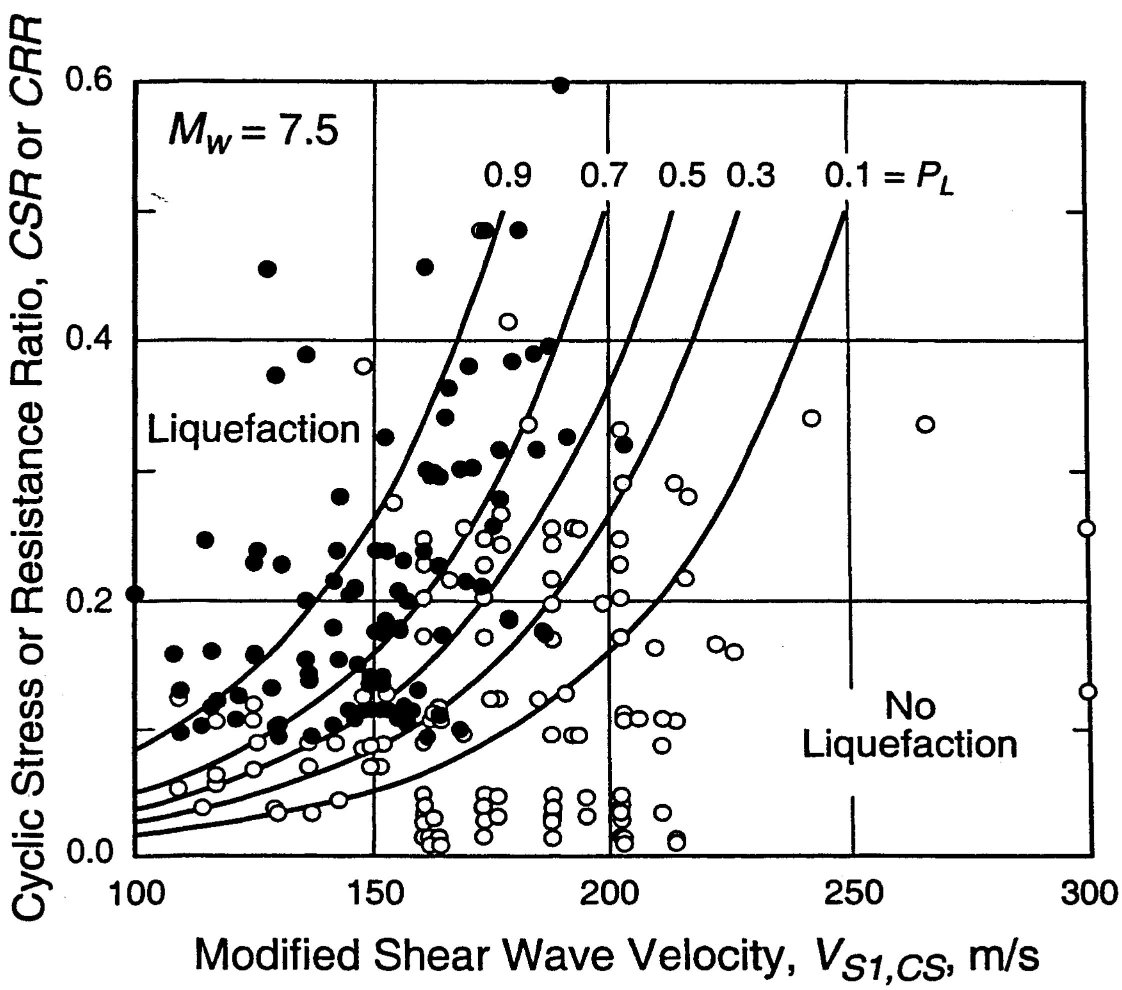

Fig. G.1 - Logistic Regression Model 1 and Case History Data Adjusted for Fines Content. (after Juang et al., 2001a)

G.1.2 Logistic Regression Model 2

To investigate the influence that the form of a regression equation might have on P_L curves, the analysis is repeated using a slightly different equation. The probability equation for this second logistic regression model, called Model 2, is defined by (as suggested by William Guthrie, NIST, to R. D. Andrus, June 1998):

$$\ln\left[\frac{P_L}{1-P_L}\right] = b_1 + b_2\, V_{S1,CS} + b_3 \ln(CSR_{7.5}) + b_4\, [\ln(CSR_{7.5})]^2 \qquad \text{(G.5)}$$

where

b_1, b_2, b_3, b_4 = regression coefficients.

The mean values of b_1, b_2, b_3 and b_4 determined by Juang et al. (2001a; 2002) are 10.0155, -0.0643, -3.9534, and -1.8381, respectively. The standard deviations associated with the coefficients are 2.6102, 0.0107, 2.1738, and 0.6302, respectively. The Nagelkerke coefficient of this regression is 0.61. A coefficient of 0.61 is slightly greater than 0.58, suggesting a slightly stronger correlation for Model 2 than Model 1. Figure G.2 presents P_L curves defined by Eq. (G.5). The Model 2 curves exhibit steeper-slopes than Model 1 curves above a CSR value of about 0.1. They reach a maximum $V_{S1,CS}$ value at CSR of about 0.33. Above CSR of 0.33, the curves trend to the left, decreasing in $V_{S1,CS}$ with increasing CSR. Nevertheless, the results clearly show that P_L curves determined by logistic regression depend on the form of the regression equation. While Model 2 provides another possible probability model, one would expect P_L curves to slope towards higher values of $V_{S1,CS}$ with increasing CSR rather than extend vertically, as suggested by the dashed lines in Fig. G.2.

G.2 BAYESIAN MAPPING MODEL

Juang et al. (1999) pioneered a Bayesian interpretation approach for mapping factor of safety, F_S, to P_L. In their approach, values of F_S are first determined for the liquefaction and non-liquefaction case histories using a deterministic evaluation curve. The V_S-based curve shown in Fig. 2.3 is the deterministic curve used in this case. Values of P_L are then estimated from the probability density functions of F_S for liquefaction and non-liquefaction case histories using Bayes' theorem. With the assumption of equal prior probability, the P_L-F_S mapping function can be expressed as (Chen and Juang, 2000; Juang et al., 2000a):

$$P_L = \frac{f_L(F_S)}{f_L(F_S) + f_{NL}(F_S)} \qquad \text{(G.6)}$$

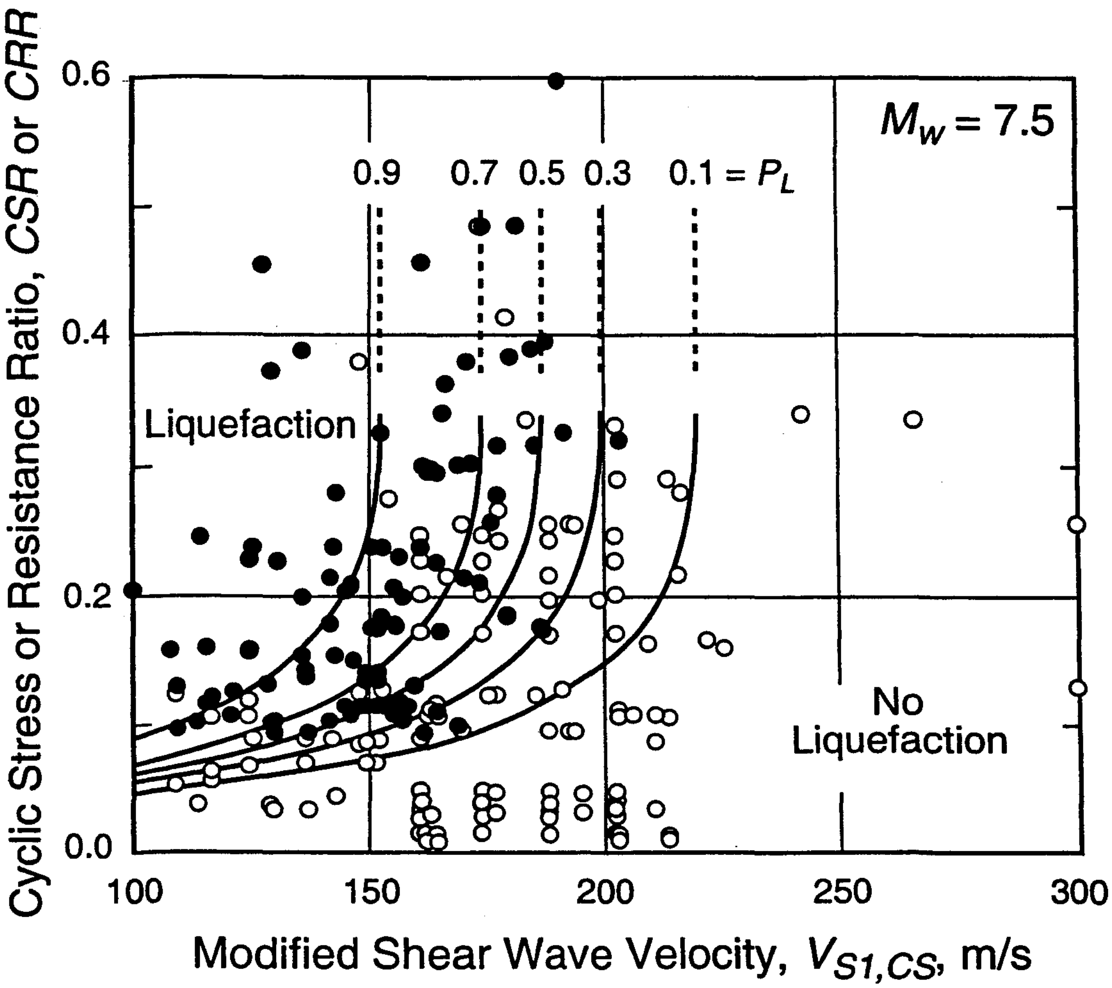

Fig. G.2 - Logistic Regression Model 2 and Case History Data Adjusted for Fines Content. (after Juang et al., 2001a) where

$f_L(F_S)$ = the probability density function of the calculated F_S for the liquefaction case histories, and

$f_{NL}(F_S)$ = the probability density function of the calculated F_S for the non-liquefaction case histories.

An analysis of the 225 case histories yields the probability density functions shown in Figs. G.3a and G.3b for the liquefaction and non-liquefaction cases, respectively. Applying Eq. (G.6), the predicted probability of liquefaction for each case history is obtained. Values of P_L and F_S for the case histories are plotted in Fig. G.4. The relationship formed by the F_S -P_L values can be approximated by (modified from Juang et al., 2001a):

$$P_L = \frac{1}{1+\left(\frac{F_S}{0.73}\right)^{3.4}} \quad (G.7)$$

In Eq. (G.7), a F_S value of 1 corresponds to points on the deterministic curve. Thus, on average, the Andrus et al. (1999) curve for clean soils (see Fig. 2.3) is characterized with a P_L value of 26 % based on Eq. (G.7). The value of 26 % is slightly less than 30 % initially determined by Juang et al. (2001a). Subsequent analysis (Juang et al., 2002) revealed that a few of the calculated P_L values corresponding to low F_S values (see Fig. G.4) were unreasonably influencing the coefficients given in Eq. G.7. Thus, Eq. G.7 has been modified slightly from the preliminary equation proposed by Juang et al. (2001a).

Figure G.5 compares the F_S-P_L relationship defined by Eq. (G.7) for the V_S-based recommended curve (Andrus et al., 1999) with the F_S-P_L relationship developed by Juang et al. (2000) for the SPT-based recommended curve (Seed et al., 1985; Youd et al., 2001). There is remarkable agreement between the V_S- and SPT-based relationships. From Fig. G.5, the SPT-based recommended curve is characterized with an average P_L value of 31 %. These findings suggest that the V_S-based deterministic evaluation curves are somewhat more conservative than the SPT-based curves.

Equation (G.7) provides an important link between the probabilistic and deterministic methods. One can obtain a family of P_L curves for probability-based design by combining Eqs. (2.8), (2.12) and (G.7). The family of P_L curves for magnitude 7.5 earthquakes and soils with $FC \leq 5$ % is presented in Fig. G.6. These curves, called the Bayesian Mapping Model, slope to the right with increasing CSR, which seems reasonable. They converge to a V_{S1} value of 215 m/s, the assumed value of V^*_{S1} for clean soils, at high values of CSR.

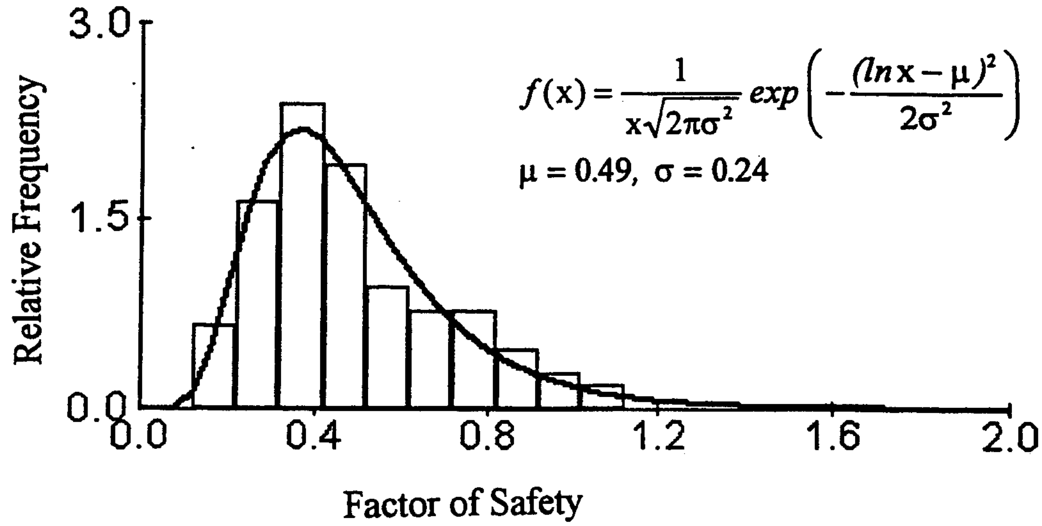

(a) Liquefaction Cases

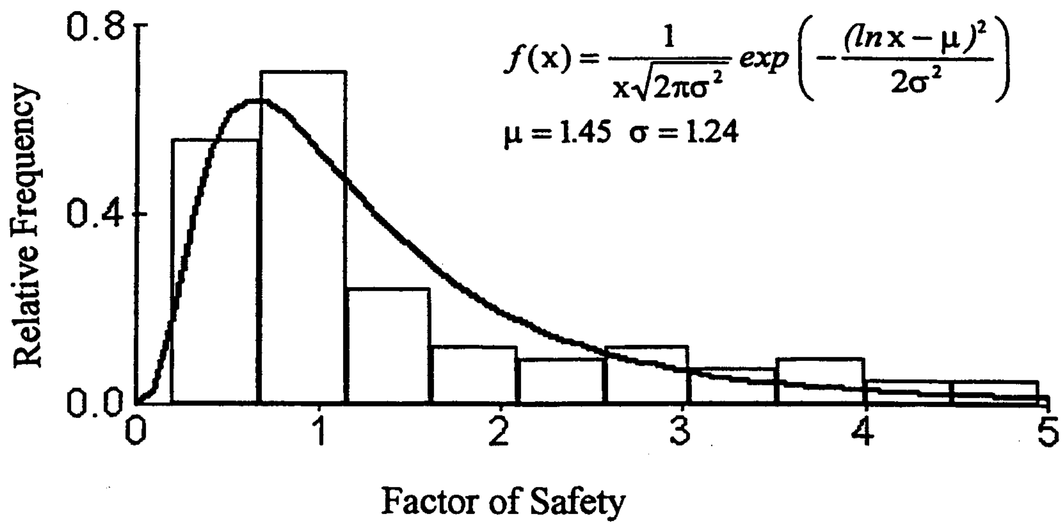

(b) Non-Liquefaction Cases

Fig. G.3 – Probability Density Functions and Calculated Factor of Safety Distributions for the 225 Case Histories.

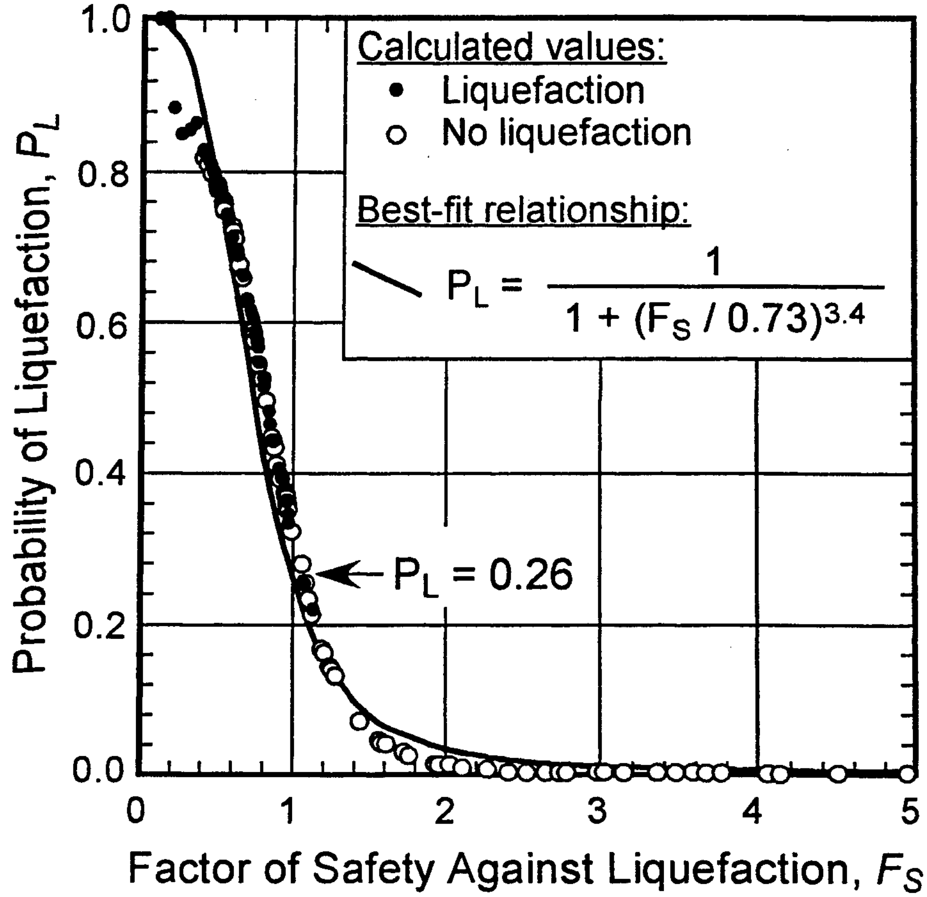

Fig. G.4 – Calculated Values of F_S and P_L for the 225 Case Histories with Best-Fit Relationship (Juang et al., 2002). Note that F_S is based on the Recommended Deterministic Evaluation Curves Shown in Fig. 2.3, and P_L is based on Eq. (G.6).

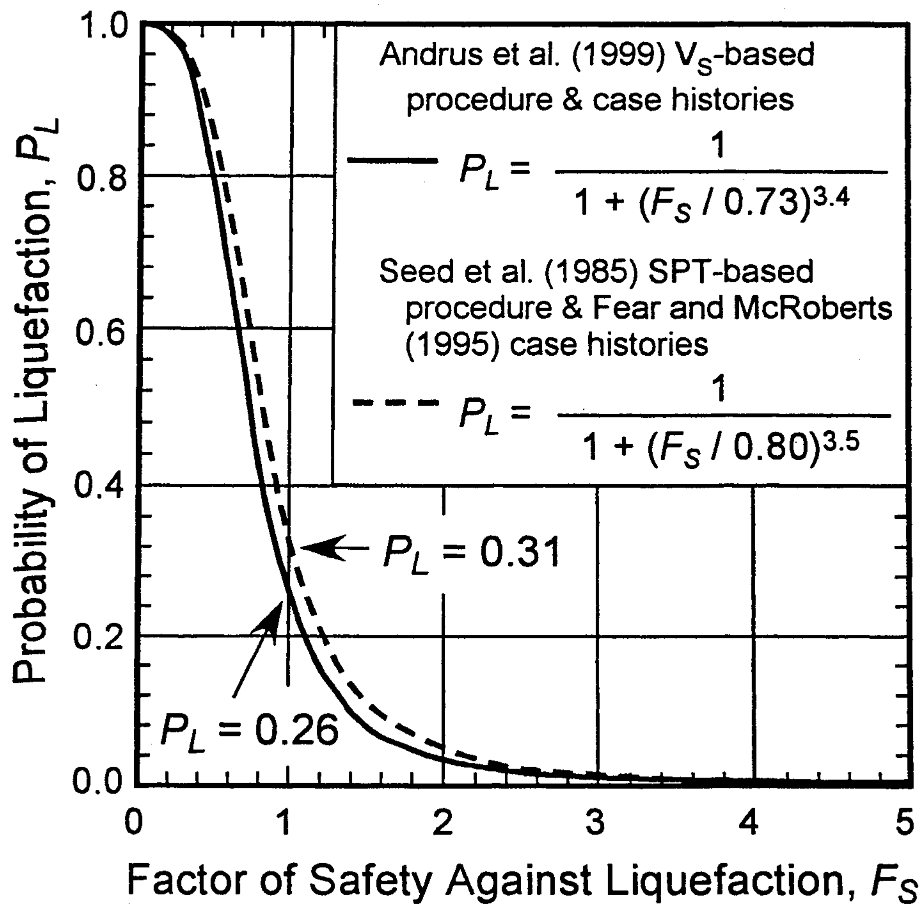

Fig. G.5 - Relationship Between P_L and F_S for the V_S-based Procedure (Juang et al., 2002) and SPT-Based Procedure (Juang et al., 2000a) Determined Using Bayes' Theorem.

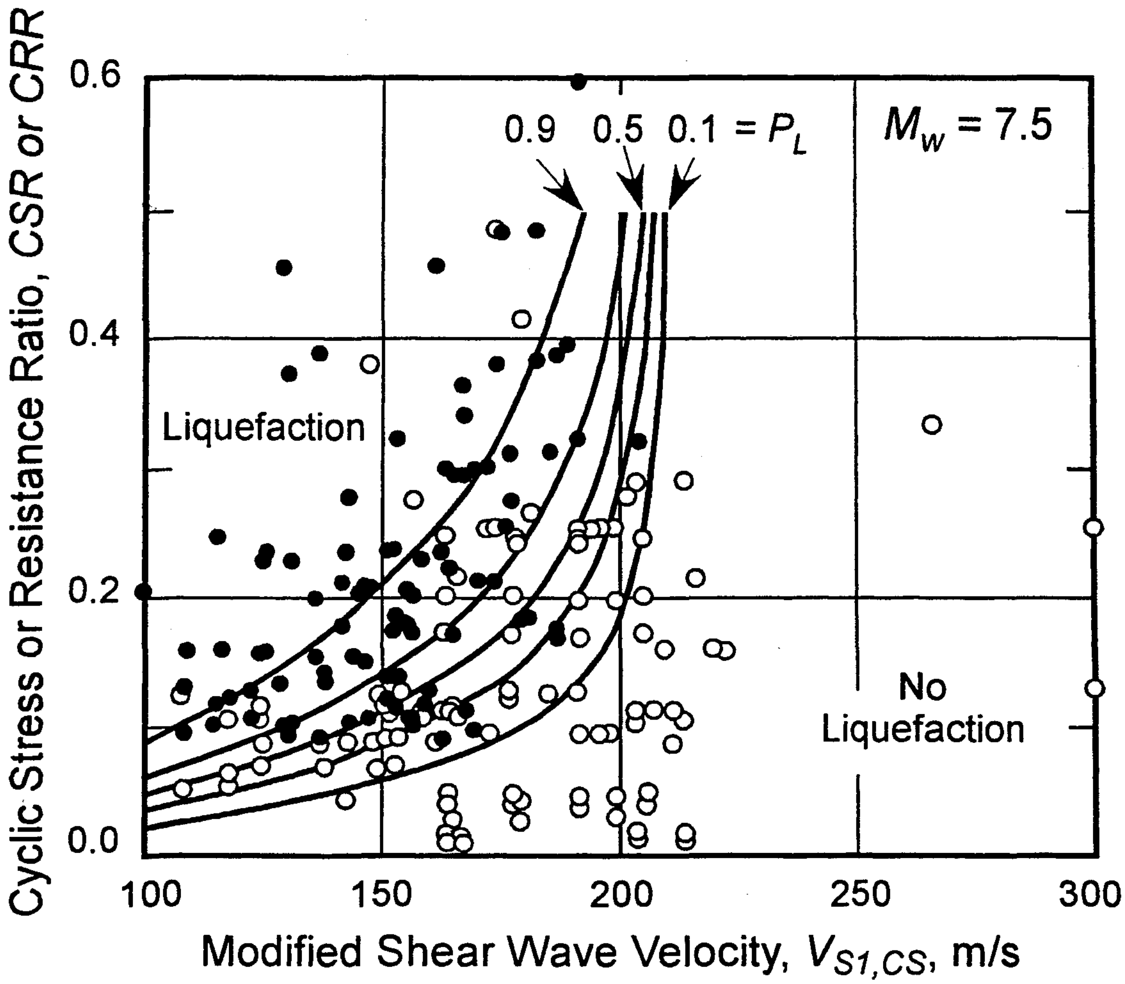

Fig. G.6 - Bayesian Mapping Model and Case History Data Adjusted for Fines Content. (Juang et al., 2002)

G.3 COMPARISON OF PROBABILITY MODELS

Figure G.7 compares the logistic regression model curves for P_L = 26 % with the Bayesian Mapping Model curve for P_L = 26 %, which corresponds to the deterministic curve developed by Andrus et al. (1999) for soils with $FC \leq 5$ %. The Bayesian Mapping Model curve lies between the two logistic regression curves below a V_{S1cs} value of about 195 m/s, indicating close agreement between the three probability models. Above 195 m/s, the Bayesian Mapping Model curve closely follows the logistic regression Model 2 curve. Thus, the logistic regression models support the Bayesian Mapping Model in characterizing the deterministic curve proposed by Andrus et al. (1999) and Andrus and Stokoe (2000) as a 26 % probability of liquefaction curve.

The tendency for the P_L curves to converge to some limiting upper value reflects the tendency of dense soils to exhibit dilative behavior at large strains, causing negative pore-water pressures. It seems reasonable that the P_L curves should not continue to diverge with increasing V_S, or penetration resistance, but should converge somewhat to reflect the behavior of dense soils, as suggested by the curves shown in Fig. G.6. The wider spread exhibited in logistic regression-based P_L curves at high values of V_S and CSR is believe to be the result of an inherent property of these models, and not a real-world phenomenon. Thus, the Bayesian Mapping Model (Fig. G.6) is considered to be an improvement over the logistic regression models, and is suggested for engineering risk-based design.

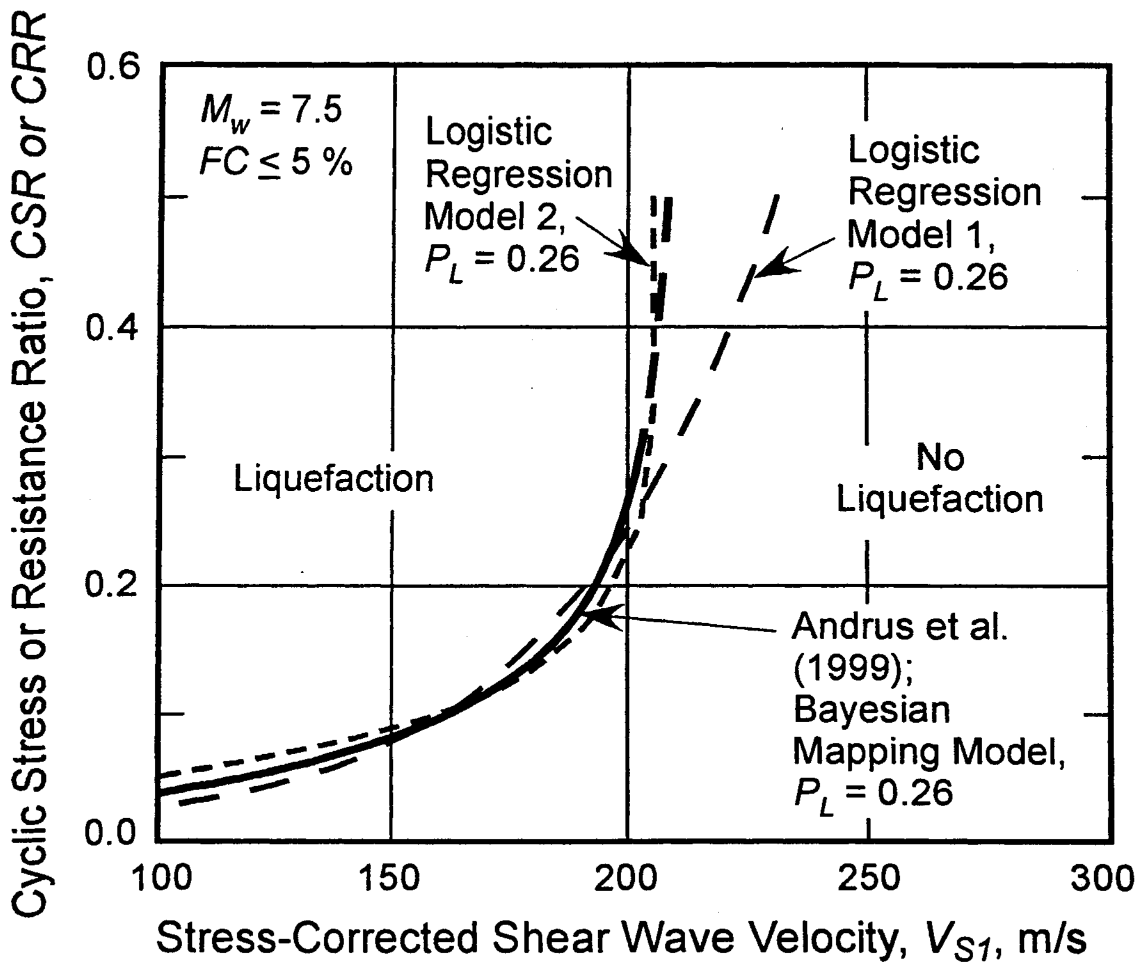

Fig. G.7 - Comparison of the Probability-Based Logistic Regression and Bayesian Mapping Models for P_L = 26 % with the Deterministic Curve Developed by Andrus et al. (1999) for Clean Soils. (modified from Juang et al., 2001a)

APPENDIX H

SUMMARY OF CASE HISTORY DATA

Table H.1 presents a summary of case history data described in Appendix E, and used in Appendix F to establish the recommended liquefaction resistance curves. This database is expanded and modified from the database presented by Andrus and Stokoe (1997). Most of the modifications are minor with the intent to have the data conform to the guidelines presented in this document. The major modifications are based on new information or correction of an error in calculations. Some case histories included in the earlier database by Andrus and Stokoe have been omitted due to one of the three following reasons: (1) The reported average downhole V_S measurement is for a depth interval much greater than the identified critical layer. (2) The critical layer is likely older than 10 000 years and contains carbonate. (3) The location of the critical layer or field behavior is uncertain. The case history data presented in Table H.1 are essentially the same as the data presented in the draft guidelines (Andrus et al., 1999), with only a few minor changes. References for the case history data are given in Table E.1.

Table H.1 - Summary Information for *Vs* -Based Liquefaction and Non-Liquefaction Case Histories.

Site	Test Type	Mw	Suf. Liq. Eff.? (1 = Y, 0 = N)	Water Table Depth (m)	amax. avg. (g)	Top of Layer Depth (m)	Thickness (m)	Soil Type	Average Fines Content (%)	Deposit Type	Age	No. of Values in Average	Depth (m)	Vert. Stress (kPa)	Eff. Vert. Stress (kPa)	rd	Vs (m/s)	Vs1 (m/s)	CSR	CSR 7.5
						----General Characteristics of Critical Layer----						----Average Value for Critical Layer ----								
1906 SAN FRANCISCO, CALIFORNIA EARTHQUAKE																				
Coyote Creek, S-R1	Xhole	7.7	1	2.4	0.36	3.5	2.5	sand & gravel	<5	AF	H	3	4.6	83.3	61.9	0.97	136	153	0.30	0.32
Coyote Creek, R1-R2	Xhole	7.7	1	2.4	0.36	3.5	2.5	sand & gravel	<5	AF	H	2	4.2	75.2	58.0	0.97	154	177	0.29	0.31
Coyote Creek, R1-R3	Xhole	7.7	1	2.4	0.36	3.5	2.5	sand & gravel	<5	AF	H	2	4.2	75.2	58.0	0.97	161	185	0.29	0.31
Coyote Creek, R2-R3	Xhole	7.7	1	2.4	0.36	3.5	2.5	sand & gravel	<5	AF	H	3	4.6	83.3	61.9	0.97	169	191	0.30	0.32
Salinas River North, S-R1	Xhole	7.7	0	6.1	0.32	9.1	2.3	sandy silt (ML to SM)	44	A	H	3	9.9	177.2	139.8	0.90	177	163	0.24	0.25
Salinas River North, R1-R2	Xhole	7.7	0	6.1	0.32	9.1	2.3	sandy silt (ML to SM)	44	A	H	3	9.9	177.2	139.8	0.90	195	179	0.24	0.25
Salinas River North, R1-R3	Xhole	7.7	0	6.1	0.32	9.1	2.3	sandy silt (ML to SM)	44	A	H	3	9.9	177.2	139.8	0.90	200	184	0.24	0.25
Salinas River North, R2-R3	Xhole	7.7	0	6.1	0.32	9.1	2.3	sandy silt (ML to SM)	44	A	H	3	9.9	177.2	139.8	0.90	199	183	0.24	0.25
Salinas River South, S-R1	Xhole	7.7	1	6.1	0.32	6.6	5.3	sand & silty sand (SP to SM)	14	A	H	2	8.0	141.2	122.6	0.93	131	124	0.22	0.24
Salinas River South, R1-R2	Xhole	7.7	1	6.1	0.32	6.6	5.3	sand & silty sand (SP to SM)	14	A	H	2	8.0	141.2	122.6	0.93	149	141	0.22	0.24
Salinas River South, R1-R3	Xhole	7.7	1	6.1	0.32	6.6	5.3	sand & silty sand (SP to SM)	14	A	H	2	8.0	141.2	122.6	0.93	158	151	0.22	0.24
Salinas River South, R2-R3	Xhole	7.7	1	6.1	0.32	6.6	5.3	sand & silty sand (SP to SM)	14	A	H	2	8.0	141.2	122.6	0.93	168	159	0.22	0.24
1957 DALY CITY, CALIFORNIA EARTHQUAKE																				
Marina District, No. 2	SASW	5.3	0	2.9	0.11	2.9	7.1	sand to silty sand (SP-SM)	~8	FH	R	1	6.4	117.0	82.2	0.94	120	129	0.09	0.04
Marina District, No. 3	SASW	5.3	0	2.9	0.11	2.9	7.1	sand to silty sand (SP to SM)	~12	FH	R	1	6.4	117.0	82.2	0.94	105	113	0.09	0.04
Marina District, No. 4	SASW	5.3	0	2.9	0.11	2.9	2.1	sand (SP)	<5	FH	R	1	3.9	69.9	59.6	0.98	120	137	0.08	0.03
Marina District, No. 5	SASW	5.3	0	5.9	0.11	5.9	4.1	sand (SP)	<5	Dune?	H?	1	7.9	140.6	120.5	0.93	220	211	0.08	0.03
Marina District, school	Dhole	5.3	0	2.7	0.11	2.7	1.6	sand (SP)	2	FU	R	2	3.5	62.3	54.1	0.98	112	130	0.08	0.03
1964 NIIGATA, JAPAN EARTHQUAKE																				
Niigata, Railway Station	?	7.5	1	2.0	0.16	2.0	2.7	sand	<5	?	?	2	3.2	56.7	45.2	0.98	131	160	0.13	0.13
Niigata, Site A1	SASW	7.5	0	5.0	0.16	5.0	2.5	sand	<5	?	?	1	6.2	109.9	97.7	0.95	162	164	0.12	0.12
Niigata, Site C1	SASW	7.5	1	1.2	0.16	1.6	6.5	sand	<5	?	?	2	4.5	82.8	50.7	0.97	112	136	0.15	0.15
Niigata, Site C2	SASW	7.5	1	1.2	0.16	1.2	4.8	sand	<5	?	?	1	4.0	73.4	46.5	0.97	118	147	0.15	0.15
1975 HAICHENG, PRC EARTHQUAKE																				
Chemical Fibre	Dhole	7.3	1	1.5	0.12	6.0	5.5	sand to silty clay	61	?	?	3	8.6	159.7	90.3	0.92	147	151	0.13	0.12
Construction Building	Dhole	7.3	1	1.5	0.12	3.0	6.5	clayey silt to silty clay	83	?	?	2	6.8	124.8	73.6	0.95	103	111	0.13	0.12
Fisheries & Shipbuilding	Dhole	7.3	1	0.5	0.12	2.5	4.0	silty sand to clayey silt	90	?	?	4	4.4	81.7	43.7	0.97	101	124	0.14	0.13
Glass Fiber	Dhole	7.3	1	0.8	0.12	2.7	3.8	sandy silt to clayey silt	42	?	?	3	4.8	89.8	50.3	0.97	98	117	0.13	0.13
Middle School	Dhole	7.3	0	1.0	0.12	5.0	6.0	clayey silt to silty clay	92	?	?	2	10.2	191.6	100.9	0.90	143	143	0.13	0.12
Paper Mill	Dhole	7.3	1	1.0	0.12	2.5	2.5	clayey silt to silty clay	72	?	?	1	3.0	54.7	35.2	0.98	122	158	0.12	0.11

Test Type
Xhole = crosshole seismic test
Dhole = downhole seismic test
SCPT = Seismic Cone Penetration Test
SASW = Spectral-Analysis-of-Surface-Waves test
Susp. = suspension logger test

Deposit Type
F = fill
FH = fill, hydraulic
FD = fill, dumped
FU = fill, uncompacted
FI = fill, improved

A = Alluvial
AF = Alluvial, fluvial
VDF = volcanic debris flow

Age
R = Recent (< 500 years)
H = Holocene (< 10 000 years)

CSR 7.5 = $CSR/(M_w/7.5)^{-2.56}$
? = unknown

Table H.1 - Summary Information for *Vs* -Based Liquefaction and Non-Liquefaction Case Histories.

Site	Test Type	Mw	Suf. Liq. Eff.? 1 = Y 0 = N	Water Table Depth (m)	amax. avg. (g)	Top of Layer Depth (m)	Thickness (m)	Soil Type	Average Fines Content (%)	Deposit Type	Age	No. of Values in Average	Depth (m)	Vert. Stress (kPa)	Eff. Vert. Stress (kPa)	rd	Vs (m/s)	Vs1 (m/s)	CSR	CSR 7.5
1979 IMPERIAL VALLEY EARTHQUAKE																				
Heber Road Channel Fill, R1-R2	Xhole	6.5	1	1.8	0.50	2.0	2.7	silty sand (SM)	22	AF	R	4	3.5	63.2	46.8	0.98	131	159	0.42	0.29
Heber Road Channel Fill, S-R1	Xhole	6.5	1	1.8	0.50	2.0	2.7	silty sand (SM)	22	AF	R	4	3.5	63.2	46.8	0.98	133	161	0.42	0.29
Heber Road Point Bar, R1-R2	Xhole	6.5	0	1.8	0.50	1.8	2.4	sand w/silt (SP-SM)	10	AF	R	4	3.4	60.3	45.4	0.98	164	201	0.42	0.29
Heber Road Point Bar, S-R1	Xhole	6.5	0	1.8	0.50	1.8	2.4	sand w/silt (SP-SM)	10	AF	R	4	3.4	60.3	45.4	0.98	173	211	0.42	0.29
Kornbloom	SASW	6.5	0	2.4	0.12	2.5	3.5	sandy silt (ML)	75	AF	R	5	4.2	75.1	58.1	0.97	105	120	0.10	0.07
McKim	SASW	6.5	1	1.5	0.51	1.5	3.5	silty sand (SM)	20	AF	R	4	3.0	54.1	39.7	0.98	126	160	0.43	0.30
Radio Tower	SASW	6.5	1	2.0	0.21	2.7	3.4	silty sand to sandy silt (SM to ML)	35	AF	H?	5	4.4	79.2	55.8	0.97	90	104	0.19	0.13
Vail Canal	SASW	6.5	0	2.7	0.12	2.7	2.8	sand w/ silt to silty sand (SP-SM to SM)	13	AF	R	4	4.0	70.4	58.4	0.98	101	116	0.09	0.06
Wildlife	SASW	6.5	0	1.5	0.13	2.5	4.3	silty sand to sandy silt (SM to ML)	27	AF	R	5	4.7	86.7	55.3	0.97	114	133	0.13	0.09
Wildlife, 1	Xhole	6.5	0	1.5	0.13	2.5	4.3	silty sand to sandy silt (SM to ML)	27	AF	R	4	4.6	83.8	53.9	0.97	127	148	0.13	0.09
Wildlife, 2	Xhole	6.5	0	1.5	0.13	2.5	4.3	silty sand to sandy silt (SM to ML)	27	AF	R	4	4.6	83.8	53.9	0.97	124	146	0.13	0.09
1980 MID-CHIBA, JAPAN EARTHQUAKE																				
Owi Island No. 1, layer 1	dhole	5.9	0	1.3	0.08	4.5	3.3	silty sand	20	FH	R	1	6.1	111.4	65.3	0.96	155	173	0.08	0.04
Owi Island No. 1, layer 2	dhole	5.9	0	1.3	0.08	13.0	3.6	silty sand	35	A	H	1	14.8	255.8	124.5	0.77	195	185	0.08	0.04
1981 WESTMORLAND, CALIFORNIA EARTHQUAKE																				
Heber Road Channel Fill, R1-R2	Xhole	5.9	0	1.8	0.02	2.0	2.7	silty sand (SM)	22	AF	R	4	3.5	63.2	46.8	0.98	131	159	0.02	0.01
Heber Road Channel Fill, S-R1	Xhole	5.9	0	1.8	0.02	2.0	2.7	silty sand (SM)	22	AF	R	4	3.5	63.2	46.8	0.98	133	161	0.02	0.01
Heber Road Point Bar, R1-R2	Xhole	5.9	0	1.8	0.02	1.8	2.4	sand w/silt (SP-SM)	10	AF	R	4	3.4	60.3	45.4	0.98	164	201	0.02	0.01
Heber Road Point Bar, S-R1	Xhole	5.9	0	1.8	0.02	1.8	2.4	sand w/silt (SP-SM)	10	AF	R	4	3.4	60.3	45.4	0.98	173	211	0.02	0.01
Kornbloom	SASW	5.9	1	2.4	0.36	2.5	3.5	sandy silt (ML)	75	AF	R	5	4.2	75.1	58.1	0.97	105	120	0.29	0.16
McKim	SASW	5.9	0	1.5	0.06	1.5	3.5	silty sand (SM)	20	AF	R	4	3.0	54.1	39.7	0.98	126	160	0.05	0.03
Radio Tower	SASW	5.9	1	2.0	0.20	2.7	3.4	silty sand to sandy silt (SM to ML)	35	AF	H?	5	4.4	79.2	55.8	0.97	90	104	0.18	0.10
Vail Canal	SASW	5.9	1	2.7	0.30	2.7	2.8	sand w/ silt to silty sand (SP-SM to SM)	13	AF	R	4	4.0	70.4	58.4	0.98	101	116	0.23	0.12
Wildlife	SASW	5.9	1	1.5	0.27	2.5	4.3	silty sand to sandy silt (SM to ML)	27	AF	R	5	4.7	86.7	55.3	0.97	114	133	0.26	0.14
Wildlife, 1	Xhole	5.9	1	1.5	0.27	2.5	4.3	silty sand to sandy silt (SM to ML)	27	AF	R	4	4.6	83.8	53.9	0.97	127	148	0.26	0.14
Wildlife, 2	Xhole	5.9	1	1.5	0.27	2.5	4.3	silty sand to sandy silt (SM to ML)	27	AF	R	4	4.6	83.8	53.9	0.97	124	146	0.26	0.14

Test Type
Xhole = crosshole seismic test
Dhole = downhole seismic test
SCPT = Seismic Cone Penetration Test
SASW = Spectral-Analysis-of-Surface-Waves test
Susp. = suspension logger test

Deposit Type
F = fill
FH = fill, hydraulic
FD = fill, dumped
FU = fill, uncompacted
FI = fill, improved

A = Alluvial
AF = Alluvial, fluvial
VDF = volcanic debris flow

Age
R = Recent (< 500 years)
H = Holocene (< 10 000 years)

CSR 7.5 = CSR/$(M_w/7.5)^{-2.56}$
? = unknown

Table H.1 - Summary Information for *Vs* -Based Liquefaction and Non-Liquefaction Case Histories.

Site	Test Type	Mw	Suf. Liq. Eff.? (1 = Y, 0 = N)	Water Table Depth (m)	amax. avg. (g)	Top of Layer Depth (m)	Thickness (m)	Soil Type	Average Fines Content (%)	Deposit Type	Age	No. of Values in Average	Depth (m)	Vert. Stress (kPa)	Eff. Vert. Stress (kPa)	rd	Vs (m/s)	Vs1 (m/s)	CSR	CSR 7.5
1983 BORAH PEAK, IDAHO EARTHQUAKE																				
Andersen Bar, SA-1	SASW	6.9	1	0.8	0.29	0.8	2.4	sandy gravel (GP-GW)	<5	AF	R	3	1.9	39.0	27.8	0.99	105	141	0.25	0.20
Andersen Bar, X1-X2	Xhole	6.9	1	0.8	0.29	0.8	2.4	sandy gravel (GP-GW)	<5	AF	R	8	2.0	40.6	28.7	0.99	106	143	0.26	0.21
Goddard Ranch, SA-2	SASW	6.9	1	1.2	0.30	1.2	2.0	sandy gravel (GP)	<5	AF	H	2	2.4	49.7	37.3	0.97	122	157	0.25	0.20
Goddard Ranch, SA-4	SASW	6.9	1	1.2	0.30	1.2	2.0	sandy gravel (GP)	<5	AF	H	2	2.4	49.8	37.4	0.97	105	136	0.25	0.20
Mackay Dam, Toe	SASW	6.9	0	2.3	0.23	2.3	2.7	silty sandy gravel (GW to GM)	6	?	H	2	2.8	57.2	52.3	0.98	270	318	0.16	0.13
North Gravel Bar, Bar Site	SASW	6.9	0	1.0	0.46	1.8	1.2	sandy gravel	~<5	A	H?	2	2.4	51.0	36.0	0.99	206	266	0.41	0.33
North Gravel Bar, Terrace	SASW	6.9	0	3.0	0.46	3.0	1.3	sandy gravel	~<5	A	H?	2	3.7	75.2	69.2	0.98	274	301	0.32	0.26
Pence Ranch, SA-1	SASW	6.9	1	1.7	0.36	1.8	1.9	gravelly sand to sandy gravel	<5	AF	H	4	2.8	57.3	46.2	0.98	103	125	0.28	0.23
Pence Ranch, SA-2	SASW	6.9	1	1.5	0.36	1.5	2.8	gravelly sand to sandy gravel	<5	AF	H	3	3.1	60.3	44.7	0.98	94	115	0.30	0.25
Pence Ranch, SA-3	SASW	6.9	1	1.4	0.36	1.4	1.8	gravelly sand to sandy gravel	<5	AF	H	3	2.4	45.8	36.8	0.98	102	131	0.28	0.23
Pence Ranch, SA-4	SASW	6.9	1	1.8	0.36	1.8	2.8	gravelly sand to sandy gravel	<5	AF	H	2	3.1	62.1	49.4	0.98	109	131	0.28	0.23
Pence Ranch, SA-5	SASW	6.9	1	1.5	0.36	1.5	1.9	gravelly sand to sandy gravel	<5	AF	H	2	3.0	60.5	45.6	0.98	123	151	0.29	0.24
Pence Ranch, SA-A	SASW	6.9	1	2.0	0.36	2.0	1.7	gravelly sand to sandy gravel	<5	AF	H	1	2.8	57.5	46.3	0.98	134	164	0.28	0.23
Pence Ranch, SA-B	SASW	6.9	1	1.5	0.36	1.5	1.7	gravelly sand to sandy gravel	<5	AF	H	2	2.1	38.8	32.9	0.99	128	170	0.27	0.21
Pence Ranch, SA-C	SASW	6.9	1	1.5	0.36	1.5	1.9	gravelly sand to sandy gravel	<5	AF	H	2	2.1	38.4	32.4	0.99	107	142	0.27	0.21
Pence Ranch, SA-D	SASW	6.9	1	1.5	0.36	1.5	1.7	gravelly sand to sandy gravel	<5	AF	H	2	2.1	39.4	33.8	0.99	131	173	0.26	0.21
Pence Ranch, SA-E	SASW	6.9	1	1.7	0.36	1.7	1.5	gravelly sand to sandy gravel	<5	AF	H	2	2.3	43.3	38.3	0.99	122	155	0.26	0.21
Pence Ranch, XD-XE	Xhole	6.9	1	1.5	0.36	2.8	1.0	gravelly sand to sandy gravel	<5	AF	H	3	3.4	64.7	46.8	0.98	146	176	0.32	0.26
1985 CHIBA-IBARAGI, JAPAN EARTHQUAKE																				
Owi Island No. 1, layer 1	Dhole	6.0	0	1.3	0.05	4.5	3.3	silty sand	20	FH	R	1	6.1	111.4	65.3	0.96	155	173	0.05	0.03
Owi Island No. 1, layer 2	Dhole	6.0	0	1.3	0.05	13.0	3.6	silty sand	35	A	H	1	14.8	255.8	124.5	0.77	195	185	0.05	0.03
10/26/85 TAIWAN EARTHQUAKE (EVENT LSST2)																				
Lotung LSST, L2-L5/L6	Xhole	5.3	0	0.5	0.05	3.7	5.2	silty sand to sandy silt (SM-ML)	50	A	H	3	6.1	114.1	45.4	0.96	137	167	0.08	0.03
Lotung LSST, L2-L7	Xhole	5.3	0	0.5	0.05	3.7	5.2	silty sand to sandy silt (SM-ML)	50	A	H	3	6.1	114.1	45.4	0.96	127	155	0.08	0.03
Lotung LSST, L8-L3	Xhole	5.3	0	0.5	0.05	4.1	4.8	silty sand to sandy silt (SM-ML)	50	A	H	3	6.1	114.1	45.4	0.96	156	191	0.08	0.03
Lotung LSST, L8-L4	Xhole	5.3	0	0.5	0.05	3.0	5.9	silty sand to sandy silt (SM-ML)	50	A	H	4	5.3	99.8	40.4	0.96	142	179	0.08	0.03

Test Type
Xhole = crosshole seismic test
Dhole = downhole seismic test
SCPT = Seismic Cone Penetration Test
SASW = Spectral-Analysis-of-Surface-Waves test
Susp. = suspension logger test

Deposit Type
F = fill
FH = fill, hydraulic
FD = fill, dumped
FU = fill, uncompacted
FI = fill, improved
A = Alluvial
AF = Alluvial, fluvial
VDF = volcanic debris flow

Age
R = Recent (< 500 years)
H = Holocene (< 10 000 years)

CSR 7.5 = CSR/$(M_w/7.5)^{-2.56}$
? = unknown

Table H.1 - Summary Information for *Vs* -Based Liquefaction and Non-Liquefaction Case Histories.

Site	Test Type	Mw	Suf. Liq. Eff.? 1 = Y 0 = N	Water Table Depth (m)	amax. avg. (g)	Top of Layer Depth (m)	Thickness (m)	Soil Type	Average Fines Content (%)	Deposit Type	Age	No. of Values in Average	Depth (m)	Vert. Stress (kPa)	Eff. Vert. Stress (kPa)	rd	Vs (m/s)	Vs1 (m/s)	CSR	CSR 7.5
						----General Characteristics of Critical Layer----						----Average Value for Critical Layer ----								
11/7/85 TAIWAN EARTHQUAKE (EVENT LSST 3)																				
Lotung LSST, L2-L5/L6	Xhole	5.5	0	0.5	0.02	3.7	5.2	silty sand to sandy silt (SM-ML)	50	A	H	3	6.1	114.1	45.4	0.96	137	167	0.03	0.01
Lotung LSST, L2-L7	Xhole	5.5	0	0.5	0.02	3.7	5.2	silty sand to sandy silt (SM-ML)	50	A	H	3	6.1	114.1	45.4	0.96	127	155	0.03	0.01
Lotung LSST, L8-L3	Xhole	5.5	0	0.5	0.02	4.1	4.8	silty sand to sandy silt (SM-ML)	50	A	H	3	6.1	114.1	45.4	0.96	156	191	0.03	0.01
Lotung LSST, L8-L4	Xhole	5.5	0	0.5	0.02	3.0	5.9	silty sand to sandy silt (SM-ML)	50	A	H	4	5.3	99.8	40.4	0.96	142	179	0.03	0.01
1/16/86 TAIWAN EARTHQUAKE (EVENT LSST 4)																				
Lotung LSST, L2-L5/L6	Xhole	6.6	0	0.5	0.22	3.7	5.2	silty sand to sandy silt (SM-ML)	50	A	H	3	6.1	114.1	45.4	0.96	137	167	0.34	0.25
Lotung LSST, L2-L7	Xhole	6.6	0	0.5	0.22	3.7	5.2	silty sand to sandy silt (SM-ML)	50	A	H	3	6.1	114.1	45.4	0.96	127	155	0.34	0.25
Lotung LSST, L8-L3	Xhole	6.6	0	0.5	0.22	4.1	4.8	silty sand to sandy silt (SM-ML)	50	A	H	3	6.1	114.1	45.4	0.96	156	191	0.34	0.25
Lotung LSST, L8-L4	Xhole	6.6	0	0.5	0.22	3.0	5.9	silty sand to sandy silt (SM-ML)	50	A	H	4	5.3	99.8	40.4	0.96	142	179	0.34	0.24
4/8/86 TAIWAN EARTHQUAKE (EVENT LSST 6)																				
Lotung LSST, L2-L5/L6	Xhole	5.4	0	0.5	0.04	3.7	5.2	silty sand to sandy silt (SM-ML)	50	A	H	3	6.1	114.1	45.4	0.96	137	167	0.06	0.03
Lotung LSST, L2-L7	Xhole	5.4	0	0.5	0.04	3.7	5.2	silty sand to sandy silt (SM-ML)	50	A	H	3	6.1	114.1	45.4	0.96	127	155	0.06	0.03
Lotung LSST, L8-L3	Xhole	5.4	0	0.5	0.04	4.1	4.8	silty sand to sandy silt (SM-ML)	50	A	H	3	6.1	114.1	45.4	0.96	156	191	0.06	0.03
Lotung LSST, L8-L4	Xhole	5.4	0	0.5	0.04	3.0	5.9	silty sand to sandy silt (SM-ML)	50	A	H	4	5.3	99.8	40.4	0.96	142	179	0.06	0.03
5/20/86 TAIWAN EARTHQUAKE (EVENT LSST 7)																				
Lotung LSST, L2-L5/L6	Xhole	6.6	0	0.5	0.18	3.7	5.2	silty sand to sandy silt (SM-ML)	50	A	H	3	6.1	114.1	45.4	0.96	137	167	0.28	0.20
Lotung LSST, L2-L7	Xhole	6.6	0	0.5	0.18	3.7	5.2	silty sand to sandy silt (SM-ML)	50	A	H	3	6.1	114.1	45.4	0.96	127	155	0.28	0.20
Lotung LSST, L8-L3	Xhole	6.6	0	0.5	0.18	4.1	4.8	silty sand to sandy silt (SM-ML)	50	A	H	3	6.1	114.1	45.4	0.96	156	191	0.28	0.20
Lotung LSST, L8-L4	Xhole	6.6	0	0.5	0.18	3.0	5.9	silty sand to sandy silt (SM-ML)	50	A	H	4	5.3	99.8	40.4	0.96	142	179	0.27	0.20
5/20/86 TAIWAN EARTHQUAKE (EVENT LSST 8)																				
Lotung LSST, L2-L5/L6	Xhole	6.2	0	0.5	0.04	3.7	5.2	silty sand to sandy silt (SM-ML)	50	A	H	3	6.1	114.1	45.4	0.96	137	167	0.06	0.04
Lotung LSST, L2-L7	Xhole	6.2	0	0.5	0.04	3.7	5.2	silty sand to sandy silt (SM-ML)	50	A	H	3	6.1	114.1	45.4	0.96	127	155	0.06	0.04
Lotung LSST, L8-L3	Xhole	6.2	0	0.5	0.04	4.1	4.8	silty sand to sandy silt (SM-ML)	50	A	H	3	6.1	114.1	45.4	0.96	156	191	0.06	0.04
Lotung LSST, L8-L4	Xhole	6.2	0	0.5	0.04	3.0	5.9	silty sand to sandy silt (SM-ML)	50	A	H	4	5.3	99.8	40.4	0.96	142	179	0.06	0.04

Test Type
Xhole = crosshole seismic test
Dhole = downhole seismic test
SCPT = Seismic Cone Penetration Test
SASW = Spectral-Analysis-of-Surface-Waves test
Susp. = suspension logger test

Deposit Type
F = fill
FH = fill, hydraulic
FD = fill, dumped
FU = fill, uncompacted
FI = fill, improved
A = Alluvial
AF = Alluvial, fluvial
VDF = volcanic debris flow

Age
R = Recent (< 500 years)
H = Holocene (< 10 000 years)

CSR 7.5 = $CSR/(M_w/7.5)^{-2.56}$
? = unknown

Table H.1 - Summary Information for *Vs* -Based Liquefaction and Non-Liquefaction Case Histories.

Site	Test Type	Mw	Suf. Liq. Eff.?	Water Table Depth	amax. avg.	Top of Layer Depth	Thick-ness	---General Characteristics of Critical Layer--- Soil Type	Average Fines Content	Deposit Type	Age	---Average Value for Critical Layer--- No. of Values in Average	Depth	Vert. Stress	Eff. Vert. Stress	rd	Vs	Vs1	CSR	CSR 7.5
			1 = Y 0 = N	m	g	m	m		%				m	kPa	kPa		m/s	m/s		
7/30/86 TAIWAN EARTHQUAKE (EVENT LSST 12)																				
Lotung LSST, L2-L5/L6	Xhole	6.2	0	0.5	0.18	3.7	5.2	silty sand to sandy silt (SM-ML)	50	A	H	3	6.1	114.1	45.4	0.96	137	167	0.28	0.17
Lotung LSST, L2-L7	Xhole	6.2	0	0.5	0.18	3.7	5.2	silty sand to sandy silt (SM-ML)	50	A	H	3	6.1	114.1	45.4	0.96	127	155	0.28	0.17
Lotung LSST, L8-L3	Xhole	6.2	0	0.5	0.18	4.1	4.8	silty sand to sandy silt (SM-ML)	50	A	H	3	6.1	114.1	45.4	0.96	156	191	0.28	0.17
Lotung LSST, L8-L4	Xhole	6.2	0	0.5	0.18	3.0	5.9	silty sand to sandy silt (SM-ML)	50	A	H	4	5.3	99.8	40.4	0.96	142	179	0.27	0.17
7/30/86 TAIWAN EARTHQUAKE (EVENT LSST 13)																				
Lotung LSST, L2-L5/L6	Xhole	6.2	0	0.5	0.05	3.7	5.2	silty sand to sandy silt (SM-ML)	50	A	H	3	6.1	114.1	45.4	0.96	137	167	0.08	0.05
Lotung LSST, L2-L7	Xhole	6.2	0	0.5	0.05	3.7	5.2	silty sand to sandy silt (SM-ML)	50	A	H	3	6.1	114.1	45.4	0.96	127	155	0.08	0.05
Lotung LSST, L8-L3	Xhole	6.2	0	0.5	0.05	4.1	4.8	silty sand to sandy silt (SM-ML)	50	A	H	3	6.1	114.1	45.4	0.96	156	191	0.08	0.05
Lotung LSST, L8-L4	Xhole	6.2	0	0.5	0.05	3.0	5.9	silty sand to sandy silt (SM-ML)	50	A	H	4	5.3	99.8	40.4	0.96	142	179	0.08	0.05
11/14/86 TAIWAN EARTHQUAKE (EVENT LSST 16)																				
Lotung LSST, L2-L5/L6	Xhole	7.6	0	0.5	0.14	3.7	5.2	silty sand to sandy silt (SM-ML)	50	A	H	3	6.1	114.1	45.4	0.96	137	167	0.22	0.23
Lotung LSST, L2-L7	Xhole	7.6	0	0.5	0.14	3.7	5.2	silty sand to sandy silt (SM-ML)	50	A	H	3	6.1	114.1	45.4	0.96	127	155	0.22	0.23
Lotung LSST, L8-L3	Xhole	7.6	0	0.5	0.14	4.1	4.8	silty sand to sandy silt (SM-ML)	50	A	H	3	6.1	114.1	45.4	0.96	156	191	0.22	0.23
Lotung LSST, L8-L4	Xhole	7.6	0	0.5	0.14	3.0	5.9	silty sand to sandy silt (SM-ML)	50	A	H	4	5.3	99.8	40.4	0.96	142	179	0.21	0.22
1987 CHIBA-TOHO-OKI, JAPAN EARTHQUAKE																				
Sunamachi, Tokyo Bay	Dhole	6.5	0	6.2	0.10	6.2	5.8	sand with silt to silty sand	15	FH	R	2	9.0	166.8	138.8	0.92	150	141	0.06	0.04
1987 ELMORE RANCH EARTHQUAKE																				
Heber Road Channel Fill, R1-R2	Xhole	5.9	0	1.8	0.03	2.0	2.7	silty sand (SM)	22	AF	R	4	3.5	63.2	46.8	0.98	131	159	0.03	0.01
Heber Road Channel Fill, S-R1	Xhole	5.9	0	1.8	0.03	2.0	2.7	silty sand (SM)	22	AF	R	4	3.5	63.2	46.8	0.98	133	161	0.03	0.01
Heber Road Point Bar, R1-R2	Xhole	5.9	0	1.8	0.03	1.8	2.4	sand w/silt (SP-SM)	10	AF	R	4	3.4	60.3	45.4	0.98	164	201	0.03	0.01
Heber Road Point Bar, S-R1	Xhole	5.9	0	1.8	0.03	1.8	2.4	sand w/silt (SP-SM)	10	AF	R	4	3.4	60.3	45.4	0.98	173	211	0.03	0.01
Kornbloom	SASW	5.9	0	2.4	0.24	2.5	3.5	sandy silt (ML)	75	AF	R	5	4.2	75.1	58.1	0.97	105	120	0.19	0.10
McKim	SASW	5.9	0	1.5	0.06	1.5	3.5	silty sand (SM)	20	AF	R	4	3.0	54.1	39.7	0.98	126	160	0.05	0.03
Radio Tower	SASW	5.9	0	2.0	0.11	2.7	3.4	silty sand to sandy silt (SM to ML)	35	AF	H?	5	4.4	79.2	55.8	0.97	90	104	0.10	0.05
Vail Canal	SASW	5.9	0	2.7	0.13	2.7	2.8	sand w/ silt to silty sand (SP-SM to SM)	13	AF	R	4	4.0	70.4	58.4	0.98	101	116	0.10	0.05
Wildlife	SASW	5.9	0	1.5	0.13	2.5	4.3	silty sand to sandy silt (SM to ML)	27	AF	R	5	4.7	86.7	55.3	0.97	114	133	0.13	0.07
Wildlife, 1	Xhole	5.9	0	1.5	0.13	2.5	4.3	silty sand to sandy silt (SM to ML)	27	AF	R	4	4.6	83.8	53.9	0.97	127	148	0.13	0.07
Wildlife, 2	Xhole	5.9	0	1.5	0.13	2.5	4.3	silty sand to sandy silt (SM to ML)	27	AF	R	4	4.6	83.8	53.9	0.97	124	146	0.13	0.07

Test Type

Xhole = crosshole seismic test
Dhole = downhole seismic test
SCPT = Seismic Cone Penetration Test
SASW = Spectral-Analysis-of-Surface-Waves test
Susp. = suspension logger test

Deposit Type

F = fill
FH = fill, hydraulic
FD = fill, dumped
FU = fill, uncompacted
FI = fill, improved

A = Alluvial
AF = Alluvial, fluvial
VDF = volcanic debris flow

Age

R = Recent (< 500 years)
H = Holocene (< 10 000 years)

CSR 7.5 = $CSR/(M_w/7.5)^{-2.56}$
? = unknown

Table H.1 - Summary Information for *Vs* -Based Liquefaction and Non-Liquefaction Case Histories.

Site	Test Type	Mw	Suf. Liq. Eff.? 1 = Y 0 = N	Water Table Depth (m)	amax. avg. (g)	Top of Layer Depth (m)	Thick-ness (m)	Soil Type	Average Fines Content (%)	Deposit Type	Age	No. of Values in Average	Depth (m)	Vert. Stress (kPa)	Eff. Vert. Stress (kPa)	rd	Vs (m/s)	Vs1 (m/s)	CSR	CSR 7.5
1987 SUPERSTITION HILLS, CALIFORNIA EARTHQUAKE																				
Heber Road Channel Fill, R1-R2	Xhole	6.5	0	1.8	0.18	2.0	2.7	silty sand (SM)	22	AF	R	4	3.5	63.2	46.8	0.98	131	159	0.15	0.11
Heber Road Channel Fill, S-R1	Xhole	6.5	0	1.8	0.18	2.0	2.7	silty sand (SM)	22	AF	R	4	3.5	63.2	46.8	0.98	133	161	0.15	0.11
Heber Road Point Bar, R1-R2	Xhole	6.5	0	1.8	0.18	1.8	2.4	sand w/silt (SP-SM)	10	AF	R	4	3.4	60.3	45.4	0.98	164	201	0.15	0.10
Heber Road Point Bar, S-R1	Xhole	6.5	0	1.8	0.18	1.8	2.4	sand w/silt (SP-SM)	10	AF	R	4	3.4	60.3	45.4	0.98	173	211	0.15	0.10
Kornbloom	SASW	6.5	0	2.4	0.21	2.5	3.5	sandy silt (ML)	75	AF	R	5	4.2	75.1	58.1	0.97	105	120	0.17	0.12
McKim	SASW	6.5	0	1.5	0.19	1.5	3.5	silty sand (SM)	20	AF	R	4	3.0	54.1	39.7	0.98	126	160	0.16	0.11
Radio Tower	SASW	6.5	0	2.0	0.20	2.7	3.4	silty sand to sandy silt (SM to ML)	35	AF	H?	5	4.4	79.2	55.8	0.97	90	104	0.18	0.12
Vail Canal	SASW	6.5	0	2.7	0.20	2.7	2.8	sand w/ silt to silty sand (SP-SM to SM)	13	AF	R	4	4.0	70.4	58.4	0.98	101	116	0.15	0.10
Wildlife	SASW	6.5	1	1.5	0.20	2.5	4.3	silty sand to sandy silt (SM to ML)	27	AF	R	5	4.7	86.7	55.3	0.97	114	133	0.20	0.14
Wildlife, 1	Xhole	6.5	1	1.5	0.20	2.5	4.3	silty sand to sandy silt (SM to ML)	27	AF	R	4	4.6	83.8	53.9	0.97	127	148	0.19	0.13
Wildlife, 2	Xhole	6.5	1	1.5	0.20	2.5	4.3	silty sand to sandy silt (SM to ML)	27	AF	R	4	4.6	83.8	53.9	0.97	124	146	0.19	0.13
1989 LOMA PRIETA, CALIFORNIA EARTHQUAKE																				
Bay Farm Island, Dike	SASW	7.0	0	3.6	0.27	3.6	2.8	sand with fines (SP-SM)	10	FI	R	1	5.2	91.9	77.0	0.96	204	219	0.20	0.16
Bay Farm Island, Dike S-R1	Xhole	7.0	0	3.6	0.27	3.6	2.8	sand with fines (SP-SM)	10	FI	R	5	4.9	87.1	75.2	0.97	193	207	0.20	0.16
Bay Farm Island, Dike R1-R2	Xhole	7.0	0	3.6	0.27	3.6	2.8	sand with fines (SP-SM)	10	FI	R	4	4.9	81.4	72.4	0.97	205	222	0.19	0.16
Bay Farm Island, Loop	SASW	7.0	1	3.5	0.27	3.5	1.7	sand with fines	<12	FH	R	1	3.8	66.7	61.4	0.98	125	142	0.18	0.15
Bay Farm Island, Loop S-R1	Xhole	7.0	1	3.5	0.27	3.5	1.7	sand with fines	<12	FH	R	3	4.3	75.6	68.2	0.98	98	107	0.19	0.16
Bay Farm Island, Loop R1-R2	Xhole	7.0	1	3.5	0.27	3.5	1.7	sand with fines	<12	FH	R	3	4.3	75.6	68.2	0.98	113	124	0.19	0.16
Coyote Creek, S-R1	Xhole	7.0	0	2.4	0.18	3.5	2.5	sand & gravel	<5	AF	H	3	4.6	83.3	61.9	0.97	136	153	0.15	0.13
Coyote Creek, R1-R2	Xhole	7.0	0	2.4	0.18	3.5	2.5	sand & gravel	<5	AF	H	2	4.2	75.2	58.0	0.97	154	177	0.15	0.12
Coyote Creek, R1-R3	Xhole	7.0	0	2.4	0.18	3.5	2.5	sand & gravel	<5	AF	H	2	4.2	75.2	58.0	0.97	161	185	0.15	0.12
Coyote Creek, R2-R3	Xhole	7.0	0	2.4	0.18	3.5	2.5	sand & gravel	<5	AF	H	3	4.6	83.3	61.9	0.97	169	191	0.15	0.13
Harbor Office, UC-12	SCPT	7.0	1	1.9	0.25	3.0	1.6	silty sand	15	?	H	2	4.1	74.3	52.6	0.97	150	176	0.22	0.19
Marina District, No. 2	SASW	7.0	1	2.9	0.15	2.9	7.1	sand to silty sand (SP-SM)	~8	FH	R	1	6.4	117.0	82.2	0.94	120	129	0.12	0.10
Marina District, No. 3	SASW	7.0	1	2.9	0.15	2.9	7.1	sand to silty sand (SP to SM)	~12	FH	R	1	6.4	117.0	82.2	0.94	105	113	0.12	0.10
Marina District, No. 4	SASW	7.0	1	2.9	0.15	2.9	2.1	sand (SP)	<5	FH	R	1	3.9	69.9	59.6	0.98	120	137	0.11	0.09
Marina District, No. 5	SASW	7.0	0	5.9	0.15	5.9	4.1	sand (SP)	<5	Dune?	H?	1	7.9	140.6	120.5	0.93	220	211	0.10	0.09
Marina District, school	Dhole	7.0	1	2.7	0.15	2.7	1.6	sand (SP)	2	FU	R	2	3.5	62.3	54.1	0.98	112	130	0.11	0.09
Port of Oakland, POO7-1	SCPT	7.0	1	3.0	0.24	5.0	4.0	sand (SP)	<5	FH	R	3	7.2	131.5	90.4	0.94	148	152	0.21	0.18
Port of Oakland, POO7-2	SASW	7.0	1	3.0	0.24	5.0	4.0	sand (SP)	<5	FH	R	2	6.4	115.7	82.9	0.95	157	165	0.21	0.17
Port of Oakland, POO7-2	SCPT	7.0	1	3.0	0.24	5.0	4.0	sand (SP)	<5	FH	R	3	7.2	131.8	90.7	0.94	151	155	0.21	0.18
Port of Oakland, POO7-2, S-R1	Xhole	7.0	1	3.0	0.24	5.0	4.0	sand (SP)	<5	FH	R	6	7.0	127.4	88.5	0.95	147	152	0.21	0.18
Port of Oakland, POO7-2, R1-R2	Xhole	7.0	1	3.0	0.24	5.0	4.0	sand (SP)	<5	FH	R	6	7.0	127.4	88.5	0.95	181	186	0.21	0.18

Test Type
Xhole = crosshole seismic test
Dhole = downhole seismic test
SCPT = Seismic Cone Penetration Test
SASW = Spectral-Analysis-of-Surface-Waves test
Susp. = suspension logger test

Deposit Type
F = fill
FH = fill, hydraulic
FD = fill, dumped
FU = fill, uncompacted
FI = fill, improved

A = Alluvial
AF = Alluvial, fluvial
VDF = volcanic debris flow

Age
R = Recent (< 500 years)
H = Holocene (< 10 000 years)

CSR 7.5 = $CSR/(M_w/7.5)^{-2.56}$
? = unknown

Table H.1 - Summary Information for *Vs* -Based Liquefaction and Non-Liquefaction Case Histories.

Site	Test Type	Mw	Suf. Liq. Eff.? (1 = Y, 0 = N)	Water Table Depth (m)	amax. avg. (g)	Top of Layer Depth (m)	Thickness (m)	Soil Type	Average Fines Content (%)	Deposit Type	Age	No. of Values in Average	Depth (m)	Vert. Stress (kPa)	Eff. Vert. Stress (kPa)	rd	Vs (m/s)	Vs1 (m/s)	CSR	CSR 7.5
Port of Oakland, POO7-3	SCPT	7.0	1	3.0	0.24	5.5	1.5	sand with silt (SP-SM)	10	FH	R	1	6.2	112.7	81.3	0.95	176	185	0.21	0.17
Port of Richmond, POR-2	SCPT	7.0	1	3.5	0.16	4.0	4.0	silt (ML)	57	FH	R	4	5.8	102.9	80.9	0.96	145	152	0.13	0.10
Port of Richmond, POR-2	SASW	7.0	1	3.5	0.16	4.0	4.0	silt (ML)	57	FH	R	2	5.3	93.6	76.4	0.97	117	125	0.12	0.10
Port of Richmond, POR-2, S-R1	Xhole	7.0	1	3.5	0.16	4.0	4.0	silt (ML)	57	FH	R	7	6.1	109.4	84.1	0.95	143	150	0.13	0.11
Port of Richmond, POR-2, R1-R2	Xhole	7.0	1	3.5	0.16	4.0	4.0	silt (ML)	57	FH	R	7	6.1	109.4	84.0	0.95	135	141	0.13	0.11
Port of Richmond, POR-3	SCPT	7.0	1	3.5	0.16	4.0	3.0	silt to silty sand (ML to SM)	>25	FH	R	3	5.2	93.4	76.3	0.96	110	118	0.13	0.11
Port of Richmond, POR-4	SCPT	7.0	1	3.5	0.16	3.8	3.2	silty sand (ML to SM)	>32	FH	R	3	5.2	93.4	76.3	0.96	128	137	0.12	0.10
Salinas River North, S-R1	Xhole	7.0	0	6.1	0.15	9.1	2.3	sandy silt (ML to SM)	44	A	H	3	9.9	177.2	139.8	0.90	177	163	0.11	0.09
Salinas River North, R1-R2	Xhole	7.0	0	6.1	0.15	9.1	2.3	sandy silt (ML to SM)	44	A	H	3	9.9	177.2	139.8	0.90	195	179	0.11	0.09
Salinas River North, R1-R3	Xhole	7.0	0	6.1	0.15	9.1	2.3	sandy silt (ML to SM)	44	A	H	3	9.9	177.2	139.8	0.90	200	184	0.11	0.09
Salinas River North, R2-R3	Xhole	7.0	0	6.1	0.15	9.1	2.3	sandy silt (ML to SM)	44	A	H	3	9.9	177.2	139.8	0.90	199	183	0.11	0.09
Salinas River South, S-R1	Xhole	7.0	0	6.1	0.15	6.6	5.3	sand & silty sand (SP to SM)	14	A	H	2	8.0	141.2	122.6	0.93	131	124	0.10	0.09
Salinas River South, R1-R2	Xhole	7.0	0	6.1	0.15	6.6	5.3	sand & silty sand (SP to SM)	14	A	H	2	8.0	141.2	122.6	0.93	149	141	0.10	0.09
Salinas River South, R1-R3	Xhole	7.0	0	6.1	0.15	6.6	5.3	sand & silty sand (SP to SM)	14	A	H	2	8.0	141.2	122.6	0.93	158	151	0.10	0.09
Salinas River South, R2-R3	Xhole	7.0	0	6.1	0.15	6.6	5.3	sand & silty sand (SP to SM)	14	A	H	2	8.0	141.2	122.6	0.93	168	159	0.10	0.09
Sandholdt Road, UC-4 Layer 1	SCPT	7.0	1	1.8	0.25	2.1	0.6	sand	2	?	H	1	2.5	44.3	37.4	0.99	91	116	0.19	0.16
Sandholdt Road, UC-4 Layer 2	SCPT	7.0	0	1.8	0.25	5.9	4.1	sand	4	?	H	4	8.0	148.0	87.2	0.94	209	216	0.26	0.22
Sandholdt Road, UC-6	SCPT	7.0	0	1.7	0.25	3.0	4.3	sand	1	?	H	5	4.7	85.5	56.4	0.97	171	199	0.24	0.20
Santa Cruz, SC02	SCPT	7.0	1	0.6	0.42	1.3	3.2	silty sand	~35?	A	H	11	2.9	53.6	31.2	0.98	122	161	0.45	0.38
Santa Cruz, SC03	SCPT	7.0	1	2.1	0.42	2.1	2.4	sand to silty sand	~12?	A	H	8	3.4	59.8	47.9	0.98	145	175	0.33	0.28
Santa Cruz, SC04	SCPT	7.0	0	1.8	0.42	1.8	2.1	silty sand	~35?	A	H	7	2.9	51.7	41.3	0.98	163	202	0.33	0.28
Santa Cruz, SC05	SCPT	7.0	0	2.8	0.42	3.0	1.8	silty sand to sandy silt	>35?	A	H	6	4.0	70.2	58.9	0.98	149	170	0.32	0.26
Santa Cruz, SC13	SCPT	7.0	0	1.8	0.42	2.0	1.3	silty sand	~35?	A	H	4	2.8	48.9	39.9	0.98	119	149	0.33	0.27
Santa Cruz, SC14	SCPT	7.0	1	1.2	0.42	1.5	1.5	sand	<5?	A	H	5	2.3	41.2	30.7	0.99	126	169	0.36	0.30
State Beach, UC-15	SCPT	7.0	1	1.8	0.25	1.8	2.8	sand	1	?	H	3	3.5	62.0	45.4	0.98	116	142	0.21	0.18
State Beach, UC-16	SCPT	7.0	1	2.3	0.25	2.3	7.1	sand	1	?	H	7	5.5	99.8	68.2	0.96	162	179	0.22	0.18
TI Fire Station, Redpath	Dhole	7.0	1	1.4	0.13	4.5	2.5	silty sand(SM)	24	FH	R	1	6.9	127.1	73.3	0.95	129	142	0.14	0.11
TI Fire Station, Gibbs et al.	Dhole	7.0	1	1.4	0.13	4.5	2.5	silty sand(SM)	24	FH	R	1	5.8	107.0	63.7	0.96	133	150	0.14	0.11
TI Fire Station, 1992	SASW	7.0	1	1.4	0.13	4.5	2.5	silty sand(SM)	24	FH	R	1	5.3	98.4	59.6	0.96	131	149	0.14	0.11
TI Fire Station	SCPT	7.0	1	1.4	0.13	4.5	2.5	silty sand(SM)	24	FH	R	1	5.3	98.4	59.6	0.96	133	152	0.13	0.11
TI Fire Station, B1-B4	Xhole	7.0	1	1.4	0.13	4.5	2.5	silty sand(SM)	24	FH	R	3	5.5	101.3	60.9	0.96	137	155	0.14	0.11
TI Fire Station, B2-B3	Xhole	7.0	1	1.4	0.13	4.5	2.5	silty sand(SM)	24	FH	R	8	5.5	101.3	60.9	0.96	129	146	0.14	0.11
TI Fire Station, B2-B4	Xhole	7.0	1	1.4	0.13	4.5	2.5	silty sand(SM)	24	FH	R	3	5.5	101.3	60.9	0.96	132	149	0.14	0.11
TI Fire Station, B4-B5	Xhole	7.0	1	1.4	0.13	4.5	2.5	silty sand(SM)	24	FH	R	3	5.5	101.3	60.9	0.96	131	148	0.14	0.11
TI Fire Station, Portable	Xhole	7.0	1	1.4	0.13	4.5	2.5	silty sand(SM)	24	FH	R	7	5.8	97.0	63.5	0.96	130	145	0.14	0.11
TI Perimeter, UM03	SCPT	7.0	0	1.5	0.14	6.5	5.2	sand to clayey silty sand	13	FH	R	17	9.1	174.7	99.8	0.92	173	173	0.15	0.12
TI Perimeter, UM05	SCPT	7.0	1	2.4	0.14	3.3	2.3	sand to silty sand	5	FH	R	8	4.6	83.7	62.5	0.97	151	169	0.12	0.10
TI Perimeter, UM06	SCPT	7.0	1	1.4	0.14	2.0	1.7	sand to silty sand	5	FH	R	5	2.9	53.4	38.7	0.98	123	157	0.12	0.10

Test Type
Xhole = crosshole seismic test
Dhole = downhole seismic test
SCPT = Seismic Cone Penetration Test
SASW = Spectral-Analysis-of-Surface-Waves test
Susp. = suspension logger test

Deposit Type
F = fill
FH = fill, hydraulic
FD = fill, dumped
FU = fill, uncompacted
FI = fill, improved

A = Alluvial
AF = Alluvial, fluvial
VDF = volcanic debris flow

Age
R = Recent (< 500 years)
H = Holocene (< 10 000 years)

CSR 7.5 = CSR/$(M_w/7.5)^{-2.56}$
? = unknown

Table H.1 - Summary Information for *Vs* -Based Liquefaction and Non-Liquefaction Case Histories.

							----General Characteristics of Critical Layer----						----Average Value for Critical Layer ----							
Site	Test Type	Mw	Suf. Liq. Eff.? 1 = Y 0 = N	Water Table Depth m	amax. avg. g	Top of Layer Depth m	Thickness m	Soil Type	Average Fines Content %	Deposit Type	Age	No. of Values in Average	Depth m	Vert. Stress kPa	Eff. Vert. Stress kPa	rd	Vs m/s	Vs1 m/s	CSR	CSR 7.5
TI Perimeter, UM09	SCPT	7.0	1	2.7	0.14	2.7	3.8	sand to silty sand	14	FH	R	12	4.6	83.1	64.8	0.97	143	160	0.11	0.09
TI Approach to Pier, SA-5b	SASW	7.0	0	2.0	0.14	2.0	10.8	sand to sand with silt (SP to SP-SM)	5	FI	R	3	6.6	123.7	78.1	0.94	189	206	0.13	0.11
TI Approach to Pier, SA-6	SASW	7.0	0	2.0	0.14	2.0	10.8	sand to sand with silt (SP to SP-SM)	5	FI	R	5	5.8	104.0	67.1	0.95	187	211	0.13	0.11
TI Approach to Pier, SA-7	SASW	7.0	0	2.0	0.14	2.0	10.8	sand to sand with silt (SP to SP-SM)	5	FI	R	3	6.6	123.7	78.1	0.98	187	203	0.13	0.11
Bay Bridge Toll Plaza, S-R1	Xhole	7.0	1	3.0	0.24	5.0	2.5	sand to silty sand (SP-SM)	~9	FU	R	4	6.4	116.0	82.5	0.95	143	150	0.21	0.17
Bay Bridge Toll Plaza, R1-R2	Xhole	7.0	1	3.0	0.24	5.0	2.5	sand to silty sand (SP-SM)	~9	FU	R	4	6.4	116.0	82.5	0.95	144	151	0.21	0.17
Bay Bridge Toll Plaza, SFOBB-1	SCPT	7.0	1	3.0	0.24	5.0	2.5	sand to silty sand (SP-SM)	~9	FU	R	2	6.5	117.8	83.4	0.95	148	155	0.21	0.18
Bay Bridge Toll Plaza, SFOBB-2	SCPT	7.0	1	3.0	0.24	6.0	3.0	sand to silty sand (SP-SM)	~13	FU	R	4	7.5	98.9	92.4	0.94	148	151	0.22	0.18
1993 KUSHIRO-OKI, JAPAN EARTHQUAKE																				
Kushiro Port, No. 2	Susp.	8.3	1	0.9	0.41	2.7	3.0	sand with silt (SP-SM)	7	A	H	3	4.2	74.8	41.9	0.97	152	189	0.46	0.60
Kushiro Port, No. D	Susp.	8.3	1	1.9	0.41	1.9	6.8	sand	5	FU	R	2	4.5	82.3	56.6	0.97	135	161	0.35	0.46
1993 HOKKAIDO-NANSEI-OKI, JAPAN EARTHQUAKE																				
Pension House, BH-1	Dhole	8.3	1	1.0	0.19	1.0	2.5	sandy gravel	<5	VDF	H	2	2.0	40.4	30.4	0.99	74	98	0.16	0.20
Hakodate Port, No. 1	Susp.	8.3	1	1.2	0.15	2.7	7.0	silty sand to sand with silt (SM to SP-SM)	20	?	?	7	7.0	112.5	55.7	0.94	131	154	0.18	0.23
Hakodate Port, No. 2	Susp.	8.3	0	1.4	0.15	2.1	8.2	sand with silt (SP-SM)	8	?	?	8	6.5	107.7	57.8	0.95	143	166	0.17	0.22
Hakodate Port, No. 3	Susp.	8.3	1	1.4	0.15	1.5	11.5	silty sand (SM)	54	?	?	11	7.0	117.1	62.2	0.93	124	141	0.16	0.21
1994 NORTHRIDGE, CALIFORNIA EARTHQUAKE																				
Rory Lane, M-20	SCPT	6.7	1	3.4	0.51	3.4	4.9	silty sand	~10	A	?	3	5.6	100.6	78.4	0.97	160	170	0.40	0.30
Rory Lane, M-32	SCPT	6.7	1	3.4	0.51	3.4	3.3	silty sand	~10	A	?	2	5.4	97.0	76.7	0.96	152	161	0.40	0.30
Rory Lane, M-33	SCPT	6.7	1	3.4	0.51	3.4	2.1	silty sand	~10	A	?	1	4.4	78.6	67.9	0.97	129	142	0.37	0.28
1995 HYOGOKEN-NANBU, JAPAN EARTHQUAKE																				
Hanshin Expressway 5, 3	Susp.	6.9	1	2.1	0.50	2.1	3.2	gravelly silty sand (SP-SM to SM)	18	FD	R	1	5.6	96.6	62.8	0.96	160	180	0.48	0.39
Hanshin Expressway 5, 10	Susp.	6.9	1	1.8	0.58	3.5	3.5	silty sandy gravel (SM)	16	FD	R	4	5.5	100.8	64.6	0.96	112	126	0.56	0.45
Hanshin Expressway 5, 14	Susp.	6.9	1	4.3	0.63	4.5	4.1	silty sandy gravel	~12	FD	R	4	6.5	115.7	94.2	0.95	175	178	0.48	0.38
Hanshin Expressway 5, 25	Susp.	6.9	1	3.2	0.65	5.3	6.3	gravelly silty sand to gravelly sand	9	FD	R	5	8.8	151.6	96.7	0.92	172	173	0.60	0.48
Hanshin Expressway 5, 29	Susp.	6.9	1	2.5	0.65	3.0	8.3	silty sand to sandy gravel with silt	12	?	?	3	7.2	123.1	77.8	0.94	167	179	0.60	0.48
KNK	Dhole	6.9	0	2.0	0.12	2.0	15.0	silt, sand, gravel	~10	?	H	2	6.6	128.5	83.4	0.94	139	147	0.10	0.08
Kobe-Nishinomiya EWY, 3	Susp.	6.9	0	3.7	0.63	4.4	6.1	gravelly sand-sandy gravel with silt	7	?	?	6	7.0	126.1	93.8	0.95	175	178	0.51	0.41
Kobe-Nishinomiya EWY, 17	Susp.	6.9	0	2.0	0.53	2.0	2.5	gravelly sand with silt	8	?	?	1	3.3	60.9	49.0	0.98	200	239	0.42	0.34
Kobe-Nishinomiya EWY, 23	Susp.	6.9	0	2.9	0.63	2.9	3.1	gravelly sand-sandy gravel with silt	11	?	?	1	4.0	71.5	60.8	0.98	130	147	0.47	0.38

Test Type
Xhole = crosshole seismic test
Dhole = downhole seismic test
SCPT = Seismic Cone Penetration Test
SASW = Spectral-Analysis-of-Surface-Waves test
Susp. = suspension logger test

Deposit Type
F = fill
FH = fill, hydraulic
FD = fill, dumped
FU = fill, uncompacted
FI = fill, improved
A = Alluvial
AF = Alluvial, fluvial
VDF = volcanic debris flow

Age
R = Recent (< 500 years)
H = Holocene (< 10 000 years)

CSR 7.5 = $CSR/(M_w/7.5)^{-2.56}$
? = unknown

Table H.1 - Summary Information for *Vs* -Based Liquefaction and Non-Liquefaction Case Histories.

							----General Characteristics of Critical Layer----					----Average Value for Critical Layer ----								
Site	Test Type	Mw	Suf. Liq. Eff.? 1 = Y 0 = N	Water Table Depth m	amax. avg. g	Top of Layer Depth m	Thick-ness m	Soil Type	Average Fines Content %	Deposit Type	Age	No. of Values In Average	Depth m	Vert. Stress kPa	Eff. Vert. Stress kPa	rd	Vs m/s	Vs1 m/s	CSR	CSR 7.5
Kobe-Nishinomiya EWY, 28	Susp.	6.9	0	2.2	0.65	3.0	3.0	sand with gravel	2	?	?	1	6.0	110.7	74.0	0.96	160	173	0.60	0.48
Kobe Port, 7C	Dhole	6.9	1	4.4	0.55	7.5	15.0	sand to silty sand	10	FD	R	1	15.0	299.3	195.4	0.88	160	135	0.48	0.39
LPG Tank Yard, Kobe	Dhole	6.9	1	1.5	0.50	2.0	6.0	gravelly sand with silt	10	FD	R	1	4.0	79.3	54.6	0.98	110	129	0.46	0.37
Port Island, 1C	Dhole	6.9	1	3.0	0.50	4.0	12.2	gravelly sand to silty gravelly sand	13	FD	R	1	8.6	171.4	116.3	0.88	170	164	0.42	0.34
Port Island, 2C	Dhole	6.9	1	1.5	0.50	5.0	10.5	sand with silt	10	FD	R	1	11.5	232.3	134.4	0.87	200	186	0.49	0.40
Port Island, Common Factory	Dhole	6.9	0	3.2	0.50	3.2	11.8	gravelly sand with silt (SP-SM)	6	R	R	12	9.0	183.3	126.4	0.90	214	202	0.41	0.33
Port Island, Common Factory	Susp.	6.9	0	3.2	0.50	3.2	11.8	gravelly sand with silt (SP-SM)	6	R	R	22	9.2	188.6	129.3	0.90	193	183	0.41	0.33
Port Island, Dhole Array '91	Dhole	6.9	1	2.4	0.50	2.4	14.6	sandy gravel with silt	10	FD	R	2	7.2	140.5	93.0	0.92	190	201	0.40	0.32
Port Island, Dhole Array '95	Dhole	6.9	1	2.4	0.50	2.4	14.6	sandy gravel with silt	10	FD	R	2	7.8	152.8	99.4	0.93	165	165	0.45	0.36
SGK	Dhole	6.9	0	7.0	0.45	7.0	5.0	silt, sand, gravel	~10	F?	R?	1	8.5	151.6	136.9	0.93	190	176	0.30	0.24

Test Type
Xhole = crosshole seismic test
Dhole = downhole seismic test
SCPT = Seismic Cone Penetration Test
SASW = Spectral-Analysis-of-Surface-Waves test
Susp. = suspension logger test

Deposit Type
F = fill
FH = fill, hydraulic
FD = fill, dumped
FU = fill, uncompacted
FI = fill, improved

A = Alluvial
AF = Alluvial, fluvial
VDF = volcanic debris flow

Age
R = Recent (< 500 years)
H = Holocene (< 10 000 years)

CSR 7.5 = $CSR/(M_w/7.5)^{-2.56}$
? = unknown